



The
University
Of
Sheffield.

Investigating the role of the type VI secretion system-associated genes of *Burkholderia thailandensis*

By:

Jamie Hall

A thesis submitted in partial fulfilment of the requirements for the degree of
Doctor of Philosophy

The University of Sheffield
Faculty of Medicine
Department of Infection, Immunity and Cardiovascular Disease

Acknowledgements

I would like to thank my supervisor, Dr Mark Thomas for his guidance and support throughout my PhD. It should be noted that this work would not have been possible without the BBSRC who provided the funding. I am indebted to Dr Trong Khoa Pham in the department of Chemical and Biological Engineering as well as Drs Mark Collins and Richard Beniston in the biOMICS facility who performed the mass spectrometry analysis vital to this work.

I am also extremely grateful to all of the past and present lab members of LU103 who have helped keep me going on the many occasions when nothing seemed to work. This gratitude is extended to the entire department of Infection and Immunity, many of whom have given me training, equipment or reagents over the last few years.

Outside of work, a great deal of credit must be given to those who have kept me sane and put up with me; housemates, teammates and just plain mates. I am particularly indebted to Elaine, who helped so much throughout.

Finally, I would like to thank all of my family. Particular appreciation goes to my sister, Robyn, who has made sure I didn't miss every single family occasion over the past four years despite my best efforts (and allowed me to put my name to presents that were all her idea). And of course my parents, Bryan and Sherrie, for all of the support they have given me, not just over the course of my PhD, but for as long as I can remember.

Abstract

The type VI secretion system (T6SS) is a relatively recently discovered nanomachine found in many Gram-negative bacterial species which is capable of delivering effector proteins directly into target cells. Composed of at least 13 protein subunits, the T6SS is capable of targeting both prokaryotic cells and eukaryotic cells. *Burkholderia pseudomallei* is a soil-dwelling saprophyte found in Southeast Asia and Northern Australia. It is of interest because it is an opportunistic human (and animal) pathogen which causes the potentially fatal disease melioidosis. One of the histopathological features of melioidosis is the appearance of multinucleated giant cells (MNGCs) formed by the fusion of neighbouring cells which is believed to facilitate intercellular spread of the bacteria. The fusion of neighbouring cells has previously been shown to be induced by T6SS-5, one of six T6SSs encoded in the genome of *B. pseudomallei*.

The T6SS-5 gene cluster contains four genes which are not found in all T6SS gene clusters, *tagA*, *tagB*, *tagC* and *tagD*. One aim of this study was to elucidate the role of these genes in the function of T6SS-5 and to identify the proteins which are secreted by T6SS-5. To avoid the complications of working with *B. pseudomallei*, the closely related, but non-virulent species *Burkholderia thailandensis* was employed, which also induces MNGC formation using T6SS-5.

Each *tag* gene in the *B. thailandensis* T6SS-5 gene cluster was deleted and it was determined that all four genes were required for *B. thailandensis* induced MNGC formation in a macrophage-like cell line. To determine whether or not the *tag* genes were required for protein export by T6SS-5, expression of the T6SS-5 gene cluster was induced by introducing the regulatory *virA* and *virG* genes into the *tag* mutants. Analysis of supernatant samples using a custom antibody prepared against the secreted T6SS component, TssD, showed that all four of the *tag* mutants were T6SS-5 deficient. Mass spectrometry was used to identify proteins secreted by T6SS-5. However, apart from the expected secretion of the TssD and TssI components of the T6SS, no novel secreted proteins were detected.

Plasmids expressing FLAG epitope-tagged Tag proteins were constructed and introduced into the *B. thailandensis tag* mutant strains. Although TagC_{FLAG} and TagD_{FLAG} were non-functional as determined by MNGC formation assays and TssD-5 secretion assays, TagA_{FLAG} and TagB_{FLAG} demonstrated the same behaviour as their WT counterparts and were used in co-immunoprecipitation experiments. Mass spectrometric analysis of the co-immunoprecipitations suggested that TagA interacts with the T6SS-5 baseplate protein TssF-5 and the tail spike protein TssI-5. Although TssI-5 was enriched in the TagB_{FLAG} pull down it was not statistically significant. Bacterial adenylate cyclase two-hybrid (BACTH) assays

were performed in an attempt to identify specific Tag protein interaction partners. However, none were found. An attempt to produce the Tag proteins in *E. coli* for structural studies was unsuccessful. The role of the *tssA-5* gene in *B. thailandensis* was also investigated through generation of a *B. thailandensis tssA-5* mutant by allelic replacement. Although the *B. thailandensis tssA-5* mutant was unable to induce the formation of MNGCs, TssD-5 secretion appeared to be reduced, rather than abolished entirely. Under the culture conditions used in the TssD-5 secretion assay, another T6SS gene cluster, T6SS-1, is expressed. Based on the hypothesis that the *tssA* gene from this cluster might be partially compensating for a loss of *tssA-5*, a *tssA-5* and *tssA-1* double mutant was constructed. However, *tssA-1* had no effect on T6SS-5 function.

Table of Contents

Acknowledgements	2
Abstract	3
List of tables	12
List of figures	13
Abbreviations	16
Chapter 1 Introduction	20
1.1 Meloidosis.....	21
1.1.1 Route of infection	21
1.1.2 Symptoms	21
1.1.3 Diagnosis	22
1.1.4 Risk factors.....	22
1.1.5 Treatment and prevention.....	23
1.1.6 Global distribution of <i>B. pseudomallei</i> and melioidosis	24
1.2 The <i>Burkholderia pseudomallei</i> group	26
1.2.1 <i>Burkholderia pseudomallei</i>	26
1.2.2 <i>Burkholderia mallei</i>	27
1.2.3 <i>Burkholderia thailandensis</i>	27
1.2.4 <i>Burkholderia oklahomensis</i>	28
1.3 <i>Burkholderia pseudomallei</i> virulence factors	29
1.3.1 Intracellular motility.....	29
1.3.2 Flagella	31
1.3.3 Capsule.....	31
1.3.4 Lipopolysaccharide.....	31
1.3.5 Pili.....	32
1.3.6 Anti-microbial resistance mechanisms	32
1.3.7 Type III secretion system.....	32
1.3.8 The type VI secretion system	33
1.4 Secretion systems in Gram-negative bacteria.....	36
1.4.1 Sec-independent protein secretion systems	37
1.4.2 Sec-dependent protein secretion systems	41
1.5 Type VI Secretion System	43
1.5.1 Membrane complex.....	43
1.5.2 Baseplate.....	47

1.5.3	Inner tube and contractile sheath	50
1.5.4	TssA	52
1.5.5	TssH	52
1.5.6	Mechanism of secretion by the T6SS.....	52
1.5.7	T6SS-exported effectors.....	53
1.6	Hypothesis	56
1.7	Aims of this study	57
Chapter 2 Materials and methods.....		58
2.1	Bioinformatic analysis.....	59
2.2	Bacterial Strains and plasmids.....	59
2.3	Growth media	65
2.3.1	Lysogeny Broth (LB)	65
2.3.2	Iso-Sensitest Broth (IST).....	65
2.3.3	Brain-Heart Infusion Broth (BHI).....	65
2.3.4	M9 Minimal medium	65
2.3.5	MacConkey agar.....	66
2.3.6	Media supplements	66
2.4	Culture techniques	68
2.4.1	<i>Escherichia coli</i>	68
2.4.2	<i>Burkholderia thailandensis</i>	68
2.4.3	RAW 264.7 cells.....	68
2.5	DNA extraction methods	69
2.5.1	Boiled lysate genomic DNA isolation	69
2.5.2	Plasmid DNA extraction	69
2.6	DNA manipulation techniques	69
2.6.1	Polymerase Chain Reaction (PCR).....	69
2.6.2	PCR purification.....	72
2.6.3	Agarose gel electrophoresis.....	72
2.6.4	DNA Extraction from agarose Gels.....	73
2.6.5	Restriction digestion	73
2.6.6	Ligation.....	73
2.6.7	Nucleotide sequencing.....	73
2.7	Transfer of DNA into bacteria.....	73
2.7.1	Preparation of competent cells	73
2.7.2	Transformation	74

2.7.3	Conjugation.....	75
2.7.4	Deletion of genes in <i>Burkholderia thailandensis</i> by allelic replacement.....	75
2.8	Protein techniques	76
2.8.1	Overexpression of proteins from plasmids containing T7 RNAP-dependent promoters.	76
2.8.2	Purification of soluble His-tagged Proteins by IMAC.....	76
2.8.3	TCA precipitation of <i>B. thailandensis</i> culture supernatants	77
2.8.4	SDS polyacrylamide gel electrophoresis (SDS-PAGE).....	78
2.8.5	Western Blotting.....	79
2.8.6	In-Gel Trypsin digestion for mass spectrometry.....	80
2.9	Infection assays	82
2.9.1	Multinucleate giant cell formation assay.....	82
2.9.2	Intracellular replication assay	82
2.10	Interaction assays	83
2.10.1	Co-immunoprecipitation.....	83
2.10.2	Bacterial adenylate cyclase two-hybrid assay.....	83

Chapter 3 Bioinformatic analysis of the *B. thailandensis* tag genes and their protein products..... 85

3.1	Introduction.....	86
3.2	Genetic organisation	86
3.3	TagA-5.....	86
3.3.1	TagA proteins in <i>Burkholderia pseudomallei</i> group members	88
3.3.2	Protein family analysis of TagA.....	88
3.3.3	Cellular location of TagA-5.....	88
3.3.4	Amino acid sequence alignments of TagA homologues	90
3.3.5	Structure prediction of TagA-5	90
3.4	TagB-5.....	97
3.4.1	TagB proteins in <i>Burkholderia pseudomallei</i> group members.....	97
3.4.2	Protein family analysis of TagB	97
3.4.3	Cellular location of TagB-5.....	99
3.4.4	Amino acid sequence alignments of TagB homologues	99
3.4.5	Structure prediction of TagB-5.....	99
3.4.6	Relationship of TagB with 'evolved' TagA.....	104
3.4.7	PipB and PipB2	104
3.5	TagC-5.....	104
3.5.1	TagC proteins in <i>Burkholderia pseudomallei</i> group members.....	109

3.5.2	Protein family analysis of TagC	109
3.5.3	Cellular location of TagC-5	109
3.5.4	Amino acid sequence alignments of TagC homologues	109
3.5.5	Structure prediction of TagC-5.....	112
3.6	TagD-5.....	112
3.6.1	TagD proteins in <i>Burkholderia pseudomallei</i> group members	112
3.6.2	Protein family analysis of TagD	116
3.6.3	Cellular location prediction of TagD-5	116
3.6.4	Amino acid sequence alignments of TagD homologues	116
3.6.5	Structure prediction of TagD-5	119
3.7	Discussion	124
Chapter 4 Investigating the role of the T6SS-5 tag genes in multinucleated giant cell formation and intracellular replication of <i>B. thailandensis</i>		127
4.1	Introduction.....	128
4.2	MNGC formation assays	129
4.2.1	<i>B. thailandensis</i> induces the formation of MNGCs in vitro.....	129
4.2.2	Construction of a <i>B. thailandensis tssK-5</i> mutant.....	129
4.2.3	Effect of deletion of <i>tssK-5</i> on MNGC formation induced by <i>B. thailandensis</i>	133
4.2.4	Construction of a <i>tssK-5</i> complementation plasmid.....	135
4.2.5	Re-introduction of the WT <i>tssK-5</i> gene into the <i>tssK-5</i> mutant restores MNGC formation <i>in trans</i>	138
4.2.6	Construction of a <i>B. thailandensis tagABCD-5</i> deletion mutant.....	138
4.2.7	The <i>B. thailandensis tagABCD-5</i> deletion mutant is incapable of inducing MNGC formation	139
4.2.8	Construction of a <i>tagABCD</i> complementation plasmid	141
4.2.9	Re-introduction of the WT <i>tagA-D-5</i> genes into the <i>tagA-D-5</i> mutant restores MNGC formation <i>in trans</i>	141
4.3	The Effect of deletion of each <i>tag</i> gene on MNGC formation induced by <i>B. thailandensis</i>	141
4.3.1	Construction of a <i>B. thailandensis</i> of <i>tagA-5</i> mutant	141
4.3.2	<i>B. thailandensis tagA-5</i> is required for MNGC formation <i>in vitro</i>	142
4.3.3	Construction of a <i>tagA-5</i> complementation plasmid	142
4.3.4	Introduction of WT <i>tagA-5</i> into the <i>B.t tagA-5</i> mutant restores MNGC formation ...	144
4.3.5	Construction of a <i>B. thailandensis</i> of <i>tagB-5</i> mutant	144
4.3.6	<i>B. thailandensis tagB-5</i> is required for MNGC formation <i>in vitro</i>	144
4.3.7	Construction of a <i>tagB-5</i> complementation plasmid.....	146
4.3.8	Introduction of WT <i>tagB-5</i> into the <i>B.t tagB-5</i> mutant restores MNGC formation ...	146

4.3.9	Construction of a <i>B. thailandensis</i> of <i>tagC-5</i> mutant.....	146
4.3.10	<i>B. thailandensis tagC-5</i> is required for MNGC formation <i>in vitro</i>	148
4.3.11	Construction of a <i>tagC-5</i> complementation plasmid.....	148
4.3.12	Introduction of WT <i>tagC-5</i> into the <i>B.t tagC-5</i> mutant restores MNGC formation....	148
4.3.13	Construction of a <i>B. thailandensis tagD-5</i> mutant	148
4.3.14	<i>B. thailandensis tagD-5</i> is required for MNGC formation <i>in vitro</i>	149
4.3.15	Construction of a <i>tagD-5</i> complementation plasmid	149
4.3.16	Introduction of WT <i>tagD-5</i> into the <i>B.t tagD-5</i> mutant restores MNGC formation...	150
4.4	Quantitative determination of MNGC formation in <i>tag</i> mutants and complemented strains.	150
4.5	Intracellular Replication of <i>B. thailandensis tag</i> mutants	153
4.5.1	Inactivation of the <i>tssK</i> and <i>tag</i> genes has no effect on intracellular replication	153
4.6	Discussion	153
Chapter 5 Role of the <i>tagA-tagD</i> genes in T6SS-5 activity		157
5.1	Introduction	158
5.1.1	Construction of pSCrhaB2- <i>virAG</i> for T6SS-5 induction in <i>B.t</i> growing in bacteriological medium	159
5.1.2	Induction of T6SS-5 activity by the pSCrhaB2- <i>virAG</i> plasmid	161
5.1.3	Identification of potential TssD-5 protein band by mass spectrometry	165
5.2	Purification of TssD-5 for antibody generation	165
5.2.1	Construction of a TssD-5 overexpression vector	165
5.2.2	Expression and solubility test of TssD-5.....	168
5.2.3	Purification of histidine-tagged TssD-5 by IMAC	170
5.2.4	Generation of antibodies	170
5.2.5	Assaying the antibody raised against TssD-5	173
5.2.6	Confirmation that the <i>B.t ΔtssK-5</i> mutant lacks a functional T6SS-5	176
5.3	Mass spectrometry analysis of T6SS-5 secretome	176
5.3.1	Comparing the WT secretome to a <i>tssK</i> mutant secretome	179
5.4	Requirement of the Tag proteins for T6SS-5 activity	181
5.4.1	A <i>B. thailandensis</i> strain lacking all four <i>tag</i> genes is deficient in TssD-5 secretion...	181
5.4.2	Each individual <i>tag</i> gene is required for secretion of TssD-5	181
5.4.3	Generation of pSCrhaB2- <i>virAG</i> plasmid derivatives for complementation of <i>tssK</i> and <i>tag</i> mutants.....	183
5.4.4	pSCrhaB2- <i>virAG-tssK</i> restores T6SS-5 activity to a <i>tssK</i> mutant	186
5.4.5	pSCrhaB2- <i>virAG-tagA</i> , pSCrhaB2- <i>virAG-tagB</i> , pSCrhaB2- <i>virAG-tagC</i> and pSCrhaB2- <i>virAG-tagD</i> restore T6SS-5 activity to their respective mutants	187

5.5	Glutathione induction of the <i>B. thailandensis</i> T6SS-5.....	187
5.5.1	Glutathione induces T6SS-5 to a similar level as <i>virAG</i>	187
5.6	Discussion	191
Chapter 6 Functional studies on the <i>B. thailandensis</i> T6SS-5 Tag proteins.....		195
6.1	Introduction	196
6.2	Identification of Tag protein interacting partners by co-immunoprecipitation .	196
6.2.1	Construction of plasmids for expression of FLAG-tagged Tag proteins in MNGC assays	196
6.2.2	Analysis of FLAG-tagged Tag protein production from pBBR1MCS in <i>B. thailandensis</i>	198
6.2.3	Assessment of ability of FLAG-tagged Tag proteins to participate in T6SS-5 dependent stimulation of MNGC formation	200
6.2.4	Construction of plasmids for expression of FLAG-tagged Tag proteins in secretion assays	203
6.2.5	Assessment of the ability of TagA _{FLAG} and TagB _{FLAG} to restore T6SS-5 activity in <i>B.t tagA</i> and <i>tagB</i> mutants	203
6.2.6	Co-immunoprecipitation using TagA _{FLAG} as bait.....	207
6.2.7	Co-immunoprecipitation using TagB _{FLAG} as bait.....	212
6.2.8	Mass spectrometry analysis of FLAG eluted samples	214
6.3	Identification of Tag protein-interacting partners by two-hybrid analysis.....	217
6.3.1	Cloning of <i>tagA</i> -5 into pKNT25 and pUT18.....	219
6.3.2	Cloning of <i>tagB</i> -5 into pKNT25 and pUT18.....	220
6.3.3	Cloning of <i>tagC</i> -5 into pKT25 and pUT18C	221
6.3.4	Cloning of <i>tagD</i> -5 into pKT25 and pUT18C	222
6.3.5	Cloning of <i>tssI</i> -5 into pKT25, pKNT25, pUT18 and pUT18C	222
6.3.6	Cloning of other selected <i>tss</i> genes into two hybrid vectors.....	224
6.3.7	BACTH analysis of Tag protein interactions	225
6.4	Overexpression of the Tag proteins for structure analysis	228
6.4.1	Construction of a TagA expression vector	228
6.4.2	Construction of a TagB expression vector and a TagA and TagB dual expression vector	229
6.4.3	Construction of a TagC expression vector	229
6.4.4	Construction of a TagD expression vector and a TagC and TagD dual expression vector	229
6.4.5	Induction of Tag protein production.....	230
6.4.6	Analysis of TagA and TagC solubility.....	232
6.5	Discussion	234

Chapter 7 Investigation into the <i>tssA-5</i> gene of <i>B. thailandensis</i>	237
7.1 Introduction.....	238
7.2 Construction of a <i>B. thailandensis tssA-5</i> mutant.....	238
7.3 MNGC formation in a <i>B. thailandensis tssA-5</i> mutant	242
7.4 Construction of a <i>tssA-5</i> complementation plasmid.....	244
7.5 Secretion of TssD-5 by a <i>tssA-5</i> mutant	244
7.6 Creation of a <i>B. thailandensis ΔtssA-1</i> and <i>ΔtssA-5</i> double mutant	246
7.7 Secretion of TssD-5 by a <i>B. thailandensis tssA-1</i> and <i>tssA-5</i> double mutant.....	248
7.8 Interaction of TssA-5 with itself.....	248
7.9 Secretion of TssD-1 by a <i>B. thailandensis tssA-1</i> and <i>tssA-5</i> double mutant.....	250
7.10 Discussion	253
Chapter 8 General discussion	256
8.1 Findings.....	257
8.2 Limitations	258
8.3 Future work	258
References	261
Appendix	280
10.1 Accession numbers.....	280
10.2 Ladders	281
10.2.1 DNA ladders	281
10.2.2 Protein ladders.....	282

List of tables

Chapter 1

Table 1.1 T6SS gene clusters in <i>B.p</i> , <i>B.t</i> and <i>B.m</i>	34
Table 1.2 Standardised names of genes encoding core components of the T6SS	46

Chapter 2

Table 2.1 Tools used in bioinformatics analysis.....	59
Table 2.2 Bacterial strains used in this study.....	59
Table 2.3 Plasmids used in this study	60
Table 2.4 Antibiotic working concentrations in <i>E. coli</i> and <i>B.t</i>	67
Table 2.5 PCR components for reactions using KOD polymerase	70
Table 2.6 PCR components for reactions using Q5 polymerase.....	71
Table 2.7 PCR components for reactions using GoTaq polymerase	71
Table 2.8 SDS-Polyacrylamide gel ingredients.....	79
Table 2.9 Antibodies used in this work.....	80
Table 2.10 Solutions used for in-gel trypsin digestion.....	81

Chapter 3

Table 3.1 Summary of bioinformatic predictions	126
--	-----

Chapter 5

Table 5.1 Band identification result with the highest Mascot score	166
Table 5.2 Proteins present in the culture supernatant of WT <i>B.t</i> samples but absent from those of the T6SS mutant.....	180

Chapter 6

Table 6.1 Predicted molecular weight of protein bands marked by red arrows in Figure 6.8	211
Table 6.2 TagA interaction partners identified by mass spec.....	215
Table 6.3 TagB interaction partners identified by mass spec.....	216
Table 6.4 Interactions of the Tag proteins as determined by BACTH assay	227

Chapter 7

Table 7.1 Identities of the five TssD-5 proteins of <i>B. thailandensis</i> with <i>B. cenocepacia</i> BCAL0343	252
---	-----

Appendix

Table 10.1 Accession numbers of proteins used in alignments.....	280
Table 10.2 Locus tags of T6SS-5 genes in <i>B.p</i> , <i>B.t</i> and <i>B.m</i>	283
Table 10.3 List of primers used in this work	284
Table 10.4 Proteins detected in all three WT <i>B.t</i> supernatant samples.....	288
Table 10.5 Proteins detected in all three <i>B.t</i> Δ tssK supernatant samples.....	293

List of figures

Chapter 1

Figure 1.1 Global distribution of <i>Burkholderia pseudomallei</i>	25
Figure 1.2 Proposed mechanism of invasion and intercellular spread utilised by <i>Burkholderia pseudomallei</i> during infection	30
Figure 1.3 <i>B. thailandensis</i> T6SS-5 gene cluster.....	38
Figure 1.4 Gram-negative secretion systems.....	39
Figure 1.5 Mechanism of action of the T6SS	44
Figure 1.6 Comparison of the delivery mechanisms of contractile bacteriophages and the T6SS	45
Figure 1.7 Structures of the T6SS membrane complex and baseplate components.....	48
Figure 1.8 Structure of the T6SS inner tube and contractile sheath	51
Figure 1.9 Mechanisms of T6SS effector delivery.....	55

Chapter 3

Figure 3.1 <i>tag</i> genes in T6SS gene clusters.....	87
Figure 3.2 Amino acid sequence of <i>B.t</i> TagA-5	89
Figure 3.3 Amino acid sequence alignment of TagA proteins	93
Figure 3.4 Amino acid sequence alignment of the CTDs of TagA proteins containing pentapeptide repeats	94
Figure 3.5 Predicted secondary structure of <i>B.t</i> TagA-5	96
Figure 3.6 Predicted structure of <i>B.t</i> TagA-5	98
Figure 3.7 Amino acid sequence of <i>B.t</i> TagB-5	98
Figure 3.8 Amino acid sequence alignment of TagB proteins	101
Figure 3.9 Predicted secondary structure of <i>B.t</i> TagB-5	102
Figure 3.10 Predicted structure of <i>B.t</i> TagB-5	103
Figure 3.11 Amino acid sequence alignment of the CTDs of pentapeptide-containing TagA proteins with TagB proteins	107
Figure 3.12 Comparison of the predicted 'solenoid' structures of TagA-5 and TagB-5 with the solved structure of QnrB1	108
Figure 3.13 Amino acid sequence of <i>B.t</i> TagC-5	110
Figure 3.14 Amino acid sequence alignment of TagC proteins	111
Figure 3.15 Predicted secondary structure of <i>B.t</i> TagC-5	113
Figure 3.16 Predicted structure of <i>B.t</i> TagC-5.....	114
Figure 3.17 Amino acid sequence alignment of TagC and phage GpV proteins.....	115
Figure 3.18 Amino acid sequence of <i>B.t</i> TagD-5	117
Figure 3.19 Amino acid sequence alignment of selected 'DUF4150' family proteins	118
Figure 3.20 Amino acid sequence alignment of TagD proteins with PAAR_1 proteins	120
Figure 3.21 Predicted secondary structure of <i>B.t</i> TagD-5.....	121
Figure 3.22 Structure of c1882 with gp5	122
Figure 3.23 Comparison of known structures of PAAR proteins with the predicted structure of TagD-5	123

Chapter 4

Figure 4.1 Confirmation of giant cell formation in RAW 264.7 cells infected with <i>B. thailandensis</i> ..	130
Figure 4.2 Schematic illustration of the deletion of <i>B. thailandensis</i> genes by splice overlap extension PCR and homologous recombination.	132
Figure 4.3 Construction of the <i>B. thailandensis</i> Δ tssK strain	134
Figure 4.4 Effects of the deletion of tssK gene of the <i>B. thailandensis</i> T6SS-5 gene cluster	136
Figure 4.5 Construction of pBBR1MCS-tssK.....	137
Figure 4.6 Effect of the deletion of all four tag genes on MNGC formation by <i>B. thailandensis</i>	140
Figure 4.7 Effect of deletion of tagA-5 on MNGC formation induced by <i>B. thailandensis</i>	143
Figure 4.8 Effect of the deletion of tagB-5 on MNGC formation induced by <i>B. thailandensis</i>	145
Figure 4.9 Effect of the deletion of tagC-5 on MNGC formation induced by <i>B. thailandensis</i>	147
Figure 4.10 Effect of the deletion of tagD-5 on MNGC formation induced by <i>B. thailandensis</i>	151
Figure 4.11 Quantitative analysis of MNGC formation induced by <i>B. thailandensis</i> tag mutants	152
Figure 4.12 Intracellular replication of <i>B.t</i> tag mutants	154

Chapter 5

Figure 5.1 pSCrhaB2-virAG vector.....	160
Figure 5.2 Rhamnose induction of cultures of <i>B. thailandensis</i> containing pSCrhaB2 or pSCrhaB2-virAG grown in dialysed brain heart infusion broth.....	162
Figure 5.3 Induction of T6SS-5 in <i>B.t</i> growing in M9 glycerol	164
Figure 5.4 pET14b-tssD-5	167
Figure 5.5 Overproduction of TssD-5 in <i>E. coli</i>	169
Figure 5.6 IMAC purification of TssD-5	171
Figure 5.7 Testing of anti-TssD-5 serum taken from the rat 45 days after the initial injection of purified TssD-5	172
Figure 5.8 Testing of polyclonal antibody raised against TssD-5 in <i>Burkholderia thailandensis</i> samples	175
Figure 5.9 Validation of the <i>B.t</i> tssK mutant.....	177
Figure 5.10 TssD-5 secretion by <i>B. thailandensis</i> lacking all four tag genes	182
Figure 5.11 TssD-5 secretion by <i>B. thailandensis</i> mutants lacking individual tag genes.....	182
Figure 5.12 Maps of the LITMUS28i-tssK and pSCrhaB2-virAG-tssK plasmids	184
Figure 5.13 Construction of pSCrhaB2-virAG-tssK.....	185
Figure 5.14 Complementation of a <i>B.t</i> tssK mutant in a T6SS-5 secretion assay	188
Figure 5.15 Complementation of Δ tagA, Δ tagB, Δ tagC and Δ tagD in TssD-5 secretion assays.....	189
Figure 5.16 Induction of TssD-5 synthesis and secretion in <i>B.t</i> when glutathione is added to cultures	190

Chapter 6

Figure 6.1 Expression of FLAG-tagged Tag proteins in <i>B. thailandensis</i>	199
Figure 6.2 Induction of MNGC formation by <i>B.t</i> mutants complemented by genes encoding FLAG-tagged Tag proteins	201
Figure 6.3 Fusion Indexes calculated from RAW 264.7 cells infected with <i>B. thailandensis</i> tag mutants complemented with genes encoding FLAG-tagged proteins.....	202
Figure 6.4 pSCrhaB2-virAG-tagA _{FLAG} restores T6SS-5 function to a <i>B.t</i> tagA mutant	205
Figure 6.5 pSCrhaB2-virAG-tagB _{FLAG} restores T6SS-5 function to a tagB mutant.....	206
Figure 6.6 T6SS-5 activity in glutathione-induced <i>B.t</i> tagC and tagD mutants complemented with TagC _{FLAG} and TagD _{FLAG}	208

Figure 6.7 Co-immunoprecipitation using TagA _{FLAG} as bait.....	209
Figure 6.8 Eluted proteins from co-immunoprecipitation assays.....	211
Figure 6.9 Co-immunoprecipitation using TagB _{FLAG} as bait.....	213
Figure 6.10 Principle of the bacterial two hybrid system.....	218
Figure 6.11 IPTG induction of BL21(λDE3) cells harbouring the tag expression vectors.....	231
Figure 6.12 TagA and TagC solubility test.....	233

Chapter 7

Figure 7.1 Amino acid sequence alignment of selected TssA proteins	241
Figure 7.2 Effect of deleting <i>tssA-5</i> on MNGC formation <i>in vitro</i>	243
Figure 7.3 Analysis of TssD-5 secretion by the <i>B. thailandensis</i> Δ <i>tssA-5</i> mutant.....	247
Figure 7.4 Secretion of TssD-5 by a <i>B. thailandensis</i> <i>tssA-1</i> and <i>tssA-5</i> double mutant.....	249
Figure 7.5 Self-interaction of TssA determined by BACTH assay.....	251
Figure 7.6 Cross reactivity of BCAL0343 with <i>B. thailandensis</i> TssD-1	254

Appendix

Figure 10.1 GeneRuler DNA ladder mix	281
Figure 10.2 Supercoiled DNA ladder.....	281
Figure 10.3 EZ-Run Rec protein ladder.....	282
Figure 10.4 EZ-Run Rec prestained ladder.....	282

Abbreviations

ATP	Adenosine triphosphate
AmB	Ammonium bicarbonate
Ap	Ampicillin
<i>B.m</i>	<i>Burkholderia mallei</i>
<i>B.o</i>	<i>Burkholderia oklahomensis</i>
<i>B.p</i>	<i>Burkholderia pseudomallei</i>
<i>B.t</i>	<i>Burkholderia thailandensis</i>
BHI	Brain-heart infusion
bp	Base pairs
cAMP	Cyclic adenosine monophosphate
CA	Cell associated
CAA	Casamino acids
CAP	Catabolite activator protein
Cm	Chloramphenicol
CTD	C-terminal domain
Da	Daltons
DTT	Dithiothreitol
dBHI	Dialysed Brain-Heart Infusion
ddH ₂ O	HPLC grade sterile water
DMEM	Dulbecco's modified eagle medium
DMEM-FCS	Dulbecco's modified eagle medium containing 10% FCS
DMSO	Dimethyl sulfoxide
DNA	Deoxyribonucleic acid

DNase	Deoxyribonuclease
dNTP	Deoxynucleotide triphosphate
EDTA	Ethylenediaminetetraacetic acid
FCS	Foetal calf serum
g	Grams
GSH	Glutathione
HRP	Horseradish peroxidase
IM	Inner membrane
IMAC	Immobilised metal ion affinity chromatography
IPTG	Isopropyl β -D-1-thiogalactopyranoside
IST	Iso-sensitest
kb	Kilobase pairs
Km	Kanamycin
l	Litres
LB	Lysogeny broth
m	Metre
M	Molar concentration (moles/l)
Mbp	Megabase pairs
MCS	Multiple cloning site
MeCN	Acetonitrile
MNGC	Multi-nucleated giant cell
MOPS	4-morpholinepropanesulfonic acid
MW	Molecular weight
MWCO	Molecular weight cut-off

NTD	N-terminal domain
°C	Degrees centigrade
OD	Optical density
OM	Outer membrane
ORF	Open reading frame
PAGE	Polyacrylamide gel electrophoresis
PAAR	Proline alanine alanine arginine repeat protein
PBS	Phosphate buffered saline
PCS	Polymerase chain reaction
PDB	Protein data bank
PG	Peptidoglycan
PMSF	Phenylmethylsulfonyl fluoride
PVDF	Polyvinylidene fluoride
rRNA	Ribosomal ribonucleic acid
RNAP	RNA polymerase
S	Supernatant
SDS	Sodium dodecyl sulphate
T1SS	Type I secretion system
T2SS	Type II secretion system
T3SS	Type III secretion system
T4SS	Type IV secretion system
T5SS	Type V secretion system
T6SS	Type VI secretion system
T7SS	Type VII secretion system

T8SS	Type VIII secretion system
T9SS	Type IX secretion system
TAE	Tris-acetate-EDTA buffer
TBS	Tris-buffered saline
TBS-T	Tris-buffered saline with tween
TCA	Trichloroacetic acid
TE	Tris-EDTA buffer
Tp	Trimethoprim
Tris	Tri (hydroxymethyl) methylamine
UV	Ultra violet
V	Volts
v/v	Volume/volume ratio
w/v	Weight/volume ratio
x g	Gravitational acceleration
X-gal	5-Bromo-4-chloro-3-indolyl- β -D-galactopyranoside
Δ	Deletion

Chapter 1 Introduction

1.1 Melioidosis

Melioidosis is an important disease of humans and is caused by infection by the environmental saprophyte *Burkholderia pseudomallei* (*B.p*). The vast majority of cases occur in Southeast Asia in people who are exposed to bacteria living in the environment. The intrinsic resistance of the bacterium to a variety of antibiotics make it difficult to treat, resulting in a high mortality rate (Wiersinga et al. 2012). The mortality rate itself varies considerably depending on a number of factors including the geographic location, underlying health problems and the site of the body that is affected. Mortality rates of between 19 and 68% have been reported (Cheng & Currie 2005).

It is also possible for animals to suffer from melioidosis, in particular livestock such as sheep, goats and pigs (Choy et al. 2000) and while transmission from animal hosts to humans is rare, the infection of animals does represent a potential financial impact of the disease. The relatively high mortality rate and ability of the causative agent to survive in the environment have led to the classification of *B.p* as a category B bioterror threat (Rotz et al. 2002).

1.1.1 Route of infection

Infection with *B.p* can occur at a number of sites. Inhalation of aerosolized bacteria is believed to be the most common route. Infection via broken skin is also commonly observed. It is also thought to be possible to be infected by drinking contaminated water (Limmathurotsakul et al. 2014). Determination of the site of infection can be difficult as *B.p* is capable of dissemination to a variety of sites within the body in a process predicted to be facilitated by dendritic cells (Williams et al. 2014).

1.1.2 Symptoms

As a consequence of the range of sites the bacteria can spread to within the infected host, melioidosis can present itself as a wide range of symptoms. Pneumonia is commonly associated with *B.p* infection (Meumann et al. 2012) and in cases of melioidosis-associated chronic pneumonia, is often mistaken for tuberculosis due to the similar lung X-rays observed (Wiersinga et al. 2006). Skin lesions are also commonly observed in patients with melioidosis (Gibney et al. 2008). Parotitis (infection of the parotid glands) is particularly prevalent children with melioidosis (observed in 38% of cases in children) compared to adults (observed in 6.3% of all cases) (Dance et al. 1989).

One of the fascinating aspects of melioidosis its ability to persist in the body asymptotically. A case of melioidosis in an 82-year-old patient in Texas, USA was speculated to have occurred as a result of exposure to *B.p* during his imprisonment in Japanese labour camps in parts of Southeast Asia, including Thailand, during the Second World War. The disease had remained dormant for 62 years, until a cut on the man's thumb became ulcerated. It was not until initial treatments failed and in depth

background questioning was performed that the unlikely (at least in his part of the world) cause was identified. The man had not left the United States since returning from the war, suggesting that the disease had originated during his ordeal over half a century previously (Ngauy et al. 2005).

Although a remarkable case due to the large time period involved, it is not unique, with another case of the disease from the same conflict re-emerging after 26 years (Mays & Ricketts 1975). The Vietnam War has also been the source of infection and subsequent relapse (Mays & Ricketts 1975). This has raised concerns that as veterans of this conflict age, more will suffer from melioidosis, hence why some have labelled the disease the 'Vietnam time bomb'.

1.1.3 Diagnosis

The current gold standard for clinical diagnosis of individuals suspected of having melioidosis is culture on Ashdowns agar, a technique which has a low sensitivity and takes a number of days to yield results (Limmathurotsakul et al. 2010). Given that early diagnosis is crucial for the successful treatment of melioidosis, a great deal of work is underway to develop novel diagnostic techniques. In northeast Thailand, an area where melioidosis is endemic, an immunofluorescence assay (IFA) using a fluorescently labelled antibody specific to *B.p* is used to aid diagnosis. The drawbacks of this approach are its low sensitivity and the requirement of specialised operators (Tandhavanant et al. 2013).

Another technique that is sometimes used is the latex agglutination assay, which uses latex beads coated in a *B.p* specific antibody (Ekpo et al. 2007). Although the assay has good sensitivity and specificity, it still requires culture of *B.p* from the patient sample. Recently a lateral flow immunoassay (LFI) has been developed. The LFI uses a monoclonal antibody against *B.p* capsular polysaccharide and generates results with good sensitivity and specificity within 15 minutes. The tests can also be carried out by individuals with minimal training and the results are easy to interpret (Houghton et al. 2014). A study using blood samples found that the LFI offered poor (40%) sensitivity (Robertson et al. 2015). A real time PCR assay which targets a type three secretion system (T3SS) is available (Meumann et al. 2006), although it is not in regular use, possibly due to PCR inhibitors present in patient samples (Richardson et al. 2012).

1.1.4 Risk factors

Unsurprisingly melioidosis is most prevalent in those who are commonly in contact with *B. pseudomallei*. In North-east Thailand, rice farmers make up almost 85% of patients infected (Suputtamongkol et al. 1999). The constant exposure of these workers to soil and water containing *B. pseudomallei* makes them a very high risk group.

Like many pathogens that can also exist in soil environments, *B.p* is opportunistic, and most commonly infects patients who have other factors which make infection more likely. In a study performed in Northern Australia, 80% of patients who presented with the disease had one or more risk factor. The most common risk factors were excessive alcohol consumption, diabetes and chronic lung disease. These risk factors also increased the chances of succumbing to the condition, in one study only 1 patient in 51 who had no associated risk factor died, while 48 out of 201 people who had one or more risk factor succumbed (Currie et al. 2000).

Of all of the risk factors, Type 2 diabetes is particularly associated with the disease. In Thailand, up to 60% of patients with melioidosis suffer from the condition (Limmathurotsakul et al. 2010). The reason for this increased susceptibility may be the impaired phagocytic activity observed in Human polymorphonuclear neutrophils (PMN) isolated from diabetic subjects compared with those isolated from healthy subjects (Chanchamroen et al. 2009). PMNs from diabetic subjects are also impaired in migration in response to interleukin-8 and in their apoptotic response to infection (Chanchamroen et al. 2009). Additionally, Woods et al. (1993) found the growth of *B. pseudomallei* in rat and human serum was increased when insulin was depleted artificially, and in experiments where the levels of insulin were reduced in infant rats, the LD₅₀ for intraperitoneal infection was reduced. Furthermore, the growth of *B. pseudomallei* in M9 medium was inhibited when insulin was added. However research has since indicated that the inhibitory effect was likely to be a result of a preservative present in the insulin preparations used (Simpson 2000).

1.1.5 Treatment and prevention

The most effective treatment of melioidosis is with ceftazidime which has been shown to reduce mortality by 50% compared to other antibiotic treatment methods but mortality rates remain high, particularly during the first 48 hours following diagnosis (Wiersinga et al. 2012). Ceftazidime treatment is usually followed by a regime of co-trimoxazole to eradicate the bacteria (Limmathurotsakul & Peacock 2011)(Dance 2014).

A range of vaccines have been trialled in animal models. A number of vaccines have attempted to use live strains attenuated by the mutation of genes, including those encoding components of biosynthetic pathways (Breitbach et al. 2008) and virulence factors (Stevens 2004). Others have used whole, killed *B.p* cells, in inactivated vaccines (Barnes & Ketheesan 2007). Purified *B.p* proteins including type III and type IV secretion system proteins have also been tested as antigens (Druar et al. 2008)(Burtnick et al. 2011). Although some of these vaccines have elicited partial protection, to date none have offered complete protection from infection and there is currently no vaccine available against (Silva & Dow 2013).

At present the only method of preventing the disease would be the recommendation that those who are most at risk avoid contact with environmental reservoirs of *B.p*. However, this is impractical given how widespread the bacterium is in the environment where melioidosis is endemic (Suputtamongkol et al. 1999). Prophylactic antibiotic treatment following exposure to *B.p* is also not considered a viable preventative measure (Dance 2014).

1.1.6 Global distribution of *B. pseudomallei* and melioidosis

Since the first identification of melioidosis in Myanmar in 1912 (Whitmore & Krishnaswami 1912; Whitmore 1913) the disease (and bacteria) has been identified throughout parts of Southeast Asia and Northern Australia. Historically generally considered endemic to just these areas, the list of countries in which melioidosis is considered endemic has been increasing and *B.p* has since been identified in Bangladesh (Jilani et al. 2016), Malawi (Katangwe et al. 2013), Brazil, India and southern China (Currie et al. 2008). A map highlighting the current understanding of the global distribution of *B.p* and melioidosis is shown in Figure 1.1. One of the factors which makes determination of the global distribution of *B. pseudomallei* difficult is a lack of awareness of melioidosis and the absence of coherent strategies to identify *B.p* in the soil.

The perceived increase in global distribution and incidence of *B.p* can largely be attributed to researchers trying to identify endemic areas as well as advances in detection methodology. However, it is also likely that human impacts on the environment increase the suitability of areas for *B.p* colonisation. Soil altered by human activities such as farming and waste disposal is classified as 'anthrosol'. The presence of *B.p* is higher in anthrosol (Limmathurotsakul et al. 2016) and as the incidence of this type of soil increases with the growth of human populations, a greater area will be suitable for *B.p* habitation.

Like the distribution of *B.p*, increases observed in the distribution and incidence of melioidosis are likely to be a consequence of increasing awareness and improvements in diagnosis. As the prevalence of diabetes and kidney disease (both risk factors for melioidosis) increases across the world, so too does the number of humans acutely susceptible to *B.p* infection. The increase in suitable niches for *B.p* combined with an increase in the number of people at risk from infection means that the impact of melioidosis is likely to increase. There is currently a great deal of research directed towards identifying the true global distribution of *B. pseudomallei*, particularly in areas where there is little awareness of the bacteria and the ability of diagnostic techniques is limited. It is likely that the incidence and distribution of melioidosis is currently underestimated (Limmathurotsakul et al. 2016). Identifying the true global burden of melioidosis will be important for the implementation of effective strategies to combat the disease.

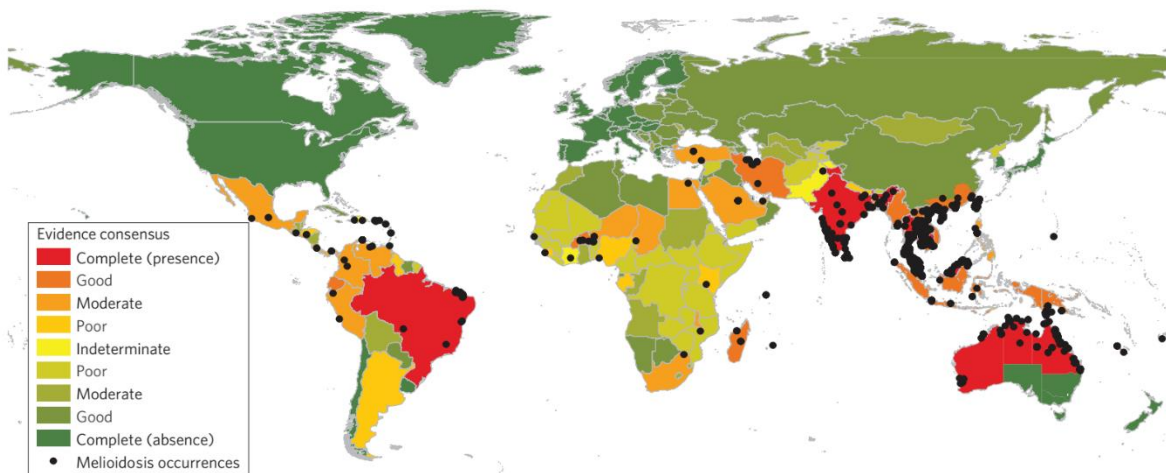


Figure 1.1 Global distribution of *Burkholderia pseudomallei*

Countries coloured according to confidence of evidence supporting the presence (red) of absence (green) of *B.p.* Black dots indicate a recorded case of melioidosis or *B.p.* in the environment. Reproduced, with permission, from Limmathurotsakul et al. 2016.

Although *B.p* is not generally found environmentally outside of the tropics, there have been a number of cases of melioidosis in individuals outside of these areas. These are normally cases where people have contracted melioidosis while visiting endemic regions before returning home and developing symptoms (Ezzedine et al. 2007; Bodilsen et al. 2015). This was a particular problem in the wake of the Vietnam war which saw thousands of US military personnel who had potentially come into contact with *B.p* return from endemic areas (Patterson 1967; Morrison et al. 1988). However, there have been a few cases where melioidosis has been contracted outside of an endemic area. The most serious incident was an outbreak of the disease in the Paris Zoo in 1975 which spread to other zoos in France; at least two people died as well as a number of animals (Sprague & Neubauer 2004). There have also been cases where individuals handling *B.p* in a laboratory have been infected (Green & Tuffnell 1968; Schlech et al. 1981)

1.2 The *Burkholderia pseudomallei* group

The *Burkholderia* genus is comprised of at least 60 species and includes soil, plant and clinical isolates which were previously classified as pseudomonads. However, based on a number of physical characteristics and 16S rRNA analysis they were classified as a new genus in 1992 (Yabuuchi et al. 1992). Subsequent analysis has indicated that there are two major clusters of *Burkholderia*; 'A' which contains plant-associated and saprophytic species and 'B' which contains plant pathogens and the *Burkholderia pseudomallei* group.

The pseudomallei group (Taxonomy ID: 111527) contains a number of species which are closely related to *B.p*. Members of the group include the equine pathogen *Burkholderia mallei* (*B.m*), the non-virulent environmental isolate, *B. thailandensis* (*B.t*), and *B. oklahomensis* (*B.o*) which was isolated in the USA.

1.2.1 *Burkholderia pseudomallei*

B.p was formally identified in 1913 and has been given a variety of names, the most enduring of which was *Pseudomonas pseudomallei* (until the introduction of the *Burkholderia* genus). The genome of *B.p* has been sequenced and is comprised of two chromosomes made up of 4.07 and 3.17 megabase pairs (Holden et al. 2004). The total size of 7.24 Mbp makes it one of the larger bacterial genomes to be sequenced so far and perhaps reflects the variety of niches *B.p* can occupy. *B.p* is predominantly a soil dwelling saprophyte that is also capable of living in standing water, in fact it has been demonstrated to survive in distilled water for 16 years (Pumpuang et al. 2011).

The ability to cause disease in humans and other animals seems likely to have arisen as a result of the fiercely hostile niche provided by the soil. The capacity to combat predatory amoebae that would feed on *B.p* could have provided the bacterium with an armoury of genes that are also capable of infection

of more complex eukaryotes. Given that the methods phagocytic cells employ to combat infection are similar to the methods used by amoebae to feed (German et al. 2013), this would also explain how *B.p* has become so adept at immune evasion.

1.2.2 *Burkholderia mallei*

B.m is a clonal derivative of *B.p*, thought to have become host adapted during a melioidosis infection, and unlike *B.p*, *B.m* is incapable of surviving in the environment (Godoy et al. 2003). This is reflected in its genome sequence, which lacks functional versions of a large number of genes which are present in *B.p*, including those involved in nitrate metabolism and amino acid synthesis (Nierman et al. 2004).

B.m is the causative agent of glanders, a disease which primarily affects horses, donkeys and mules, but can also be spread to humans who are in close contact with equines. Glanders has been recognised since ancient times and was once considered a major disease (Sharrer 1995). Today, glanders has largely been eradicated from Western countries where the use of horses as a beast of burden has declined, an exception being a laboratory acquired infection in an American military laboratory (Deitchman & Sokas 2001). However, in parts of Africa, Asia, Central and South America and the middle East it remains endemic in horses (Khan et al. 2013). The disease presentation in humans is similar to melioidosis, indeed one of the initial reports of melioidosis reported a “glanders-like disease” (Whitmore 1913). Depending on the site of infection it can cause ulceration, abscesses and pneumonia, dissemination can lead to septicaemia (Van Zandt et al. 2013).

Cultures of *B. mallei* were used in the First World War as a clandestine biological weapon by German agents who infected horses awaiting shipment in America (Wheelis 1998). More recently, a previous employee at a biological defence facility in the former Soviet Union has also indicated that *B.m* was weaponised and used in the 1979-1989 Soviet-Afghan war (Alibek & Handelman 1999). Like *B.p*, *B.m* it is considered a potential bioterror agent (Rotz et al. 2002).

1.2.3 *Burkholderia thailandensis*

Initially *B.t* was identified as a *B.p* strain isolated from the environment which showed a drastic increase in LD₅₀ in a hamster infection model in comparison to virulent strains (Brett et al. 1997) and an ability to utilize L-arabinose, a property not found in pathogenic *B.p* (Smith et al. 1997). Latterly, 16S rRNA sequence analysis determined that it was actually a separate species (Brett et al. 1998).

Although generally considered non-virulent in humans (Smith et al. 1997), there have been a number of cases where *B.t* has been isolated from a human (Lertpatanasuwan et al. 1999; Glass, Gee, et al. 2006). However, in one of these cases there were circumstances that had compromised the immune

system so that it was unable to fight infection; a car accident which led to the affected 2-year-old almost drowning. Although it is presumed that a large inoculum *B.t* was ingested during the trauma, the bacterium could not be isolated from the location of the accident (Glass, Gee, et al. 2006).

B.t represents a useful tool for the study of *B.p* as its reduced virulence has resulted in its classification as a hazard group 2 pathogen, in comparison to *B.p*, which belongs to hazard group 3. This makes working with *B.t* far more convenient. The reduction in virulence is most markedly observed in Syrian Hamster and mouse models of infection, where the LD₅₀ for infection with *B.p* is <10 and ~100, respectively (Brett et al. 1997; Smith et al. 1997). These numbers contrast with the LD₅₀ of >1 x 10⁶ in hamsters (Brett et al. 1997) and >1 x 10³ in mice (Smith et al. 1997) for *B.t*. In addition to this, experiments using cultured epithelial cells show that *B.t* is less capable of adherence and invasion (Kespichayawattana et al. 2004). This highlights that there are differences in the two species and therefore caution must be taken when making assumptions about one based on the other.

Despite the differences, *B.t* still exhibits similar properties and methods of infection, making it an attractive model organism for the study of melioidosis. In particular, the induction of the formation of multinucleated giant cells (MNGCs) is an obvious feature in *in vitro* infection assays (French et al. 2011). While the MNGCs induced by *B.p* infection express increased levels of osteoclast (a multinucleated bone cell) markers, those induced by *B.t* infection do not (Boddey et al. 2007). This is thought to be due to the absence of the *IfpA* gene in *B.t*. Genes absent from *B.t*, but present in *B.p* make good candidates for genes involved in the virulence of the agent that causes melioidosis (Reckseidler et al. 2001). An example of such a gene is BPSL1549 which encodes Burkholderia lethal factor 1, a helicase inhibitor present in *B.p* but absent from *B.t* (Cruz-Migoni et al. 2011).

1.2.4 *Burkholderia oklahomensis*

B.o was initially identified in the wound of a farmer from Oklahoma, USA, who had sustained a serious injury which had become contaminated with soil. The bacterium was cultured from the patient and demonstrated similar results to *B.p* in diagnostic tests (which was named *Pseudomonas pseudomallei* at the time of initial identification) that led to it being initially classed as a *B.p*-like organism. Environmental samples taken from where the injury occurred also contained the bacterium (McCormick et al. 1977). In another case, a man who had suffered injuries in a car accident in Georgia, USA, was infected with a *B.p*-like organism (Nussbaum et al. 1980). Subsequent analysis of the strains isolated from these two cases has resulted in their classification as *B.o*, distinct from *B.p* (Glass, Steigerwalt, et al. 2006). *B.o* is non-virulent in mice (DeShazer 2007) and unlike the other pseudomallei group members, it does not induce the formation of MNGCs or actin tails *in vitro* (Wand et al. 2011).

1.3 *Burkholderia pseudomallei* virulence factors

The large genome of *B.p* encodes a diverse repertoire of genes which facilitate the infection of a broad range of host species. An outline of the steps involved in cell infection, replication and intercellular spread is shown in Figure 1.2. Like some other bacterial diseases, such as tuberculosis, one of the major histopathological features associated with melioidosis is the observation of MNGCs in infected tissues (Wong et al. 1995). *B.p* (as well as *B.m* and *B.t*) is capable of inducing the formation of MNGCs in a range of cell types, both phagocytic and non-phagocytic (Harley et al. 1998). Indeed, MNGC formation caused by *B.p* is not restricted to mammalian hosts; it can also induce the fusion of cells in the Madagascar hissing cockroach (Fisher et al. 2012). It is thought that MNGC formation allows the bacterium to spread between host cells while evading the immune system. Upon invasion of host cells the expression of a range of *B.p* genes is induced, the global regulatory factor RpoS is believed to be involved (Utai-incharoen et al. 2006).

1.3.1 Intracellular motility

To propel itself within infected host cells, *B.p* is capable of polymerising actin, resulting in distinctive 'comet tails' when cells are stained with phalloidin (Kespichayawattana et al. 2000). The mechanism by which *B.p* induces actin polymerisation to achieve intracellular motility is different to other actin-motile intracellular pathogens (Breitbach et al. 2003). Instead of utilising host N-WASP or Ena/VASP proteins, *B.p* relies on the BimA protein which can induce polymerisation of actin alone. *B.p* *bimA* null mutants are unable to form actin tails *in vitro* (M. P. Stevens et al. 2005) and display a 10 fold reduction in median lethal dose compared to the wild type in a BALB/c mouse model of infection (Lazar Adler et al. 2015). *B.p* BimA is a trimeric autotransported (type V secretion system) protein in which each subunit contains three WASP homology 2 (WH2) motifs, but only two are required for activity (Sitthidet et al. 2011; Benanti et al. 2015).

Proteins similar to BimA are found in *B.m* and *B.t* and have been shown to restore actin based motility to *B.p* mutants lacking BimA (J. M. Stevens et al. 2005). *B.m* BimA induces actin polymerisation in a similar fashion to *B.p* BimA, directly polymerising host actin, although each subunit of the *B.m* BimA trimer only contains a single WH2 domain (Benanti et al. 2015).

Although able to restore motility to a *B.p* BimA mutant, the mechanisms by which *B.t* induces actin filament polymerisation is markedly different; *B.t* BimA recruits the host Arp2/3 complex which results in the formation of shorter, curved tails. Compared with the direct movement of *B.p* and *B.m* within cells, the movement of *B.t* is much more erratic. It has been suggested that the variations in actin polymerisation mechanisms in pseudomallei group species is a consequence of evolution to suit

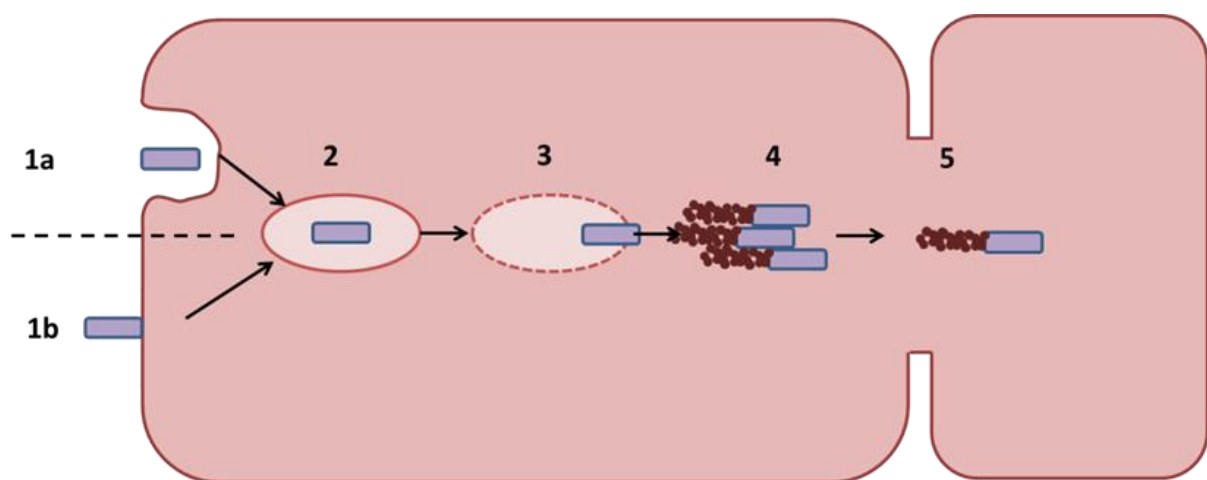


Figure 1.2 Proposed mechanism of invasion and intercellular spread utilised by *Burkholderia pseudomallei* during infection

Entry into host cells is either facilitated by phagocytic cells (**1a**) or induced by factors present in the bacteria that facilitate its entry into non-phagocytic cells (**1b**). Bacteria inside the cell are initially sequestered inside endosomes (**2**) before escape in a process mediated by T3SS-3 (**3**). Once inside the cytoplasm the bacteria replicate and can move by the polymerisation of actin by BimA resulting in the formation of actin tails (**4**). Bacteria spread between cells by inducing membrane fusion, a process dependent on T6SS-5 which leads to the formation of distinctive multi-nucleate giant cells (MNGC).

replication within different hosts (Benanti et al. 2015). Surprisingly, a knockout of *bimA* in *B. mallei* did not display reduced virulence in hamsters (Schell et al. 2007) despite its apparent importance.

1.3.2 Flagella

B.p is motile by means of a tuft of two to four polar flagella (DeShazer et al. 1997). There is currently a lack of clarity in the role that the flagella of *B.p* play during infection. Syrian hamsters and diabetic rats showed no attenuation in virulence when injected with transposon mutants that were motility deficient as a result of disruption of the gene *fliC* (DeShazer et al. 1997). However mice infected via the nasal route with an aflagellate mutant showed a significant reduction in death and number of bacteria recovered from the lungs (Chua et al. 2003). This was in contrast to results from the same study which showed no difference in replication of bacteria lacking flagella in human lung cells *in vitro*. Other work in the amoeba *Acanthamoeba astronyxis* found that flagella aided in invasion in a manner that was not just a result of increasing chances of contact, but the relevance of this finding to infection of higher eukaryotes is unclear (Inglis et al. 2003).

Interestingly, *B.t* encodes another flagellum, *fla2*, which is predicted to be a lateral system and can partially compensate for a lack of actin polymerisation in *bimA* mutants to drive intracellular movement (French et al. 2011). Some *B.p* strains possess this system, while it is absent in others. It is unclear if this system plays a major role in melioidosis (Tuanyok et al. 2007).

1.3.3 Capsule

The capsule of *B.p* plays a key role in infection. Mutations in genes encoding capsule components result in drastic attenuation in a mouse model (Atkins et al. 2002). The capsule is composed of -3)-2-O-acetyl-6-de-oxy- β -D-manno-heptopyranose-(1- (Perry et al. 1995) and has been shown to prevent the binding of a component of the innate immune response, complement factor C3b, to *B.p* (Reckseidler-Zenteno et al. 2005). This could potentially reduce the effect of the innate immune response. A capsule mutant was also impaired in its ability to enter and replicate within macrophages (Wikraiphat et al. 2009).

1.3.4 Lipopolysaccharide

Lipopolysaccharide (LPS) is found in the outer membrane of Gram-negative bacteria and is important in recognition by the innate immune response. It is composed of three major components: lipid A, which is part of the phospholipid bilayer; core-oligosaccharide and O-antigen. *B.p* LPS is a type II O-polysaccharide and is required for virulence in guinea pigs, mice and infant diabetic rats (DeShazer et al. 1998)(Wikraiphat et al. 2009). Unlike wild type *B.p*, LPS mutants are incapable of growth in 10-30%

normal human serum (DeShazer et al. 1998). In contrast to other pathogens, *B.p* LPS is not believed to stimulate inducible nitric oxide synthase, an important part of the host cell defence (Utai-incharoen et al. 2003).

1.3.5 Pili

Another important factor in *B.p* infection is the ability of the bacteria to adhere to host cells (Brown et al. 2002). One of the methods some pathogenic bacteria employ to facilitate this is the use of type IV pili (Craig et al. 2004). The *Burkholderia pseudomallei* genome possesses a number of genes for type IV pili. Deletion of the structural gene, *pilA*, decreased virulence in both a mouse and nematode model of infection and also led to an *in vitro* reduction in adherence to human cells (Essex-Lopresti et al. 2005).

1.3.6 Anti-microbial resistance mechanisms

B.p has an intrinsic resistance to a range of anti-microbials, mediated by a range of mechanisms. The drug efflux pump AmrAB-OprA confers resistance to aminoglycoside and macrolides (Moore et al. 1999). The BpeEF-OprC efflux pump has been found to responsible for resistance to trimethoprim (Podnecky et al. 2013), one of the drugs used in the eradication phase of treatment. Although resistance to ceftazidime (the drug of choice for the intensive phase of treatment) is low (Wuthiekanun et al. 2011), some strains show resistance by upregulation or modification of PenA β -lactamase or deletion of BPSS1219, which encodes penicillin binding protein 3 (Schweizer 2012).

1.3.7 Type III secretion system

Type III secretion systems (T3SS) are critical to the virulence of a variety of Gram-negative human pathogens. The *B. pseudomallei* genome encodes three T3SSs. One of these systems, T3SS-3 (also referred to as the *Burkholderia* secretion apparatus, or Bsa), is similar to one found to be important to the virulence characteristics of *Salmonella enterica* (Stevens et al. 2002).

The knockout of the T3SS-3 translocator gene *bipD* in *B.p* resulted in a reduced virulence in a mouse infection model (Stevens 2004). The effect of T3SS-3 on the non-phagocytic HeLa cell line has also been investigated; inactivation of the gene encoding the T3SS secreted effector protein *bopE* resulted in *B.p* cells that displayed a poor level of invasion but did not lead to a reduction in intracellular replication in a mouse macrophage-like cell line. However, deletion of *bsaZ*, a component of the secretion apparatus greatly reduced the number of intracellular bacteria recovered post infection (Stevens et al. 2002).

Delivery of a *B.t* mutant lacking a functioning T3SS-3 directly to the cytosol of HEK293 cells using a device known as a 'photothermal nanoblade' resulted in the induction of MNGC formation similar to

the wild type. However, when the same mutant was used in regular infection assays, no MNGC formation occurred (French et al. 2011). This suggests that this secretion system plays a role in the initial infection of bacteria, possibly in escape from endosomes. This finding also suggests that the bacteria travel between cells in a method other than by the formation of membrane protrusions into neighbouring cells resulting in the formation of vacuoles, as a mutant in T3SS-3 would be unable to escape from these and would therefore be unable to form MNGCs.

1.3.8 The type VI secretion system

The type VI secretion system (T6SS) is a macromolecular machine found in a variety of Gram-negative bacteria which is capable of delivering proteins into a target cell (a more in depth description of general T6SSs is given in section 1.5). Six T6SSs have been identified in *B.p* (Schell et al. 2007; Shalom et al. 2007). These are labelled T6SS-1 to T6SS-6 using the nomenclature of Shalom et al. (2007). As indicated in Table 1.1, some of these systems are also present in *B.m* and *B.t*. *B.m* lacks a functional T6SS-1 and T6SS-2, while in *B.t*, T6SS-3 is absent (Schell et al. 2007). To date, only the activities of T6SS-1 and T6SS-5 have been determined. Thus, while T6SS-1 is involved in inter-bacterial competition, T6SS-5 is a key virulence factor required for virulence in multicellular eukaryotes (Schwarz et al. 2010).

Using *in vivo* expression technology (IVET) it is possible to determine how the expression of genes within bacteria are affected during infection (Mahan et al. 1993). Using this technique it was determined that T6SS-5 a likely virulence factor as expression of a number of genes within this system are increased during infection of a macrophage cell line (Shalom et al. 2007). The deletion of the core T6SS-5 component, *tssD-5*, in *B.p* confirmed the suspicion that T6SS was involved in virulence. Mutants lacking this gene had at least a 1,000-fold higher LD₅₀ in a hamster model of infection when compared with wild type cells. Deletion of all of the *tssD* genes present in the other five T6SS gene clusters in *B.p* had no effect (Burtnick et al. 2011).

The deletion of other genes essential to the function of T6SS-5 in *B.m* resulted in mutants that were unable to induce MNGC formation following infection of the murine macrophage-like RAW 264.7 cell line (Burtnick et al. 2010). When T6SS-5 was knocked out in *B.t*, the resulting mutants showed a reduction in virulence in a mouse model (Schwarz et al. 2010). Interestingly, deletion of an apparently core component of the T6SS, *tssA-5* (referred to as *bimE* by the authors), in *B.m* did not have an effect on virulence in a hamster model of infection (Schell et al. 2007). This was despite mutants in other core components being non-virulent (Schell et al. 2007).

Table 1.1 T6SS gene clusters in *B.p*, *B.t* and *B.m*

T6SS gene cluster	Locus tag		
	<i>B. pseudomallei</i> K96243	<i>B. thailandensis</i> E264	<i>B. mallei</i> ATCC 23344
1	BPSSL3097-BPSSL3111	BTH_I294-BTH_I2968	BMA2826-BMA2833 ^a
2	BPSS0095-BPSS0116	BTH_II0119-BTH_II0140	Absent
3	BPSS0167-BPSS0185	Absent	BMAA1897-BMAA1915
4	BPSS0515-BPSS0532	BTH_II1885-BTH_II1902	BMAA0438-BMAA0455
5	BPSS1493-BPSS1511)	BTH_II0873-BTH_II0854	BMAA0729-BMAA0744
6	BPSS2093-BPSS2109	BTH_II0249-BTH_II0265	BMAA0396-BMAA0412

^aThe T6SS-1 gene cluster in *B.m* ATCC 23344 is thought to be non-functional as it lacks *tssB*, *tssC*, *tssD*, *tssJ*, *tssK* and *tssL*

In contrast to similar experiments using a T3SS-3 mutant, a *B.t* T6SS-5 mutant is incapable of inducing MNGC formation when delivered directly to the cytosol of a mammalian cell line (French et al. 2011). By bypassing the internalisation and phagosome escape steps, this demonstrated that MNGC formation is mediated specifically by T6SS-5. It also demonstrated that a single intracellular *B.t* cell was capable of inducing the host cell to fuse with its neighbour, supporting the argument for a role of MNGC formation in facilitating intercellular spread.

Currently the precise mechanism by which T6SS-5 facilitates MNGC formation by *B.p*, *B.m* and *B.t* is unclear. However, recent investigations have suggested a critical role for the C-terminal domain of TssI-5 (Schwarz et al. 2014; Toesca et al. 2014). TssI proteins are components of the T6SS that are secreted along with TssD, their presence in culture supernatants is considered a 'hallmark' of a functional T6SS. Some TssI proteins (referred to as 'evolved' TssI) contain C-terminal extensions that serve as effectors. The deletion of the C-terminal domain of TssI-5 (retaining the 'core' TssI region conserved amongst all TssI proteins) in *B.p* and *B.t* abolished their ability to induce the formation of MNGCs (Schwarz et al. 2014; Toesca et al. 2014) and rendered *B.t* avirulent in a mouse model of infection (Schwarz et al. 2014). However, unlike mutations in genes encoding structural subunits of the T6SS-5, which affected MNGC formation and secretion of TssD-5 (a marker of T6SS activity), the removal of the CTD of TssI-5 did not have a detrimental effect on the secretion of TssD-5 (Toesca et al. 2014). Although the CTD of TssI-5 is necessary for the induction of cell fusion, it is unclear if any other factors are required. Given that MNGC formation can be induced in a wide range of cells, it is likely that cell fusion is mediated either by bacterial proteins alone, or the host factor that is utilised by the T6SS-5 is well conserved. Although *B.o* does not induce the formation of MNGCs *in vitro*, *B.o* *tssI-5* was able to restore MNGC induction to a *B.p* *tssI-5* mutant when it was expressed *in trans* (Toesca et al. 2014). This suggests that either TssI is not secreted in *B.o* or one or more of the virulence factors required for earlier infection steps is absent (Wand et al. 2011).

An unusual property of the T6SS-5 machinery is its position within the cell. When the *B.t* T6SS-5 subunit, TssH-5, was fluorescently labelled with GFP it clearly demonstrated that T6SS-5 localises to the poles of the bacterium (Schwarz et al. 2014). This is in contrast to *B.t* T6SS-1, which is randomly distributed around the cell like the *Vibrio cholerae* and enteroaggregative *Escherichia coli* T6SSs (Basler et al. 2012; Durand et al. 2015). The significance of the specific localisation of T6SS-5 is unclear.

The regulation of the T6SS-5 gene cluster appears to be fairly complex and co-ordinated with T3SS-3. They are both dependent on host signals for their activation, with T3SS-3 being most upregulated during the early stages of infection and without internalisation. This suggests that the upregulation of T3SS-3 is based on signals received from contact with host cells rather than intracellular triggers. In

contrast, T6SS-5 is not upregulated when internalisation of *B.p* by a macrophage cell line is inhibited by cytochalasin D (Chen et al. 2011) indicating that an intracellular component or property was the signal for induction of T6SS-5 expression.

A two-component regulatory system composed of the histidine kinase sensor VirA and the DNA binding response regulator VirG is a critical component of the regulation of T6SS-5 during *B.p* infection. Under standard laboratory growth conditions (i.e. LB media) T6SS-5 is not expressed, as determined by the absence of secreted TssD-5, however when the *virA* and *virG* genes are introduced *in trans* and overexpressed, T6SS-5 expression is increased (Burtnick et al. 2011). The same result was observed in *B.m* (Schell et al. 2007). The intracellular signals for induction of expression of T6SS-5 are host thiols, in particular glutathione. When glutathione is depleted from host cells infected with *B.t*, the level of *tssD-5* expression and the ability of the bacterium to form MNGCs are reduced. Glutathione reduces the thiol group of a periplasmic cysteine residue of VirA (VirA is embedded in the bacterial inner membrane by 9-10 predicted transmembrane helices) which results in its monomerization and the induction of T6SS-5, presumably via VirG (Wong et al. 2015).

As well as results in animal and *in vitro* models, evidence for the role of T6SS-5 in human infections has been found in serum from patients infected with *B.p*. Western blotting of serum from 10 patients with melioidosis gave a positive result for TssD-5, while TssD subunits from the other T6SSs present in the organism were absent. Moreover, TssD-5 was absent from uninfected controls (Burtnick et al. 2011). This is in accordance with other experiments suggesting T6SS-5 is expressed during infection.

In addition to those conserved across all T6SSs, the T6SS-5 gene cluster also contains four additional genes, the type six associated genes (*tagA*, *tagB*, *tagC* and *tagD*), which are located immediately downstream of *tssI-5* (which encodes the secreted tail-spike protein) (Figure 1.3). As the effectors of other T6SSs are often encoded downstream of *tssI* genes, the *tag* genes could encode T6SS-5 secreted effector proteins. The locus tag of each ORF of the T6SS-5 gene clusters in *B.p*, *B.t* and *B.m* is shown in Table 1.1 and in Figure 1.3.

1.4 Secretion systems in Gram-negative bacteria

For many bacteria, the ability to secrete proteins into their environment is crucial for their survival. This is true of both Gram-negative and Gram-positive species, although for the former there is an added complexity, the presence of an extra membrane. To overcome this challenge, Gram-negative bacteria have evolved a diverse repertoire of secretion systems, to date nine have been identified (Type I-Type IX Secretion Systems: T1SS-T9SS). To confuse matters, a Gram-negative protein secretion system has also been designated as a 'type VII secretion system' (Abdallah et al. 2007). As this

mechanism is only present in Gram-positive species its designation as a type VII secretion system remains controversial.

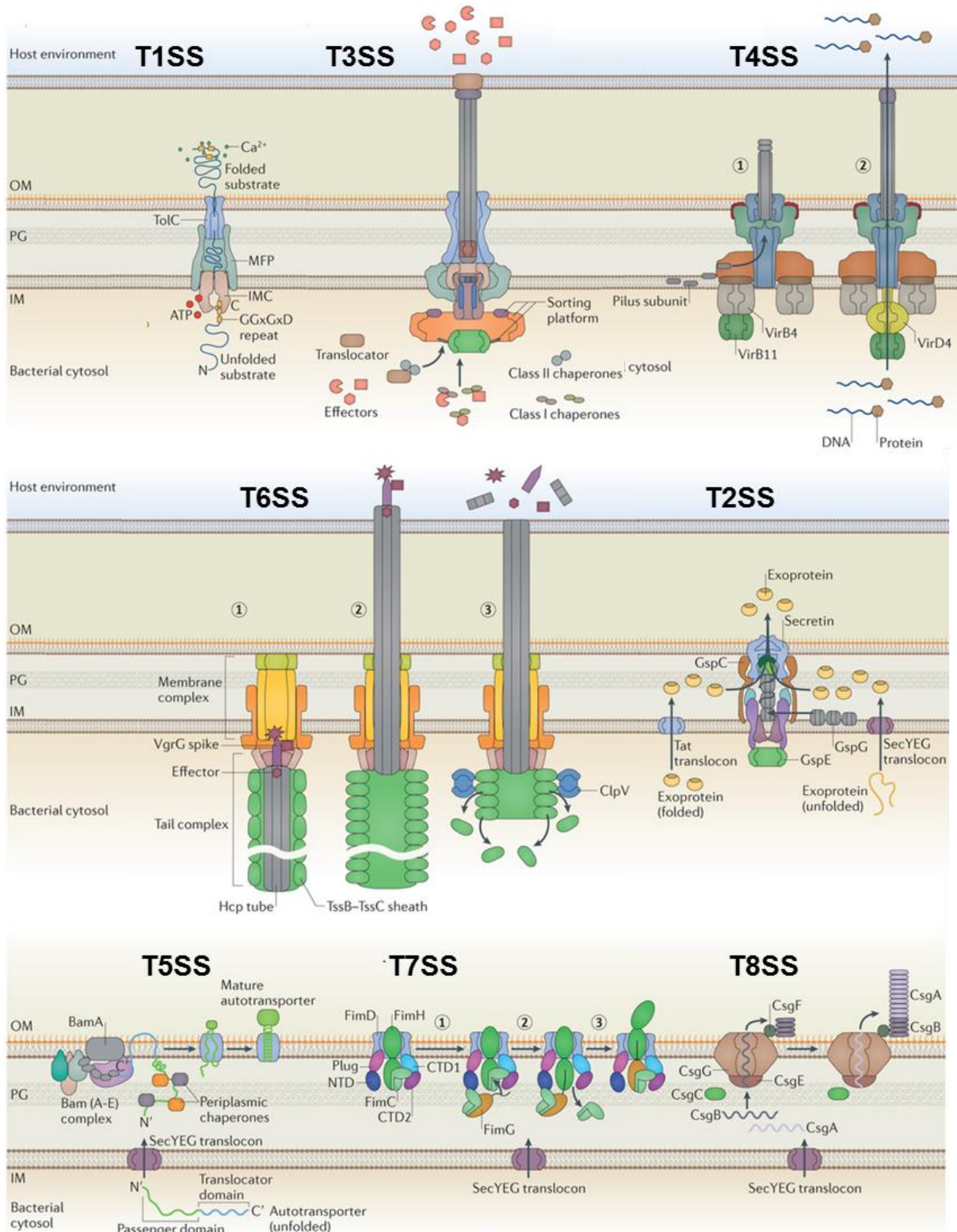
Apart from the chaperone-usher system (T7SS), the Gram-negative secretion systems are classified I to IX according to the order in which they were formally identified. They are broadly categorised into two groups, the Sec-dependent systems, which secrete their substrates in a two-step process and the Sec-independent systems which translocate proteins across both membranes in a single step. A simple outline of T1SS to T8SS is given in Figure 1.4.

1.4.1 Sec-independent protein secretion systems

As their classification suggests, the Sec-independent systems do not rely on Sec to transport proteins across the inner membrane. Instead, they translocate substrates across both membranes in a single step. This means that there is no periplasmic intermediate.

1.4.1.1 Type I Secretion System (T1SS)

The T1SS is comprised of two inner membrane proteins, the ABC (ATP binding cassette) protein, the membrane fusion protein (MFP, which also spans the periplasm) and a porin-like outer membrane (OM) protein (Costa et al. 2015). The T1SS ABC protein is a member of the ABC transporter protein family. The ABC transporter family facilitates the transport of a wide range of substrates including ions, amino acids and antibiotics in a mechanism energised by the hydrolysis of ATP (Higgins 1992). The family is widespread, examples of ABC transporters can also be found in eukaryotes and archaea. Proteins secreted by the T1SS are predicted to bind to the ABC before the energy provided from the hydrolysis of ATP transfers the unfolded protein into the periplasmic cavity of the MFP. The OM component then opens to form a pore which allows the release of the substrate into the extracellular space where it folds (Costa et al. 2015). The T1SS is capable of secreting a wide range of protein substrates (which contain a C-terminal signal sequence) of various molecular weights from 20 to 900 kDa (Thomas et al. 2014). Some substrates of the T1SS are associated with the acquisition of nutrients and include the *Serratia marcescens* iron scavenging protein HasA (Kanonenberg et al. 2013), while others, such as *E. coli* HlyA are virulence factors (Thomas et al. 2014).



Nature Reviews | Microbiology

Figure 1.4 Gram-negative secretion systems

Outline of the mechanisms used to secrete proteins in Gram-negative species, the T9SS is not shown. OM, outer membrane; PG, peptidoglycan; IM, inner membrane. Image modified and reproduced, with permission, from Costa et al. (2015)

1.4.1.2 Type III Secretion System (T3SS)

The T3SS is a nanomachine composed of over 20 protein subunits which is capable of translocating proteins across the bacterial envelope and delivering effectors into target eukaryotic cells (Marlovits & Stebbins 2010). While this section deals with the eukaryotic targeting 'injectisome' T3SSs, distinct T3SSs are also key components of bacterial flagella where they export extracellular components, the two types of T3SS share an evolutionary ancestor (Abby & Rocha 2012). Effectors delivered by the T3SS act on a variety of host cell proteins. T3SSs in *Salmonella* alone deliver effectors that act on the host cytoskeleton, the ubiquitin pathway and host signalling (Burkinshaw & Strynadka 2014).

The T3SS forms a syringe-like structure which is made up of two major sub-structures: a base which spans both bacterial membranes and a needle-like structure which extends from the outer membrane into the extracellular space (Schraidt & Marlovits 2011). The base contains two inner rings, a neck which spans the periplasm, and two outer rings (Galán & Wolf-Watz 2006). The needle is made up of multiple copies (over 120) of a single protein which form a 50 nm long filament with an 8 nm external diameter and a 2 nm inner diameter (Burkinshaw & Strynadka 2014). T3SS substrates are translocated through this needle in an unfolded state (Radics et al. 2013) The tip complex is found at the end of the needle which senses contact with host cells and regulates effector secretion. The tip complex interacts with the translocon which is believed to form a pore in the target membrane, facilitating translocation of effector proteins (Sato & Frank 2011).

1.4.1.3 Type IV Secretion System (T4SS)

As well as Gram negative bacteria, the T4SS can also be found in Gram positive species as well as some archaea (Alvarez-Martinez & Christie 2009). Uniquely, the T4SSs is capable of secreting DNA, proteins or a combination of both DNA and protein. T4SSs are diverse, with few components conserved throughout all systems, as such there are a number of classification systems in place. A recent "evolutionary based" system places T4SSs into eight groups based on an ATPase (VirB4) found in all known systems (Guglielmini et al. 2013).

A number of human pathogens utilise a T4SS. A T4SS known as Dot/Icm in *Legionella pneumophila* is required for trafficking of the bacteria to an ER-derived vacuole in which it replicates (Berger & Isberg 1993). One of the causative agents of cat scratch disease, *Bartonella henselae*, uses a T4SS to modify host cytoskeletal proteins to facilitate its internalisation (Rhombert et al. 2009).

1.4.1.4 Type VI Secretion System (T6SS)

The T6SS is outlined in detail in section 1.5.

1.4.2 Sec-dependent protein secretion systems

As their name suggests, the Sec-dependent systems are reliant on the Sec-translocase pathway which transports unfolded proteins across the inner membrane in an ATP dependent manner. Proteins translocated by Sec are either maintained in an unfolded state by chaperones before they are directed to the system, or translated directly from the ribosome into the Sec apparatus, although the latter technique is primarily utilised by membrane proteins (Natale et al. 2008). Non-membrane proteins which are transported across the inner membrane by the Sec system are directed to the motor protein SecA, which hydrolyses ATP to translocate the unfolded protein through the SecYEG channel. The SecDF complex is thought to liberate the protein and release it into the periplasm (Lycklama a Nijeholt & Driessen 2012). An N-terminal signal sequence marks proteins for export by the Sec-translocase (Natale et al. 2008).

1.4.2.1 Type II Secretion System (T2SS)

Although considered a Sec-dependent system, T2SS substrates can also be delivered to the periplasm by the twin-arginine translocation (Tat) protein export pathway which translocates folded proteins across the inner membrane (Nivaskumar & Francetic 2014). The T2SS is also unique amongst Sec-dependent secretion systems in that the delivery apparatus spans both membranes (Nivaskumar & Francetic 2014). The folded protein is loaded onto a type VI pilus-like structure within the periplasmic chamber of the T2SS which polymerises and pushes the protein out of the cell (Korotkov et al. 2012). T2SSs are capable of secreting a wide range of proteins, at least 18 proteins are secreted by the T2SS in *V. cholerae* alone (Sikora et al. 2011), including cholera toxin (Sánchez & Holmgren 2008). While it is a virulence factor in many species, including *Pseudomonas aeruginosa*, and the fish pathogen *Aeromonas hydrophila*, its primary role is in nutrient acquisition (Nivaskumar & Francetic 2014).

1.4.2.2 Type V Secretion System (T5SS)

The T5SS can secrete virulence factors as well as mediate intercellular interactions and biofilm formation (Leyton et al. 2012). There are five classes of T5SS, labelled T5SSa to T5SSe according to their transmembrane domain (Leo et al. 2012). Although the transport and effector domains of most T5SS proteins are part of the same polypeptide (prior to processing), in the T5SSb class the two domains are separate, they are still considered autotransporters according to the definition of Leo et al. (2012) as they do not rely on cytosolic energy sources. Members of the T5SSa class facilitate their own movement across the outer membrane by the formation of a pore (Henderson & Nataro 2001). Once the unfolded T5SSa protein has been released from the Sec system its C-terminal domain is recognised by the outer membrane protein BamA which inserts the C-terminal β -barrel domain into the outer membrane which forms a pore. The secreted portion of the protein (the N-terminal domain)

then passes through this pore before it is cleaved, leaving behind an α -helix which plugs the pore (Leo et al. 2012).

As mentioned, the T5SSb class utilises a separate protein to cross the outer membrane. The T5SSc proteins form trimers but are exported using a similar mechanism to the T5SSa class. However, once the N-terminal domain of the subunits passes through the membrane pore, the protein is not cleaved and remains attached to the outer membrane (Leo et al. 2012). T5SSd and T5SSe are not as well characterised. Proteins of the T5SSd class are predicted to be a fusion of the two domains of T5SSb class, while the T5SSe class appears to be inverted, i.e. the C-terminal domain passes through the N-terminal domain which is embedded in the membrane (Leo et al. 2012).

1.4.2.3 Type VII Secretion System (T7SS, also known as the chaperone-usher pathway)

The T7SS is used to assemble pili which are multisubunit appendages that extend from the cell and facilitate attachment to host cells and biofilm formation (Wright et al. 2007). To date, the most well studied T7SSs are those which assemble the type I and P pili. Pili can be up to 2 μm long and are composed of a rod which contains multiple FimA subunits in the type I pili or PapA subunits in the P pili. Once the subunits of the pili have crossed the inner membrane, they are folded and stabilised by a chaperone (FimC in type I and PapD in P pili). The subunits pass through an outer membrane pore (known as an 'usher') made up of either FimD or PapC and assemble on the outside of the cell (Costa et al. 2015). The tip of the type I pilus is made up of one subunit each of FimF, FimG and FimH (found at the end of the tip), while the P pilus tip contains multiple copies of PapE and one copy of PapF, PapG (found at the end of the tip) and PapK (Costa et al. 2015).

1.4.2.4 Type VIII Secretion System (T8SS, also known as the curli biogenesis system)

The T8SS is commonly known as the 'curli biogenesis system'. It secretes the amyloid-like curli protein CsgA, which is found in large quantities in *E. coli* bio-films. A periplasmic protein, CsgE, directs CsgA to an outer membrane pore formed by 8 CsgG subunits. CsgF interacts with CsgG at the outer membrane where it stabilises and localises another amyloid-like subunit, CsgB. CsgA travels through the CsgG pore and interacts with CsgB (Evans & Chapman 2014). The role of curli in pathogenesis is not entirely clear, although they do bind to many host proteins including the extracellular matrix proteins fibronectin and laminin as well as the antigen presenting major histocompatibility (MHC) class I proteins (Barnhart & Chapman 2006).

1.4.2.5 Type IX Secretion System (T9SS)

The T9SS was recently identified in *Porphyromonas gingivalis*, where it is required for secretion of a protease (Saiki & Konishi 2007). *P. gingivalis* is a member of the Bacteroidetes, a diverse phylum of bacteria, many members are motile by gliding motility. As well as secreting effectors, the T9SS also

exports outer membrane proteins necessary for gliding motility in Bacteroidetes (Sato et al. 2010). Bioinformatic analysis has demonstrated that T9SSs are common amongst the *Bacteroidetes*, but not found in other phyla (McBride & Zhu 2013).

1.5 Type VI Secretion System

The T6SS is a macromolecular machine which is capable of delivering proteins into target cells. T6SS genes have been found in roughly a quarter of all Gram-negative genomes which have been sequenced (Bingle et al. 2008). The bacterial T6SS was first identified in 2006 in the human pathogen *Vibrio cholerae* (Pukatzki et al. 2006). A transposon mutant screen was performed to identify genes critical for the bacterium to avoid predation by the phagocytic amoeba *Dictyostelium discoideum*. A number of the mutants were identified as having a reduced protein secretion profile and it was determined that the disrupted genes encoded components of a novel secretion system which was designated the “type VI secretion system” or T6SS. The system itself is thought to operate by the formation of a contractile tubule (sheath) surrounding an inner tube. On contraction of the sheath the inner tube, capped by ‘spike’ proteins, is driven out of the bacterium and injected into the target cell (Bönemann et al. 2010), the components of the T6SS and the mechanism of secretion is displayed in Figure 1.5. This mechanism is not unique; in fact, it is remarkably similar to the way the contractile bacteriophage T4 delivers DNA and proteins into target cells (Figure 1.6). Some components of the T6SS share sequence and structural homology with a variety of bacteriophage components (Leiman et al. 2009). As the T6SS is a fairly recent discovery, inroads into the roles of the components of the system are constantly being made.

Currently there are a variety of different naming conventions in place for components of the T6SS; these vary depending on organism being investigated and the groups that are studying them. For convenience, the nomenclature proposed by Shalom et al. (2007) is used here, demonstrated in Table 1.2, this labels the 13 core components as TssA-TssM.

1.5.1 Membrane complex

The minimal T6SS membrane complex anchors the injection apparatus to the bacterial cell envelope and is made up of three components, TssJ, TssL and TssM. TssJ is an outer membrane lipoprotein. It resides in the periplasm and is tethered to the outer membrane lipid bilayer by an acylated cysteine that is located at the N-terminus of the protein following removal of the signal peptide (Aschtgen et al. 2008). TssJ interacts with the periplasmic domain of TssM with a stoichiometry of 1:1 (Felisberto-Rodrigues et al. 2011). TssM is embedded in the inner membrane by three transmembrane helices in its N-terminal domain which also facilitates self-interaction (Zheng & Leung 2007; Ma et al. 2009).

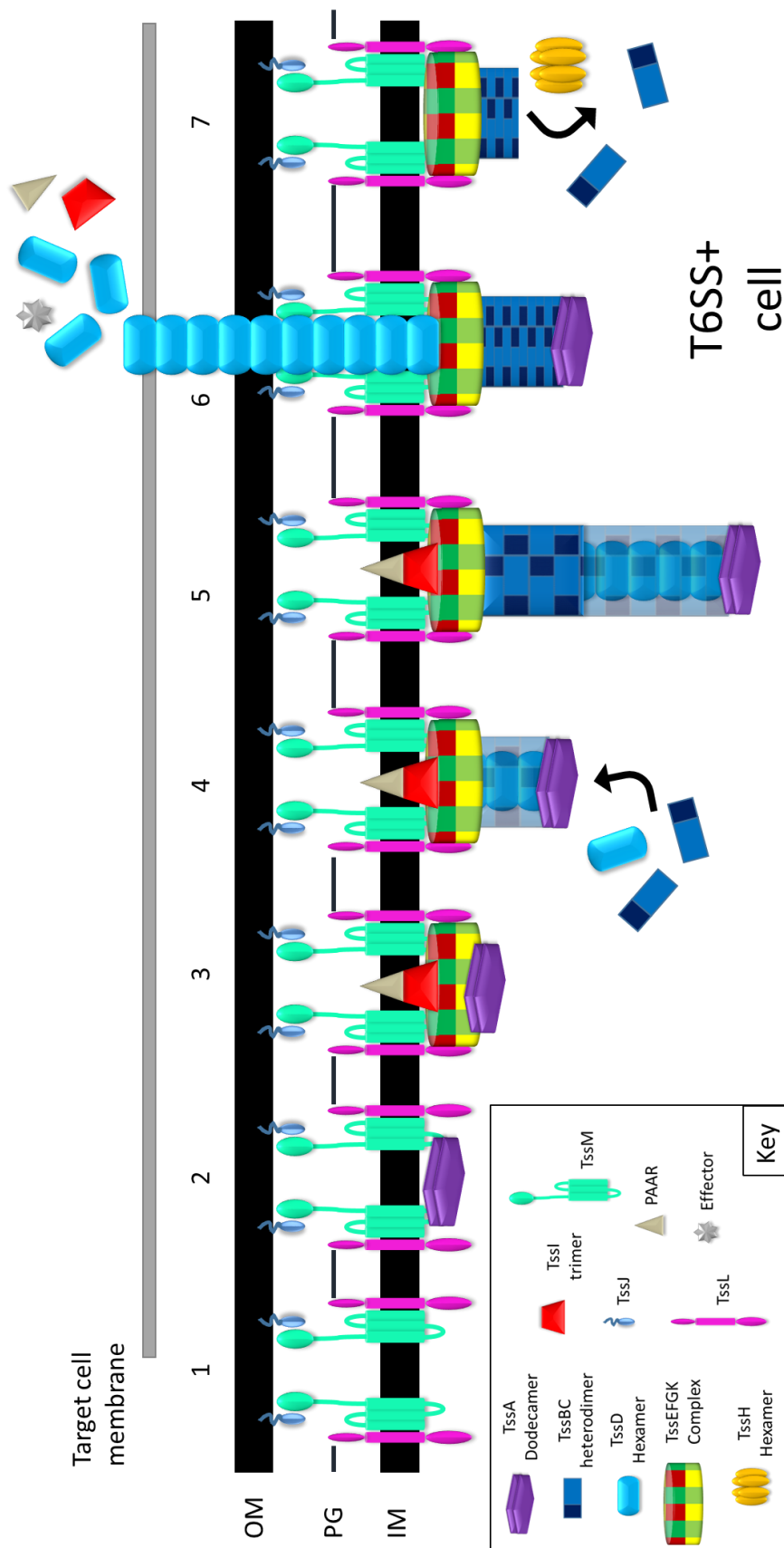


Figure 1.5 Mechanism of action of the T6SS

Schematic representation of effector translocation by the T6SS showing progression from left to right. 1, the membrane complex of TssI, TssL and TssM assembles; 2, TssA is recruited to the membrane complex; 3, the base plate complex of TssE, TssF, TssG, TssH (tipped with the PAAR protein) and TssK interacts with the membrane complex; 4, the base plate acts as a nucleation site for the TssD inner tube and TssB/TssC sheath which extends away from the membrane; 5, the tube is fully extended and 'primed'; 6, a signal triggers the sheath to contract, pushing the inner tube and the PAAR-tipped TssI into the target cell, delivering any associated effectors; 7, TssH hydrolyses ATP to disassemble the sheath.

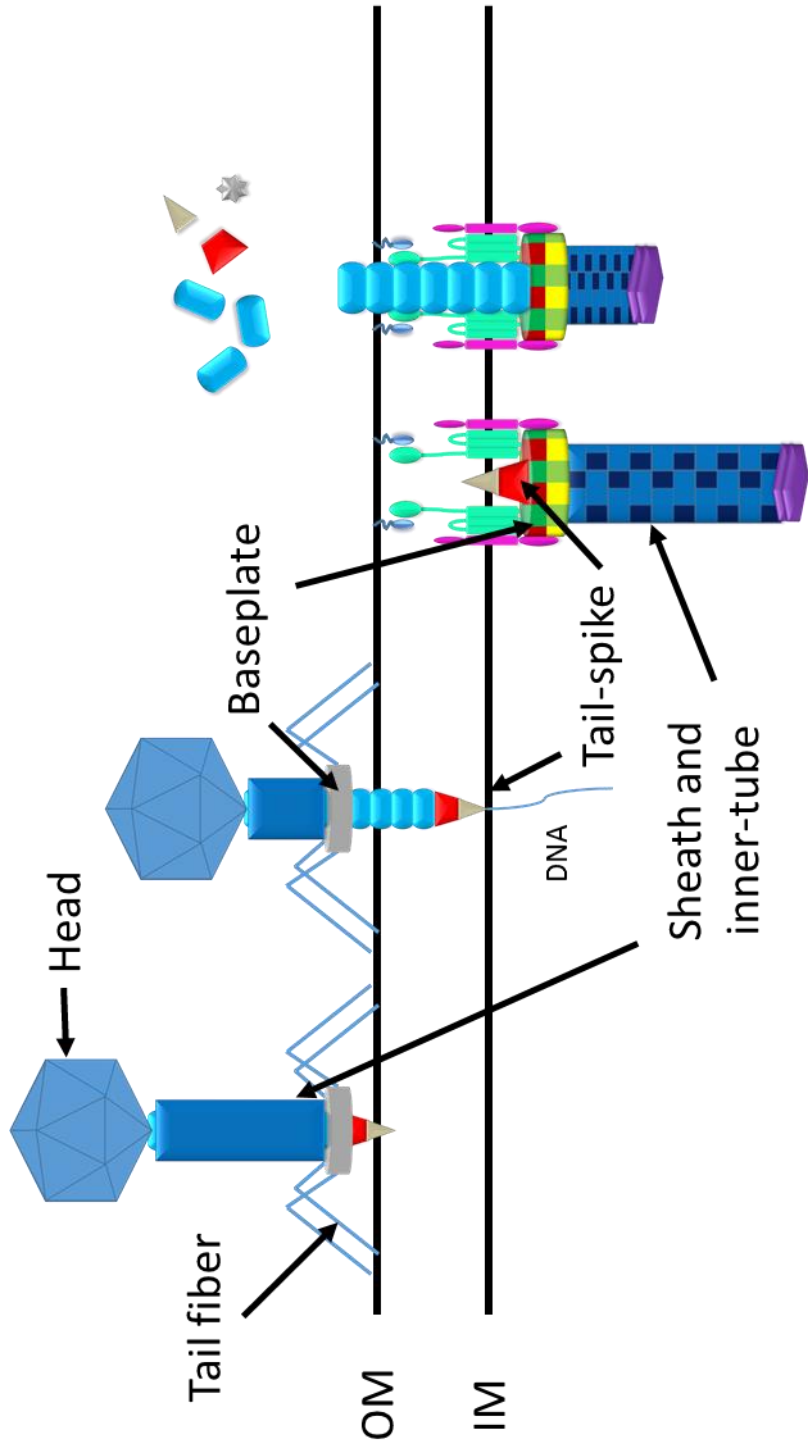


Figure 1.6 Comparison of the delivery mechanisms of contractile bacteriophages and the T6SS

Diagram showing a comparison of the overall structure and mechanism of action of contractile bacteriophages (left) and the T6SS (right). Note the assembly of an inner tube surrounded by a contractile sheath which delivers a tail-spike into the target cell.

Table 1.2 Standardised names of genes encoding core components of the T6SS

Standardised gene name	Common alternative gene name	COG	<i>Burkholderia mallei</i>	<i>Vibrio cholerae</i>	<i>Pseudomonas aeruginosa</i>		<i>Edwardsiella tarda</i>
					HSI-I	HSI-II	
<i>tssA</i>		COG3515	<i>bimE</i>	<i>vasJ</i>	<i>tssA1</i>	<i>hsiA2</i>	<i>evpK</i>
<i>tssB</i>		COG3516	<i>tssA</i>	<i>vipA</i>	<i>tssB1</i>	<i>hsiB2</i>	<i>evpA</i>
<i>tssC</i>		COG3517	<i>tssB</i>	<i>vipB</i>	<i>tssC1</i>	<i>hsiC2</i>	<i>evpB</i>
<i>tssD</i>	<i>hcp</i>	COG3157	<i>hcp1</i>	<i>hcp</i>	<i>hcp1</i>	<i>hcpC</i>	<i>evpC</i>
<i>tssE</i>		COG3518	<i>tssC</i>	VCA0109	<i>tssE1</i>	<i>hsiF2</i>	<i>evpE</i>
<i>tssF</i>		COG3519	<i>tssD</i>	<i>vasA</i>	<i>tssF1</i>	<i>hsiG2</i>	<i>evpF</i>
<i>tssG</i>		COG3520	<i>tssE</i>	<i>vasB</i>	<i>tssG1</i>	<i>hsiH2</i>	<i>evpG</i>
<i>tssH</i>	<i>clpV</i>	COG0542	<i>clpV1</i>	<i>vasG</i>	<i>clpV1</i>	<i>clpV2</i>	<i>evpH</i>
<i>tssI</i>	<i>vgrG</i>	COG3501	<i>vgrG1</i>	<i>vgrG</i>	<i>vgrg1</i>	<i>vgrG2</i>	<i>evpI</i>
<i>tssJ</i>		COG3521	<i>tssJ</i>	<i>vasD</i>	<i>tssJ1</i>	<i>lip2</i>	<i>evpL</i>
<i>tssK</i>		COG3522	<i>tssK</i>	<i>vasE</i>	<i>tssK1</i>	<i>hsiJ2</i>	<i>evpM</i>
<i>tssL</i>		COG3455	<i>tssL</i>	<i>vasF</i>	<i>tssL1</i>	<i>dotU2</i>	<i>evpN</i>
<i>tssM</i>		COG3523	<i>icmF1</i>	<i>vasK</i>	<i>tssM1</i>	<i>icmF2</i>	<i>evpO</i>

A recent study by Durand et al. (2015) demonstrated that the C-terminal region of TssM forms an arch which crosses the periplasm. Each membrane complex has ten TssM subunits which form a dynamic periplasm-spanning double ring structure. In an active T6SS, TssM is at least partially exposed to the extracellular environment, suggesting it may form an outer membrane pore to facilitate the passage of TssI and TssD through the outer membrane of the T6SS-containing cell (Durand et al. 2015). Most TssM proteins contain a Walker A motif in the cytoplasmic N-terminal domain. Such motifs are commonly found in ATPases. The role of the Walker A motif in TssM is unclear; In *Edwardsiella tarda* the Walker A motif of TssM is dispensable for TssD secretion (Zheng & Leung 2007), however in *Agrobacterium fabrum*, modification of this motif abolished TssD secretion (Ma et al. 2009). As well as mediating self-interaction, the N-terminal region of TssM also facilitates interaction with the other membrane complex protein, TssL (Ma et al. 2009). TssL contains a cytoplasmic N-terminal domain that is anchored to the lipid bilayer by a single transmembrane helix (Durand et al. 2012). Many TssL proteins carry a periplasmic C-terminal peptidoglycan binding domain which interacts with the cell wall to stabilise the T6SS membrane complex (Ma et al. 2009, Aschtgen et al. 2010). When this domain is absent, an additional protein compensates, by interacting with both peptidoglycan and another T6SS component. For example, TagL interacts with TssL to anchor the T6SS membrane complex to the cell wall (Aschtgen et al. 2010).

The membrane complex is composed of ten subunits each of TssJ, TssL and TssM. Unlike most other T6SS components and complexes which demonstrate 3 or 6-fold symmetry, the T6SS membrane complex is unusual in that it demonstrates 5-fold symmetry (Figure 1.7). Thus, It is unclear how interactions with the tail tube and sheath components are facilitated (Durand et al. 2015).

1.5.2 Baseplate

In bacteriophages which share the contractile delivery mechanism of T6SS, one of the essential components is the baseplate. The bacteriophage T4 baseplate is a complex structure made up of 6 wedges each composed of seven proteins which surround a central hub. Each wedge contains gp11, gp10, gp7, gp8, gp6, gp52 and gp25 (Leiman & Shneider 2012). The central hub, which penetrates the outer membrane of the target bacterium, is made up of a complex of three gp27 and three gp5 subunits (Kanamaru et al. 2002). In the T6SS, the baseplate is held close to the inner face of the cytoplasmic membrane by the TssJLM membrane complex. The baseplate has been proposed to be made up of TssE, TssF, TssG TssI and TssK (Brunet et al. 2015). TssE exhibits a remarkable 40% amino acid sequence similarity to the bacteriophage T4 base plate protein, gp25 (Leiman et al. 2009); although its precise role is unknown, it is required for the correct assembly of the TssD inner tube (Brunet et al. 2015) and it interacts with the sheath component, TssC (Zoued et al. 2016).

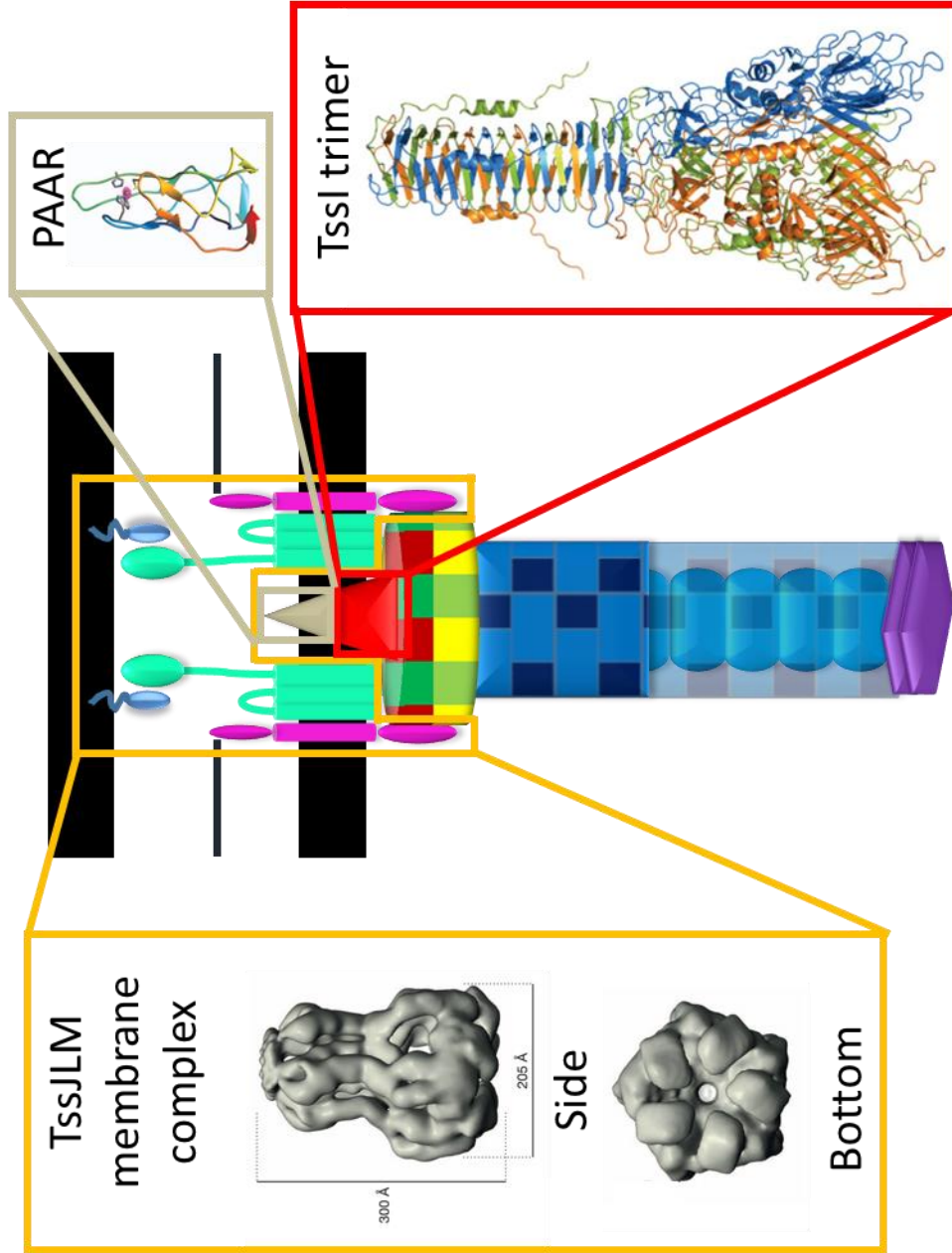


Figure 1.7 Structures of the T6SS membrane complex and baseplate components

Solved structures of the T6SS membrane complex and components of the baseplate. Orange box, 11.6 Å resolution three-dimensional structure of the TssJLM complex of enteroaggregative *E. coli* solved by cryo-electron microscopy, image taken, with permission from (Durand et al. 2015). Tan box, 1.9 Å resolution crystal structure of the PAAR protein, VCA0105, of *Vibrio cholerae* image reproduced, with permission, from (Shneider et al. 2013). Red box, 2.0 Å resolution crystal structure of the TssI-1 trimer from *Pseudomonas aeruginosa*, reproduced with permission of the International Union of Crystallography (Spinola-Amilbia et al. 2016).

Another baseplate protein critical to the operation of the T6SS is TssK (Zheng & Leung 2007, Schwarz et al. 2010) which forms a trimeric structure (Zoued et al. 2013). This protein interacts with the TssF-TssG heterodimer to form a complex which is recruited to the cytoplasmic side of the inner membrane by interaction with the inner membrane proteins TssL and TssM (Zoued et al. 2013; English et al. 2014). TssK also interacts with the TssC and TssD proteins, suggesting it may act as a link between the membrane complex formed by TssJ-TssL-TssM and the contractile sheath composed of TssB-TssC surrounding the TssD inner tube (English et al. 2014).

TssG is almost always found downstream of TssF in T6SS gene clusters (Boyer et al. 2009) and in the Uropathogenic *E. coli* strain O6:K2:H1 CFT073, they are expressed as a fusion protein from a single ORF (Brunet et al. 2015). TssF and TssG are homologues to the baseplate proteins J and I of bacteriophage P2, respectively (Brunet et al. 2015). The baseplate of bacteriophage P2 is more straightforward than bacteriophage T4 and contains four proteins; protein V which is equivalent to the central hub, protein W, a homologue of gp25, I a homologue of gp6 and J, a homologue of gp53 (Leiman & Shneider 2012). Unsurprisingly, given their genetic co-localisation, TssF and TssG interact with each other. TssG interacts with TssE and the sheath component-TssC. Both TssG and TssF interact with the inner tube protein, TssD. The TssF-TssG complex interacts with TssI and TssK (Brunet et al. 2015).

Also commonly referred to as valine-glycine repeat protein G (VgrG), TssI is a core component of the T6SS which is also secreted. Its presence in culture supernatants alongside TssD indicates a functional T6SS. Some TssI proteins have an additional region at their C-terminus which serves as an effector. Such subunits are referred to as 'evolved' TssI proteins (Pukatzki et al. 2007). It forms trimers which are similar to the tail spikes used by bacteriophages to puncture target cells (Pukatzki et al. 2007). In particular, the N-terminus and C-terminus of non-evolved (i.e. 'ancestral') TssI proteins resemble the bacteriophage gp27 and gp5 proteins, respectively (Pukatzki et al. 2007). The TssI trimer sits on the top of the inner tube, thereby forming the spike (Figure 1.7). TssI interacts with the inner tube subunit TssD (Lin et al. 2013) and is required for the assembly of functional (i.e. stacked in the correct orientation) inner tubes (Brunet et al. 2014).

Recently another component of the T6SS was identified; PAAR (proline-alanine-alanine-arginine) superfamily proteins form a sharp conical extension to the TssI trimer (Figure 1.7) and are thought to facilitate the transport of some effectors. It is also essential for T6SS activity (Shneider et al. 2013).

1.5.3 Inner tube and contractile sheath

Further evidence of the similarities between the T6SS and bacteriophages can be found in the structures that project from the T6SS baseplate into the bacterial cytoplasm prior to secretion (Basler et al. 2012). This is made up of an inner tube composed of stacked hexameric rings of TssD which are surrounded by a sheath made of TssB and TssC subunits.

TssD (also referred to as haemolysin co-regulated protein, Hcp) was one of the earliest components of the T6SS to be identified. In fact, it was identified as an unusual *V. cholerae* secreted protein in 1996 (Williams et al. 1996), years before the identification of the T6SS. The presence of TssD in culture supernatants is one of the hallmarks of a functional T6SS (the other being TssI).

The crystal structures of a number of TssD proteins have been elucidated. All of the structures determined so far have demonstrated that TssD forms hexameric rings which stack on top of each other (Mougous 2006, Jobichen et al. 2010, Osipiuk et al. 2011). Although in each structure solved, TssD rings interacted with one another, the apparent orientation of the stacking varied between different TssD proteins studied; *P. aeruginosa* TssD-1 rings stacked 'head-to-tail' forming long tubes (Figure 1.8) (Mougous 2006), *P. aeruginosa* TssD-3 formed double rings which adopted a head-to-head conformation (Osipiuk et al. 2011) while the rings formed by *Edwardsiella tarda* TssD adopted a tail-to-tail conformation (Jobichen et al. 2010). Work by Brunet et al. (2014) subsequently demonstrated that the head-to-tail conformation represented the physiological structure of TssD hexamers.

The hexameric rings formed by TssD typically have an internal and external diameter of ~40 Å and ~85 Å, respectively and resemble those formed by gp19 which makes up the phage T4 tail tube (Leiman et al. 2009). Accordingly, TssD forms a structure which is equivalent to the tail tube of contractile bacteriophages, TssD hexamers assemble into long tubes in the cytoplasm which are surrounded by the TssB-TssC sheath. The sheath and inner tube extend from the membrane across almost the entire diameter of the T6SS-containing cell. On contraction of the sheath, the inner tube is pushed out of the cell, delivering the TssI tail spike protein along with the PAAR protein, into the target (Basler et al. 2012). Although primarily regarded as a structural component of the T6SS, TssD has been proposed to perform a number of other roles; In *P. aeruginosa*, TssD has been shown to act as a chaperone for a secreted effector protein, Tse2, preventing its degradation prior to secretion (Silverman et al. 2013).

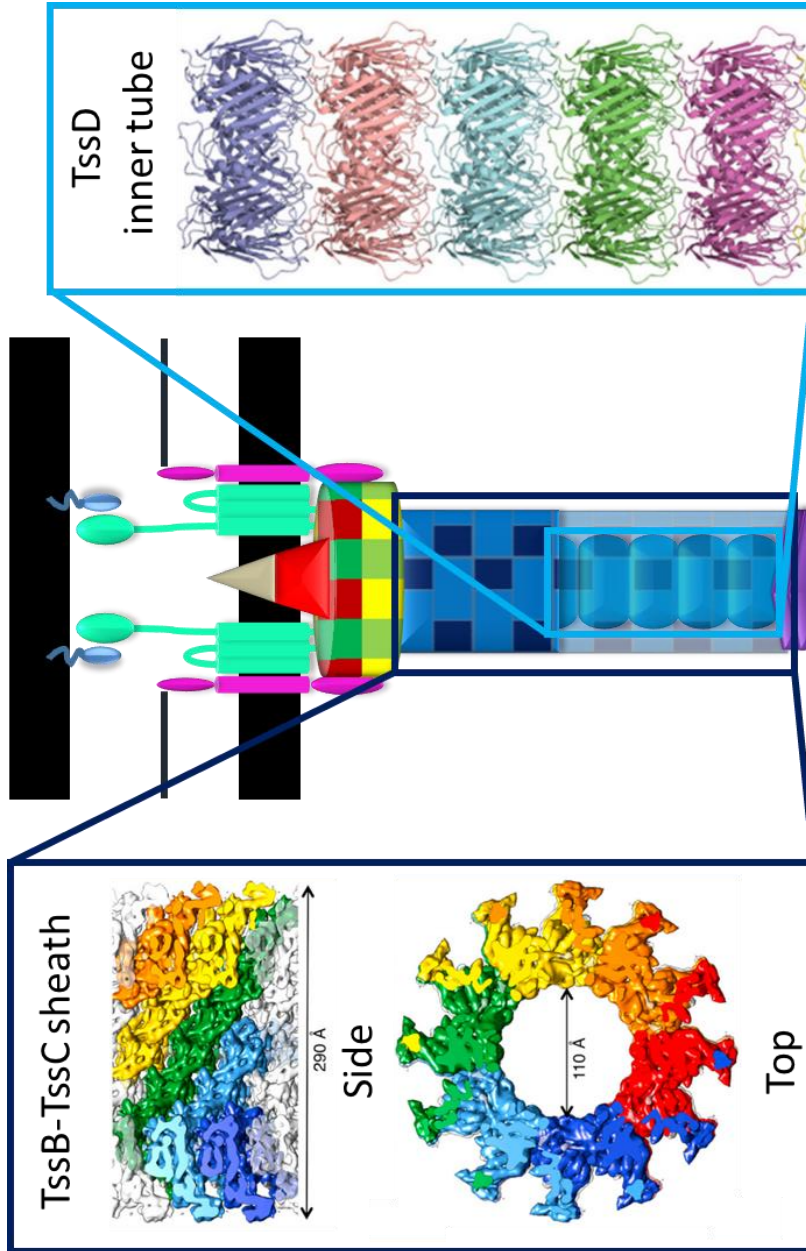


Figure 1.8 Structure of the T6SS inner tube and contractile sheath

Selected solved structures of the T6SS inner tube and contractile sheath. Dark blue box, 6 Å resolution three-dimensional structure of the TssBC contractile sheath of *V. cholerae* solved by cryo-electron microscopy, note that this structure is likely to represent the contracted conformation of the sheath rather than the extended form, image reproduced, with permission from (Kube et al. 2014). Light blue box, 1.95 Å resolution crystal structure of the TssD-1 inner tube of *P. aeruginosa* showing the head to tail stacking of the heaxamers (colour represents a separate heaxamer) image reproduced, with permission from (Osipiuk et al. 2011)

Bioinformatic analysis of genes encoding T6SS components demonstrated that *tssB* immediately precedes *tssC* in most T6SS gene clusters (Boyer et al. 2009) and TssC is similar to phage sheath proteins. It has been found that TssB and TssC interact to form a contracted bacteriophage sheath-like structure *in vitro* (Lossi et al. 2013; Kube et al. 2014) with an internal diameter which is sufficient to accommodate the TssD inner tube (Figure 1.8) (Lossi et al. 2013). Although TssD was not co-purified with the TssB-TssC sheath, it is likely that the sheath adopts its contracted conformation which pushes out the TssD inner tube in the absence of other T6SS components (Basler et al. 2012).

1.5.4 TssA

An unusual component of the T6SS is TssA, this protein forms dodecamers that interact with TssD and TssC (components of the inner tube and sheath respectively). It also co-purifies with the T6SS membrane complex, to form a structure which is visible by electron microscopy (Zoued et al. 2016) suggesting it forms a component of the baseplate. However, when fluorescently labelled TssA was observed in *E. coli* alongside fluorescently labelled TssB, it was observed to move away from the membrane as the sheath was extended and therefore it was predicted to incorporate inner tube and sheath components into the growing “tail tube” during assembly of the T6SS (Zoued et al. 2016).

1.5.5 TssH

Also known as ClpV, TssH is an AAA⁺ ATPase which facilitates the disassembly of the TssB-TssC tubules following contraction (Bönemann et al. 2009). TssH is unable to access the TssC when the tubule is in its extended conformation. However, following contraction of the sheath when the T6SS is ‘fired’, the N-terminus of TssC is exposed, allowing access to TssH and subsequent disassembly of tubules (Kube et al. 2014). Another protein involved in the disassembly of the sheath in some T6SSs is TagJ. TagJ recruits the respective TssH of the T6SS to the TssB subunit of the sheath rather than TssC (Förster et al. 2014). Thus, TssH allows recycling of sheath subunits in contrast to the contracted phage sheath.

1.5.6 Mechanism of secretion by the T6SS

An outline of the mechanism of secretion by the T6SS is shown in Figure 1.5. Based on assays which used fluorescently labelled TssL and TssM, the first stage of membrane complex assembly is believed to be the anchoring of the lipoprotein TssJ in the outer membrane. In *E. coli* and other species, the localisation of the T6SS machinery is randomly distributed around the cell. However, in *B.t* it specifically localises to the poles of the cell (Schwarz et al. 2014), suggesting another factor is involved in the membrane localisation of *B.t* (and presumably other pseudomallei group members). Insertion of TssJ into the outer membrane is followed by the addition of TssM and then TssL to produce the cell envelope anchoring complex. TssA is then recruited to the membrane complex which is followed by assembly of the baseplate. Rings of TssD surrounded by the TssB-TssC sheath then assemble from this

baseplate complex in a structure which eventually stretches across almost the entire width of the cell (Basler et al. 2012). As the inner tube/sheath extends, the TssA protein moves away from the membrane with the growing end of the tube/sheath (Zoued et al. 2016).

Once the system is assembled, firing is induced by a mechanism that has not been elucidated to date, although it is suspected that a conformational change in the membrane components is involved (Durand et al. 2015). Whatever the cause, the sheath contracts which pushes the TssI-tipped TssD tube out of the attacker cell and into the target cell. This also delivers the PAAR protein and any other proteins associated with TssI and TssD into the target. The TssH ATPase is then recruited to the contracted sheath to dismantle it. After the system has fired and disassembled, the membrane complex remains, allowing further rounds of secretion.

1.5.7 T6SS-exported effectors

One of the most striking observations regarding the effectors secreted by T6SSs is their sheer diversity, both in terms of their function and method of delivery. One of the earliest 'evolved' TssI proteins to be identified was *V. cholerae* TssI-1, which contains an RtxA domain at the C-terminus, which is capable of cross-linking actin in its purified monomeric form, in eukaryotic cell lysates and in whole J774.2 cells (Pukatzki et al. 2007). This TssI contributes to inflammation and is required for infection of the intestine in a mouse model of infection (Ma & Mekalanos 2010). *Aeromonas hydrophila* TssI-1 induces the rounding and eventual apoptosis of HeLa cells by the modification of host cell actin in a mechanism that is distinct from *V. cholerae* TssI-1 (Suarez et al. 2010).

A number of effectors secreted by T6SSs target the peptidoglycan of bacterial cell walls, and they are classified according to their specific activities. Type VI secretion amidase effectors (Tae), cleave the peptides and cross bridges of peptidoglycan. The Tae group are further divided into four clades based on evolutionary history (Tae1-4), each clade has a different specificity (Russell et al. 2012).

T6SS-exported peptidoglycan glycoside hydrolases which cleave the glycan strands of peptidoglycan are referred to as 'Tge' and are further divided into three families (Tge1-3) (Whitney et al. 2013). Another peptidoglycan targeting effector of *V. cholerae*, TssI-3, is an evolved TssI with a C-terminal domain which binds to and degrades peptidoglycan, increasing the ability of the bacteria to compete with *E. coli* (Brooks et al. 2013). A further set of T6SS effectors are phospholipases which have been classified (sticking with a similar naming convention to the Tae and Tge effectors) as Tle1-5 (type VI lipase effectors 1-5) based on phylogenetic distribution and sequence comparisons (Russell et al. 2013). A *B.t* Tle1, a *V. cholerae* Tle2 and a *P. aeruginosa* Tle5 have all been shown to exert lytic effects on bacteria (Russell et al. 2013; Dong et al. 2013; Jiang et al. 2014). As the substrates for lipases are not confined to bacteria, these effectors are also capable of targeting eukaryotic cells, indeed the *P.*

aeruginosa T6SS secreted phospholipases PldA and PldB have effects on bacterial and eukaryotic cells (Jiang et al. 2014). Some Tle effectors appear to be more specific; a Tle5 of *Klebsiella pneumoniae* is essential for virulence in a mouse model of infection but does not appear to exert an effect on *E. coli* (Lery et al. 2014). Type VI DNase effectors (Tde) have recently been identified, in *Agrobacterium fabrum* (*tumefaciens*) a pair of Tde proteins allow *A. fabrum* to outcompete *P. aeruginosa* in a plant co-infection model (Ma et al. 2014).

1.5.7.1 Mechanisms of effector delivery

The mechanisms utilised by the T6SS to deliver effector proteins are outlined in Figure 1.9. As mentioned previously, some TssI proteins, referred to as ‘evolved’ TssI proteins contain additional domains at the C-terminus which act upon target cells. These domains are dispensable for the activity of the T6SS as judged by the maintenance of the secretion of TssD and the remaining ‘core’ TssI when the effector region is removed. Effectors that are fused to structural components of the T6SS are referred to as ‘specialised effectors’. As these effector domains are covalently linked to the spike protein, they are delivered to the recipient cell as part of the puncturing device. Other effectors (so-called cargo effectors) must associate with the T6SS in order to be secreted.

It has been speculated that some types of effector proteins interact with TssI proteins and are carried across the membrane (Shneider et al. 2013, Durand et al. 2014). This is based on the observation that the Tle2 effector of *V. cholerae* interacts with TssI-3 (Dong et al. 2013). Effectors that interact with components of the T6SS are referred to as ‘cargo effectors’. The delivery of some effector proteins is believed to be enabled by an ‘accessory protein’ which interacts with both TssI and the effector. For example, *V. cholerae* VasW is dispensable for TssI secretion, but essential for secretion of the effector protein VasX (Miyata et al. 2013).

The recently discovered PAAR proteins may facilitate further methods of transportation for effectors. Like evolved TssI proteins, some PAAR proteins possess extended C-terminal regions which contain putative specialised effectors, including proteases, lipases and nucleases (Shneider et al. 2013). Additionally, some PAAR proteins contain a transthyretin domain. Such domains facilitate interaction with other proteins and therefore may act like an adaptor to enable the secretion of additional cargo effectors (Shneider et al. 2013).

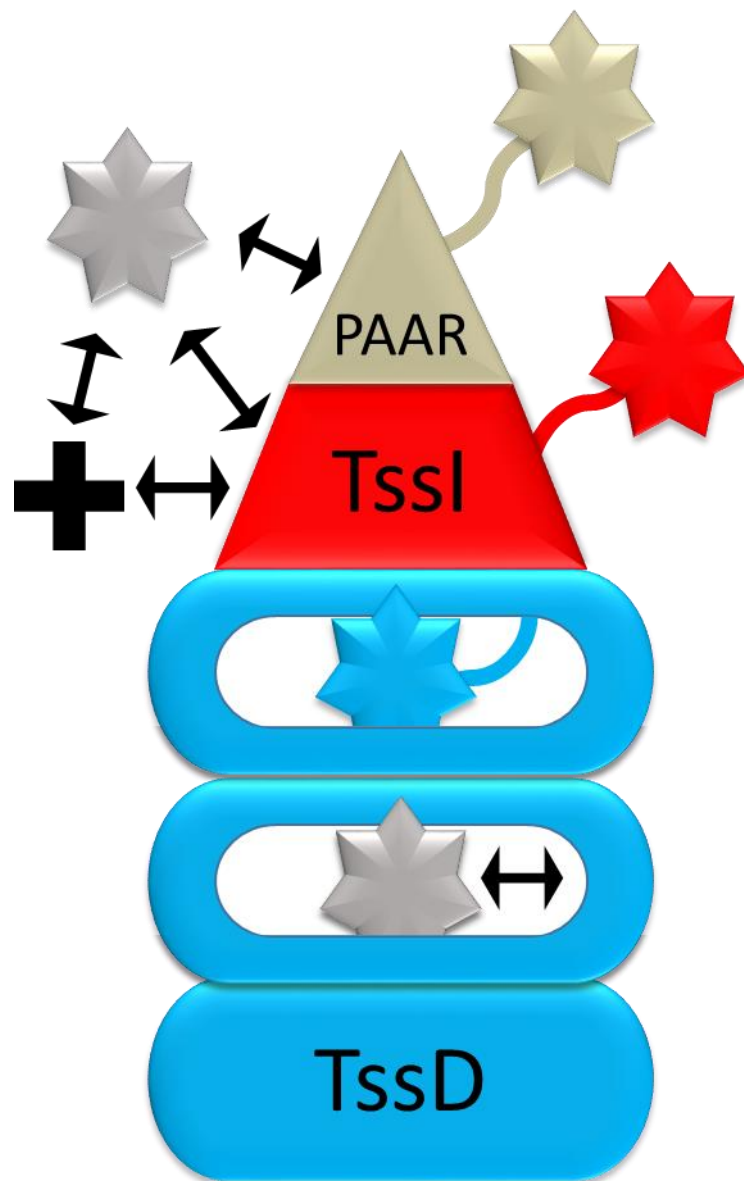


Figure 1.9 Mechanisms of T6SS effector delivery

Diagram showing the predicted mechanisms employed by the T6SS to translocate effectors into target cells. Grey stars, 'cargo effectors' which interact with TssD, TssI, PAAR proteins or an intermediate accessory protein (black cross); stars on stalks, 'specialised effectors' which are fused to secreted core components of the T6SS. Black arrows indicate an interaction.

In addition to its structural role, some small effectors, such as many of the Tae effectors, are thought to insert inside the TssD inner-tube. Here, TssD may act as chaperones as described in section 1.5.3, a TssD of *P. aeruginosa* is believed to facilitate the delivery of the Tse2 protein into the target cell. This is based on the observation that Tse2 occupies the central pore of TssD hexamers when analysed by electron microscopy (Silverman et al. 2013). A putative TssD protein in *Salmonella enterica* subspecies *arizonae* contains a putative bacteriocin domain and has been designated an 'evolved-Hcp' (using the alternative nomenclature for TssD), However, it is unclear whether or not it is functional as a TssD protein or toxin (Blondel et al. 2009).

1.5.7.2 Immunity proteins

As many of the effectors secreted by T6SSs are anti-bacterial, one would expect such effectors (i.e. DNases, peptidoglycan hydrolases and lipases) to harm the cell which produces them or its siblings. Therefore, to avoid self-toxicity and detrimental effects from accidental targeting by neighbouring siblings, many effectors have cognate immunity proteins which bind to and inhibit their function. Immunity proteins are almost always encoded immediately upstream or downstream of the effector to which they provide immunity.

Type VI secreted effectors are not thought to be exposed to the periplasm during delivery by the T6SS and therefore Tae proteins secreted by the attacker cell will not come into contact with the cell wall. However, cells are still at risk of the toxic effects of amidases delivered by siblings. To protect from fratricide, Tae proteins have cognate type VI amidase immunity proteins, referred to as Tai1-4 (corresponding to Tae1-4) which are transported into the periplasm, where they either exist as soluble proteins or outer membrane bound lipoproteins (Russell et al. 2011; Russell et al. 2012; English et al. 2012). Another periplasmic immunity protein class is the type VI secretion lipase immunity (Tle) proteins which are labelled Tli1-5 according to the effector protein (Tle1-5) they provide protection from (Russell et al. 2013). Unsurprisingly the Tde proteins also have cognate immunity proteins referred to as Tdi (Ma et al. 2014). An unusual example of immunity proteins is the Rap1b and Rap2b (resistance associated protein) proteins. These Tai4 family members are encoded on the *Serratia marcescens* genome but do not interact with any *S. marcescens* Tae4 proteins. It has therefore been suggested that Rap1b and Rap2b may protect the cell from amidases which are not produced by *S. marcescens* and are expressed purely for defence against proteins secreted by other species or strains (English et al. 2012; Srikannathasan et al. 2013).

1.6 Hypothesis

Based on the fact that they are not conserved amongst all T6SSs and their genomic location, immediately downstream of TssI-5, I predict that the *tag* genes encode effector proteins secreted by

T6SS-5 which are required for *B.t* to induce the formation of MNGCs *in vitro*. It is also possible that T6SS-5 secretes other effector proteins required for virulence. Although *tssA* is generally considered an essential component of the T6SS, Schell et al. (2007) found that a *B.m tssA-5* mutant was still virulent in a hamster model of infection, while mutation of other *tss* genes rendered *B.m* non-virulent. Thus, I intend to determine whether or not a *B.t tssA-5* mutant is capable of inducing MNGC formation and if the deletion of *tssA-5* has an effect on T6SS-5 activity.

1.7 Aims of this study

- Determine whether the *tag* genes are required for MNGC formation
- Determine whether the *tag* genes are required for T6SS-5 activity
- Identify proteins secreted by T6SS-5
- Identify interaction partners of the Tag proteins
- Determine the role of TssA-5 in T6SS-5

Chapter 2 Materials and methods

2.1 Bioinformatic analysis

Bioinformatic tools utilised in this work are shown in Table 2.1. DNA and amino acid sequences were obtained from the *Burkholderia* Genome Database (Winsor et al. 2008).

Table 2.1 Tools used in bioinformatics analysis

Tool	Function	Reference(s)
BoxShade	Shading of multiple alignments for display.	No publication, tool available at http://www.ch.embnet.org/software/BOX_form.html
Culstal omega	Multiple sequence alignment.	(Goujon et al. 2010; Sievers et al. 2014)
EMBOSS Needle	Pairwise sequence alignment.	(Li et al. 2015)
InterProScan	Scans sequences against the InterPro database to provide functional analysis.	(Jones et al. 2014)
Phyre²	Protein 3D structure prediction.	(Kelley et al. 2015)
PSIPRED	Protein secondary structure prediction.	(Buchan et al. 2013)
PSORTb	Protein subcellular location prediction.	(Yu et al. 2010)
PyMOL v1.8	Manipulation and visualisation of 3D protein structures.	(Schrodinger LLC 2015)
ScanProsite	Scans a protein for matches against the PROSITE motif collection.	(de Castro et al. 2006)

2.2 Bacterial Strains and plasmids

Bacterial strains used in this work are shown in Table 2.2, plasmids are shown in Table 2.3

Table 2.2 Bacterial strains used in this study

Bacterial Strain	Description	Source
<i>Burkholderia thailandensis</i> E264	Soil isolate obtained from a rice field in central Thailand.	(Brett et al. 1998)
<i>B.t</i> Δ tssA-5	E264 with a markerless in-frame deletion of 1,671bp of the central portion of <i>tssA-5</i> (BTH_II0873)	This study

<i>B.t ΔtssA-5, ΔtssA-1</i>	E264 with a markerless in-frame deletion of 1,671 bp of the central portion of <i>tssA-5</i> and 963 bp of <i>tssA-1</i> (BTH_I2957)	This study
<i>B.t ΔtssK</i>	E264 with a markerless in-frame deletion of 1,194 bp of the central portion of <i>tssK-5</i> (BTH_II0857)	This study
<i>B.t ΔtagA-D</i>	E264 with a markerless in-frame deletion of <i>tagA-5</i> (BTH_II0862), <i>tagB-5</i> (BTH_II0861), <i>tagC-5</i> (BTH_II0860) and <i>tagD-5</i> (BTH_II0859)	This study
<i>B.t ΔtagA</i>	E264 with a markerless in-frame deletion of 2,493 bp of the central portion of <i>tagA-5</i> (BTH_II0862)	This study
<i>B.t ΔtagB</i>	E264 with a markerless in-frame deletion of 927 bp of the central portion of <i>tagB-5</i> (BTH_II0861)	This study
<i>B.t ΔtagC</i>	E264 with a markerless in-frame deletion of 621 bp of the central portion of <i>tagC-5</i> (BTH_II0860)	This study
<i>B.t ΔtagD</i>	E264 with a markerless in-frame deletion of 816 bp of the central portion of <i>tagD-5</i> (BTH_II0859)	This study
<i>Escherichia coli</i> JM83	F ⁻ <i>ara Δ(lac-proAB) Φ80dlacZΔM15</i> (Sm ^R)	(Yanisch-Perron et al. 1985)
<i>Escherichia coli</i> SM10λpir	<i>thi-1 thr leu tonA lacY supE recA</i> RP4-2-Tc::Mu (Km ^R) (λpir)	(Simon et al. 1983)
<i>Escherichia coli</i> BL21λDE3	F ⁻ <i>ompT hsdS_B(r_B⁻m_B⁺) dcm gal λ(DE3)</i>	(Studier & Moffatt 1986)
<i>Escherichia coli</i> BTH101	F ⁻ , <i>cya</i> , (Sm ^R)	(Karimova et al. 1998)

Abbreviations: Tp^R, trimethoprim resistant; Sm^R streptomycin resistant; Ap^R, ampicillin resistant; Km^R, Kanamycin resistant.

Table 2.3 Plasmids used in this study

Plasmid	Description	Source
pET14b	<i>E. coli</i> specific vector for expression. Introduces N-terminal hexa-histidine tag. (Ap ^R)	Novagen
pET14b-His ₆ .TssD	pET14b containing <i>tssD</i> cloned between NdeI and BamHI. (Ap ^R)	This study

pETDuet-1	<i>E. coli</i> specific vector for expression. Contains two multiple cloning sites (Ap ^R)	Novagen
pETDuet- <i>tagA</i>	pETDuet containing <i>tagA</i> cloned between NcoI and HindIII of MCS1	This study
pETDuet- <i>tagB</i>	pETDuet containing <i>tagB</i> cloned between NdeI and BamHI of MCS2	This study
pETDuet- <i>tagA-tagB</i>	pETDuet containing <i>tagA</i> cloned between NcoI and HindIII of MCS1 and <i>tagB</i> cloned between NdeI and BamHI of MCS2	This study
pACYCDuet	<i>E. coli</i> specific vector for expression. Contains two multiple cloning sites (Cm ^R)	Novagen
pACYCDuet- <i>tagC</i>	pACYCDuet containing <i>tagC</i> cloned between NcoI and BamHI of MCS1	This study
pACYCDuet- <i>tagD</i>	pACYCDuet containing <i>tagD</i> cloned between NdeI and BglIII of MCS2	This study
pACYCDuet- <i>tagC-tagD</i>	pACYCDuet containing <i>tagC</i> cloned between NcoI and BamHI of MCS1 and <i>tagD</i> cloned between NdeI and BglIII of MCS2	This study
pBBR1MCS	Broad host range cloning vector, (Cm ^R)	(Kovach et al. 1995)
pBBR1MCS- <i>tssA</i>	pBBR1MCS containing <i>tssA</i> cloned between HindIII and BamHI, (Cm ^R)	This study
pBBR1MCS- <i>tssK</i>	pBBR1MCS containing <i>tssK</i> cloned between HindIII and BamHI, (Cm ^R)	This study
pBBR1MCS- <i>tagA-D</i>	pBBR1MCS containing <i>tagA</i> , <i>tagB</i> , <i>tagC</i> and <i>tagD</i> cloned between HindIII and BamHI, (Cm ^R)	This study
pBBR1MCS- <i>tagA</i>	pBBR1MCS containing <i>tagA</i> cloned between HindIII and BamHI, (Cm ^R)	This study
pBBR1MCS- <i>tagA_{FLAG}</i>	pBBR1MCS containing <i>tagA</i> modified to contain a C-terminal FLAG epitope, cloned between HindIII and BamHI, (Cm ^R)	This study
pBBR1MCS- <i>tagB</i>	pBBR1MCS containing <i>tagB</i> cloned between HindIII and BamHI, (Cm ^R)	This study

pBBR1MCS- <i>tagB_{FLAG}</i>	pBBR1MCS containing <i>tagB</i> modified to contain a C-terminal FLAG epitope, cloned between HindIII and BamHI, (Cm ^R)	This study
pBBR1MCS- <i>tagC</i>	pBBR1MCS containing <i>tagC</i> cloned between HindIII and BamHI, (Cm ^R)	This study
pBBR1MCS- <i>tagC_{FLAG}</i>	pBBR1MCS containing <i>tagC</i> modified to contain a C-terminal FLAG epitope, cloned between HindIII and BamHI, (Cm ^R)	This study
pBBR1MCS- <i>tagD</i>	pBBR1MCS containing <i>tagD</i> cloned between HindIII and BamHI, (Cm ^R)	This study
pBBR1MCS- <i>tagD_{FLAG}</i>	pBBR1MCS containing <i>tagD</i> modified to contain a C-terminal FLAG epitope, cloned between HindIII and BamHI, (Cm ^R)	This study
pSCrhaB2	Broad-host-range vector, expression inducible by rhamnose (Tp ^R)	(Cardona & Valvano 2005)
pSCrhaB2- <i>virAG</i>	pSCrhaB2 containing <i>virA</i> and <i>virG</i> cloned between NdeI and BamHI (Tp ^R)	This study
pSCrhaB2- <i>virAG-tssA</i>	pSCrhaB2- <i>virAG</i> containing <i>tssA</i> cloned between BamHI and XbaI, taken from digesting LITMUS 28i- <i>tssA</i> with BglIII and XbaI	This study
pSCrhaB2- <i>virAG-tssK</i>	pSCrhaB2- <i>virAG</i> containing <i>tssK</i> cloned between BamHI and XbaI, taken from digesting LITMUS 28i- <i>tssK</i> with BglIII and XbaI	This study
pSCrhaB2- <i>virAG-tagA</i>	pSCrhaB2- <i>virAG</i> containing <i>tagA</i> cloned between BamHI and XbaI, taken from digesting LITMUS 28i- <i>tagA</i> with BglIII and XbaI	This study
pSCrhaB2- <i>virAG-tagA_{FLAG}</i>	pSCrhaB2- <i>virAG</i> containing <i>tagA_{FLAG}</i> cloned between BamHI and XbaI, taken from digesting LITMUS 28i- <i>tagA_{FLAG}</i> with BglIII and XbaI	This study
pSCrhaB2- <i>virAG-tagB</i>	pSCrhaB2- <i>virAG</i> containing <i>tagB</i> cloned between BamHI and XbaI, taken from digesting LITMUS 28i- <i>tagB</i> with BglIII and XbaI	This study

pSCrhaB2- <i>virAG-tagB_{FLAG}</i>	pSCrhaB2- <i>virAG</i> containing <i>tagB_{FLAG}</i> cloned between BamHI and XbaI, taken from digesting LITMUS 28i- <i>tagB_{FLAG}</i> with BglII and XbaI	This study
pSCrhaB2- <i>virAG-tagC</i>	pSCrhaB2- <i>virAG</i> containing <i>tagC</i> cloned between BamHI and XbaI, taken from digesting LITMUS 28i- <i>tagC</i> with BglII and XbaI	This study
pSCrhaB2- <i>virAG-tagD</i>	pSCrhaB2- <i>virAG</i> containing <i>tagD</i> cloned between BamHI and XbaI, taken from digesting LITMUS 28i- <i>tagD</i> with BglII and XbaI	This study
LITMUS 28i	<i>E. coli</i> plasmid vector for transcription of double stranded RNA (Ap ^R)	NEB, (Kovach et al. 1995)
LITMUS 28i- <i>tssA</i>	LITMUS 28i containing <i>tssA</i> cloned between NcoI and XbaI taken from digesting pBBR1MCS- <i>tssA</i> with NcoI and XbaI	This study
LITMUS 28i- <i>tssK</i>	LITMUS 28i containing <i>tssK</i> cloned between NcoI and XbaI taken from digesting pBBR1MCS- <i>tssA</i> with NcoI and XbaI	This study
LITMUS 28i- <i>tagA</i>	LITMUS 28i containing <i>tagA</i> cloned between NcoI and XbaI taken from digesting pBBR1MCS- <i>tssA</i> with NcoI and XbaI	This study
LITMUS 28i- <i>tagA_{FLAG}</i>	LITMUS 28i containing <i>tagA_{FLAG}</i> cloned between NcoI and XbaI taken from digesting pBBR1MCS- <i>tssA</i> with NcoI and XbaI	This study
LITMUS 28i- <i>tagB</i>	LITMUS 28i containing <i>tagB</i> cloned between NcoI and XbaI taken from digesting pBBR1MCS- <i>tssA</i> with NcoI and XbaI	This study
LITMUS 28i- <i>tagB_{FLAG}</i>	LITMUS 28i containing <i>tagB_{FLAG}</i> cloned between NcoI and XbaI taken from digesting pBBR1MCS- <i>tssA</i> with NcoI and XbaI	This study
LITMUS 28i- <i>tagC</i>	LITMUS 28i containing <i>tagC</i> cloned between NcoI and XbaI taken from digesting pBBR1MCS- <i>tssA</i> with NcoI and XbaI	This study

LITMUS 28i- <i>tagD</i>	LITMUS 28i containing <i>tagD</i> cloned between NcoI and XbaI taken from digesting pBBR1MCS- <i>tssA</i> with NcoI and XbaI	This study
pEX18Tp- <i>pheS</i>	Suicide vector containing the mutant <i>pheS</i> gene for allelic replacement in <i>Burkholderia</i> species. (Tp ^R)	(Barrett et al. 2008)
pEX18Tp- <i>pheS</i> - Δ <i>tssA-5</i>	pEX18Tp- <i>pheS</i> with the deleted <i>tssA-5</i> SOE PCR product cloned between Acc65I and BamHI (Tp ^R)	This study
pEX18Tp- <i>pheS</i> - Δ <i>tssA-1</i>	pEX18Tp- <i>pheS</i> with the deleted <i>tssA-1</i> SOE PCR product cloned between Acc65I and BamHI (Tp ^R)	This study
pEX18Tp- <i>pheS</i> - Δ <i>tssK</i>	pEX18Tp- <i>pheS</i> with the deleted <i>tssK</i> SOE PCR product cloned between Acc65I and BamHI (Tp ^R)	This study
pEX18Tp- <i>pheS</i> - Δ <i>tagA</i>	pEX18Tp- <i>pheS</i> with the deleted <i>tagA</i> SOE PCR product cloned between Acc65I and BamHI (Tp ^R)	This study
pEX18Tp- <i>pheS</i> - Δ <i>tagB</i>	pEX18Tp- <i>pheS</i> with the deleted <i>tagB</i> SOE PCR product cloned between Acc65I and BamHI (Tp ^R)	This study
pEX18Tp- <i>pheS</i> - Δ <i>tagC</i>	pEX18Tp- <i>pheS</i> with the deleted <i>tagC</i> SOE PCR product cloned between Acc65I and BamHI (Tp ^R)	This study
pEX18Tp- <i>pheS</i> - Δ <i>tagD</i>	pEX18Tp- <i>pheS</i> with the deleted <i>tagD</i> SOE PCR product cloned between Acc65I and BamHI (Tp ^R)	This study
pEX18Tp- <i>pheS</i> - Δ <i>tagA-D</i>	pEX18Tp- <i>pheS</i> with the deleted <i>tagA-D</i> SOE PCR product cloned between Acc65I and BamHI (Tp ^R)	This study
pKT25- <i>tssA</i>	pKT25 with <i>tssA</i> cloned between XbaI and BamHI	This study
pUT18C- <i>tssA</i>	pUT18C with <i>tssA</i> cloned between XbaI and BamHI	This study
pKT25- <i>tssC</i>	pKT25 with <i>tssC</i> cloned between PstI and XbaI	This study
pKNT25- <i>tssC</i>	pKNT25 with <i>tssC</i> cloned between PstI and XbaI	This study
pUT18- <i>tssC</i>	pUT18 with <i>tssC</i> cloned between PstI and XbaI	This study
pUT18C- <i>tssC</i>	pUT18C with <i>tssC</i> cloned between PstI and XbaI	This study
pKT25- <i>tssI</i>	pKT25 with <i>tssI</i> cloned between PstI and BamHI	This study
pKNT25- <i>tssI</i>	pKNT25 with <i>tssI</i> cloned between XbaI and KpnI	This study
pUT18- <i>tssI</i>	pUT18 with <i>tssI</i> cloned between XbaI and KpnI	This study
pUT18C- <i>tssI</i>	pUT18C with <i>tssI</i> cloned between PstI and BamHI	This study
pKNT25- <i>tagA</i>	pKNT25 with <i>tagA</i> cloned between PstI and BamHI	This study
pUT18- <i>tagA</i>	pUT18 with <i>tagA</i> cloned between PstI and BamHI	This study
pKNT25- <i>tagB</i>	pKT25 with <i>tagB</i> cloned between HindIII and BamHI	This study

pUT18- <i>tagB</i>	pUT18C with <i>tagB</i> cloned between HindIII and BamHI	This study
pKT25- <i>tagC</i>	pKNT25 with <i>tagC</i> cloned between PstI and BamHI	This study
pUT18C- <i>tagC</i>	pUT18 with <i>tagC</i> cloned between PstI and BamHI	This study
pKT25- <i>tagD</i>	pKNT25 with <i>tagD</i> cloned between XbaI and BamHI	This study
pUT18C- <i>tagD</i>	pUT18 with <i>tagD</i> cloned between XbaI and BamHI	This study

Abbreviations: Tp^R, trimethoprim resistant; Sm^R streptomycin resistant; Ap^R, ampicillin resistant; Km^R, Kanamycin resistant.

2.3 Growth media

2.3.1 Lysogeny Broth (LB)

For the preparation of 1 L of LB, the following were weighed out: 10 g tryptone (BD), 10 g NaCl (Fisher), 5 g yeast extract (BD). The components were dissolved in ddH₂O and autoclaved for 20 minutes. Agar (Oxoid) was added to 1.5% (w/v) prior to autoclaving if plates were being prepared.

2.3.2 Iso-Sensitest Broth (IST)

IST broth was prepared by dissolving 21.4 g IST broth powder in 1 L ddH₂O and autoclaving. Agar (Oxoid) was added to 1.5% (w/v) prior to autoclaving if plates were being prepared.

2.3.3 Brain-Heart Infusion Broth (BHI)

BHI broth was prepared by dissolving 37 g of BHI powder (Oxoid) in 1 L ddH₂O and autoclaving.

2.3.3.1 Dialysed Brain-Heart Infusion Broth (dBHI)

BHI contains large MW proteins which could interfere with downstream analysis when analysing culture supernatants, to remove these dialysis was performed. For 1 L of dBHI, 37 g of BHI powder was dissolved in 50 ml of ddH₂O and poured into a suitable length of 12000-14000 MWCO dialysis tubing (Thermo) which had been soaked in ddH₂O and sealed at one end with a dialysis clip. A dialysis clip was added to the other end to seal the concentrated BHI solution. The tubing was placed in a container with 1 L of ddH₂O and incubated at 4°C overnight. The dialysate dBHI (i.e. the larger volume) was sterilised by autoclaving.

2.3.4 M9 Minimal medium

For the preparation of 100 ml of M9 minimal agar, 0.5 g of glucose and 1.5 g of agar were dissolved in 90 ml of ddH₂O before autoclaving. The solution was allowed to cool to roughly 50°C before 10 ml of 10X M9 salts were added along with 0.1 ml of 1 M MgSO₄ and 0.1 ml of 0.1 M CaCl₂ before pouring. If 0.1% w/v *p*-chlorophenylalanine (cPhe) plates were being prepared, 0.1 g of cPhe was dissolved in the

medium prior to addition of agar and autoclaving. When preparing plates for the blue/white colony screening of DNA inserts cloned into pEX18Tp-*PheS*, glucose was omitted and casamino acids added to 1.0% (w/v). The following were added after cooling: 1 ml 50% glycerol, 50 μ l 1% thiamine, 20 μ l 20 mg ml⁻¹ Xgal dissolved in DMSO, 10 μ l 1 M IPTG.

10X M9 Salts

The following were dissolved in 1 L ddH₂O before autoclaving.

- 60 g Na₂HPO₄
- 30 g KH₂PO₄
- 5 g NaCl
- 10 g NH₄Cl

2.3.5 MacConkey agar

MacConkey agar used in bacterial conjugations was prepared by adding 43 g of MacConkey agar base (Difco) to 1 litre of distilled water. The solution was mixed and then autoclaved for 20 minutes. 1 g of lactose (Fisher) was added immediately before pouring the plates. If the plates were to be used for the BACTH assay, 43 g of MacConkey agar base was added to 950 ml of distilled water which was mixed and autoclaved for 20 minutes. 50 ml of a 20% (w/v) maltose (Fisher) stock solution (filter sterilised) was added immediately before pouring the plates.

2.3.6 Media supplements

2.3.6.1 Glutathione (GSH)

A stock solution was prepared immediately prior to use by dissolving reduced glutathione (Sigma) in ddH₂O to a concentration of 100 mM and filter sterilising. An appropriate volume of the stock solution was added the media being used to give a working concentration of 200 μ M.

2.3.6.2 Isopropyl β -D-1-thiogalactopyranoside (IPTG)

An IPTG stock solution was prepared by dissolving in water to give a concentration of 1 M. The stock solution was filter sterilised and stored at -20°C. In solid media (i.e. agar plates) a working concentration of 0.1 mM was used, in liquid media a working concentration of 1 mM was used.

2.3.6.3 Thiamine

A stock solution was prepared immediately prior to use by dissolving thiamine (Sigma) in ddH₂O to a concentration of 1% (w/v) and filter sterilising. An appropriate volume of the stock solution was added to the media being used to give a working concentration of 0.0005 % (w/v).

2.3.6.4 5-Bromo-4-chloro-3-indolyl- β -D-galactopyranoside (X-Gal)

A 20 mg/ml stock solution was prepared by dissolving X-Gal in DMSO. The stock solution was protected from light and stored at -20°C.

2.3.6.5 Antibiotics

Antibiotics were stored at -20°C and used at the working concentrations indicated in Table 2.9.

Ampicillin (Ap)

A stock solution was prepared by dissolving ampicillin (Thermo) in ddH₂O to a concentration of 100 mg/ml. The solution was filter sterilised.

Chloramphenicol (Cm)

A stock solution was prepared by dissolving chloramphenicol (Sigma) in 100% ethanol to a concentration of 50 mg/ml.

Kanamycin (Km)

A stock solution was prepared by dissolving kanamycin (Thermo) in ddH₂O to a concentration of 25 mg/ml. The solution was filter sterilised.

Trimethoprim (Tp)

A stock solution was prepared by dissolving trimethoprim (Sigma) in 100% DMSO to a concentration of 50 mg/ml.

Table 2.4 Antibiotic working concentrations in *E. coli* and *B.t*

Supplement	Medium	Working concentration ($\mu\text{g/ml}$)	
		<i>E. coli</i>	<i>B.t</i>
Ampicillin (Ap)	LB	100	-
Chloramphenicol (Cm)	LB	25	50
	M9	-	250
Kanamycin (Km)	LB	50	50
	DMEM-FCS	-	250
Trimethoprim (Tp)	IST	25	50
	M9	25	50

2.4 Culture techniques

2.4.1 *Escherichia coli*

E. coli cells were grown on Lysogeny Broth (LB) agar plates containing appropriate antibiotic(s), or Iso-Sensitest (IST) agar when trimethoprim was used as a selectable marker. When DNA inserts cloned into pEX18Tp-*pheS* were being screened, M9 glycerol + thiamine + Xgal + IPTG Agar was used. Liquid broth cultures were grown overnight by inoculating the growth medium with a single colony picked from a plate using either a sterile toothpick or loop. Cultures were incubated at 37°C with aeration. Colonies growing on agar plates were sealed and stored for up to a month at 4°C. For longer term storage glycerol stocks were prepared using 700 µl of overnight culture mixed with 300 µl of 50% glycerol in a cryovial and stored at -80°C.

2.4.2 *Burkholderia thailandensis*

Cultures of *B.t* were grown for 48 hours at 37°C on M9 minimal plates supplemented with 0.5% (w/v) glucose. Overnight cultures were grown in LB at 37°C with shaking. Glycerol stocks were prepared as for *E. coli*.

2.4.3 RAW 264.7 cells

The mouse macrophage-like cell line was maintained in Dulbecco's modified Eagles medium (DMEM) supplemented with 10% foetal calf serum (FCS). Cells were grown on standard tissue culture plastic in a 37°C incubator with a 5% CO₂ atmosphere to a confluence of up to 80%. To passage, all but 10 ml of the culture medium was removed and the cells were detached from the surface using a cell scraper. The cell density was determined using a Neubauer improved haemocytometer and viability determined by trypan blue staining. 2×10^6 viable cells were added to T75 flasks and the final volume made up to 20 ml with fresh DMEM + 10% FCS.

To freeze, cells were detached from culture plastic using a cell scraper and the cell suspension was centrifuged at 400 x g for 5 minutes. The growth medium was removed and the cell pellet was resuspended to a density of 1×10^7 cells/ml in ice cold freezing solution containing 10% (v/v) DMSO and 90% (v/v) FCS. 1 ml aliquots were dispensed into 1.2 ml cryovials which were transferred to a polystyrene ice box lined with paper towel which was placed in a -80°C freezer for ~90 minutes before storage of the cryovial in liquid nitrogen.

To thaw, cryovials were placed in a 37°C water bath. Just before complete thawing occurred, the outside of the cryovial was wiped with 70% ethanol and the cell mixture in freezing solution was transferred to a T-25 culture flask. 9 ml of serum free DMEM was then slowly added to the flask which was placed in the incubator.

2.5 DNA extraction methods

2.5.1 Boiled lysate genomic DNA isolation

Burkholderia genomic DNA for use as a template in PCRs was prepared by picking a single colony growing on an agar plate using a sterile loop and resuspending it in 100 µl of TE buffer in a screw-capped microcentrifuge tube. This tube was then transferred to a boiling water bath for 10 minutes to lyse cells. The tube was allowed to cool before centrifuging at 13,000 x g for 5 minutes to remove insoluble cell debris. The supernatant was transferred to a clean microcentrifuge tube and stored at -20°C until required.

TE buffer

- 10 mM Tris
- 1 mM EDTA

2.5.2 Plasmid DNA extraction

Purification of plasmid DNA was performed using a GeneJET Plasmid Miniprep kit (Thermo). The protocol provided by the manufacturer was followed with the addition of an extra wash step after the clarified cell lysate was passed through the column. The added wash added 500 µl of buffer PB (Qiagen) to the column which was eluted by centrifugation. The step was added to completely remove endonucleases present in the *E. coli* strain harbouring the plasmid.

2.6 DNA manipulation techniques

2.6.1 Polymerase Chain Reaction (PCR)

Reaction components detailed for each polymerase used were prepared at room temperature in 50 µl PCR tubes (Fisher Scientific). The respective polymerase enzyme was added immediately prior to commencing thermal cycling. All PCRs were performed in either a G-STORM GS1 or a Bio-Rad T100 thermal cycler using the cycling settings shown below. Primer annealing temperature was calculated using the NEB Tm Calculator or determined empirically by using a gradient annealing step, whereby a number of identical reactions were carried out over a range of annealing temperatures. As a rule, primers used to amplify *B.t* genomic DNA were at least 20 bp long with a ~50% GC content. Oligonucleotide primers used in this study are listed in Table 10.3.

Step	Temperature (°C)	Time (s)	Cycles
Initial Denaturation	95	120	1
Denaturation	95	30	
Annealing	(Primer dependent)	30	30-35
Extension	70	30 s/kb	
Storage	10	-	-

2.6.1.1 KOD DNA polymerase

For amplification of DNA that was to be used in downstream applications where a low error rate was essential, such as insertion into an expression vector or the generation of mutants, KOD Hot start polymerase was used (Merck Millipore). The components of each KOD PCR are given in Table 2.5, the MgSO₄ concentration was typically 1 mM, but could be adjusted when amplifying difficult targets.

Table 2.5 PCR components for reactions using KOD polymerase

Reagent (stock concentration)	Volume for a 50 µl reaction
Genomic DNA	3.0 µl
Forward primer (10 µM)	3.0 µl
Reverse primer (10 µM)	3.0 µl
DMSO	2.5 µl
KOD x10 Buffer	5.0 µl
dNTP mixture (2 mM each dNTP)	5.0 µl
MgSO ₄ (25 mM)	2.0-4.0 µl
KOD Hot Start DNA polymerase (1 unit/µl)	0.5 µl
ddH ₂ O	(to a final volume of 50 µl)

2.6.1.2 Q5 DNA polymerase

PCRs were performed with Q5 polymerase (NEB) as an alternative to KOD polymerase for difficult templates. The components of each Q5 PCR are given in Table 2.6. The same conditions outlined previously were used with the exception of the extension temperature which was 72°C.

Table 2.6 PCR components for reactions using Q5 polymerase

Reagent (stock concentration)	Volume for a 50 µl reaction
Genomic DNA	3.0 µl
Forward primer (10 µM)	2.5 µl
Reverse primer (10 µM)	2.5 µl
Q5 5x Reaction Buffer	10.0 µl
Q5 GC enhancer	10.0 µl
dNTP mixture (2 mM each dNTP)	5.0 µl
Q5 High-Fidelity DNA Polymerase (2 units/ml)	0.5 µl
ddH ₂ O	(To a final volume of 50 µl)

2.6.1.3 GoTaq DNA polymerase

For PCRs where the amplified DNA was not being used for downstream applications which required high-fidelity replication (i.e. in PCR screening experiments), GoTaq polymerase (Promega) was used. Template DNA was provided by either single bacterial colonies for *E. coli* or boiled lysate for *B.t.* MgCl₂ concentration could be adjusted, but was typically 2 mM. Reactions were set up as indicated in Table 2.7 and the temperature cycling steps shown above were used but with the extension temperature increased to 72°C.

Table 2.7 PCR components for reactions using GoTaq polymerase

Reagent (Stock concentration)	Volume for a 50 µl reaction
Genomic DNA	3.0 µl
Forward primer (10 µM)	3.0 µl
Reverse primer (10 µM)	3.0 µl
DMSO	2.5 µl
GoTaq green buffer	5.0 µl
dNTP mixture (10 mM each dNTP)	1.0 µl
MgCl ₂ (25 mM)	4.0 µl
GoTaq polymerase (5 units/µl)	0.25 µl
ddH ₂ O	(to a final volume of 50 µl)

2.6.1.4 Deletion by splice overlap extension

For the marker-less in-frame deletion of genes, it was necessary to generate PCR fragments containing a deleted version of the gene with homology either side to allow allelic replacement.

In practice, two DNA fragments were first created; the first (fragment α) was composed of ~500 bp sequence upstream of the start codon and ~15 bp downstream, the forward primer contained a restriction site to allow its cloning into the plasmid pEX18Tp-*PheS*. The second fragment (fragment β) contained ~15 bp upstream of the stop codon and ~500 bp downstream. The primers were designed so that the primer pairs annealing to the region within the gene added a region complementary to each other. This meant that when the shorter fragments were used as templates for third PCR an amplicon (fragment γ) was produced with the middle portion of the gene deleted. It was important that the primers were designed so that the deletion was in-frame to minimise polar effects. For a more comprehensive guide, see (Heckman & Pease 2007).

2.6.2 PCR purification

For the removal of contaminating enzymes and other molecules such as dNTPs and primers from DNA samples following technique such as PCR or restriction digestion, the GeneJET PCR purification kit (Thermo) was used as per manufacturers instruction.

2.6.3 Agarose gel electrophoresis

For the separation of DNA molecules based on their size and for rough estimation of DNA concentration, agarose gel electrophoresis was performed. To prepare gels, between 0.8 and 1.2 g/ml of agarose (Fisher Scientific) was dissolved in TAE buffer (0.04 M Tris, 0.1142% (v/v) acetic acid, 0.001 M EDTA) by boiling in a microwave oven. Volumes of gels varied between 50 and 200 ml depending on number of samples. After dissolving the agarose, the volume of the solution was returned to the desired volume with distilled water to compensate for evaporation and allowed to cool to roughly 55°C before pouring into a cast and adding a suitable comb. For gel extraction of DNA, larger wells accommodating greater sample volumes were used. The gel was left at room temperature for 1 hour to set before the comb was removed and the gel transferred to an electrophoresis tank with the wells positioned at the cathode end. The gel was covered with TAE buffer. Typically, 1 μ l of 6X DNA gel loading dye (Thermo) was mixed with 5 μ l of sample before loading into wells. Suitable DNA ladders were run with a volume recommended by the manufacturer.

The gel was electrophoresed at a voltage dependent on gel size (80-120V were normally used) until the bromophenol blue dye front was approximately 2 cm from the end of the gel. The gel was transferred to a suitable container and covered in ethidium bromide staining solution (0.5 μ g/ml). Staining was performed by gentle shaking on an orbital shaker for 20-30 minutes before rinsing the

gel with water. DNA was visualised using a UV transilluminator and images captured using an EDAS 290 imaging system (Kodak).

2.6.4 DNA Extraction from agarose Gels

When PCRs gave rise to a background of incorrect bands/smears, or different sized DNA fragments needed to be separated, gel extraction was performed. The entire sample was loaded into an agarose gel with wells large enough to accommodate it. The DNA was electrophoresed and the desired DNA fragment (visualised using a UV transilluminator) excised from the gel with a scalpel after staining with ethidium bromide. The excised gel slice was transferred to a sterile microcentrifuge tube, weighed and a volume of buffer QX1 (Qiagen) equivalent to 1 µl per mg of gel slice was added to the tube. The agarose in the gel slice was dissolved by incubation at 50°C for 10 minutes to release immobilised DNA. DNA was then extracted using the PCR purification method (section 2.6.2).

2.6.5 Restriction digestion

Restriction enzyme digestion of DNA was performed as per the enzyme manufacturer's (Promega) instructions in a volume of 50 µl. Prior to use in downstream applications, DNA from the digestions was purified by PCR purification (section 2.6.2 **Error! Reference source not found.**).

2.6.6 Ligation

Ligation of digested DNA was performed in a volume of 30 µl using a roughly 3:1 molar insert to vector ratio judged by band intensity on an agarose gel. T4 DNA ligase (Promega) was used overnight as manufacturer's instructions. For most instances involving ligation of DNA fragments into a linearized plasmid, a vector control containing no ligase enzyme was included. This vector control allowed the assessment of the efficiency of digestion. A ligation control containing no insert DNA was also included to account for the occurrence of self-ligation of the plasmid which could occur if one of the enzymes had not cut effectively. These controls aided assessment of how many colonies to screen after transformation.

2.6.7 Nucleotide sequencing

To check the integrity of the DNA cloned into plasmids, constructs were sent for sequence analysis at the University of Sheffield core sequencing facility.

2.7 Transfer of DNA into bacteria

2.7.1 Preparation of competent cells

Escherichia coli cells were prepared to allow them to take up genetic material using Hanahans method (Hanahan 1983). A single colony of the *E. coli* strain being prepared was grown overnight and used to

inoculate 50 ml of appropriate media. The culture was grown at 37°C with shaking to an OD₆₀₀ 0.3-0.5 and placed on ice for 15 minutes before centrifuging at 4000 x g for 10 minutes at 10°C. The supernatant was discarded and cells were gently resuspended in 16 ml of RF1 before placing on ice for 30 minutes. The cells were centrifuged again at 4000 x g for 10 minutes at 4°C and the supernatant was discarded before the addition of 4 ml of RF2 solution and gentle resuspension. The cell suspension was placed on ice for 15 minutes and aliquots of 200-400 µl were transferred to microcentrifuge tubes. Competent cells could be used immediately or stored indefinitely at -80°C.

RF1

- 100 mM KCl
- 61.1 mM MnCl₂
- 30 mM CH₃CO₂K
- 10 mM CaCl₂
- 15% (w/v) glycerol

The components were dissolved in distilled water before adjusting the pH to 5.8 with 0.2 M acetic acid. The solution was filter sterilised through a 0.22 µm membrane into a sterile container which was then stored at 4°C.

RF2

Solution RF2 was prepared fresh by adding 0.2 ml of Solution A to 9.8 ml of solution B.

Solution A:

- 0.5 M MOPS (4-morpholinepropanesulfonic acid)

MOPS was dissolved in distilled water before the pH was adjusted to 8.0, filter sterilised through a 0.22 µm membrane and stored at 4°C.

Solution B:

- 10 mM KCl
- 75 mM CaCl₂
- 15% (w/v) glycerol

The components were dissolved in distilled water, filter sterilised through a 0.22 µm membrane and stored at 4°C.

2.7.2 Transformation

E. coli competent cells were thawed on ice and 1 µl of plasmid DNA (for ligations, 15 µl of the ligation reaction was used) was added to a microcentrifuge tube placed on ice. 100 µl of competent cells were

added to the microcentrifuge tube containing the plasmid and this mixture was then left on ice for 30 minutes, and agitated by flicking the tube every 5 minutes.

Transformation mixtures were transferred to a 42°C water bath for 2 minutes 30 seconds to heat shock then returned to ice for 5 minutes. To allow the expression of antibiotic resistance genes prior to plating on selective agar, 1 ml of LB or BHI broth (IST broth if using trimethoprim resistance as the selectable marker) was added to the transformation mixtures which were incubated at 37°C for 1 hour. 100 µl of the transformation mixture was then spread onto an appropriate agar plate to select for transformant *E. coli* cells which contained the plasmid.

2.7.3 Conjugation

Bacterial conjugation was used routinely to introduce plasmid DNA into *B. thailandensis*. To accomplish this, the *E. coli* conjugal donor strain, SM10(λpir), was used. This strain has the self-transmissible plasmid RP4 integrated into the chromosome. Separate overnight cultures of 10 ml of each of the donor and the recipient cells were prepared. Cells were harvested by transferring 1 ml of each culture to microcentrifuge tubes and centrifuging at 13,000 x g for 5 minutes. The supernatant was discarded and pelleted cells were washed by resuspension in 1 ml of 0.85% (w/v) saline and re-centrifuging to remove any antibiotics/debris that might hinder the growth of either cell type. The cells were centrifuged again at 13,000 x g for 5 minutes before the supernatant was discarded and the pellets resuspended in 100 µl of 0.85% (w/v) saline.

Donor and recipient cells suspended in saline (25 µl of each) were added to a microcentrifuge tube and mixed by tapping the tube. A 25 mm circular nitrocellulose filter membrane with a pore size of 0.45 µm was placed on a nutrient rich (e.g. MacConkey-lactose) agar plate with sterile forceps. The cell suspensions were then carefully pipetted onto the membrane. The plates with the inoculated nitrocellulose filters were then placed in the incubator at 37°C for 8 hours before the cells were recovered. This was achieved by transferring the nitrocellulose filter to 4 ml of 0.85% saline in a 25 ml universal tube followed by thorough vortexing. This cell suspension was then plated out. For transfer of suicide vectors, 100 µl of undiluted cell suspension as well as a 1 in 10 dilution was plated out. When a plasmid capable of replication inside the host strain was delivered, undiluted, 1 in 10, 1 in 100 and 1 in 1,000 dilutions were plated out.

2.7.4 Deletion of genes in *Burkholderia thailandensis* by allelic replacement

For the generation of deletion mutants the method of Barrett et al. (2008) was employed using the pEX18Tp-*pheS* plasmid. This system utilises a mutant *pheS* gene under control of a strong promoter which, when introduced into *Burkholderia* species, causes cell death in the presence of p-chlorophenylalanine (cPhe). By using the trimethoprim resistance gene as positive selection for

incorporation of the plasmid into the chromosome, a second recombination event can subsequently be selected by growth on plates containing cPhe.

Once the deleted gene had been cloned into pEX18Tp-*pheS* (see section 2.6.1.4) the plasmid was used to transform an *E. coli* strain encoding the RP4 transfer functions for delivery into *Burkholderia thailandensis* by conjugation. Single recombinants that were resistant to trimethoprim were selected for and purified by streaking on trimethoprim containing plates. Single colonies were then streaked on the same medium containing 0.1% (w/v) cPhe to select for a second crossover event, resulting in the loss of the plasmid along with the wild type or deletion allele. Genomic DNA was prepared from a single colony growing on the cPhe plate and the deletion was confirmed by PCR with primers flanking the original cloned region.

2.8 Protein techniques

2.8.1 Overexpression of proteins from plasmids containing T7 RNAP-dependent promoters

A single colony of an *E. coli* strain (BL21(λDE3)) encoding bacteriophage T7 RNA polymerase harbouring a plasmid containing the gene of interest located downstream of a T7 RNAP-dependent promoter was inoculated into 10 ml of BHI broth containing the appropriate antibiotic. This culture was grown overnight at 37°C with aeration and used to inoculate fresh antibiotic containing medium at a dilution of 1 in 100. The culture was incubated at 37°C with shaking until the OD₆₀₀ reached 0.5, at which point IPTG was added to a final concentration of 1 mM and the culture incubated for a further 3 hours. Protein over production was assessed by comparing samples taken before and after induction which were adjusted to the same number of cells based on their OD₆₀₀ prior to centrifugation at 13,000 x g. After the supernatant was discarded the pellet was resuspended in 50 µl of 1 x Laemmli sample buffer before analysis by SDS-PAGE.

2.8.2 Purification of soluble His-tagged Proteins by IMAC

Cells were harvested by centrifugation at 4,000 x g for 30 mins at 4°C. The supernatant was discarded and the cell pellet resuspended in 0.5 volumes of wash buffer containing 25 mM Tris-HCl (pH 7.5), 150 mM NaCl and 2 mM EDTA. The cell suspension was centrifuged again at 4,000 x g, the supernatant discarded and the cell pellet stored at -20°C overnight to aid lysis. To complete cell lysis, the pellet was resuspended on ice in lysis buffer containing 50mM Tris-HCl (pH 8.0), 2mM EDTA, 200mM NaCl, and 5% glycerol. The volume of lysis buffer used was equivalent to 5 ml per gram of cell pellet. This suspension was subjected to repeated rounds of sonication at 15% power using a microtip. Rounds of sonication were separated by three minute intervals on ice to prevent overheating which could denature proteins. The number of times a sample was sonicated was determined by the viscosity of

the solution. Following sonication, the lysate was clarified by centrifugation at 35,000 x g for 30 minutes at 4°C. The cleared lysate containing soluble proteins was subsequently used for IMAC.

To purify proteins which had been engineered to contain a polyhistidine tag, a nickel Sepharose column was used. Before use, a 1 ml His-Trap (GE Healthcare) column was stripped and recharged. The first step involved washing with 5 ml of ddH₂O before stripping with 5 ml of 50 mM EDTA (pH 8.0) to remove the nickel followed by a second water wash step. The column was then washed with 5 ml of 500 mM guanidinium hydrochloride to denature and remove any residual proteins followed by another water wash. To replace the nickel, 5 ml of 100 mM NiCl₂ was passed through the column before a final water wash step was performed. Columns were stored in 20% ethanol at 4°C if they were not to be used immediately.

Prior to loading the protein-containing sample, the column was equilibrated in 5 ml of lysis buffer containing 10 mM imidazole. The cleared bacterial lysate was then passed through a 0.2 µm syringe driven filter before applying to the column. The flow-through, containing proteins that did not bind to the column, was collected to analyse the binding efficiency. The column was then connected to an ÄKTA purifier system (GE Healthcare) which had been washed with ethanol and equilibrated with the lysis buffer containing 10 mM imidazole. The column was washed with 10 ml of lysis buffer containing 10 mM imidazole to remove residual unbound proteins, this was also collected. The His-tagged protein was eluted by gradually increasing the concentration of imidazole from 10 mM to 500 mM over a volume of 30 ml. 1 ml fractions were collected and proteins visualised by SDS-PAGE and staining with Coomassie blue.

2.8.3 TCA precipitation of *B. thailandensis* culture supernatants

To collect extracellular proteins, the trichloroacetic precipitation method was utilised. Overnight cultures of *B. thailandensis* were used to seed 25 ml of M9 minimal medium containing 0.5% glycerol and 0.5% casamino acids to an OD₆₀₀ of 0.01 or 0.05. If the cultures were glutathione induced, reduced glutathione (Sigma) was added from a filter sterilised stock at 100 mM in water to give a final concentration of 200 µM. Once the desired optical density of the cultures was achieved the cultures were centrifuged at 3,900 x g for 20 minutes at 4°C. The supernatant was collected and filter sterilised through a 0.22 µm pore syringe filter unit (Millipore) before adding sodium deoxycholate (Sigma) to a concentration of 200 µg/ml and incubating on ice for 30 minutes. 100% (w/v) TCA (Thermo) was added to the supernatants to give a concentration of 10% (v/v) TCA and the mixture frozen overnight at -20°C. The supernatants were thawed and centrifuged at 3,900 x g for one hour at 4°C. The resulting supernatant was discarded and the pellet washed by resuspension in 5 ml ice cold 100% acetone and incubated at -20°C for one hour prior to centrifuging at 3,900 x g for one hour and removing the

supernatant. This wash was repeated and the pellet was allowed to dry for one hour before resuspending in 6 M urea containing 25 mM ammonium bicarbonate.

2.8.4 SDS polyacrylamide gel electrophoresis (SDS-PAGE)

Gels for Sodium Dodecyl Sulphate Polyacrylamide Gel Electrophoresis (SDS-PAGE) were prepared according to the recipes below in Table 2.8. The resolving gel was prepared first and carefully poured between two glass plates in a mini-protean II (Bio-Rad) gel casting system. The volume of resolving gel used was appropriate to leave sufficient space for the stacking gel and comb. Butanol was added to the surface of the resolving gel to remove any bubbles and keep the surface level, the gel was allowed to set for 30 minutes. After the gel had set, the surface was rinsed with distilled water and dried using a small piece of tissue. The stacking gel was added, the comb placed in and the gel was allowed to set for 30 minutes. If not used immediately gels were stored in tissue soaked in running buffer at 4°C.

Samples to be analysed on the gel were mixed 1:1 with 2 x Laemmli sample buffer (120 mM Tris, 4% (w/v) sodium dodecyl sulphate, 20% (v/v) glycerol, 10% (w/v) β -mercaptoethanol, 0.004% (w/v) bromophenol blue pH 6.8) and incubated in a heat block at 100°C for 10 minutes and then centrifuged at 13,000 x g for 10 minutes prior to loading. When ready, the gel running apparatus was assembled and the comb removed. The gel tank was filled with running buffer and samples were loaded using gel loading tips. The gel was electrophoresed at 100 V until the blue dye in the Laemmli sample buffer migrated through the stacking gel, at which point the voltage was increased to 140 V. Once the dye front had reached the bottom of the gel, the gel was removed from the glass plates and stained in Coomassie blue staining solution (0.1% Coomassie brilliant blue R-250, 50% methanol, 10% glacial acetic acid) for one hour. Destain solution (40% methanol, 10% glacial acetic acid) was added and replaced every 20 minutes until protein bands were visible.

Table 2.8 SDS-Polyacrylamide gel ingredients

Component	Volume (ml)			
	10% Resolving	12% Resolving	15% Resolving	5% Stacking
	Gel (x4)	Gel (x4)	Gel (x4)	Gel (x4)
ddH ₂ O	9.6	8.6	7.1	6.3
40% acrylamide: bis-acrylamide 37.5:1	5	6	7.5	1.25
1.5 M Tris-HCl (pH 8.8)		5		-
1 M Tris-HCl (pH 6.8)		-		1.25
10% (w/v) SDS		0.2		0.1
10% (w/v) ammonium persulfate		0.2		0.1
TEMED		0.01		0.005

2.8.5 Western Blotting

Samples were electrophoresed as above, but before staining the proteins were transferred to Polyvinylidene fluoride (PVDF) membranes. Proteins were transferred for one hour at 100 V using a Mini Trans-Blot cell (Bio-Rad) filled with ice cold transfer buffer containing 25 mM Tris, 190 mM glycine and 20% methanol adjusted to pH 8.3. After transfer membranes were blocked for one hour in 20 ml 5% (w/v) milk powder (Marvel) in TBS containing 0.1% (v/v) Tween-20 (TBS-T). Primary antibody was diluted between 1 in 1000 and 1 in 5000 in 5% milk in TBS-T and the membranes incubated overnight in a 50 ml centrifuge tube on a roller at 4°C. Membranes were washed three times with 20 ml TBST before the addition of horseradish peroxidase conjugated secondary antibody specific to the species the primary antibody was raised in at a dilution of between 1 in 5000 and 1 in 10,000 in 5% milk in TBST. Membranes were incubated for one hour at room temperature in a 50 ml centrifuge tube on a roller before washing three times with TBST and once with TBS. EZ-ECL (Biological Industries) was added to the membrane and emitted light was detected using a ChemiDoc XRS+ imaging system (Bio-Rad) and analysis performed using Image Lab software (Bio-Rad). Blots were stripped of primary and secondary antibodies by the addition of 20 ml Restore PLUS western blot stripping buffer (Thermo) before blocking and staining again. Antibodies are shown in Table 2.9

Table 2.9 Antibodies used in this work

Antibody	Epitope	Animal raised in	Source
Anti-TssD-5	<i>B.t</i> TssD-5	Rat (antiserum)	This study
Anti-RNAP β	B subunit of <i>E. coli</i> RNAP	Mouse (IgG1, monoclonal)	Biologend
Anti-FLAG	FLAG epitope	Mouse (IgG1 monoclonal)	Sigma
Anti-Rat	Rat IgG	Goat (polyclonal, HRP conjugate)	BioLegend
Anti-Mouse	Mouse IgG	Rabbit (polyclonal, HRP conjugate)	Thermo
Anti-BCAL0343	<i>B. cenocepacia</i> BCAL0343	Rat (antiserum)	(Spiewak 2016)

2.8.6 In-Gel Trypsin digestion for mass spectrometry

The solutions used in this section are described in Table 2.10. Protein samples were electrophoresed and stained with Coomassie blue as described in section 2.8.4. The staining and destaining of the gel was performed in a sterile plastic container using freshly prepared solutions to avoid protein contaminants. After the desired staining intensity was achieved, the gel was rinsed with ddH₂O and placed on a sterile plastic surface. A sterile scalpel blade was used to excise each lane from the gel and each lane was cut into 12 horizontal strips (cut perpendicular to the resolving direction of the gel)

To remove the Coomassie blue stain, each gel slice was transferred to a 'LoBind' microcentrifuge tube (Eppendorf) followed by the addition of 200 μ l of Solution 1 and incubation at 37°C for 30 minutes. The liquid was removed from the tube and discarded before the addition of another 200 μ l of Solution 1 and incubation at 37°C for 30 minutes. The previous step was repeated once more and the liquid discarded. 200 μ l of Solution 5 was added to the tubes which were incubated at 37°C for 30 minutes. The liquid was discarded and the remaining gel pieces were dried in a vacuum concentrator.

200 μ l of Reduction buffer was added to each gel slice followed by incubation at 55°C to reduce the proteins, thereby breaking any disulphide bonds in the protein. After a one-hour incubation, the tubes were briefly centrifuged to collect all of the liquid, which was then removed. The proteins were alkylated by the addition of 200 μ l of Alkylation buffer. The tubes were incubated for 20 minutes at room temperature away from light. This irreversibly modifies the cysteine residues so they can no longer form disulphide bonds. The tubes were briefly centrifuged to collect all of the liquid.

To wash, 200 μ l of Solution 2 was added to each tube and incubated at room temperature for 15 minutes. The tubes were briefly centrifuged and the liquid removed. This wash step was repeated twice more. The gel pieces were washed once more by the addition of 200 μ l of Solution 3 and

incubated at 37°C for 15 minutes. The tubes were briefly centrifuged and the liquid was discarded before the gel pieces were dried in a vacuum concentrator.

To digest proteins in the gel slices, 50 µl of Trypsin solution was added to each tube, the slices were submerged by the addition of 50 µl Solution 4 and the tubes were incubated at 37°C for 16 hours. The tubes were briefly centrifuged to collect all of the liquid (which contained the digested peptides) which was subsequently transferred to a new low bind tube. After the addition of 20 µl of Solution 5, the tubes containing the gel slices were incubated at 37°C for 10 minutes. 50 µl of Solution 6 was then added to the tubes which were mixed prior to incubation at 37°C for 10 minutes. The tubes were centrifuged and the liquid was transferred to the new low bind tubes containing the digested peptides. Again, 20 µl of Solution 5 was added to the tubes containing the gel pieces which were incubated at 37°C for 10 minutes followed by the addition of 50 µl of Solution 6 and incubation at 37°C for 10 minutes. The tubes containing the gel pieces were briefly centrifuged and the liquid was transferred to the tubes containing the digested peptides.

50 µl of Solution 7 was added to the tubes containing the gel pieces and incubated at 37°C for 30 minutes. The liquid (containing the remaining peptides) was collected by centrifugation and transferred to the tubes containing the rest of the digested peptides, the gel pieces were discarded. The tubes containing the digested peptides were placed in the vacuum concentrator to evaporate the liquid. The dry digested peptides were then submitted to Trong Khoa Pham at the University of Sheffield Chemical and Biological Engineering department who performed the mass spectrometry analysis of the samples.

Table 2.10 Solutions used for in-gel trypsin digestion

Solution	Components
Solution 1	200 mM ammonium bicarbonate (AmB), 40% (v/v) acetonitrile (MeCN)
Solution 2	50 mM AmB
Solution 3	50 mM AmB, 50% (v/v) MeCN
Solution 4	40 mM AmB, 10% (v/v) MeCN
Solution 5	100% MeCN
Solution 6^a	5% (v/v) formic acid
Solution 7	50% (v/v) MeCN, 5% (v/v) formic acid
Reduction buffer^a	10 mM dithiothreitol (DTT), 50 mM AmB
Alkylation buffer^a	55 mM iodoacetamide, 50 mM AmB
Trypsin solution^a	36 mM AmB, 0.1 mM HCl 9% (v/v) MeCN, 20 µg/ml trypsin (Promega)

^a Freshly prepared on the day of use

2.9 Infection assays

2.9.1 Multinucleate giant cell formation assay

To assess the ability of *B. t* strains to induce the formation of multinucleated giant cells (MNGCs), single bacterial colonies were used to inoculate overnight cultures in LB. 24 well plates were seeded with RAW 264.7 cells at a density of 2×10^5 cells/ml 16 to 24 hours before infecting. On the day of infection 1 ml of the overnight culture was transferred to a microcentrifuge tube and cells collected by centrifugation at 20,000 x g. The supernatant was discarded and the pellet resuspended in 1 ml phosphate buffered saline (PBS) before the centrifugation was repeated and the pellet resuspended in another 1 ml PBS. The optical density of the bacterial solutions at OD₆₀₀ was measured and used to adjust the OD₆₀₀ to 0.4 in PBS. An appropriate volume of this solution was then used to inoculate DMEM containing 10% FCS to 2×10^6 cells/ml. Culture medium was removed from the wells of the 24 well plate and replaced with 1 ml of the bacterial suspension in DMEM. After two hours the medium in the wells was removed and washed three times with PBS before the addition of 1 ml of culture medium supplemented with 250 µg/ml kanamycin to kill extracellular bacteria. 16 hours after the initial infection the culture medium was removed and wells washed three times with PBS before fixing with 300 µl of 100% ethanol for 30 minutes. The ethanol was then removed and the well left to dry for half an hour. Cells were stained with 300 µl of undiluted Giemsa solution (Sigma) for 5 minutes before the stain was removed and the wells gently rinsed with tap water until the desired staining intensity was achieved. Images of the wells were collected using a Leica DMI4000B microscope.

Nuclei within giant cells (as defined as having three or more nuclei within a single cell) and total nuclei per field of view were counted using the 'cell counter' tool in ImageJ software. The number of nuclei within giant cells was divided by the total number of nuclei and multiplied by 100 to give a percentage fusion index.

2.9.2 Intracellular replication assay

To assess the ability of the *B. t* strains to invade and replicate within RAW cells, overnight cultures were used to infect mammalian cells growing in 24 well plates as above. At specified time points following the addition of medium containing 250 µg/ml kanamycin, medium was removed and the wells washed three times with PBS before the mammalian cells were lysed in 250 µl 1% Triton X-100 (Sigma). The lysates containing *B. thailandensis* were serially diluted in LB and 10 µl of dilutions from 10^{-5} to 10^0 were pipetted onto LB plates and grown at 37°C until colonies could be counted and used to calculate the colony forming units per well.

2.10 Interaction assays

2.10.1 Co-immunoprecipitation

Overnight cultures of *B. thailandensis* expressing FLAG-tagged bait proteins were grown in M9 minimal medium containing 0.5% (v/v) glycerol and 0.5% (w/v) casamino acids and used to inoculate a 25 ml culture in the same medium to a starting OD₆₀₀ of 0.05. The culture was grown to an OD₆₀₀ of ~1.0 before the centrifuging at 3,900 x g for 10 minutes at 4°C and the resulting supernatant discarded. The cell pellet was gently resuspended in 5 ml Tris Buffered Saline (TBS) before centrifugation at 3,900 x g for 10 minutes at 4°C, the supernatant was discarded and the pellet frozen at -20°C to assist lysis. The pellet was resuspended in 2.5 ml of lysis buffer containing 50 mM Tris pH 7.4, 150 mM NaCl, 1 mM EDTA, 1% (v/v) Triton-X100 and 200 µg/ml lysozyme and incubated on an orbital shaker for 30 mins at room temperature. The lysate was then placed on ice and phenylmethanesulfonyl fluoride (PMSF) was added to a concentration of 50 µg/ml before ten rounds of sonication in 30 second bursts. Insoluble material was removed by centrifugation at 22,000 x g for 10 minutes at 4°C and the soluble supernatant collected. To wash the binding medium, 1 ml of TBS was added to 50 µl of ANTI-FLAG M2 affinity gel (Sigma) in a microcentrifuge tube which was gently mixed before centrifuging at 5000 x g for 30 s at 4°C to collect the affinity gel at the bottom. The supernatant was removed carefully to prevent the beads being disturbed and the process repeated twice more. 1 ml of soluble lysate was added to the washed beads and incubated for 2 hours at 4°C with inversion. After binding the mixture was centrifuged at 5000 x g for 30 s at 4°C and the supernatant removed. The beads were washed four times before bound proteins were eluted either by the addition of 50 µl 2x Laemmli buffer and boiling for 10 minutes or by the addition of 50 µl TBS containing 150 µg/ml FLAG peptide (Sigma) and incubating at 4°C for 30 minutes with inversion followed by centrifugation at 5000 x g for 30 s at 4°C and the careful collection of eluted proteins. Eluted proteins were analysed by SDS-PAGE, western blotting or mass spectroscopy.

2.10.2 Bacterial adenylate cyclase two-hybrid assay

The bacterial adenylate cyclase two hybrid (BACTH) assay utilises the catalytic domain of *Bordetella pertussis* adenylate cyclase (CyaA) which catalyses the conversion of adenosine triphosphate (ATP) to cyclic adenosine monophosphate (cAMP). cAMP binds to the catabolite activator protein (CAP) which in turn binds to the cAMP-CAP promoter. The CyaA protein is composed of two domains, T25 and T18. In the BACTH assay, an *E. coli cyaA* mutant is used and the two domains are added separately, T25 is fused to a protein of interest by cloning the respective gene into the pKT25 or pKNT25 (both kanamycin resistant) plasmids, while T18 is fused to a protein of interest by cloning the respective gene into the pUT18 or pUT18C (both ampicillin resistant) vectors. When there is no interaction

between the proteins being tested, the T25 and T18 fragments are not brought into close proximity and therefore there is no cAMP production. When the proteins do interact, they bring their fused T25 and T18 domains into close proximity, making a functional adenylate cyclase which results in an increase in intracellular cAMP levels. cAMP binds to CAP which in turn induces the genes downstream of a cAMP-CAP promoter, in BTH101 cells this promoter is upstream of the maltose operon. Therefore, when intracellular cAMP levels are high, the maltose operon is expressed and the cells can ferment maltose, which produces an acidic end product. This means that when these cells are grown on agar containing maltose and a pH indicator, such as MacConkey agar containing maltose, a red/pink colony colour indicates a protein interaction. However, when there is no interaction the levels of intracellular cAMP remain low, resulting in no maltose fermentation and an off-white/brown colony colour.

To investigate specific protein-protein interactions, *E. coli* BTH101 cells were transformed with two plasmids, one encoding a T25 fusion protein and another encoding a T18 fusion protein (i.e. a combination of pKT25/pKNT25 and pUT18/pUT18C) and spread on MacConkey agar base (Difco) plates containing 1% (w/v) maltose, 100 µg/ml ampicillin and 25 µg/ml kanamycin. The plates were incubated at 30°C and the colour of the colonies growing on the plate was assessed after three nights and five nights' incubation.

Chapter 3 Bioinformatic analysis of the
B. thailandensis tag genes and their
protein products

3.1 Introduction

To date, much of the research conducted on bacterial type VI secretion systems has focussed on the 'core' proteins, encoded by the *tssA-M* genes, which are present in all functional T6SSs. Considerable effort has also been invested in identifying and characterising the effector proteins secreted by these systems. In addition to TssI, which itself can contain a variety of C-terminal effector domains, a wide range of secreted effector proteins have been identified (although TssD is secreted, it is not normally considered an effector).

At the outset of this work there was limited information regarding the role of the 'T6SS associated genes' (*tags*) of the *B.p* T6SS-5. Homologues of *tagA-5*, *tagB-5*, *tagC-5* and *tagD-5*, are associated with a number of T6SSs in a variety of species, but are not present in all systems. As shown in Figure 3.1, the *tag* genes are not always present together. In the absence of direct experimental evidence, bioinformatic analysis offers a potent tool in the prediction of protein function. Therefore, a bioinformatics approach was employed to gain information as to the nature and possible role of the Tag proteins.

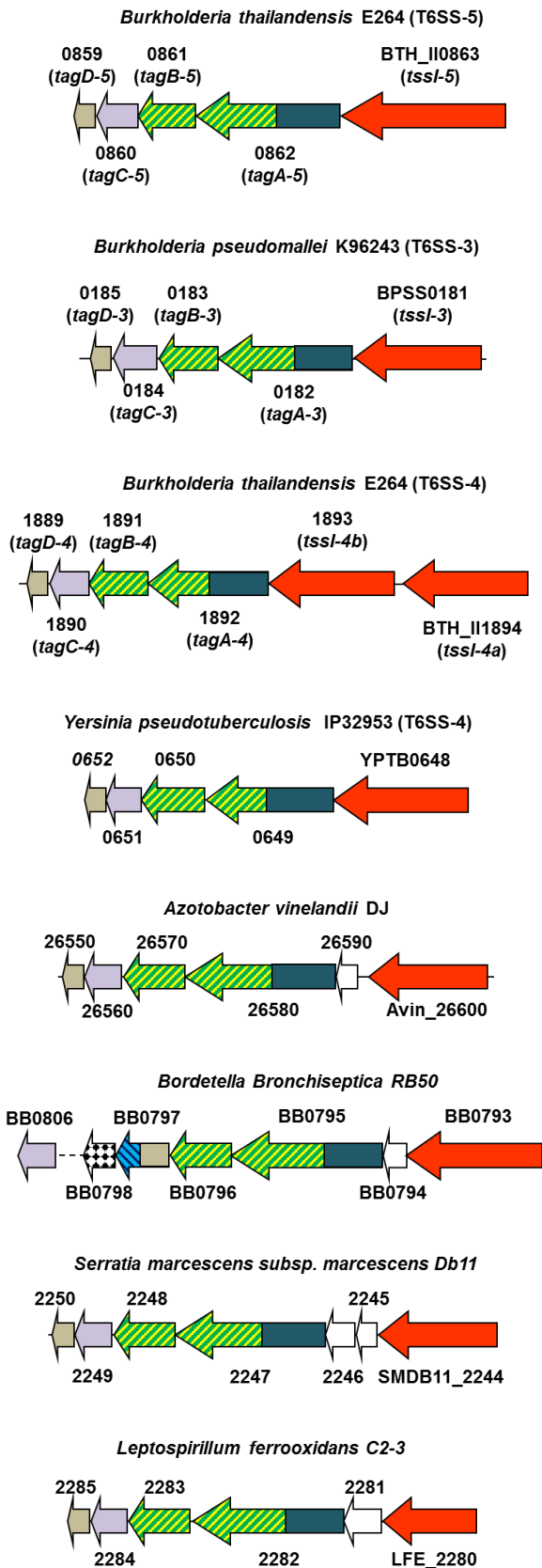
3.2 Genetic organisation

The *tag* genes are always located downstream of a *tssI* ORF suggesting they might be co-transcribed. It is not uncommon for genes located immediately downstream of *tssI* genes in T6SS gene clusters (as well as those encoded downstream of *tssI* genes present outside of T6SS gene clusters) to encode secreted effector proteins. As indicated in Figure 3.1, when the *tag* genes are found in a T6SS gene cluster, all four of them are present, or just *tagA* and *tagD*. When all four of the *tag* genes are present, *tagA* encodes a protein which contains an extended pentapeptide repeat domain which is absent when only *tagA* and *tagD* are in the gene cluster. *tagD* genes also encode TagD proteins which possess a variety of effector domains when they are present alongside *tagA* alone. In contrast, of the *tagD* genes found alongside all four *tag* genes, only the *Bordetella bronchiseptica tagD* gene encodes a protein with an effector domain. The *B.t* (and *B.p* and *B.m*) T6SS-5 gene cluster contains all four *tag* genes (see Figure 1.3 for the full *B.t* T6SS-5 gene cluster)

3.3 TagA-5

The first T6SS-associated gene in the T6SS-5 gene cluster, *tagA-5* (BTH_I10862), is found immediately downstream of *tssI-5*. This encodes the 91.2 kDa protein, TagA-5.

TagABCD



TagA&D

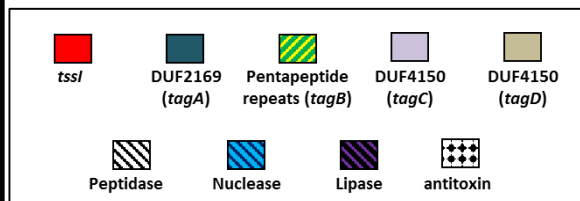
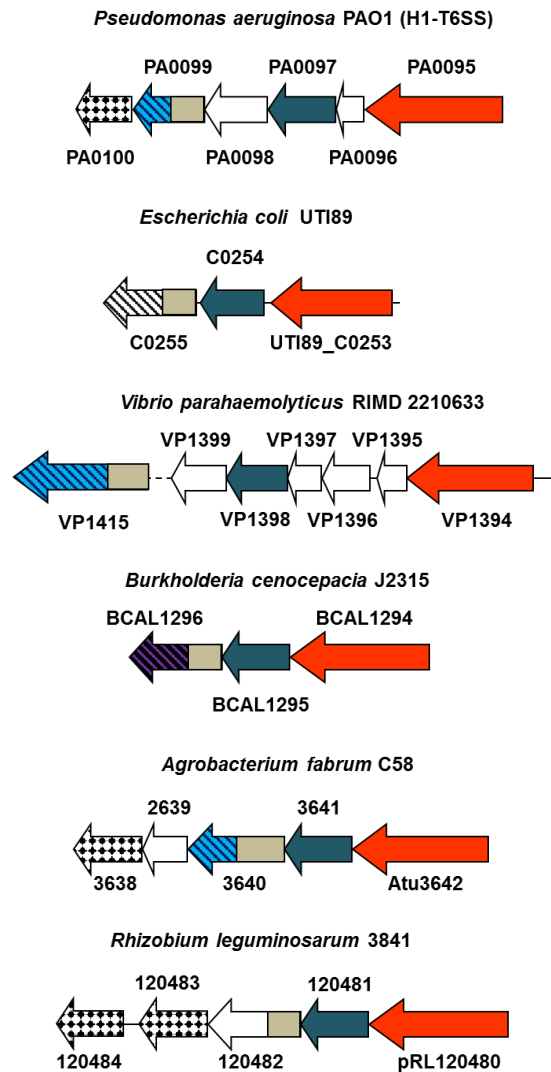


Figure 3.1 tag genes in T6SS gene clusters

Schematic diagram illustrating selected *tssI-tag* gene clusters within T6SS gene clusters. The genes are separated according to whether they contain *tagA*, *tagB*, *tagC* and *tagD* or just *tagA* and *tagD*.

3.3.1 TagA proteins in *Burkholderia pseudomallei* group members

Including TagA-5 there are two *tagA* genes present in the *B.t* E264 genome, the other is *tagA-4* (encoded by BTH_II1892) found within the T6SS-4 gene cluster. *B.p* and *B.m*, however, possess an additional *tagA* gene (*tagA-3*, BPSS0182 in *B.p* and BMAA1900 in *B.m*) which is found with the T6SS-3 gene cluster of these bacteria; this gene cluster is not present in *B.t*. *B.t* TagA-5 shares 76.7% sequence identity with *B.p* TagA-5 (encoded by BPSS1504) and 76.3% sequence identity with *B.m* TagA-5 (encoded by BMAA0736A, also known as TssF, *B.p* and *B.m* share 99.4% identity).

3.3.2 Protein family analysis of TagA

Entering the amino acid sequence of TagA-5 into the protein BLAST (BLASTp) search engine identifies a number of protein families and conserved domains. The N-terminal end of the protein contains a DUF2169 domain, while the C-terminus contains a series of pentapeptide repeats (Figure 3.2). The DUF2169 domain is found across the proteobacteria and its function is not known, but it is only present in proteins associated with the T6SS. Using the nomenclature of Shalom et al. (2007) proteins which contain the DUF2169 are named 'TagA'. This paper referred to *B.p* TagA-5 as 'TagAB-5' on account of the C-terminal pentapeptide domain which resembles the TagB protein. I refer to a TagA protein containing pentapeptide repeats as an 'evolved' TagA and those that do not (i.e. harbour only a DUF2169 domain) as an 'ancestral' TagA.

Pentapeptide repeat sequences are found among both prokaryotes and eukaryotes in numerous proteins which have a variety of roles (Vetting et al. 2006). The pentapeptide repeat has a consensus sequence of [S,T,A,V][D,N][L,F][S,T,R][G]. In the structures of pentapeptide repeat-containing proteins which have so far been experimentally determined, the repeats form a coiled-coil like structure. Each coil is formed from four faces in which each pentapeptide makes up a face. Pentapeptide repeats generally form a β -helix, however the type of turn present in the helix is variable. Each face either adopts a configuration which has type II turns and a single β bridge between faces in the coils, or has type IV turns which form a β -strand. The coils stack on top of one another and the pentapeptide repeats interact with the repeats which are positioned above and below them. The lumen of the helix is comprised of hydrophobic residues which stack on top of each other (Vetting et al. 2006).

3.3.3 Cellular location of TagA-5

The amino acid sequence of *B.t* TagA-5 was submitted to the PSORTb search tool which predicted TagA-5 is an extracellular protein. This was due to the homology between TagA-5 and the *Salmonella typhimurium* type three secreted effector PipB2. The TMHMM tool does not identify any transmembrane helices in the TagA-5 sequence and the SignalP server does not identify a signal sequence. A cell fractionation study in *Yersinia pestis* KIM6+ identified an evolved TagA, y3665

MKIVKPESLALLCRTLRFEGTDRLSIGALACFALRADAPAGPGDLAPEASLWQVARQWLGEHAPLDDGLPKPSGEFLVY
 GDACAPPGRDRAARAPFAVRARI GAACKERLVDARDAAGRALAEFRALPPSH PERSRDLGPFDERWLAARWPHLPAGTR
 AEHFHTAPRDQRIAGFWRGDEDIELVNLHADRPAIAGALPRVRARCFVERWVGGVARIDACPMRAETVWLFPGAACGIV
 LYRALVAIDDEDGDDVVVRIAGWEHADAPPLPDEAYIGRPAPEDEGSRPALAPAAAAPAIADDDARADAGDAADRAPGA
 PASAAHAHSPAAPESAEPPAPDLSALERDAAALAAQTDALLAAAGLTEADVARELLPPRDAPADMTLDELTAALAEELDA
 RTAQWQAQYDAAAERDEASSPAS PNSAAAHDA SLADLLRQADAQIRALVDQHGLSRAQMEAAAARDRPELAALADALDA
 LDAPLDIDALTAGLAAPAGDEAIVEPDAPAGPDRPAGADRPADGAPASMHAAAPSAGDAPPAEPLTREQVIERHARGLG
 FAGLDLSGLDLSSAALERADLRDARIERTCFAGCRLRGASFERALLSRADFSNADLREATFVDASAPGASFRGAALDRA
 RLAHADFTGADFTRASLADGHCAHARFDESAMTCLAAARLDGAHASFAGCALDAADFTSARMPRANFQHATLTAATFAF
 AQCDGAEWYGAQASGAQLRSASLRGSRADASTSFRQAVLSGAALDDANWDCVDLRYANLHKATLDRASLARAIASGAQL
 TLSLARRADLTKADLTHADARESNLQGASLRRARLDGTQLQSSNLYGADCYGTALGRSQLAGANVERTLFFVVPGRPELA
 SSR

Figure 3.2 Amino acid sequence of *B. t* TagA-5

Amino acid sequence of the *B. t* TagA-5 protein. Sequence highlighted in dark blue represents the coverage of the DUF2169 domain. Sequence highlighted in alternating green and yellow indicates the locations of the pentapeptide repeats.

(identical to the *Yersinia pseudotuberculosis* YPTB0649 protein shown in the alignment in Figure 3.3), in the membrane fraction of cells. However, the authors also detected TssI in the same fraction even though it is secreted (Pieper et al. 2009).

3.3.4 Amino acid sequence alignments of TagA homologues

An amino acid sequence alignment was performed with a representative selection of full length DUF2169 family proteins including a number which, like *B.t* TagA-5, contain a C-terminal pentapeptide repeat domain. As shown in Figure 3.3, the sequences show intermittent regions of homology and few residues were conserved at a single position in all the sequences. Interestingly *B.t* TagA-5 is unique in that it appears to have a gap in its sequence when compared with the other members of the DUF2169 family members. This is consistent with the InterPro analysis of the *B.t* TagA-5 amino acid sequence which predicted that its DUF2169 domain extended from residue 22 to 108 before there was a break and resumed again from residue 124 to 240. The absence of sequence in this region is also observed in the *B.p* and *B.m* TagA-5 proteins (not shown). The role of this region is unclear and the consequence of its absence (if any) is unknown. The *B. cenocepacia* protein included in the alignment (BcTagA, BCAL1295) contains a unique linker domain which does not show homology with the other sequences in the alignment.

The C-terminal regions of the 'evolved' TagA proteins did not demonstrate a high level of homology in the alignment which contained the full length 'non-evolved' and 'evolved' TagA sequences (result not shown). Therefore, the CTDs of the 'evolved' TagA proteins were aligned to ensure that all of the 'evolved' TagA proteins contained pentapeptide repeats. As shown in Figure 3.4, although there are long, non-conserved regions in the sequence, there are several sections which display homology, there are several blocks of conserved sequence. There are also a number of sites where hydrophobic residues are conserved at sites across the sequences.

3.3.5 Structure prediction of TagA-5

The secondary structure of TagA-5 was predicted using PSIPRED v3.3 (Figure 3.5). The predicted secondary structure contains a number of alpha helices and beta sheets in the region corresponding to DUF2169. There are also a series of alpha helices C-terminal to the DUF2169 before there is a disordered region after residue 486 that is rich in proline residues which could be a linker domain. Another alpha helix (541-549) is located N-terminal to the pentapeptide repeat domain (residues 550-872). The pentapeptide repeats are predicted to be disordered with a few short beta-strands, although this prediction is made with a low confidence.

A	VpTagA	1	-MQLWDIEAYPELSIKGRFQDENQDEVVWVVAKRTRQFDGEV-----WHELGD	
	EcTagA	1	MLEWKNNTPFPILSFL--EKYGRYGLLFDVIAIKMSLRKNGF-----YADLAE	
	BcTagA	1	-MEFRNLTPPLHAF--NAVDVPGNEIHVVAIKAAVRIEPAQSFDPDGDTHRCVLLSGD	
	PaTagA	1	-MELLNATPLAAAYN---QGLDAEGRESLVVIAKESLIDPLDG-----RE--ARLLD	
	AfTagA	1	-METQNRLPFPAMAF---RQFDAEGGRDCIVSVRATFTHVQDG-----T--METAR	
	RlTagA	1	-MDLINRILPFPAMAF---RQFDANGDLDCVVSVRCTFVHRQGD-----A--LALAS	
	E	BtTagA-5	1	-MKIVKPESLALIC----RTLRFEGIDRLSIGALACFALRADAPAGP-----GDLAP
		LfTagA	1	-MKVIKPMMLGLLW---KTYRRNG-HRLSVTGTVCIPFAT-----P-----DRPLT
		BpTagA-3	1	-MKIVKPLAISPLT---RVYRMHGREYLGVAALLIATLGD-----E-----PKLLA
		AvTagA	1	-MELIKPLRLGLVLIH---RTYHWRHGRLAVTATLALATLEE-----S-----PVLLP
SmmTagA		1	-MKVVKPLRLSALH---RPF SWQGNHLGVSVLALADMG A-----S-----PRIRP	
BbTagA		1	-MKIVKPLRLGLLS---RPYRMRGRQRLGLAVFALATLDE-----Q-----ALLQP	
BtTagA-4		1	-MRHKPQAALVAT---TNTQIGIQPMLGISVGMGRIRDQP-----S--TIIVH	
YpTagA		1	-MRLIRPQQLVVLK---SSYQIGHESHMGISVWAGCYLSKP-----E--HIVT	

A	VpTagA	49	--SEIFDDPQYLGEEGFSAIKVDQEFAYTKNNTDVLVYCKARSYAKK-PVTY---QECRV	
	EcTagA	47	FQKELSMDEYYGESETSSLKSETDILVLCRNTDIHVTGSAHAPSGD-K-SQ---WKACV	
	BcTagA	57	NAVPLAMSDEYEGETGKSSVKWESDLAPFKPKCDVLRATAHAPHGT-PAAS---WPARV	
	PaTagA	47	EQQTLLMVDEFYGEFGSAPRRECIFVFPKPFCDVILVLSAQAPGGR-FVQQ---LTAGL	
	AfTagA	46	EQESIQWEDAYEGDPHQTVLLRQSDLTPDKPGTDISFLGDAWSPSQE-PQKS---WRASL	
	RlTagA	46	KQEDIQWEDAYDGDPHASPLLRQTDITPEKVGTDITFLGNAYAPGGE-PAPS---WQVGL	
	E	BtTagA-5	48	EASLWQVARQWLG-E-----HAPLDDGLPKPSGEFLVYGDACAPPGR-DRAARAPFAVRA
		LfTagA	42	EQAMWPIAAECP-E-----ETVWDAGIPKDRGELLISAHGYAYGGI-PVET---RRISV
		BpTagA-3	43	ESALWRLAGDELRL---GYPLDMLPKACPEFLVSCYAYGKYAS-DPHAC-ACEVGV
		AvTagA	43	EQELWAILDEALD-E-----NEQIDLMPKPCPEFLVNGHAYNVHGT-DRRR---CRVQA
SmmTagA		43	EPELWQLADELTLTSL---GGVLDLALPKACAEFLATCNAYTHHQQ-DKTA---CAVKL	
BbTagA		43	EADLWSLAGEALG-E-----DGVLDLAMPKPCAFLVSGAAYTAHQQ-DRTA---CMARV	
BtTagA-4		43	EAAVWEALKAA-----APSLPLYEALPKQRAEWLLAGHSVHAVGGTRSRDIDWTAWV	
YpTagA		43	ESQWQAWKAA-----PLSFRMLDSAEKPFPAEFLLAGHAGIGEEVTSLSAEVSV----	

A	VpTagA	103	LIT----DGHIDKTLAVHGERVWVE-----HGGSVTLISKVPPFIEKDDIDV	
	EcTagA	102	RVNSFS-----KELSLSGVRYLQY-----ERNRWQMSLPDKIINVPRLV	
	BcTagA	113	RVFDAGTMVIDKGLRVTGPRSITK-----GWRGWKLGEPETRAMPVWRV	
	PaTagA	103	RVGRVLS-----KALTVHGPRQWEPGLLGAGAGVA-----QPFQSQDLSY	
	AfTagA	102	RVGDVLS-----KELDVGQRFWKPVIKEKWAGFYAREPKRVISDWVLNDEEPARQVAVCW	
	RlTagA	102	RVGQVLS-----KRLEVHGARFWRPVVKEKWAGFSAKEAKRELTDWQLIEAEPASSVPEICW	
	E	BtTagA-5	101	RITGAAC-----KERLVDARD-----
		LfTagA	92	QVGSILR-----KELALYGDRLWHK-----KNGEWIKSRPEPFCSMPILVY
		BpTagA-3	94	RIAGLE-----KRLRVCGDRQWAG-----AR----IAPRPFERLPIDW
		AvTagA	93	RLDDRC-----KALVVHGDRIYWAE-----GE----AGEPADFEAMPILGR
SmmTagA		94	QFDSLE-----KTLVVEGDRHWIN-----DR----PSTELPFAELRIDW	
BbTagA		93	RVGETLE-----KTLAVFGDRYWLD-----GK----PPEAPFEAMPILDH	
BtTagA-4		97	ELDGVRKIV--SCATQLGDE-----HEP---G---GCVRVAIDH	
YpTagA		93	--GSLTR-R--WCL---EGS-----NKT---GLVIKPFELRSLSDH	

A	VpTagA	143	TCALGGDLRNRIG-----GGVADSNKE-----
	EcTagA	141	ELAYGGIWQPD-----GMEKLVFSANPVGCGYYPDISQL-----
	BcTagA	157	EQAYGGTSRVALAQSAGKTSADLELNEVCFTNPLGRGWVEKRFLDRATHKSVVASLCASS
	PaTagA	142	ASAFGGSHASP-----DNPFGMDCYMANPAGCGWFPRASDT-----
	AfTagA	157	TNAFGGTIPGT-----GDTETDTPADVERRNLLGCGIVNLDMPA-----
E	RlTagA	157	SKAYGGQIPGT-----GDPENETPADVEARNPLGCGIVNLDMPW-----
	BtTagA-5	116	---AA-----
	LfTagA	131	TRSFGGKDY-----PKNPTGKGFSLD--PE-----
	BpTagA-3	129	DLAYGGAGC-----ADNPRGRGAHAR--E-----
	AvTagA	128	RRAYGGPGY-----EANPIGIGHVPESVDG-----
	SmmTagA	129	RRAYGGTQF-----ADNPHGIGATPETFPQ-----
	BbTagA	128	AHAFGGPEY-----ADNPHGRGAGDERIAG-----
	YpTagA	123	TQSWGKGC-----KENPLGRGYNDERKPT-----

A	VpTagA	165	-----LLEQKVPSVFPKKEWSS-----TSK-NLRVAGFGPVP
	EcTagA	175	-----NTSCQYKLPQITSSALSENA-----TIFNGE-SDFFGVGPVS
	BcTagA	217	IPGPLPKIAEIAAPQIEAWDIPITSLDVAEHAASGLDARQMKEVVASY-ATTEVGLGVVG
	PaTagA	178	-----AEIVGTPMPATEKLGCEPVDS-----PHG-RFTPMALGPIG
	AfTagA	196	-----DT-PPVRAPQITSPGERLD-----WKD-APEPQGFGLVS
E	RlTagA	196	-----DQ-APVAAPQITLPGKLN-----WRE-PVEPQGLGLVS
	BtTagA-5	118	-----GRALAEFRALP
	LfTagA	154	-----ESPVSLPNIESPFPFTIS-----PET-DTFPAGLGLD
	BpTagA-3	151	-----GAPRDLPNVEYAHSPMRF-----AHE-QPAPAGFCPVD
	AvTagA	153	-----GERWPLPNVEHDCQPPFA-----PGQPPGTPAGFGMRD
	SmmTagA	154	-----GRIHRLPNVEPLQRLAS-----PRQ-SALPASFDALD
	BbTagA	153	-----VRTRRLPNVEPARGRMQR-----PDQ-RPEPAGFGPVS
	YpTagA	148	-----MSLGLDGSAA-----IV-RSPLASPSVP

A	VpTagA	197	PFPEARQTLAG----TDEEWIENRKFMLELDFDRRFQSAPADQCKGF--LKGGERL
	EcTagA	212	RWWKSRLQYAG----TYNEVWREKRYPYLDDDFDERFNSAHPDMIYTG--LSGDENI
	BcTagA	276	RAWTPRLQFAG----TYDETWHKTRVYHPEVDHDFHYUNGAPADQOI-EW--PAPGLAF
	PaTagA	212	RHWQARVGFAG----RYDDAWLAERFPFLPADFDERFQSAPADQW-TDH--LRGGEEV
	AfTagA	228	PWRSRQQYTG----TYDDAWVAERHPLELRFDFDRFVQAAHPDLVATPH--LKGDEKY
E	RlTagA	228	PWRSRQQHAG----TYDETWLNERHPLELRFDFDARFVQCAHSDLVVMPH--LIGNEDY
	BtTagA-5	129	PSHPERSRDLG----PDERWLAARVPHLEPAGTRAEHHTAPRDQRIAGF--WRGDEDI
	LfTagA	186	LAWAERQSRTG----QYQFGEIGTEPPELANADWTLNQAQSDQWLSGF--WTGGESY
	BpTagA-3	183	AAWPARAGLYG----ALDRQWQEDCGPGEFRTLDPRFNLIAPADQQLPELRAFPDGAARY
	AvTagA	186	IDAPAHRAKLG----QYDEETLERDGPGLAESFDWRFFNLAPDDQWDRDRLAGGLEAY
	SmmTagA	186	ITWPRRFARIG----KNYDADWLKHGFPGFANDIDWRLFNMAESDQQFPQRDSLPPRAAY
	BbTagA	185	PLWPRRFARAG----QYHESWLDEGFPGLDLDLDPHFVNAAPDQWWPGQFGLAAGTPY
	YpTagA	171	CDWPERMQWMPTR-PGTVDAMAQDGTHTMGWPADVDLRFVQAAAPDQWARG-ECWMPGARF

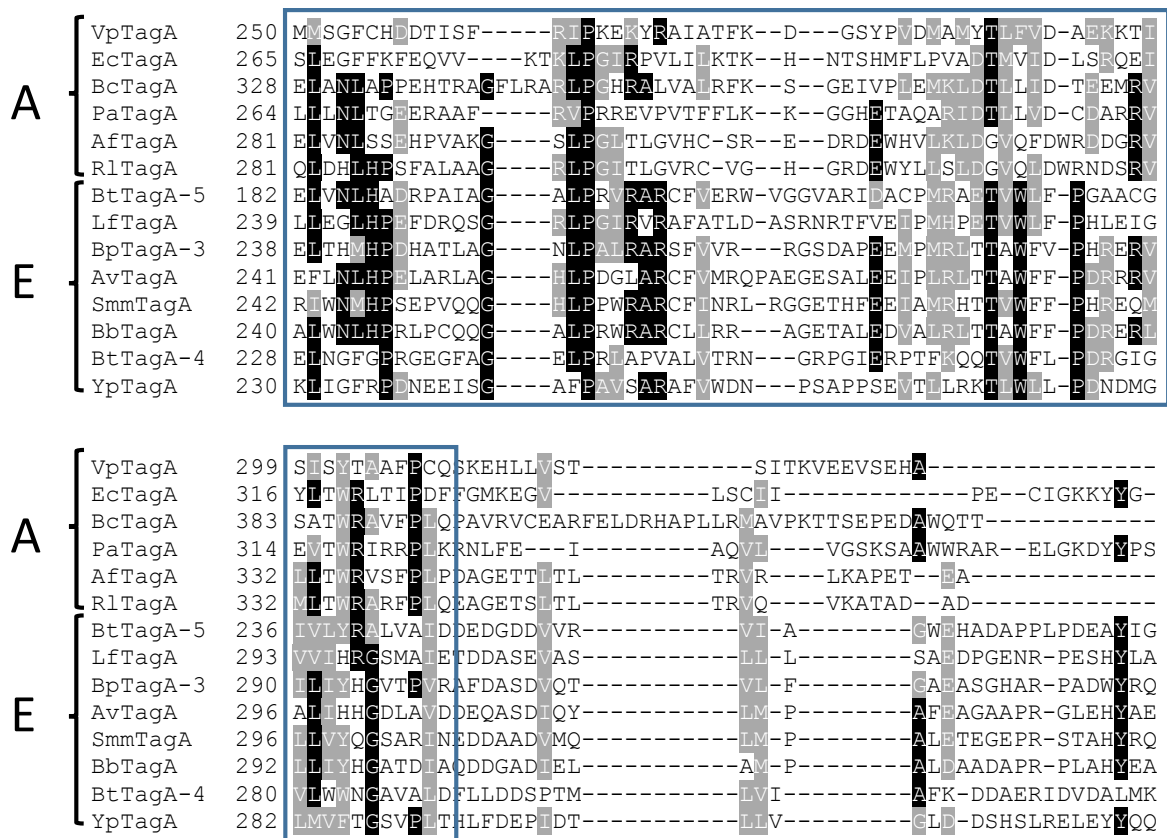


Figure 3.3 Amino acid sequence alignment of TagA proteins

Alignment of TagA proteins performed using Clustal Omega, shading performed using BoxShade. Amino acids that are identical at the corresponding position in $\geq 50\%$ of sequences are shown in white font with a black highlight while those that are similar in $\geq 50\%$ of cases are shown in white font with grey shading. The full length proteins were aligned. However only the NTDs (corresponding to DUF2169) are shown (sequence in blue box). A, 'ancestral' TagA; E, 'evolved' TagA; VpTagA, *Vibrio parahaemolyticus* VP1398; EcTagA, *E. coli* UTI89_C0254; BcTagA, *Burkholderia cenocepacia* BCAL1295; PaTagA, *Pseudomonas aeruginosa* PA0097; AfTagA, *Agrobacterium fabrum* Atu3641; RlTagA, *Rhizobium leguminosarum* pRL120481; BtTagA-5, *B.t* BTH_II0862; LfTagA, *Leptospirillum ferrooxidans* LFE_2282; BpTagA-3, *B.p* BPSS0182; AvTagA, *Azotobacter vinelandii* Avin_26580; SmmTagA, *Serratia marcescens subsp. marcescens* SMDB11_2247; BbTagA, *Bordetella bronchiseptica* BB0795; BtTagA-4, *B.t* BTH_II1892; YpTagA, *Yersinia pseudotuberculosis* YPTB0649. Accession numbers of proteins are listed in Table 10.1.

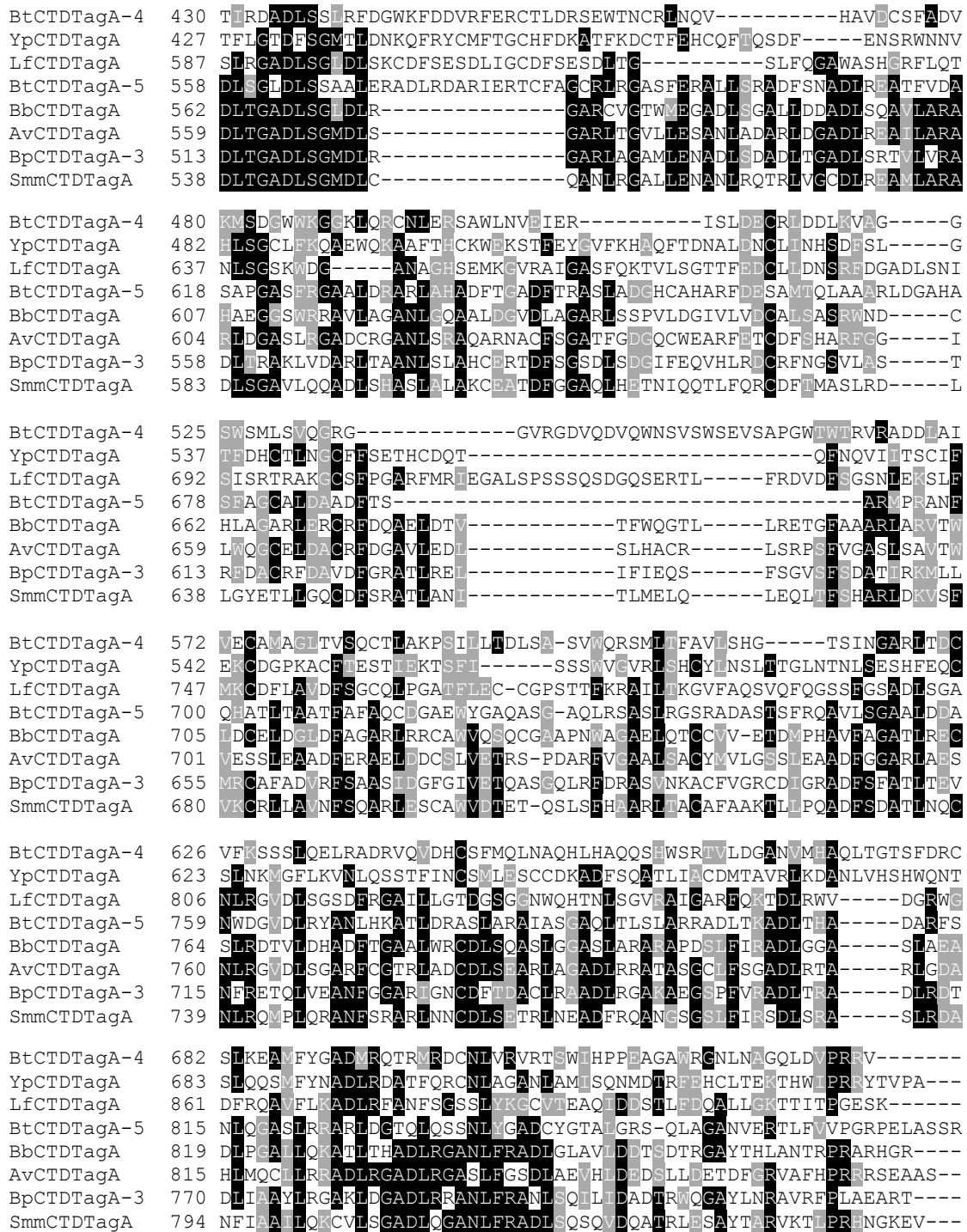


Figure 3.4 Amino acid sequence alignment of the CTDs of TagA proteins containing pentapeptide repeats

Alignment performed using Clustal Omega and shaded using Boxshade. Amino acids that are identical at the corresponding position in $\geq 50\%$ of sequences are shown in white font with a black highlight while those that are similar in $\geq 50\%$ of cases are shown in white font with grey shading. Only TagA proteins containing pentapeptide repeats was included and the region of the proteins containing the DUF2619 was excluded. BtTagA-4, *B.t* BTH_II1892; YpTagA, *Yersinia pseudotuberculosis* YPTB0649; LfTagA, *Leptospirillum ferrooxidans* LFE_2282; BtTagA-5, *B.t* BTH_II0862; BbTagA, *Bordetella bronchiseptica* BB0795; AvTagA, *Azotobacter vinelandii* Avin_26580; BpTagA-3, *B.p* BPSS0182; SmmTagA, *Serratia marcescens subsp. marcescens*. SMD11_2247. Accession numbers of proteins are listed in Table 10.1.

The 3D structure of *B.t* TagA-5 was predicted using the Phyre² server in ‘intensive’ mode. This generated a predicted structure with 35% of residues modelled at >90% confidence. The region of TagA-5 which gave the highest degree of confidence for the model was the C-terminal domain containing the pentapeptide repeats (Figure 3.6). However, The N-terminus of *B.t* TagA-5 (the region containing DUF2169) was modelled with a very low confidence due to a lack of available structures for proteins which aligned with this region. Therefore, the N-terminus of the predicted structure is probably unreliable.

Phyre² used the previously determined structures of a number of pentapeptide repeat-containing proteins to inform predictions on the structure of TagA-5. The structures used to inform this prediction included the cyanobacterium HetL protein (3DU1 in the protein data bank), *E. coli* NleL ubiquitin ligase secreted by the T3SS (3NB2 in the protein data bank) and the plasmid-mediated fluoroquinolone resistance factor QnrB1 (2XTW in the protein data bank). Therefore, it predicts the C-terminal domain of *B.t* TagA-5 to be solenoid-like with each of the pentapeptides coiling around each other to form a helix-like structure.

3.4 TagB-5

The second T6SS-associated gene, in the T6SS-5 gene cluster *tagB-5* (BTH_I10861), is located immediately downstream of *tagA-5* in the T6SS-5 gene cluster. The *tagB-5* gene encodes a 37.6 kDa protein.

3.4.1 TagB proteins in *Burkholderia pseudomallei* group members

There is one other ‘*tagB*’ gene present in the *B.t* E264 genome, *tagB-4* (BTH_I11891). Homologues of these proteins are found in *B.p* and *B.m*, which also possess an additional *tagB* gene, *tagB-3*, which is absent in *B.t*. *B.t tagB-5* shares 84.2% identity with both *B.p* TagB-5 (encoded by the BPSS1505) and *B.m* TagB-5 (encoded by BMAA0736B). The *B.p* and *B.m* TagB-5 proteins are 99.2% identical.

3.4.2 Protein family analysis of TagB

Detection of conserved domains using a BLASTP search did not identify any protein families or domains of unknown function. However, it did detect pentapeptide repeats. Searching the InterPro database with the *B.t* TagB-5 amino acid sequence was also unable to assign TagB to a protein family and again identified pentapeptide repeats. The pentapeptide repeats extend across almost the entire length of TagB (Figure 3.7). The repeats are similar to those observed at the CTD of ‘evolved’ TagA proteins and each repeat approximates to ‘[S,T,A,V][D,N][L,F][S,T,R][G]’. Using the nomenclature of Shalom et al. (2007) pentapeptide repeat proteins (which don’t contain DUF2169) encoded by genes within T6SS gene clusters are named ‘TagB’.

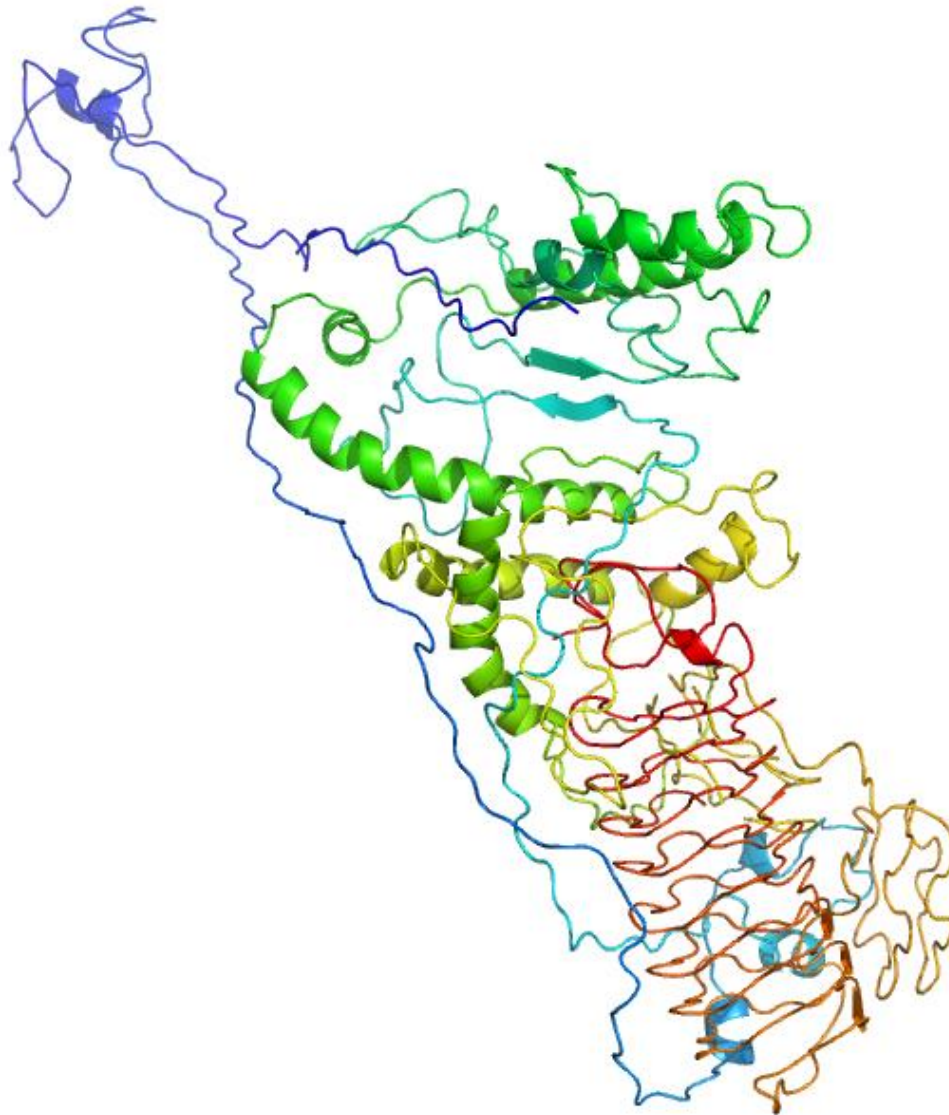


Figure 3.6 Predicted structure of *B.t* TagA-5

Structure predicted using Phyre². Displayed in rainbow colours with the N-terminus in blue and C-terminus in red.

```

MSDTVHAALAAALTDTRTLSGVDLSADLSGLDLSGCTLHRVILRGANLSAAQLDATRWLHCDLTGARVDGATLGESSWH
AVALRGASLRATTGDAFAMTDADLGGATLTDALWARATFERVDFSAQAQCARAKLLRCEAADCRFERTDFSSAELERFSA
MRADLSSARFDATRLTNALLCEADLRGQRFARCDLTMTHLNGATLAGSDFSGTSLVQTMFFAADLEGATLAGARGRHVR
FADATLVGARLAEAVFDECFARARLSSANARGLRARMRLFHADGAGATLAGGHFVYCDFSHATLSRADCTDADFSHA
NLHGIDDRAARWDGACKTGACATDPTLALAERWTAPER

```

Figure 3.7 Amino acid sequence of *B.t* TagB-5

Amino acid sequence of the *B.t* TagB-5 protein. Alternating yellow and green boxes above the sequence indicate the rough locations of pentapeptide repeats.

3.4.3 Cellular location of TagB-5

PSORTb predicts TagB-5 to be located extracellularly based on its homology with the *Salmonella enterica* serovar Typhimurium PipB2 protein which is a substrate for a T3SS. No transmembrane helices or a signal sequence were identified when the amino acid sequence was entered into the TMHMM search engine or the SignalP server, respectively. The same experiment which identified the *Y. pestis* y3665 protein (a TagA protein) in membrane fractions also detected the TagB protein y3664 (identical to the *Yersinia pseudotuberculosis* YPTB0650 protein shown in the alignment in Figure 3.8), in the same samples. Again, how much confidence can be made in this observation is debatable given a secreted TssI protein was detected in this fraction (Pieper et al. 2009).

3.4.4 Amino acid sequence alignments of TagB homologues

As shown in Figure 3.8, the TagB proteins do not contain many residues which are conserved across all of the sequences, this is likely due to the variability within the pentapeptide repeats. However, there are sections which do show a higher degree of similarity particularly at the leucine and phenylalanine residues which make up the central amino acid in the pentapeptide repeats.

3.4.5 Structure prediction of TagB-5

The secondary structure of *B.t* TagB-5 was predicted using PSIPRED V3.3. PSIPRED predicted a single alpha helix at the N-terminus of the protein, followed by an apparently disordered region that extends to the C-terminus and is interspersed with an occasional very short beta-strand. This is very similar to the prediction for the C-terminus of TagA-5 (Figure 3.9).

The 3D structure of *B.t* TagB-5 was predicted using the Phyre² server with over 90% confidence for 79% of residues. A number of known structures were used to make the structure prediction, all of which contained pentapeptide repeats, including the fluoroquinolone resistance protein QnrB1. Although an overall solenoid-like structure was predicted, like that observed for the TagA-5 C-terminal domain, the middle of the solenoid (residues 108 to 165) is interrupted by a disordered region that is extruded from the solvent (Figure 3.10). The disordered region on the structure corresponds to the residues of the amino acid sequence that were modelled with a low confidence and therefore this part of the predicted structure is probably unreliable.

YpTagB 1 MIPSD---TPMPPDSPRRITGRHFTQRQLQQLTLSEVYFIQCTFTDISFAEIAVRNIH
 BtTagB-4 1 MS---KIRSAVPPPLPEIVEGQRY-VSAQRDVALADTLFVDCHFERVEWTGCRLSNLR
 LfTagB 1 MPETQKIVDMITD---GEPVQEMDLSGFDLSGADLSHGIFINTRAIGARFDRCILKNTL
 BtTagB-5 1 MSDTVHAALAAITD---TRTSLSGVDLSDADLSGLDLSGCTLHRVILRGANLSAAQLDATR
 BpTagB-3 1 MSTRADRLRDAIRH---GRAIRDATDAGDFDGHVWSGGVFERVRFIGVSMKRVRLDEAV
 SmmTagB 1 MMSKPEQIRQRVFR---GEPTAGFDLHGLSFAGLDLAGGMFNELNNGVNFSDCDLRDSV
 AvTagB 1 -----MFR---GEATEGRALPGLRMAGLLLAGGLFRGCDLSGSDWQGTTLRACL
 BbTagB 1 --MDAETLRDWVFRQ---GRPLVGLDLRAAALQADLAGALLQDCDLRGAALAGSRWRDSR

YpTagB 57 FESCHFTHLRLDGGRVENCSEFRFCMFN-----DVSAQGVSIILNTSCIEVQ
 BtTagB-4 56 FVNGTFDANRFDRCELEKLSYESSRVR-----EGANTQSALQRVSENECE
 LfTagB 58 FDSCDLSGSNWOSSILHLASFLKCRFH-----RAGFDHAGSQNSRNVESD
 BtTagB-5 58 WIHCDLTGARVDGATLGESSWHAVALRGASLRATTGDAFAMTDADLGCATLTDALVARAT
 BpTagB-3 58 FIDCLFRDVMRQAGCARCIFDRCFLE-----RVDLSASELRDCMMNGTH
 SmmTagB 58 FSDCQLEHAQFTRADLKQTAFNQCAMS-----ASRFSESHIELTMTNDCR
 AvTagB 47 FIDCALEAADERMARLDEVQWQCALA-----DAAFAGAELEERCQLEESG
 BbTagB 56 FSGCRMEQTDWRGADVAQCAFRCFLA-----EAVFAAEACAGASVVECR

YpTagB 102 WQCYLTGCLIERWLLTSCQLDDAQLQDIOQNYWTVQDTPMTHLIMS DSKMQDSSWHGCT
 BtTagB-4 101 IDGGAMAGCLLKDVVCSQSKGAWTFDAVRGAHVSLVAGEYAGVLRGGHWSDTSWIGSR
 LfTagB 103 LSGSRFSDTLNHSSWVDCVFDGTAFDGADLEKTSFVHGSFPGTSESGAKI IKTALIGQT
 BtTagB-5 118 FERVDFSAQCARAKLLRCEAADCRFER-----TDFSSAELERFSAMRAD
 BpTagB-3 103 AAGVYFSGARASGLHCVKSDLGDCGFDDARIESAVESDTRLARAAFTRAAVRKAVFVRLD
 SmmTagB 103 IEQSDFSRLSLNQSHWMSCOLAGANFSATQHDRTIEYESPLDGAMLNQARLCLVTFERLN
 AvTagB 92 IARAVFDGALLGGLAFIQSVLAHASFEEATLAETSFNECDLRDCRFARAHLSETLLEELD
 BbTagB 101 AAGADERATPLHGSHFVQCALDGARLDRAEMREGGEAECTLEQASLAGAALRQTLERAD

YpTagB 162 IQQSVWKNSE-----ELIRQVMGSCVLECOVQAIQSDTVVWSQCQLEQVDFRHQP
 BtTagB-4 161 LVDLRLESVGLLENLIAGQSGFERAVLVECRGINVRMIDSRIERMVQCCELKQAAWSHST
 LfTagB 163 LNQAFFAGA-----IFRNPIEIKVSLKGIIDE-----SNMSPMVAASSDISETR
 BtTagB-5 163 LSSARFDAT-----RLTNAALCEADLRGQRE-----ARCDLTMTHLNGATLAGSD
 BpTagB-3 163 LLSAVFADA-----AFDDTVFAEANLAGQRL-----QGQRWHRCQFVGDLEHRAD
 SmmTagB 163 LCKTQFEGV-----NFDRVTFEFCDHKGSY-----AGQSLIACQFTDNQLDDVD
 AvTagB 152 LCSVDFAET-----RFESVTFSGSNLSGCCL-----MRTSLACQFSAALLDGCD
 BbTagB 161 LRTADLAGA-----RLRVRVVEECDLSGQRL-----AGQFLGCSQFVEARMDGCD

```

YpTagB      212 LENSNFHKSILTQCGF-----SDANLAAALFSEATLEGCDFNMAQLAAQEFVDAT
BtTagB-4    221 WATGEIHASRLPIASFDHASINGLTVINSELPQALFDSASVADSALQGVRAPIALR---
LfTagB      208 WV-----GSDIRLANFYQSDLTGAVLDGANAEKALFSESRMEGASARGAMIKMASEFQKTS
BtTagB-5    208 FS-----GTSIVQTMFFAADLEGATLAGARGRHVRFADATLVGARLAEAVFDECDFFARAR
BpTagB-3    208 FT-----GARLAGCNFQRAKLTGARLDGVDAPNTVFFEADAPDATCRDAAIRGSIWVQAD
SmmTagB     208 FS-----QAILRQSNFKGASLRRANLTSVQAQQSLWLEANLQACCRGGQFDQATFSEAT
AvTagB      197 LT-----EAVLSQAVFKDASLVGARLTGVEARYALFPDADLSDADCRCRFAQSVWAGAQQ
BbTagB      206 LR-----EASMAQCNFKGASLRRACLAGASCARAMFAQADLGGADCSGARVPOSLEWADAI

YpTagB      262 LRDCNFDTADLQNASLLRANLTRCHLTQVNLTKADLRSCMLSESSLOASKLSKTRTHGAQ
BtTagB-4    278 --DAWLTRVNLAGAQLQLDARGVRLERVDLRGAD-----CRSGNIVGQL
LfTagB      263 ARTIDLTHADLSLSQWRQSDCEGANFTDSNVSFCDFSHANLKHSLEGGCANLNRTNFRHAL
BtTagB-5    263 LSSANARGLRARMSLFSHADCATLAGGHFVYCDFSHATLSRADCTDAFDSHANLHGID
BpTagB-3    263 ARRIDFTGSLDGAVFQRATCTGARFSRAKLEGADFSYADLVGAVFEAGFARTAFHGAT
SmmTagB     263 LDAANFSQARLYQCVFQHSRSARCDYSDSLTYADFCYADLGADFRRARFMRTFMHRAH
AvTagB      252 LAGADFSQACLDMAVLQRTWARGARFERASLRHAEFSYADLVGADFAGALFERTSFHRSL
BbTagB      261 LDGAVFSGADLAQAMLHRARAAGARFDGAGLHWADFSYADLRDADLRGARCLRTQLHRAH

YpTagB      322 IPTL-----DTPLQMPDPLLSQIDNWKYGHQPGPKNNPKFSPSPSGASRYV
BtTagB-4    321 RQ--TWAAADTRDAVFEFATSAIDRLWVQVQPGARGV-----
LfTagB      323 EDGADYSGSSRPLGRETDPELQFAEDFVPRNSP-----
BtTagB-5    323 DRAARWDGACHTGACATDPTLALAEERWTAPER-----
BpTagB-3    323 APAIAWRD--HFGAVACDAELSLAQAWSRQDEQARREEC-----
SmmTagB     323 QQQTRWSD--RSGILESDEELYAAETWSAQEQSRI-----
AvTagB      312 LEDARFDS--RDGLTERDEELWA-----AEERAQAGSRR-----
BbTagB      321 QEGARWDS--RIGVLENDEALYEAEIWSARRRAGP-----

```

Figure 3.8 Amino acid sequence alignment of TagB proteins

Alignment was performed using Clustal Omega and were shaded using BoxShade. Amino acids that are identical at the corresponding position in $\geq 50\%$ of sequences are shown in white font with a black highlight while those that are similar in $\geq 50\%$ of cases are shown in white font with grey shading. YpTagB, *Yersinia pseudotuberculosis* YPTB0650; BtTagB-4, *B.t* BTH_I11891; LfTagB, *Leptospirillum ferrooxidans* LFE_2283; BtTagB-5, *B.t* BTH_I10861; BpTagB-3, *B.p* BPSS0183; SmmTagB, *Serratia marcescens* SMDDB11_2248; AvTagB, *Azotobacter vinelandii* Avin_26570; BbTagB, *Bordetella bronchiseptica* BB0796. Accession numbers of proteins are listed in Table 10.1.

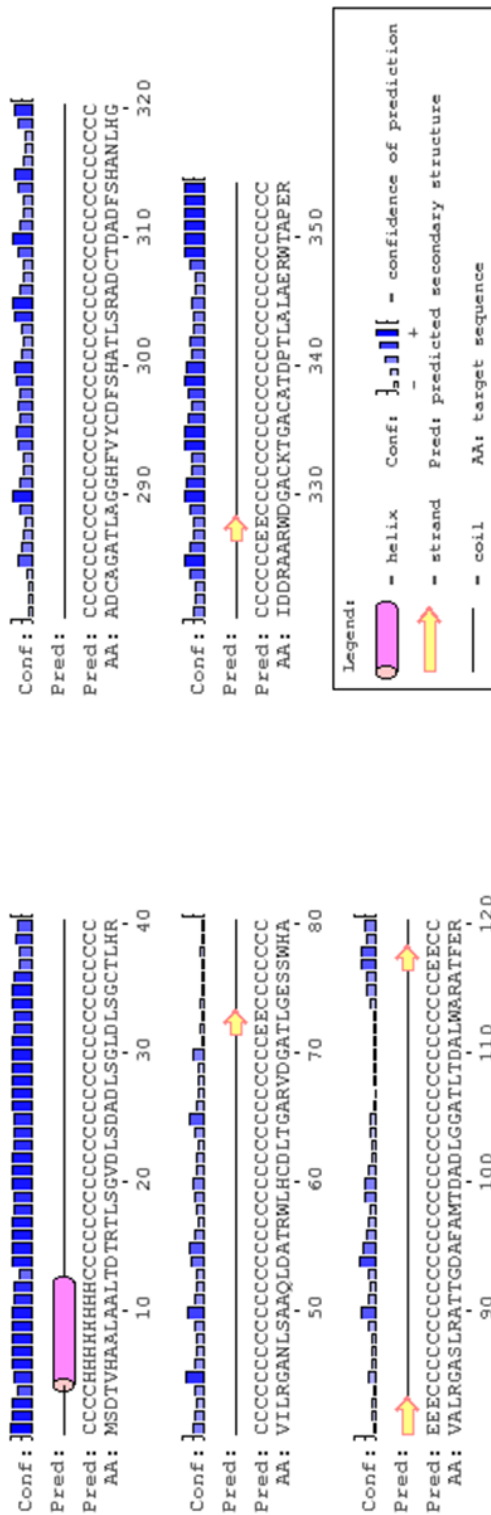


Figure 3.9 Predicted secondary structure of *B.t* TagB-5
 Secondary structure predicted using PSIPRED

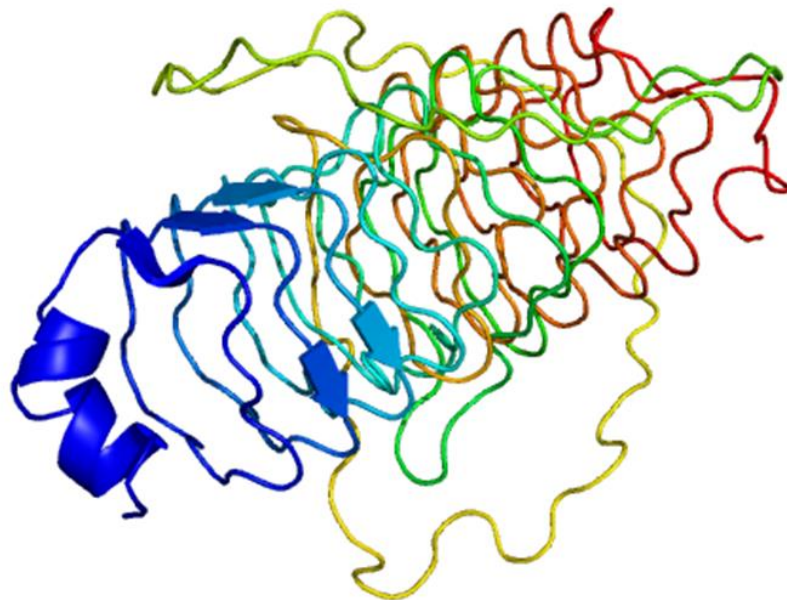


Figure 3.10 Predicted structure of *B.t* TagB-5

Structure predicted using Phyre² displayed in rainbow colours with the N-terminus in blue and C-terminus in red.

3.4.6 Relationship of TagB with 'evolved' TagA

One of the striking things about the occurrence of *tagB* genes in a genome is that, so far, they have only been identified immediately downstream of an evolved *tagA* gene. The relationship is reciprocal in that evolved *tagA* genes, which encode proteins containing an extended C-terminal pentapeptide repeat domain, are always succeeded by a *tagB* gene.

Unsurprisingly, given the presence of the pentapeptide repeats in the CTD of 'evolved' TagA proteins and the fact that TagB is comprised almost entirely of these repeats, there is clear homology between the two proteins when they are aligned (Figure 3.11). As stated previously, the authors of Shalom et al. (2007) designated TagA, 'TagAB' on account of the homology between its CTD and TagB. The proteins display the highest degree of similarity around the hydrophobic phenylalanine and leucine residues which are often the central residue in the pentapeptide repeats. The predicted structures of *B.t* TagA-5 and TagB-5 both contained solenoid-like domains corresponding to the pentapeptide repeat domains, which were similar to the experimentally determined structures of a number of pentapeptide repeat proteins including QrnB1 (Figure 3.12 A-C). The inner face of the solenoid domains is mostly populated with hydrophobic residues such as leucine and phenylalanine (Figure 3.12 D-F). These residues correspond to the central residues in the pentapeptide repeats.

3.4.7 PipB and PipB2

The second type three secretion system (T3SS-2) of *Salmonella typhimurium* secretes, amongst other effectors, PipB (Knodler et al. 2002) and PipB2 (Knodler et al. 2004). Both of these proteins are targeted to lipid rafts of the internal membranes of the infected host cell and PipB2 interacts with the molecular motor protein kinesin-1 (Henry et al. 2006) and a *S. typhimurium pipB2* mutant is attenuated in a mouse model of infection. Like TagA-5 and TagB-5, both of these *S. typhimurium* proteins contain pentapeptide repeats in their C-terminal domains and although they are associated with separate secretion systems, they could play analogous roles in host-pathogen interactions.

3.5 TagC-5

The T6SS-associated gene of the T6SS-5 gene cluster, *tagC-5* (BTH_I10860), is located immediately downstream of *tagB-5* and upstream of *tagD-5*. Comparison of the encoded product with the equivalent *B.p* and *B.m* proteins suggests that the annotation of *tagC-5* in the *B.t* E264 genome has placed the start codon 6 codons early. The corrected *B.t* TagC-5 protein consists of 258 amino acids and has a molecular weight of 27.1 kDa. The sequence of the corrected protein is shown in Figure 3.13.

BtCTDTagA-4 87 ERLSAFEEA----NRNAKLPGAP----RGGENWRTRRQAKTPEIANVTTRDADLSSLR
 YpCTDTagA 82 EQQ-KSEEQETLGDLNVPAAK-----EEAGTQWLE-SKEDTATNVTFLGTDFFSGMT
 YpTagB 1 -----MTPSDTPI MPPD-----SPRRITIGRHFTQRQLQQLT
 BtTagB-4 1 MSK--I-----RSAVPPPLPEI---VEGQRYV-----
 BbCTDTagA 210 LHA--A-----HHQPAAEAARPARAARLRRRVQALMA--GSRDLAGLDLTGADLSGLD
 AvCTDTagA 203 RDS--V-----HCCGAAPALQGAEEALRRKVAQAYA--RDRDLAGMDLTGADLSGLD
 BpCTDTagA-3 163 QQC--A-----QHQPAPARLHGAAARARRECVASAAA--AGQSLQVADLTGADLSGLD
 SmmCTDTagA 182 LMS--A-----QAQSPALRLSGDLAQIIRQRVAAAL--RDKDLSGLDLTGADLSGLD
 LfCTDTagA 235 VRS--V-----HFFAPPPEDRPN-AGRGRQKVLEQMK--SSRNFRKWSLIRGADLSGLD
 BtCTDTagA-5 262 PAS--M-----HAAAPSAGDA-----PPAEPLTREQV--IERHARGHGFACLDLSGLD
 LfTagB 1 -----MT-----PETQKIIVDMIT--DGEPVQEMDLSGFDLSGAD
 BtTagB-5 1 -----MS-----DTVHAALAAIT--DTRTSLSGVLDLSDADLSGLD
 BpTagB-3 1 -----MS-----TRADRIRDATR--HGRAIRDTAIDAGDFDGHHD
 SmmTagB 1 -----MT-----SKPEQIRQRVK--RGEPIAGEDLHGLSFAGLD
 AvTagB 1 -----MR--RGEATEGRALPGLRMAGLE
 BbTagB 1 -----MDAETLRDWR--QGRPLVGHDLRAALQCAD

BtCTDTagA-4 138 FDGWFDDVRFERCTLDRSEWTNCRINQVHAV-----
 YpCTDTagA 132 LDNKQFR----YCMFTGCHFDKATFDCDFEH-----CQFTQSDHE-----
 YpTagB 32 LSEVYFI----QCTFTDISFAEIAVENIHVES-----CHFTHLRLDGGRVENCs
 BtTagB-4 24 -----
 BbCTDTagA 259 LRGARCVGTWMEGADLSCALLDDADLSQAVLAR-----AHAEGGSRRAVLAGAN
 AvCTDTagA 252 LSGARLTGVLLLESANLADARLDGADLEAAILAR-----ARLDGASLRGADCRGAN
 BpCTDTagA-3 212 LRGARLAGAMLENADLSDADLTGADLSRTVLVR-----ADLTRAKLVDARLTAAN
 SmmCTDTagA 231 LCOANLRGALLENANLRQTRLVGCDFREAVLAR-----ADLSGAVLQOQADLSHAS
 LfCTDTagA 283 LSKCDFSS----ESDLICDFSESDLTGSFQGWASHGRFLQTNLSGSKWDGANAGHSE
 BtCTDTagA-5 306 LSSALE----RADL----RDARLERTCFAG-----CRLRGASERALLSRAD
 LfTagB 33 LSHGIFI--NTRATGARFDRCLLNTLFDSS-----CDLSSNMQASSLHLAS
 BtTagB-5 33 LSGCTLH----RVILRCANLSAAQLDATRMLH-----CDLGTGARVMDGATLGESS
 BpTagB-3 33 WSGEVEE----RVRFICVSMKRVRLDEAVFID-----CLFRDVRMRQAGCARCT
 SmmTagB 33 LAGMFIN----ELNNGVNFSDCDLDSVFSDF-----COLEHMQEITRADLQKQTA
 AvTagB 22 LAGGLFR----GCDLSCSDWQGTTLRACDFID-----CALEAADERMARLDEVQ
 BbTagB 31 LAGALLQ----DCDLRGAALAGSRWRDSRFSG-----CRMEQTDVIRGADVAQCA

BtCTDTagA-4 170 -----DCSEADVKMSDGWIKGGKLRQCNLERSAWLNVEIERIS
 YpCTDTagA 169 -----NSRNNVLSGCLFKQAEWQKAAFTHCK
 YpTagB 77 FRFCKFN----DVSAQCVSILNNTSCIEVQWQGCYLIGCLTERWLLTSCQ
 BtTagB-4 24 -----SAQRDVALADTLFVDCHEFERVEWTCRISNLRFVNCT
 BbCTDTagA 309 LGQAAD-----GVDLAGARLSSPVLDGIVLVDCALSSSRWNDCHLAGAR
 AvCTDTagA 302 LSRAQAR-----NACFSGATFGDGQCWEAFETCDFSHARFGGILWQGC
 BpCTDTagA-3 262 LSLAHCE-----RTDFSGSDLSDGIIEQVHLRDCRFNCSVLASTRFDAGR
 SmmCTDTagA 281 LALAKCE-----ATDFGGAQLHETNIQOTLFRQCFITMASLRDLLGYETL
 LfCTDTagA 338 MKGVRAIGASFQ-----KTVLSCGTTTFEDCLLDNSFDFGADLSNISLSRTRAKGCS
 BtCTDTagA-5 346 FSNADIREATFVDAS----APGASFRCAALDRARLAHADFTGADFIRASLADGHCAHAR
 LfTagB 78 FLKCRFH-----RAGFDHAGSQNSRWVESDLSGSRFSDTLNHNSSWVDCV
 BtTagB-5 78 WHAVARGLASLRATTGDAFAMTDADLGGATLTDALVARATFERVDFSAQCARAKLLRCE
 BpTagB-3 78 FDRCRFE-----RVDLSASELRDCMMNGTHAAGVYFSGARASGLHCVKSD
 SmmTagB 78 FNQCAMS-----ASRFESHIELTMNDCLLEQSDFSRLSINQSHWMSQ
 AvTagB 67 WQNCAIA-----DAAFAGAELEERCQLIESGLARAVFDALLGGLAFIQSV
 BbTagB 76 FFRCEIA-----EAVFAAEACAGASWVECFRAGADFRATPLHGSHFVQCA

BtCTDTagA-4 208 LDECRLDLKVGAS-----WSMLSVQGRGG---VRGDRVQDVQW
 YpCTDTagA 197 WE-----KSTFEYGV-FKHAQFDNALDNCLINSEDFSLGTFDHCTL
 YpTagB 122 LDDAQLQDIQLN-----YWTVQDTP-MTHLTMDSKMQDSWGHCTIQQSVWKNSEL
 BtTagB-4 61 FDANRFD-----RCE---LEKLSYESSR-VREGANTQSALQRVSENECEIDGCAMACCLL
 BbCTDTagA 354 LERCRFD-----QAE---LDTVIFWQGTLLRETGFAAARLARVTWLDCELDGLDFAGARL
 AvCTDTagA 347 LDACRFD-----GAV---LEDLSLHACR-LSRPSFVGASLSAVTWVESSLEAADFERAEL
 BpCTDTagA-5 307 FDAVDFG-----RAT---LRELITIEQS-FSGVSESDATIRKMLLMCAFADVRFSEASI
 SmmCTDTagA 326 LGQCDFS-----RAT---LANIILMELQ-LEQLTFSHARLDKVSFVKRLLAVNFSQARL
 LfCTDTagA 388 FPGAREMRIEGALSPSSSQSDGQSERL-FRDVDFSGNLEKSLFMCFLLAVDFSQCQL
 BtCTDTagA-5 401 FDESAMTQLAAARLD---GAHAFAGCA-LDAADFTSARMPRANFQATLTAATFAFAQC
 LfTagB 123 FDGTAFD-----GAD---LEKTSFVHGS-FPGTSFSGAKIIKTAFIQGTLNQAFAGAIIF
 BtTagB-5 138 AADCRFD-----R-----TDFSAELERFSAMFADLSSARFDATRL
 BpTagB-3 123 LGDCGFD-----DAR---IESAVFSDTR-LARAATRAAVRKAVFYRLDITSAVFADAAF
 SmmTagB 123 LAGANFS-----ATQ---HDRTFEYESP-LDGAMLNQARLCLVTFEELNLCKTQFEVNF
 AvTagB 112 LAHASEFD-----EAT---LAETSFNECD-LRDCRFARAHLSETLFLFDLCSVDFAETRF
 BbTagB 121 LDGARLD-----RAE---MREGGTAECT-LEQASLAGAALRQTLFEFADLRTADLAGARL

BtCTDTagA-4 244 NSVSWSEVSA-PGWTWTRVRADDLAIVECAMAGLTVSQCTLA-KPSLLTDLISASVWQRS
 YpCTDTagA 238 NGCFESETHC-DQTQENQVITTSICFEKCDG----PKACFT-ESTLEKTSFISSWVGV
 YpTagB 173 IRQVMGSCVL-----KECQYQ-AIQSDTVVWSQCQLEQV
 BtTagB-4 112 KDVVCSQSKG-GAWTFDAVRGAH-VSL-----VAGEYA-GVTLRGGHSDTSWIGS
 BbCTDTagA 406 RRCAVQSQCGA-PNMGAEI-----QTCCVV-ETDMPHAVFAGATLREC
 AvCTDTagA 398 DDCSLVETRS-PDARFVGAAL-----SACYMVLSSLEAADFGGARLAES
 BpCTDTagA-5 358 DGFGIVETQASGQLRFDRASV-----NKACFVGRCD-GRADFSFAILLTEV
 SmmCTDTagA 377 ESCAVDTET-QSLSEHAARL-----TACAFAAKTLLPQADFSDAILLNQC
 LfCTDTagA 447 PGATFLECCG-PSTTEKRAILTKGVFA-----QSVQFQ-GSSFSGADLSGANLRGV
 BtCTDTagA-5 457 DGAEWYGAQA-SGAQLRSASL-----RGSRAD-A-----STSFRAQ
 LfTagB 174 RNPFIKVSLL-KGIDFSNMSL-----PMVQAS-SSDLSETRWVGSDFRLA
 BtTagB-5 174 TNALLCEADL-RGQRFARCDL-----TMTHLN-GATLAGSDFSGTSLVQT
 BpTagB-3 174 DDTVFAEANL-AGQRLQGQRM-----HRCQFV-GADLRHADFTIGARLAGC
 SmmTagB 174 DRVTFEFCDH-RGKSYAGQSL-----IACQFT-DNQLDDVDFSQAILRQS
 AvTagB 163 ESVIISGSNL-SGQCLMRTSL-----AGCQFS-AALLDGCDLTEAVLSQA
 BbTagB 172 ERVVEVECDL-SGQRLAGQFL-----GGSQFV-EARMDGCDLREASMAQC

BtCTDTagA-4 302 MLT-----FAVLSHGTSI-----NGARLTDCEVKSSSLQELRADRVQVDHCSFMQ-
 YpCTDTagA 291 RLSHCYLNSLTG---LNTNLSSEHFQC SLNKMGLKVNLOS----STFINCSMLE-
 YpTagB 206 DFR-----HQPLENSNFHKSTLTQCGESDANLAA----AL-----
 BtTagB-4 160 RLVDLRLESVGLNLIAGQSGFERAVIVVECRGINVRMIDSRIER----MTVQGCELKQA
 BbCTDTagA 450 SLR-----DTVLDHADFTGAALWRCDLSQASLGG-----
 AvCTDTagA 442 NLR-----GVDLSGARFCGTRLADCDSLSEARLAG-----
 BpCTDTagA-5 403 NFR-----ETQLVEANFGGARIGNCDETDACLRA-----
 SmmCTDTagA 421 NLR-----QMPLQRANFSRARLNNCDLSETRLNE-----
 LfCTDTagA 496 DLS-----GSDFERGAILLGTGSGGNQHTNLSG----VRAIGARFQKT
 BtCTDTagA-5 491 VLS-----GAALDDANWDGVDLRYANLHKATLDR----ASLA-----
 LfTagB 217 NFY-----QSDLTGAVLDGANAEKALFSESRMEG-----
 BtTagB-5 217 MFF-----AADLEGATLAGARGRHVRFADATLVG-----
 BpTagB-3 217 NFQ-----RAKLTGARLDGVDAPNTVEFEADAPD-----
 SmmTagB 217 NFK-----GASLRRANLTSVQAQQSLWLEANLTQ-----
 AvTagB 206 VFK-----DASLVGARLTGVEARYALFPDADLSD-----
 BbTagB 215 NFK-----GASLRRACLAGASGARAMFAQADLGG-----

BtCTDTagA-4	347	-----LNAQHL
YpCTDTagA	341	-----SCCDKADFSQATLIACDVTAVRT-----KDA
YpTagB	237	-----FSEATLEGCDFNMAQLAAAEVVDATLRDCNF-----
BtTagB-4	215	AWSHSTWATGEIHASRLPIASFDHASVNGLTVTNSELPQATFDSASVADSATLQGVRAPRI
BbCTDTagA	479	-----ASLARARAPDSLIFIRADLGGASL-----
AvCTDTagA	471	-----ADLRRATASGCLIFSGADLRTARL-----
BpCTDTagA-5	432	-----ADLRGAKAEGSPFVVRADLTRADL-----
SmmCTDTagA	450	-----ADFRQANGSGSLIFIRSDLRSASL-----
LfCTDTagA	536	D-----LRWVDGRWCDFRQAVFLKADLRFANF-----
BtCTDTagA-5	524	-----RAIASGAQLTSLARRADLTKADL-----
LfTagB	246	-----ASARGAMLKMASFQKTSARTIDL-----
BtTagB-5	246	-----ARLAEAVFDECDLARARLSSANA-----
BpTagB-3	246	-----ATCRDAALRGSLWVQADARRIDF-----
SmmTagB	246	-----AQCRRGGQFDQATFSEATLDAANF-----
AvTagB	235	-----ADCRQCRFAQSVWAGAQLAGADF-----
BbTagB	244	-----ADCSGARMPQSLWADAILDGAVF-----

Figure 3.11 Amino acid sequence alignment of the CTDs of pentapeptide-containing TagA proteins with TagB proteins

Alignment performed using Clustal Omega and shaded using BoxShade. Amino acids that are identical at the corresponding position in $\geq 50\%$ of sequences are shown in white font with a black highlight while those that are similar in $\geq 50\%$ of cases are shown in white font with grey shading. Numbers of the TagA sequences relative to the end of DUF2169. Numbers of the TagB sequences relative to the first residue of the amino acid sequence. BtCTDTagA-4, *B. t* BTH_II0862; YpCTDTagA, *Yersinia pseudotuberculosis* YPTB0649; YpTagB, *Y. pseudotuberculosis* YPTB0650; BtTagB-4, *B. t* BTH_II1891; BbCTDTagA, *Bordetella bronchiseptica* BB0795; AvCTDTagA, *Azotobacter vinelandii* Avin_26580; BpCTDTagA-5, *B. p* BPSS0182; SmmCTDTagA, *Serratia marcescens* subsp. *marcescens* SMDB11_2247; LfCTDTagA, *Leptospirillum ferrooxidans* LFE_2282; BtCTDTagA-5, *B. t* BTH_II0862; LfTagB, *L. ferrooxidans* LFE_2283; BtTagB-5, *B. t* BTH_II0861; BpTagB-3, *B. p* BPSS0183; SmmTagB, *S. marcescens* SMDB11_2248; AvTagB, *A. vinelandii* Avin_26570; BbTagB, *B. bronchiseptica* BB0796. Accession numbers of proteins are listed in Table 10.1.

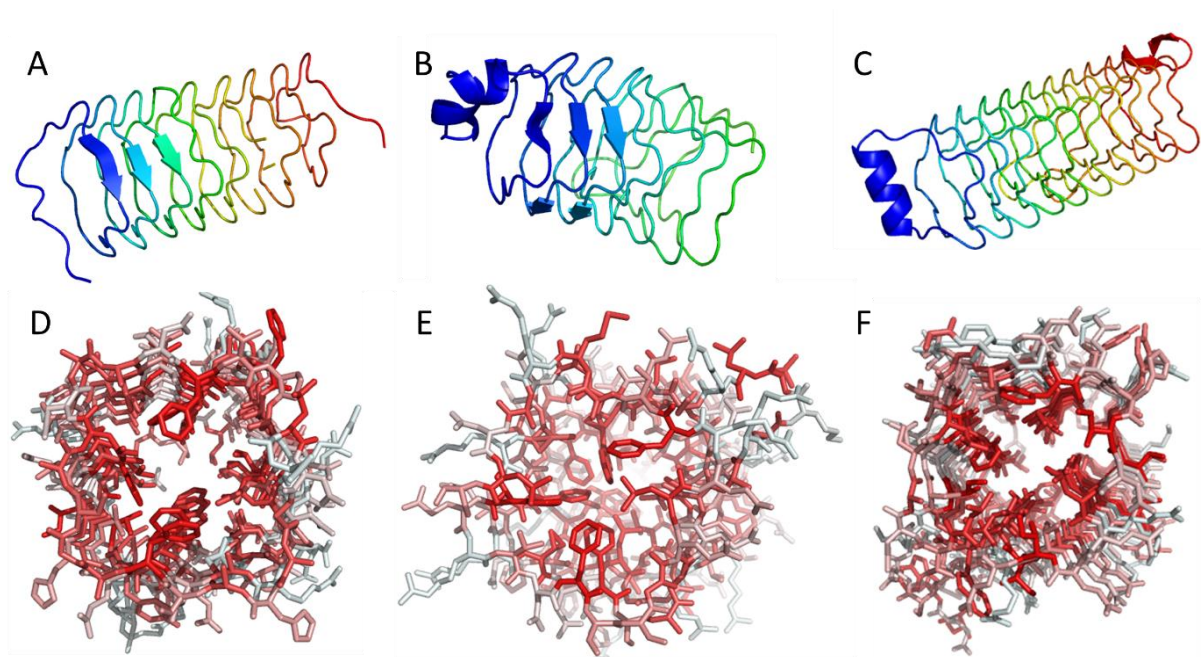


Figure 3.12 Comparison of the predicted ‘solenoid’ structures of TagA-5 and TagB-5 with the solved structure of QnrB1

A-C) Displayed in rainbow colours with the N-terminus in blue and C-terminus in red. A) Predicted solenoid-like domain of TagA-5 extending from residues 664 to 843. B) Section of the predicted TagB-5 structure extending from residues 1 to 163. C) Structure of QnrB1. D-F) View down the centre of the solenoid structures coloured according to hydrophobicity with the most hydrophobic residues displayed in red. D) Predicted solenoid-like domain of TagA-5 extending from residues 664 to 843. E) Section of the predicted TagB-5 structure extending from residues 16 to 163. F) Structure of QnrB1.

3.5.1 TagC proteins in *Burkholderia pseudomallei* group members

The *B.t* TagC-5 protein shares 76.5% identity with the *B.p* TagC-5 protein (encoded by BPSS1506) and 75.7% identity with the *B.m* TagC-5 protein (encoded by BMAA0735). The *B.p* and *B.m* TagC-5 proteins share 98.4% sequence identity. There are two *tagC* genes present in the *B.t* genome (*tagC-4* and *tagC-5*), compared with three in the *B.p* and *B.m* genomes (*tagC-3*, *tagC-4* and *tagC-5*).

3.5.2 Protein family analysis of TagC

Entering the *B.t* TagC-5 amino acid sequence into the BLASTP search engine identified amino acids 48 through to the C-terminus as corresponding to a DUF3540 domain (Figure 3.13). Proteins of this family are found only in T6SS gene clusters and little is known concerning the structure or function of this domain. Entering the same sequence into the InterPro search engine also identified the DUF3540 domain (which extends from residue 52 to 258 in *B.t* TagC-5) and a prokaryotic membrane lipoprotein lipid attachment signal sequence at the N-terminus of *B.t* TagC-5. The designation of proteins containing the DUF3540 as 'TagC' was based on the nomenclature of Shalom et al. (2007).

3.5.3 Cellular location of TagC-5

Further investigation into the putative lipoprotein signal sequence using the Prosite search suggests that *B.t* TagC-5 is post-translationally modified by the addition of a lipid to the cysteine residue at position 18 and the removal of the N-terminal 17 residues by proteolytic cleavage between residue 17 and 18 by signal peptidase II. The mature lipoprotein is then translocated across the inner membrane and anchored into either the inner or outer membranes. However, when the amino acid sequence of *B.p* TagC-5 was entered into the same Prosite search, it is not indicated as a lipoprotein. This is because the first cysteine residue is located at position 67 in *B.p* TagC-5. In fact, of the 8 TagC proteins encoded by the genomes of *B.t*, *B.p* and *B.m*, only *B.t* TagC-5 has a putative lipid attachment site according to Prosite. The absence of a signal sequence for lipid attachment in other TagC proteins suggests that TagC-5 is also not a lipoprotein.

PSORTb was unable to predict the cellular location of TagC-5 (note that PSORTb does not identify lipoproteins) and the TMHMM program did not detect any transmembrane helices. The SignalP server did not detect a Sec or Tat-dependent signal peptide in TagC-5. A TagC protein of *Yersinia pestis* KIM6+ (y3663, which is identical to the *Y. pseudotuberculosis* YPTB0651 protein in the alignment in Figure 3.14) was detected in culture supernatants, suggesting TagC proteins might be secreted.

3.5.4 Amino acid sequence alignments of TagC homologues

Proteins to enter into the alignment were selected using the InterPro database of DUF3540 proteins. As shown in Figure 3.14, there is a conserved amino acid sequence motif around the proline at residue 80 in TagC-5 as well as a hydrophobic region around the alanine at position 112. It is unclear what the

MTHDSRASMTTTPSFYSCSCASASSCAGAAAPRPPADAPSAPHADASLRACRVTGRAGDWLSLDDPAGRARRADGCLLV
PDLGDHVLIWAPAHARSHPGGDASGAPHAYVLAVLARAGAPRAALALPGGVALEAGADGLRIDAPRIALAAARERIDACA
PRFDVSAHRARVHAAHLDARAQSIDGRAHDVRLVARRFTSTIGRALHTLGDCFRRVCGVDDLRAARARWRIDERAHLHA
RDVALLADRHVGDGERIDLG

Figure 3.13 Amino acid sequence of *B.t* TagC-5

Annotated amino acid sequence of *B.t* TagC-5, highlighted sequence indicates the coverage of DUF3540 domain.

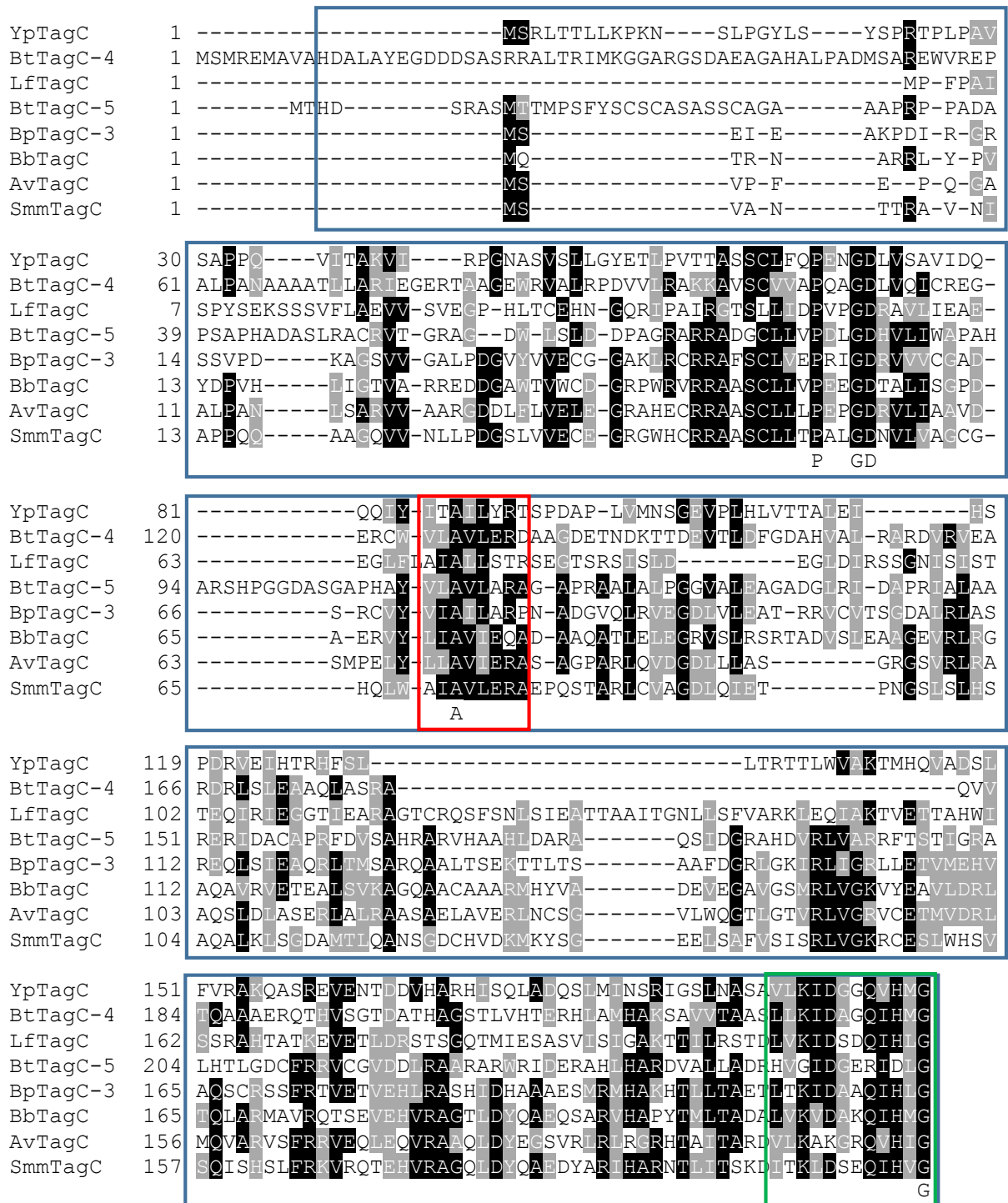


Figure 3.14 Amino acid sequence alignment of TagC proteins

Alignment was performed using Clustal Omega, shading performed using BoxShade. Amino acids that are identical at the corresponding position in $\geq 50\%$ of sequences are shown in white font with a black highlight while those that are similar in $\geq 50\%$ of cases are shown in white font with grey shading. Blue box indicates the DUF3540. Red box indicates conserved hydrophobic section. Green box indicates conserved C-terminal residues. Residues conserved across all sequences indicated below the alignments. YpTagC, *Yersinia pseudotuberculosis* YPTB0651; BtTagC-4, *B.t* BTH_II1890; LfTagC, *Leptospirillum ferrooxidans* LFE_2284; BtTagC-5, *B.t* BTH_II0860; BpTagC-3, *B.p* BPSS0184; BbTagC, *Bordetella bronchiseptica* BB0806; AvTagC, *Azotobacter vinelandii* Avin_26560; SmmTagC, *Serratia marcescens* subsp. *marcescens* SMDB11_2249. Accession numbers of proteins are listed in Table 10.1.

significance of these regions is. It is also interesting that a C-terminal glycine residue is almost absolutely conserved throughout the TagC proteins (all but four of the 545 DUF3540 proteins in the InterPro database have a C-terminal glycine residue).

3.5.5 Structure prediction of TagC-5

The secondary structure of *B.t* TagC-5 was predicted using PSIPRED, this anticipated that TagC-5 was primarily organised into beta-strands and a single alpha helix (residues 193 to 204) (Figure 3.15). The 3D structure of *B.t* TagC-5 was predicted by entering the amino acid sequence into the Phyre² server. This was only able to model 52% of residues at over 90% confidence (Figure 3.16). Interestingly the top template used to model TagC-5 was the Enterobacteria phage P2 spike protein, GpV. As such, the predicted structure bears some resemblance to a monomer of the tail spike protein. As the amino acid sequences of the DUF3540 proteins and the phage GpV spike proteins do not show a convincing alignment (Figure 3.17), it is unclear how robust this structure prediction is. Compared to the predicted secondary structure, there are few beta-strands present in the structure predicted by Phyre² and is largely disordered. There is also a single alpha helix extending from residue 191 to 213; this is in a similar location to the one predicted by PSIPRED.

3.6 TagD-5

The fourth *tag* encoded by the T6SS-5 gene cluster is *tagD-5* (BTH_II0859). According to the annotated *B.t* E264 genome the *tagD-5* open reading frame is 120 codons in length which encodes an 11.98 kDa protein. However, based on alignments with the *B.t* and *B.m* TagD-5 proteins, the actual start of the *B.t tagD-5* open reading frame is likely to be located a further 33 bp upstream, extending the open reading frame to 131 codons that gives rise to a 13.09 kDa protein. Therefore, all the bioinformatics described below was performed based on the assumption that the longer ORF is correct.

3.6.1 TagD proteins in *Burkholderia pseudomallei* group members

Of the five T6SS gene clusters present in the *B.t* genome, there is a *tagD* gene present in two of them; T6SS-4 and T6SS-5. In *B.p* and *B.m* there is an additional *tagD* encoded within T6SS-3 (TagD-3). There are no TagD proteins encoded outside of T6SS gene clusters in *B.p* and *B.m*. However, in *B.t*, the BTH_II0236 gene locus, which is not located within a T6SS gene cluster, encodes a TagD protein which does not appear to have any obvious *B.p* or *B.m* equivalent. The closest match is to *B.p* TagD-3 (the T6SS-3 gene cluster is absent in *B.t*) with which it shares 55% identity.

The *B.t* TagD-5 protein shares 90.8% identity with the *B.p* and *B.m* TagD-5 proteins (encoded by BPSS1507 and BMA0734, respectively) indicating there is a good chance that the *B.t* protein performs a similar function to its *B.p* and *B.m* homologues. The *B.p* and *B.m* TagD-5 proteins are identical.

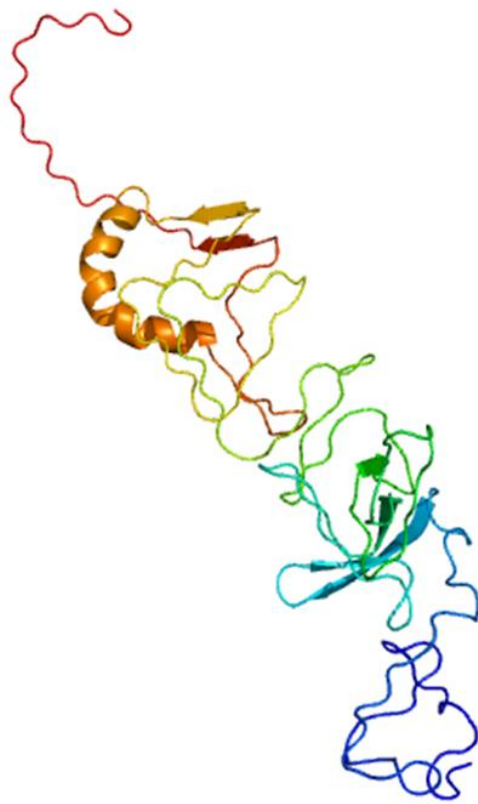


Figure 3.16 Predicted structure of *B.t* TagC-5

Structure of *B.t* TagC-5 as predicted by Phyre² displayed in rainbow colours with the N-terminus in blue and C-terminus in red.

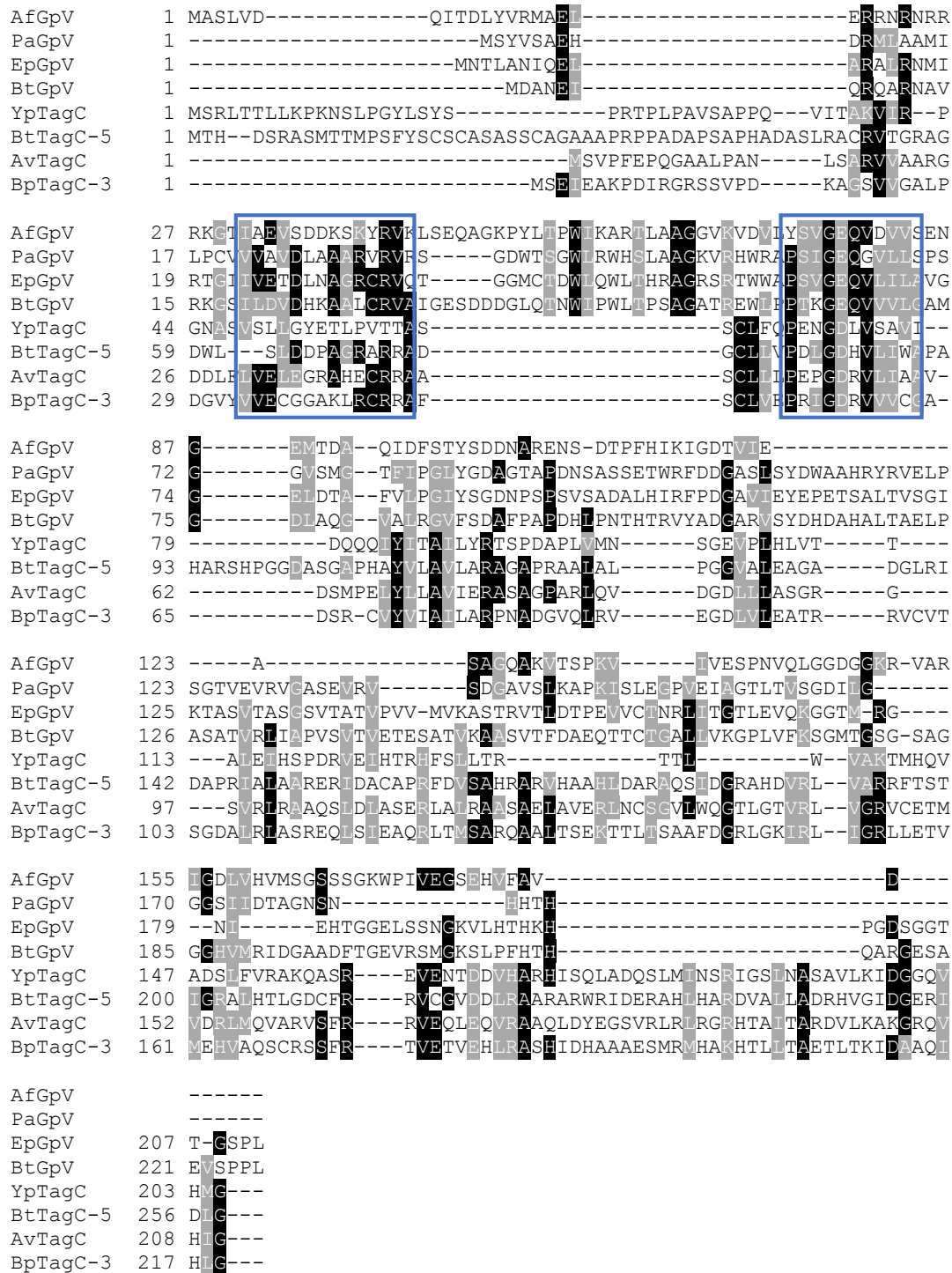


Figure 3.17 Amino acid sequence alignment of TagC and phage GpV proteins

Amino acid alignment of the indicated proteins performed using Clustal Omega and shaded using BoxShade. Amino acids that are identical at the corresponding position in $\geq 50\%$ of sequences are shown in white font with a black highlight while those that are similar in $\geq 50\%$ of cases are shown in white font with grey shading. Blue boxes indicate conserved sequences. AfGpV, *Agrobacterium fabrum* Atu0454; PaGpV, *Pseudomonas aeruginosa* PA0616; EpGpV, Enterobacteria phage P2 V; BtGpV, *B.t* BTH_II1337; YpTagC, *Yersinia pseudotuberculosis* YPTB0652; BtTagC-5, *B.t* BTH_II0860; AvTagC, *Azotobacter vinelandii* Avin_26560; BpTagC-3 *B.p* BPSS0184. Accession numbers of proteins are listed in Table 10.1.

3.6.2 Protein family analysis of TagD

When the amino acid sequence of TagD-5 was submitted to the BLASTP search tool, the conserved PAAR_4 domain was identified. The PAAR_4 family falls within the PAAR(proline-alanine-alanine-arginine) like superfamily which contains eight members, PAAR_1 to PAAR_5, PAAR_RHS, PAAR_CT_1 and PAAR_CT_2 (the final three are grouped according to their C-terminal extensions). One of the members of the PAAR superfamily, PAAR_1 has been shown to form a sharp conical extension which sits on top of the Tssl spike. The PAAR proteins are believed to assist in puncturing the target cell and may act as adapters which facilitate interactions between Tssl and effector proteins (Shneider et al. 2013). The PAAR_4 and PAAR_CT_2 families are unusual amongst the PAAR_like superfamily in that they do not possess conserved histidine or cysteine residues which are present in all other PAAR_like superfamily members. In PAAR_1 family members, these residues co-ordinate a zinc atom which stabilises the protein (Shneider et al. 2013).

The region of TagD-5 which falls within the PAAR_4 domain group based on amino acid sequence homology extends from amino acid 16 to 118. Some PAAR superfamily proteins possess effector domains (referred to as 'evolved') such as *Pseudomonas aeruginosa* PA0099 which contains an endonuclease domain. TagD-5, however, only appears to contain the 'ancestral' PAAR_4 domain.

Searching the TagD-5 sequence using the Pfam database indicates that TagD-5 contains the domain of unknown function 4150 (DUF4150). This domain extends from residue 10 to 117 (Figure 3.18) and therefore encompasses a very similar region to the PAAR_4 domain. Only the PAAR_4 family of proteins contain DUF4150 and all of the PAAR_4 proteins contain a DUF4150, suggesting that they are the same. According to InterPro, domains containing DUF4150 are found across the proteobacteria. Based on the nomenclature of Shalom et al. (2007) I consider genes encoding proteins containing DUF4150 (and hence PAAR_4) to be a '*tagD*'.

3.6.3 Cellular location prediction of TagD-5

PSORTb was unable to assign a putative cellular location for TagD-5 and submitting the amino acid sequence of TagD-5 to the SignalP 4.1 server suggested that TagD-5 is unlikely to have a signal peptide. TMHMM did not identify any transmembrane helices.

3.6.4 Amino acid sequence alignments of TagD homologues

As shown in Figure 3.19, alignment of the TagD-5 amino acid sequence with those of other selected proteins of the DUF4150 family, clearly demonstrates regions of homology which define the DUF4150 domain. The proteins appear to form two groups within the DUF4150 family. At first glance it appears that this is down to the presence or absence of a C-terminal effector domain (i.e. evolved and ancestral TagD proteins, respectively). However, the *B. bronchiseptica* protein included in the alignment has a

MFVVTASGLCMSPADVCKTPTPGGPVPIYPNTGLPMAASITTKVLVCGMPALTKKSTIPMTNGDQPGTAGGAVSGK
IMGKVEFAAGSAKVKLEGS PAVRLTPTKHNDGNATGAVLQPSQQKVMVMS

Figure 3.18 Amino acid sequence of *B. t* TagD-5

Amino acid sequence of *B. t* TagD-5. Coloured box above the sequence indicates the extent of the protein that corresponds to DUF4150. Sequences highlighted in orange indicates the putative sites of interaction with Tssl-5 based on the predicted 3D structure (Figure 3.23).

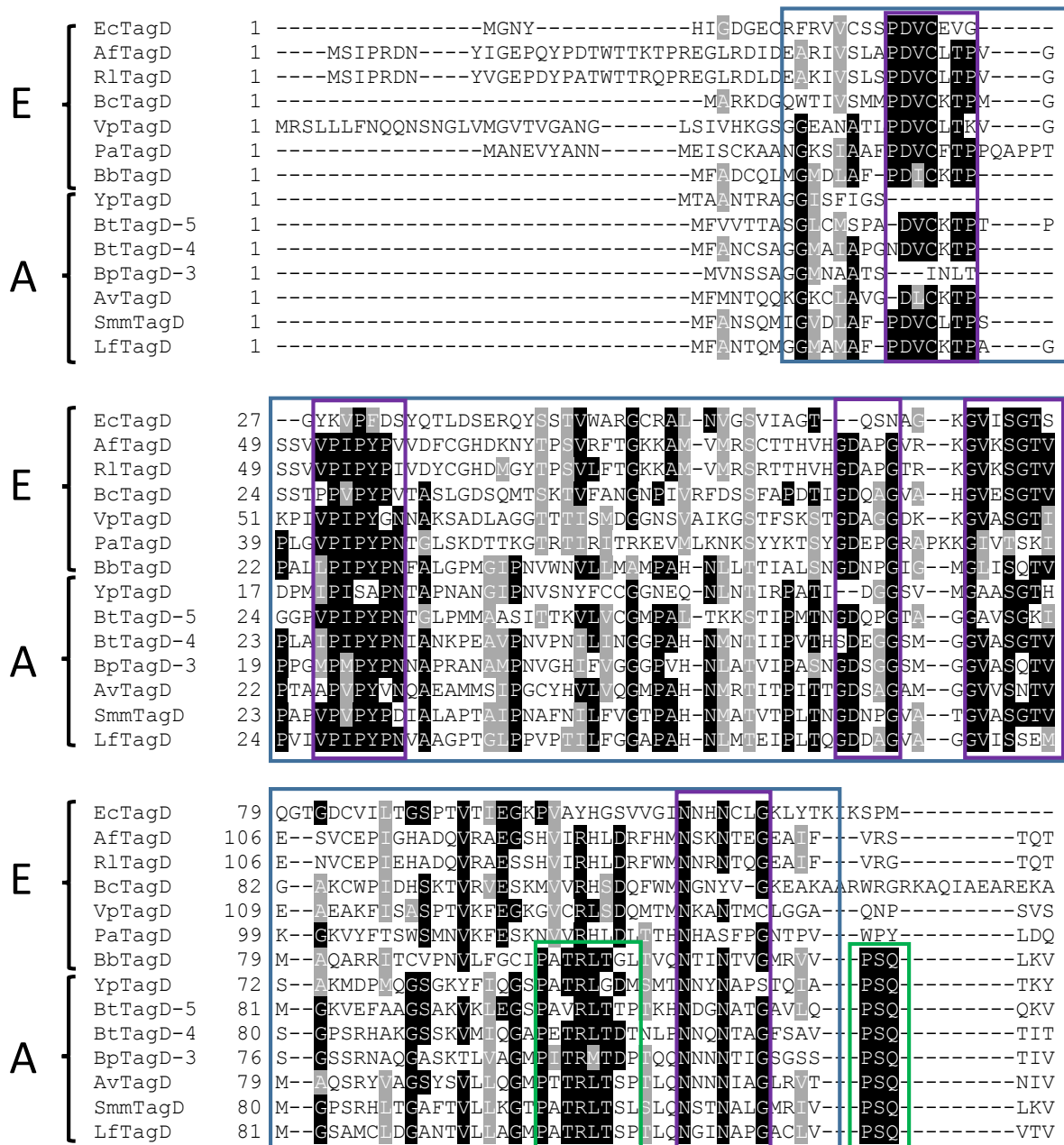


Figure 3.19 Amino acid sequence alignment of selected 'DUF4150' family proteins

Alignment carried out between members of the DUF4150 family using Clustal Omega, shading performed using BoxShade. Amino acids that are identical at the corresponding position in $\geq 50\%$ of sequences are shown in white font with a black highlight while those that are similar in $\geq 50\%$ of cases are shown in white font with grey shading. Only the region extending from the N-terminus to the C-terminal end of the DUF4150 domain for each protein is shown as there was little homology after the DUF4150. E, evolved. B, Ancestral. Blue box outlines the DUF4150. Purple boxes highlight conserved residues which make up the DUF4150. Green boxes indicate conserved residues unique to Tag proteins encoded by genes in T6SS gene clusters where all four tag genes are present. EcTagD, *E. coli* UT189_C0255; AfTagD, *Agrobacterium fabrum* Atu3640; RlTagD, *Rhizobium leguminosarum*, pRL120482; BcTagD, *Burkholderia cenocepacia* BCAL1296; VpTagD, *Vibrio parahaemolyticus* VP1415; PaTagD, *Pseudomonas aeruginosa* PA0099; BbTagD, *Bordetella bronchiseptica* BB0797; YpTagD, *Yersinia pseudotuberculosis* YPTB0652; BtTagD-5, *B.t* BTH_II0859; BtTagD-4, *B.t* BTH_II1889; BpTagD-3, *B.p* BPSS0185; AvTagD, *Azotobacter vinelandii* Avin_26550; SmmTagD, *Serratia marcescens* subsp. *marcescens* SMDB11_2250; LfTagD, *Leptospirillum ferrooxidans* LFE_2285. Accession numbers of proteins are listed in Table 10.1.

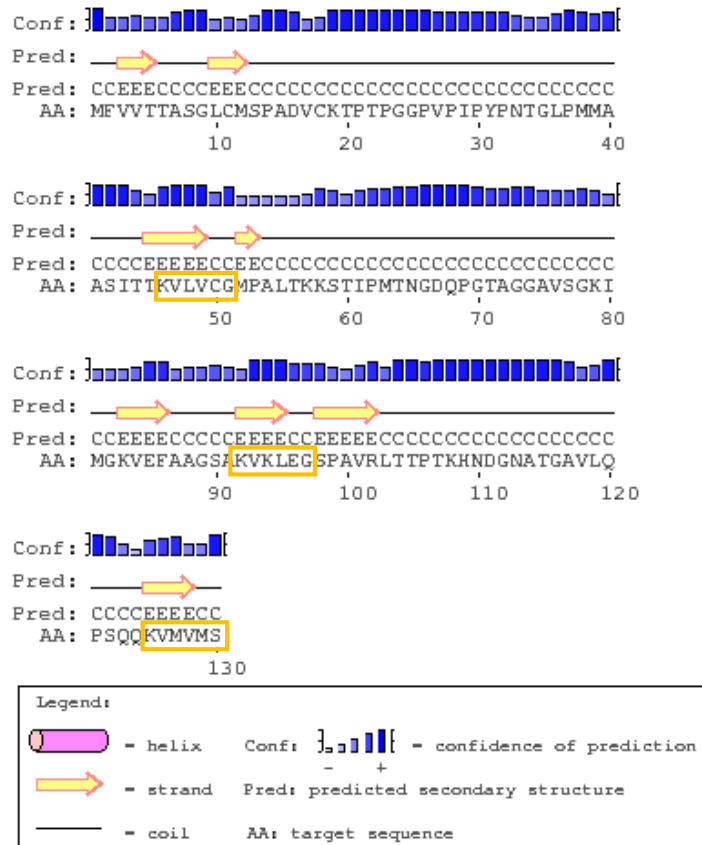


Figure 3.21 Predicted secondary structure of *B.t* TagD-5

Prediction of the secondary structure of *B.t* TagD-5 performed by PSIPRED. Orange boxes indicate sequence predicted to be at the base of the predicted 3D structure of TagD-5 (Figure 3.23).



Figure 3.22 Structure of c1882 with gp5

Crystal structure of a single *E. coli* c1882 molecule (tan) in complex with a trimeric gp5 (Enterobacteria phage T4)-TssI (c1883) chimera (red), 4JIW in the protein data bank. Image adapted from the structure solved by (Shneider et al. 2013).

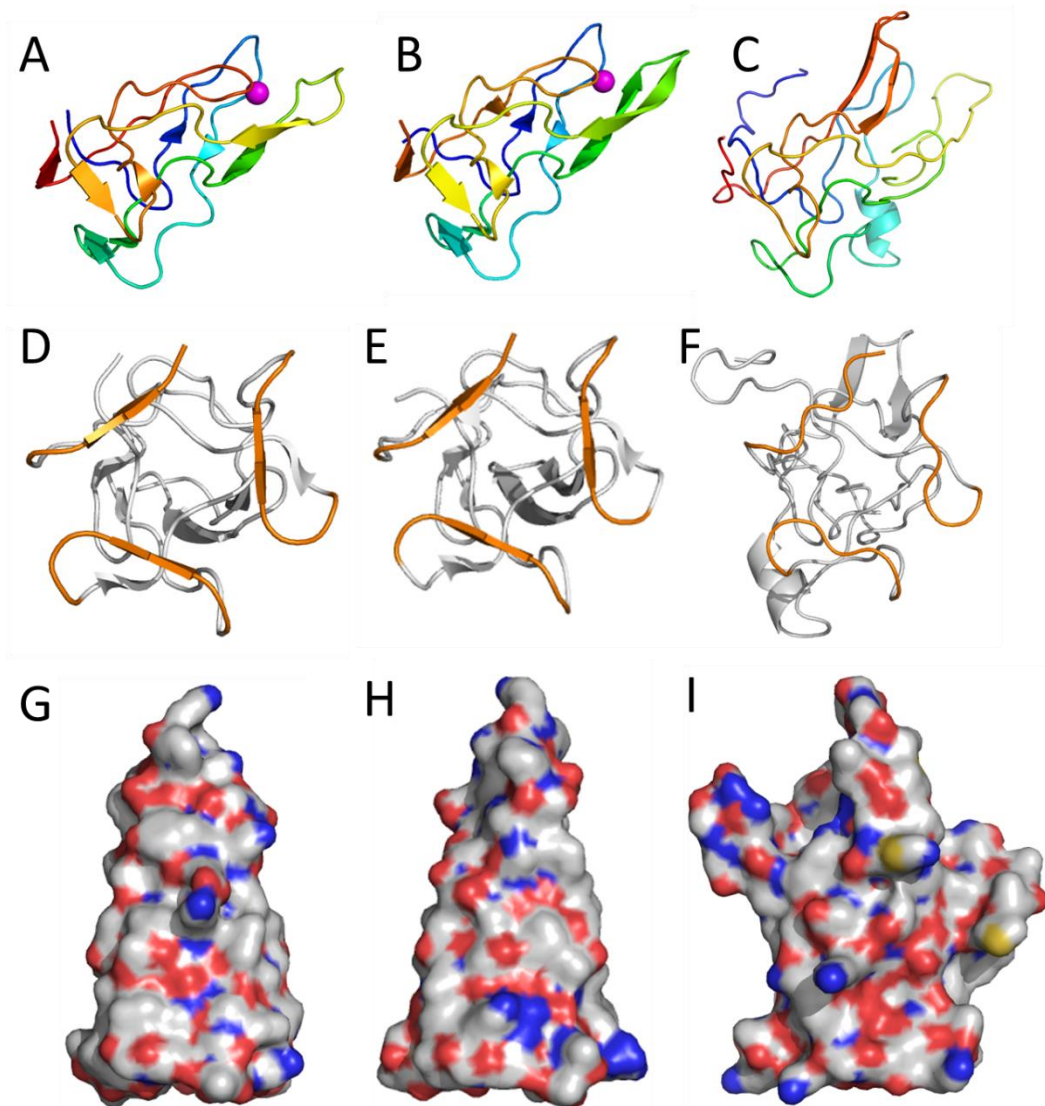


Figure 3.23 Comparison of known structures of PAAR proteins with the predicted structure of TagD-5

A-C) Displayed in rainbow colours with the N-terminus in blue and C-terminus in red, zinc atoms in magenta. A) Structure of *E. coli* c1882 (4KU0 in the protein data bank). B) Structure of *V. cholerae* VCA0105 (4JIV in the protein data bank). C) Predicted structure of *B.t* TagD-5. D-F) Structures viewed from below, coloured in grey apart from the putative interaction sites with Tssl-5 in orange. D) Structure of *E. coli* c1882. E) Structure of *V. cholerae* VCA0105. F) Predicted structure of *B.t* TagD-5. G-I) Surface representation of structures coloured by element (carbon in grey, nitrogen in blue, oxygen in red and sulphur in yellow) viewed from the side showing conical shape. G) Structure of *V. cholerae* VCA0105. H) Structure of *E. coli* c1882. I) Predicted structure of *B.t* TagD-5. Images presented using PyMol. Solved structures adapted from (Shneider et al. 2013).

triangular base-like structure (Figure 3.23 D-F). Although the predicted structure indicates these regions are unstructured in TagD-5, the secondary structure prediction (Figure 3.21) indicates that they are likely to form beta-strands as do the corresponding regions in the PAAR proteins. In the experimentally determined structures of VCA0105 and c1882, the equivalent residues which make up the base of the cone facilitate interaction with an engineered TssI protein (Figure 3.22). Therefore, in TagD-5, this platform presumably facilitates the interaction of a single TagD-5 protein with the TssI-5 trimer. The first amino acid each of the hexa-peptide motifs is a lysine which is followed by a valine residue (Figure 3.18). The alignments with other TagD proteins did not show any conserved residues around this sequence (Figure 3.19).

One of the differences observed when TagD and PAAR_1 proteins are aligned (Figure 3.20) is that TagD-5 does not contain the conserved histidine and cysteine residues which co-ordinate the zinc atom in PAAR_1 proteins (displayed in magenta in Figure 3.23 A&B). The zinc atom is believed to stabilise the fold of the PAAR protein. Although the overall shape of the PAAR proteins and the predicted shape of TagD-5, is conical (Figure 3.23 G-I), in TagD-5 there are projections, this is because the three loops (which are brought into close proximity in the PAAR proteins by the stabilising zinc atom) are further apart, preventing the formation of a sharp tip. It is possible that other residues (such as arginines, lysines or glutamines) co-ordinate a zinc atom in TagD-5 to form a sharp tip as is observed in the PAAR proteins.

3.7 Discussion

A summary of the predicted roles of the Tag proteins is given in Table 3.1. Although it is present in T6SS-related proteins from a variety of species, it is unclear what role the conserved DUF2169 core domain of TagA-5 plays. It is also not clear why in some cases it is present as the core protein with an evolved TagD and why in others it is present in the evolved form (i.e. possessing a pentapeptide repeat CTD) together with TagB, TagC and core TagD proteins. The PipB and PipB2 proteins of another intracellular pathogen, *S. typhimurium*, are secreted effectors which have C-terminal pentapeptide repeat domains. Although PipB and PipB2 are exported by the T3SS, it is logical to suggest that TagA-5 and TagB-5 could be secreted effector proteins that are attached to the TssI-5. However, the members of the pentapeptide repeat family perform a wide array of functions including conferring resistance to fluoroquinolone antibiotics (Vetting et al. 2011). The fact that, so far, *tagB* genes have only been located immediately downstream of 'evolved' *tagA* genes suggests that they might interact with one another. The observations of Pieper et al. (2009) suggest that TagA and TagB might be membrane proteins, while there are no transmembrane helices present in either protein, it is possible that they interact with another membrane bound component of the T6SS.

The same study which identified TagA and TagB as membrane proteins, also detected TagC in culture supernatants, suggesting it could be a secreted effector. Other than this, few predictions can be made of the role of TagC-5 as the DUF3540 domain has not been studied and it does not contain any known functional domains. It is possible that it interacts with TagA-5 or TagB-5 as *tagC* genes have only been found in gene clusters where the pentapeptide repeats are present.

TagD-5 demonstrated homology with the PAAR proteins, which allowed its structure to be predicted with a high degree of confidence. This suggests that TagD-5 is likely to function in a manner similar to the PAAR proteins; sharpening the TssI-5 tail spike. If this is the case, then TagD-5 would be expelled into the culture medium alongside TssI-5 during firing of T6SS-5. Although TagD-5 does not contain any of the C-terminal effector domains that are seen in evolved DUF4150 family members, it could act as an adapter, enabling the interaction of effectors with TssI-5 and facilitating their delivery into the target cell. *tagD* genes in T6SS gene clusters which also contained *tagA*, *tagB* and *tagC* encoded a conserved tripeptide sequence (PSQ) C-terminally to the DUF4150, which was not found in other TagD proteins. It is unclear what this motif is for.

Table 3.1 Summary of bioinformatic predictions

Protein	Predicted function	Similar proteins	Predicted structure
TagA	Secreted effector protein	<i>S. typhimurium</i> PipB and PipB2	TagA 'core domain' unclear, C-terminal pentapeptide repeat domain predicted to be solenoid-like.
TagB	Secreted effector protein	<i>S. typhimurium</i> PipB and PipB2	Predicted to be solenoid-like.
TagC	Secreted effector protein	None known	Unclear.
TagD	PAAR protein, sharpening the TssI 'tail spike' protein	PAAR proteins	Triangle based pyramid.

Chapter 4 Investigating the role of the
T6SS-5 *tag* genes in multinucleated giant
cell formation and intracellular
replication of *B. thailandensis*

4.1 Introduction

In tissues infected with *Burkholderia pseudomallei* (*B.p*) and *B. mallei* (*B.m*), one of the major histopathological features is the presence of distinctive multinucleated giant cells (MNGCs), formed by the fusion of neighbouring cells which is thought to facilitate the spread of the bacterium within the body of the host. This effect on eukaryotic cells can also be observed when a variety of cell types are infected with *B.p* or *B.m* *in vitro*. MNGC formation is also observed when eukaryotic cells are infected with the closely related, but non-virulent relative of *B. pseudomallei*; *B. thailandensis* (*B.t*). Previous studies have shown that strains of *B.p*, *B.m* and *B.t* containing mutations in genes encoding components of one of the type six secretion systems (T6SS-5) are capable of invasion, escape from endosomes into the cytoplasm and replication (to a varying degree) within eukaryotic cells, but not formation of giant cells, indicating that MNGC formation is a T6SS-5 specific phenotype (French et al. 2011).

To date, the specific cause of the giant cell formation has not been elucidated. However, one of the interesting features of the gene cluster encoding T6SS-5 (Figure 1.3) is the presence of four Type VI associated genes (*tags*) designated *tagA*, *tagB*, *tagC* and *tagD*. Although homologous genes are present in some of the T6SS gene clusters present in other bacteria, and indeed those encoding T6SS-4 of *B.p*, *B.m* and *B.t* and T6SS-3 of *B.p* and *B.m* (this system is absent in *B.t*), they are not present in all of them. Based on the fact that the *tag* genes are located immediately downstream of the gene encoding the tail spike protein, TssI, and the observation that it is not uncommon for effector proteins secreted by T6SSs to be encoded immediately downstream of *tssI* we hypothesised that the Tag proteins were secreted. Furthermore, due to the observation that *tagA-5* and *tagB-5* are similar to the *Salmonella typhimurium* T3SS effectors *pipB* and *pipB2*, respectively, it was hypothesised that they could encode T6SS-5 secreted effector proteins responsible for MNGC formation. If this was the case, then the inactivation of *tagA-5* and *tagB-5* would eliminate MNGC formation. Additionally, *tagD-5* encodes a protein which contains a PAAR domain, such proteins are proposed to be associated with TssI proteins and are required for its penetration of target cells. Again if this hypothesis was correct then deletion of *tagD-5* would likely impair the function of T6SS-5 and have an effect on MNGC formation. As there have so far been no investigations into the role of *tagC*-like genes it was also included as a candidate gene required for MNGC formation due to its genomic location with the T6SS-5 gene cluster.

4.2 MNGC formation assays

4.2.1 *B. thailandensis* induces the formation of MNGCs in vitro

Before it could be determined if the *tag* genes had any effect on the formation of MNGCs it was first necessary to confirm that the formation of giant cells could be observed when eukaryotic cells were infected with a wild type (WT) strain of *Burkholderia thailandensis* (E264). RAW 264.7 mouse macrophage-like cells were utilised in these assays as previous studies have shown that they form giant cells when infected with WT *B.p* and *B.m* but not when T6SS-5 is inactivated (Burtnick et al. 2010; 2011). RAW cells were seeded at 2×10^5 cells/ml and infected 14-18 hours later with *B. thailandensis* cells suspended in DMEM containing 10% foetal calf serum (DMEM-FCS), at a multiplicity of infection (MOI) of 10 bacterial cells to 1 eukaryotic cell. Wells containing RAW cells were also left uninfected to act as a control, but were treated in an identical fashion to the infected cells henceforth. Two hours after infection, each well was washed three times with PBS before the addition of 1 ml DMEM-FCS with 250 µg/ml kanamycin to kill extracellular bacteria. Sixteen hours after the initial infection, wells were washed three times with PBS and fixed with 100% ethanol for 30 minutes. The ethanol was removed and wells were left to dry for 30 minutes before the addition of 100% Giemsa. After 5 minutes staining, each well was rinsed with tap water to remove excess stain. The image of one random field of view per well was captured using the 10 x objective of a Leica DMI4000B inverted microscope. The number of nuclei contained within single membranes which contained three or more nuclei (giant cells) were counted along with the total number of nuclei. The number of nuclei within giant cells was divided by the total number of nuclei and multiplied by 100 to give the fusion index as a percentage. Three independent repeats were performed for the uninfected and *B. thailandensis* infected cells.

As shown in Figure 4.1, MNGC formation could be observed in wells infected with WT *B. thailandensis* but not in wells to which bacteria were not added. Membranes and nuclei could be distinguished, and the fusion index was calculated to be ~20%, but there was a very high standard deviation. This was probably a result of not imaging enough fields of view therefore not having many nuclei per repeat.

4.2.2 Construction of a *B. thailandensis* *tssK-5* mutant

In order to determine whether or not the *tag* genes were involved in MNGC formation it was necessary to have a control strain which lacked a functional T6SS-5 and therefore was unable to form MNGCs *in vitro*. Based on a previous study by Schwarz et al. (2010) which demonstrated that the deletion of *tssK-5* attenuates *B.t* in a mouse infection model and the observation that *tssK* is present in all T6SS gene clusters and is required for function by the T6SS (Zheng & Leung 2007), *tssk-5* (BTH_II0857) was selected for inactivation.

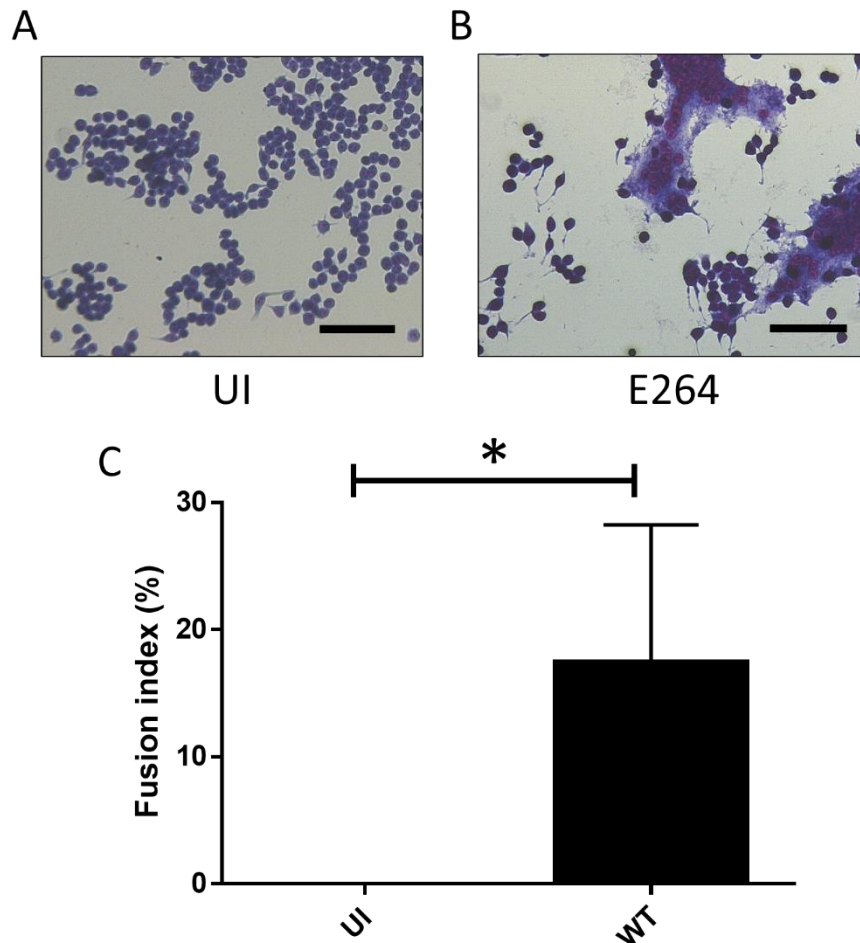


Figure 4.1 Confirmation of giant cell formation in RAW 264.7 cells infected with *B. thailandensis*

RAW 264.7 macrophage-like cells were infected at a MOI of 10:1 and stained with Giemsa diluted 1:20 in PBS. Images were obtained using the 20 x objective of a Nikon Eclipse TS100 microscope. A) Uninfected cells. B) Cells infected with *B. thailandensis*. Scale bars = 75 μ m C) Fusion index calculated over three independent repeats in; UI, uninfected cells; WT, cells infected with WT *B. thailandensis* E264. Error bars represent one standard deviation. An unpaired *t*-test was performed using GraphPad Prism **P* < 0.05.

To avoid polar effects on expression of downstream genes, it was decided to generate a markerless in-frame deletion of *tssK*. To achieve this, the splice overlap extension PCR (SOE-PCR) method was employed to generate the mutant allele (Horton et al. 1989) which was introduced into the *B. t* genome by the allelic replacement method described by Barrett et al. (2008) as outlined in Figure 4.2. For the SOE-PCR, a PCR (PCR1) was performed using KOD hot start polymerase, with a boiled lysate prepared from WT *B. thailandensis* as a template and primers *tssKSOEfor2* and *tssKSOEmidrev* (a and b, respectively, in Figure 4.2) to generate the 536 bp fragment α containing the final 416 bp of *tssJ* and the first 78 bp of *tssK*. PCR2 was performed using the same conditions but with *tssKSOErev2* and *tssKSOEmidfor* (d and c respectively in Figure 4.2) to generate the 498 bp fragment β which contained the final 123bp of *tssK* and the first 368 bp of *tssL*. These two fragments contained a 36 bp region of overlap introduced by primers *tssKSOEmidrev* and *tssKSOEmidfor* which facilitated the fusion of α and β in the next step. Fragment α and fragment β were purified by gel extraction before being combined and used as a template for PCR3 which yielded the 1034 bp fragment γ . This fragment, retaining the first 78 bp (26 codons) and final 123 bp (41 codons) of the *tssK-5* open reading frame, but lacking the central 1194 bp (398 codons), was digested with the restriction enzymes *Acc65I* and *BamHI* which cut at the restriction sites introduced by the *tssKSOEfor2* and *tssKSOErev2* primers. This digested fragment was then ligated into the pEX18Tp-*pheS* suicide plasmid (4487 bp) which had been digested using the same enzymes. Competent *E. coli* JM83 cells were transformed with the ligation mixture and plated onto M9 agar containing 25 $\mu\text{g/ml}$ trimethoprim, 1% (w/v) casamino acids, 0.5% (v/v) glycerol, 0.0005% (w/v) thiamine, 40 $\mu\text{g/ml}$ X-gal and 0.1 $\mu\text{g/ml}$ IPTG followed by incubation for two nights at 30°C. Several white colonies were used to inoculate cultures in 4 ml of IST broth containing 25 $\mu\text{g/ml}$ trimethoprim and grown at 37°C overnight. Plasmids from these cultures were isolated by plasmid miniprep and electrophoresed in an agarose gel to identify a construct of the correct size (5501 bp) which was confirmed by determining the nucleotide sequence of the insert (performed by the University of Sheffield core sequencing facility).

The resulting pEX18Tp-*pheS*- Δ *tssK* plasmid was then used to transform the *E. coli* SM10(λ pir) conjugal donor strain and subsequently delivered into WT *B. thailandensis* by conjugation. Exconjugants were selected on M9 agar containing 50 $\mu\text{g/ml}$ trimethoprim. As pEX18Tp-*pheS* derivatives are *colE1*-based replicons, they are only capable of replication in *E. coli* strains and therefore, in the context of other species, pEX18Tp-*pheS* is a suicide plasmid. Selection for the antibiotic resistance marker contained on the plasmid results in creation of strains in which the plasmid has integrated into the genome through a single crossover recombination event occurring at the locus that is homologous to the region carried on the plasmid. Therefore, trimethoprim resistant exconjugants were either the result

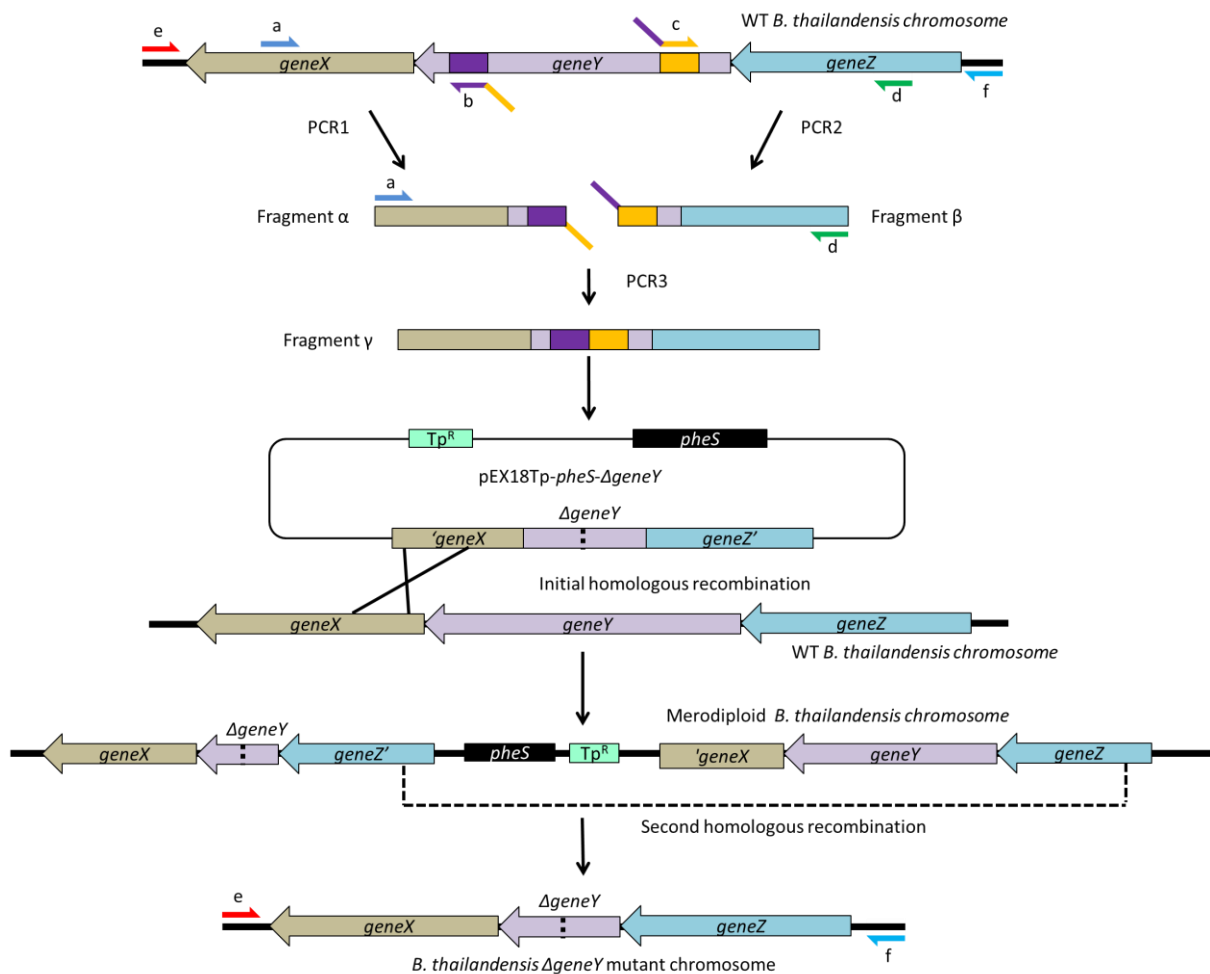


Figure 4.2 Schematic illustration of the deletion of *B. thailandensis* genes by splice overlap extension PCR and homologous recombination.

B. thailandensis boiled lysate was used as a template along with primer *a* and primer *b* in the reaction PCR1 which generated fragment α . The same template was used with primer *c* and primer *d* in PCR2 to generate fragment β . Primer *b* contained an 18 bp 3' extension which was the reverse complement of the annealing site of primer *c*. Primer *c* contained an 18 bp 5' extension which was the reverse complement of the annealing site of primer *b*. These overlapping complementary extensions facilitate the annealing of fragment α and fragment β when they are used as templates in PCR3 which used the primers *a* and *d*, generating fragment γ containing *geneY* lacking its central sequence. Fragment γ was then cloned into the *pEX18Tp-pheS* suicide vector which was introduced into *B. thailandensis* by conjugation. Integration of the plasmid into the chromosome by homologous recombination was selected for by resistance to trimethoprim. The excision of the plasmid from the chromosome was selected for by the ability to grow on plates containing chlorophenylalanine. Resulting colonies containing the deletion were identified by a PCR screen using primers *e* and *f*.

of plasmid integration into the chromosome facilitated by homologous recombination with the T6SS-5 sequence located either side of the *tssK* gene lacking its central portion present on the suicide vector, or spontaneous mutants.

Colonies of various size were streaked onto fresh M9 agar containing 50 µg/ml trimethoprim to purify them. pEX18Tp-*pheS* contains the *B.p pheS* (BPSL1941) gene engineered by codon substitution to reduce nucleotide homology and encode a PheS protein with a single A304G mutation (Barrett et al. 2008). PheS is the α subunit of the phenylalanyl tRNA synthase protein. The A304G mutant PheS protein can charge tRNA^{Phe} with the toxic phenylalanine analogue *p*-chlorophenylalanine (cPhe). Therefore, culturing bacteria containing this *pheS* marker in the presence of cPhe results in cell death and it can be used to counter-select strains harbouring the plasmid. Colonies containing the integrated pEX18Tp-*pheS*- Δ *tssK* were then streaked onto M9 agar containing 0.1% (w/v) *p*-chlorophenylalanine (cPhe) which only allowed the growth of colonies in which the mutant *pheS* gene had been lost in a second recombination event. Colonies growing on M9 cPhe agar were restreaked onto fresh M9 cPhe agar. Colonies growing on this second plate were used to prepare a boiled lysate which was used as a template in a diagnostic PCR with GoTaq using the tagDSOEmidfor and tssKscrnrev primers (corresponding to e and, f respectively, in Figure 4.2) which annealed upstream and downstream of the annealing sites for tssKSOEfor2 and tssKSOErev2 primers, respectively. When the desired deletion was introduced into the chromosome, this reaction amplified a 1749 bp fragment, in contrast to a 2942 bp fragment generated from the WT strain (Figure 4.3 D).

4.2.3 Effect of deletion of *tssK-5* on MNGC formation induced by *B. thailandensis*

The empty pBBR1MCS vector was introduced into the WT and Δ *tssK-5* strains of *B. thailandensis* by conjugation. The resulting exconjugants were chloramphenicol resistant, allowing the overnight cultures used in the infection assays to be grown in LB containing chloramphenicol to reduce the risk of contamination.

Overnight cultures of WT pBBR1MCS and Δ *tssK* pBBR1MCS were grown in LB containing 250 µg/ml chloramphenicol. The cultures were washed twice with PBS before the OD₆₀₀ was determined. This solution was used to inoculate DMEM-FCS with 1 x 10⁶ cells/ml *B. thailandensis*. RAW267.4 cells seeded at 1 x 10⁵ cells/well of a 24 well plate 12-16 hours previously were infected by replacing the culture medium with 1 ml of the *B. thailandensis* cell solution. Two hours' post-infection, the wells were washed twice with PBS before the addition of 1 ml DMEM containing 10% FCS and 250 µg/ml kanamycin. 16 hours post infection, wells were washed three times with PBS and fixed with ethanol for 30 minutes. After fixing, wells were allowed to dry and cells were stained using 100% Giemsa for five minutes before rinsing with tap water to achieve the desired staining intensity.

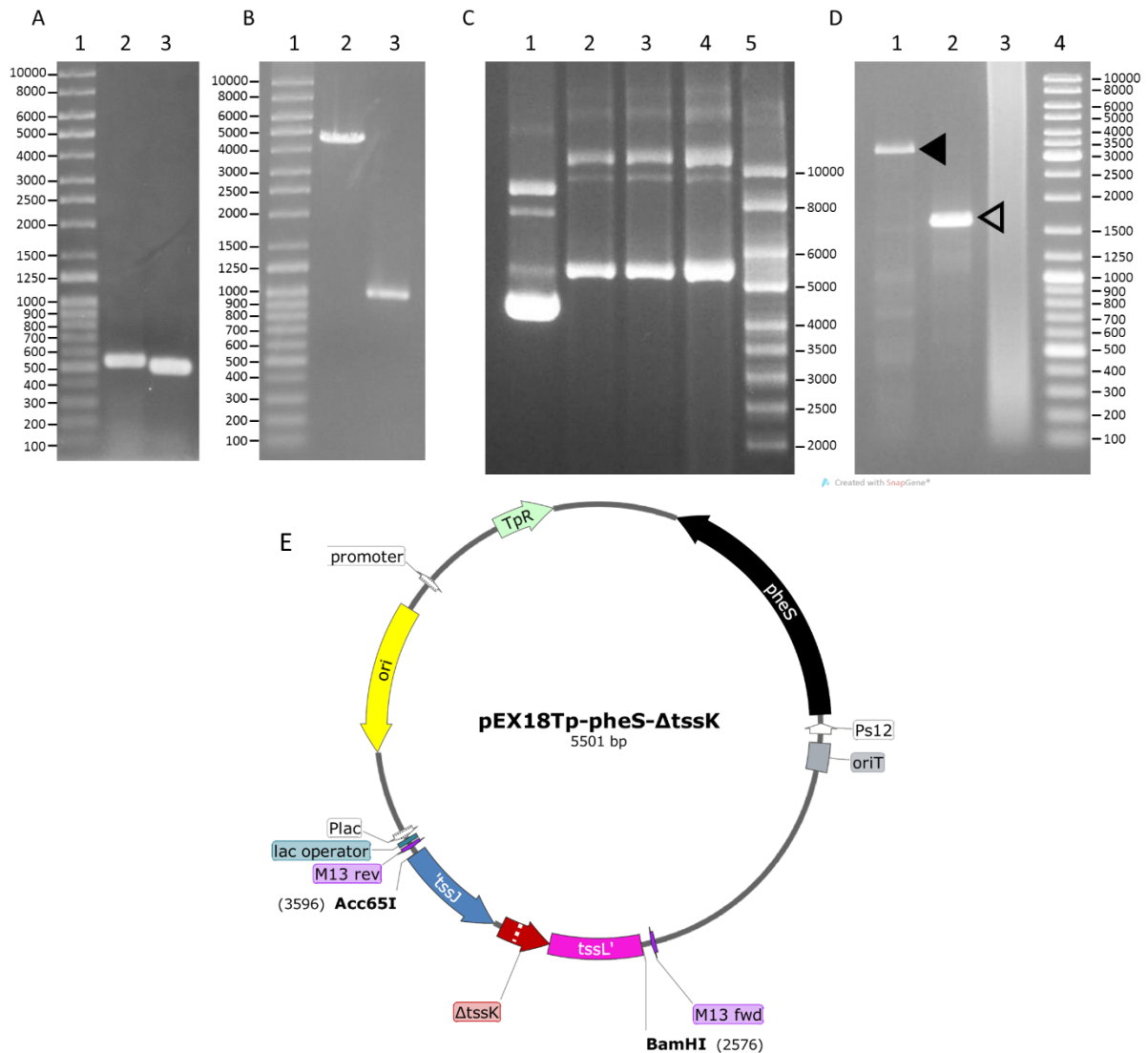


Figure 4.3 Construction of the *B. thailandensis* $\Delta tssK$ strain

A) Agarose gel electrophoresis analysis of DNA fragments amplified from a WT boiled lysate template using KOD polymerase. Lane 1, QStep4 DNA ladder; lane 2, Fragment α produced using *tssKSOEfor2* and *tssKSOEmidrev* primers, lane 3; Fragment β produced using *tssKSOErev2* and *tssKSOEmidfor* primers. B) Agarose gel electrophoresis of digested pEX18Tp-*pheS* and the DNA fragment γ amplified by KOD PCR using fragments α and β as a template and the primers *tssKSOEfor2* and *tssKSOErev2*. Lane 1, Qstep4 DNA ladder; lane 2, pEX18Tp-*pheS* digested with Acc65I and BamHI; lane 3, Fragment γ digested with Acc65I and BamHI. C) Agarose gel electrophoresis analysis of plasmid DNA prepared by miniprep from cultures inoculated with colonies of JM83 transformed with the products of a ligation between pEX18Tp-*pheS* and *tssK* fragment γ . Lane 1; empty pEX18Tp-*pheS* vector; lanes 2-4, plasmid DNA isolated from cultures inoculated with colonies of JM83 predicted to contain pEX18Tp-*pheS*- $\Delta tssK$; lane 5 supercoiled DNA ladder. D) PCR screen to identify $\Delta tssK$. A *B.t*-pEX18Tp-*pheS*- $\Delta tssK$ recombinant was challenged with cPhe and cPhe-resistant Tp-sensitive colonies were screened by PCR screen with the primers *tagDSOEmidfor* and *tssKscrnrev*. Products were analysed by agarose gel electrophoresis. Lanes 1-3, cPhe-resistant colonies; lane 4, Generuler DNA ladder. Solid black arrowhead indicates the size fragment expected when the WT gene is present, open arrowhead indicates the size expected when $\Delta tssK$ is present. Numbers indicate size in base pairs E) Plasmid map of pEX18Tp-*pheS*- $\Delta tssK$ created using SnapGene.

As indicated in Figure 4.4 B the WT *B. thailandensis* strain containing pBBR1MCS was able to form MNGCs in RAW cells, indicating that the presence of this vector did not effect that ability of *B.t.* to form MNGCs *in vitro*. However, the $\Delta tssK-5$ strain was incapable of MNGC formation (Figure 4.4 C), suggesting that *tssK-5* is required for T6SS-5 activity, validating the use of this strain as a control.

4.2.4 Construction of a *tssK-5* complementation plasmid

Although the marker-less in-frame deletion method had been used to minimise potential polar effects, it was necessary to confirm that the observed changes in phenotype were due to the specific mutations introduced rather than polar effects resulting from, for example, the altered expression of neighbouring genes caused by these mutations. This was carried out by performing a complementation experiment in which a wild type copy of the inactivated gene is introduced into the mutant gene *in trans*. To re-introduce the wild type copy of the deleted genes *in trans* they were amplified and cloned into the broad host-range pBBR1MCS plasmid (Kovach et al. 1995). This vector was chosen as it confers resistance to the antibiotic chloramphenicol. It was necessary to avoid plasmids which contained a kanamycin resistance gene as kanamycin would be used in the MNGC formation and replication assays to prevent the extracellular growth of bacteria. Previous studies have also successfully used pBBR1MCS to re-introduce the WT versions of genes into mutants in *B.p* (Suparak et al. 2005), suggesting that the *lac* promoter present upstream of the multiple cloning site is sufficiently active in *B.p* to provide adequate expression of the cloned gene. Given the similarities between *B.t* and *B.p* it was reasoned that pBBR1MCS would be suitable for complementation in *B.t* also. It is also convenient that the vector allows blue/white screening, making the cloning process easier.

To prevent the generation of a LacZ fusion protein when the gene was cloned into the multiple cloning site of pBBR1MCS, in each case, the forward primer was designed to introduce a stop codon in frame with the *lacZ* start codon. To illustrate the principle, the example of the construction of pBBR1MCS-*tssK* is outlined. The strategy for cloning the wild type copies of the other genes used in complementation experiments was identical but using the appropriate primers and restriction enzymes. Boiled lysate was prepared from WT *B. thailandensis* and used as a template for a PCR using the proofreading Q5 polymerase and the *tssK*compfor and *tssK*comprev primers to generate a 1428 bp DNA fragment containing the *tssK* gene together with 16 bp of the upstream transcribed region that includes the native Shine-Dalgarno sequence. The forward and reverse primers contained a HindIII and a BamHI restriction site, respectively, at their 5' end. These restriction enzymes were then used to digest the *tssK* gene amplicon and the pBBR1MCS vector to give a linear fragment of 4683 bp (Figure 4.5 A). The resulting fragments were ligated together and the ligation mixtures were used to

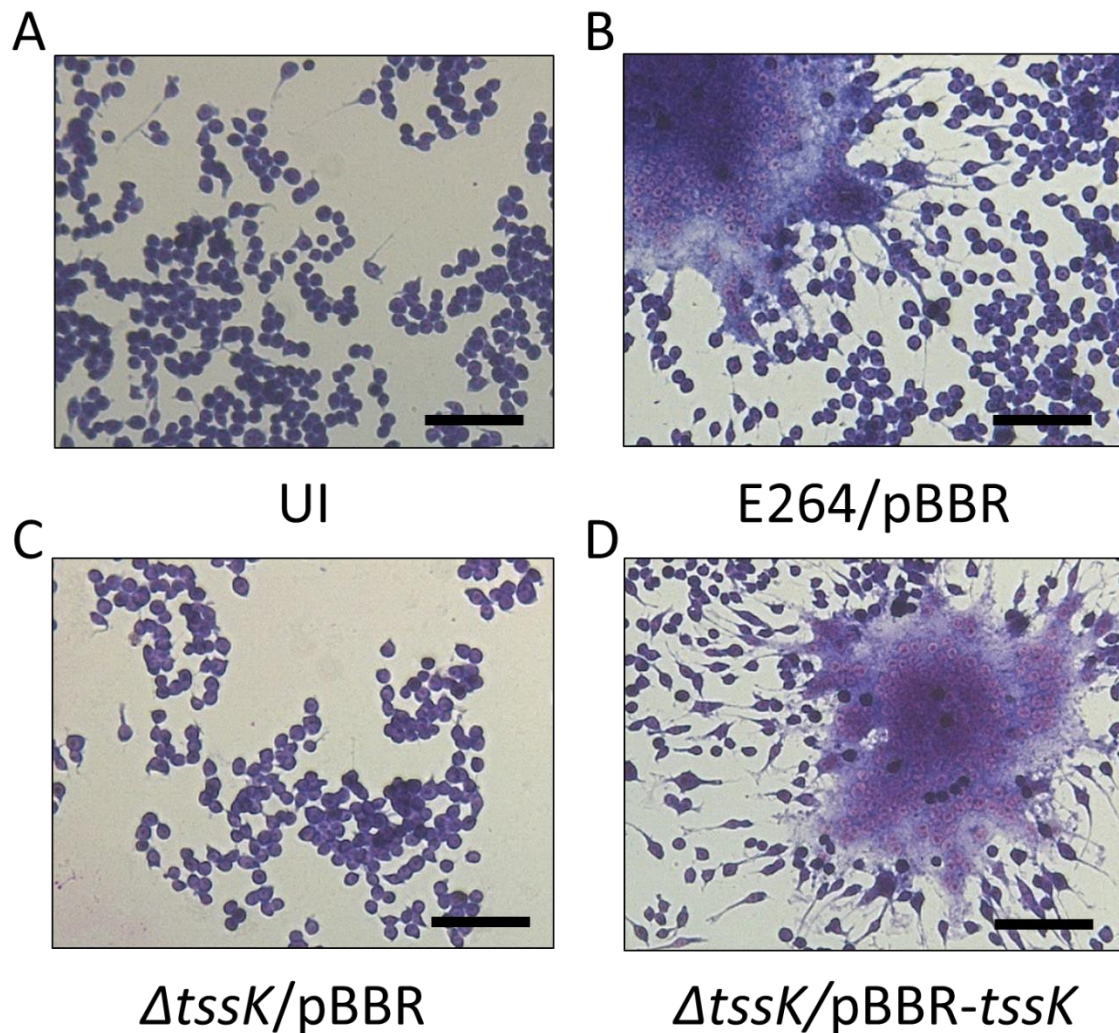


Figure 4.4 Effects of the deletion of *tssK* gene of the *B. thailandensis* T6SS-5 gene cluster

RAW 264.7 cells infected at a MOI of 10:1 for 16 hours before fixing with ethanol and staining with Giemsa. Images acquired using the 10x objective of a Leica DMI4000B inverted microscope magnified to make nuclei visible. A) UI, Uninfected. B) E264/pBBR, WT *B. thailandensis* containing pBBR1MCS. C) $\Delta tssK/pBBR$, *B.t* $\Delta tssK$ containing pBBR1MCS. D) $\Delta tssK/pBBR-tssK$, *B.t* $\Delta tssK$ containing pBBR1MCS-*tssK*. Scale bar = 75 μ m.

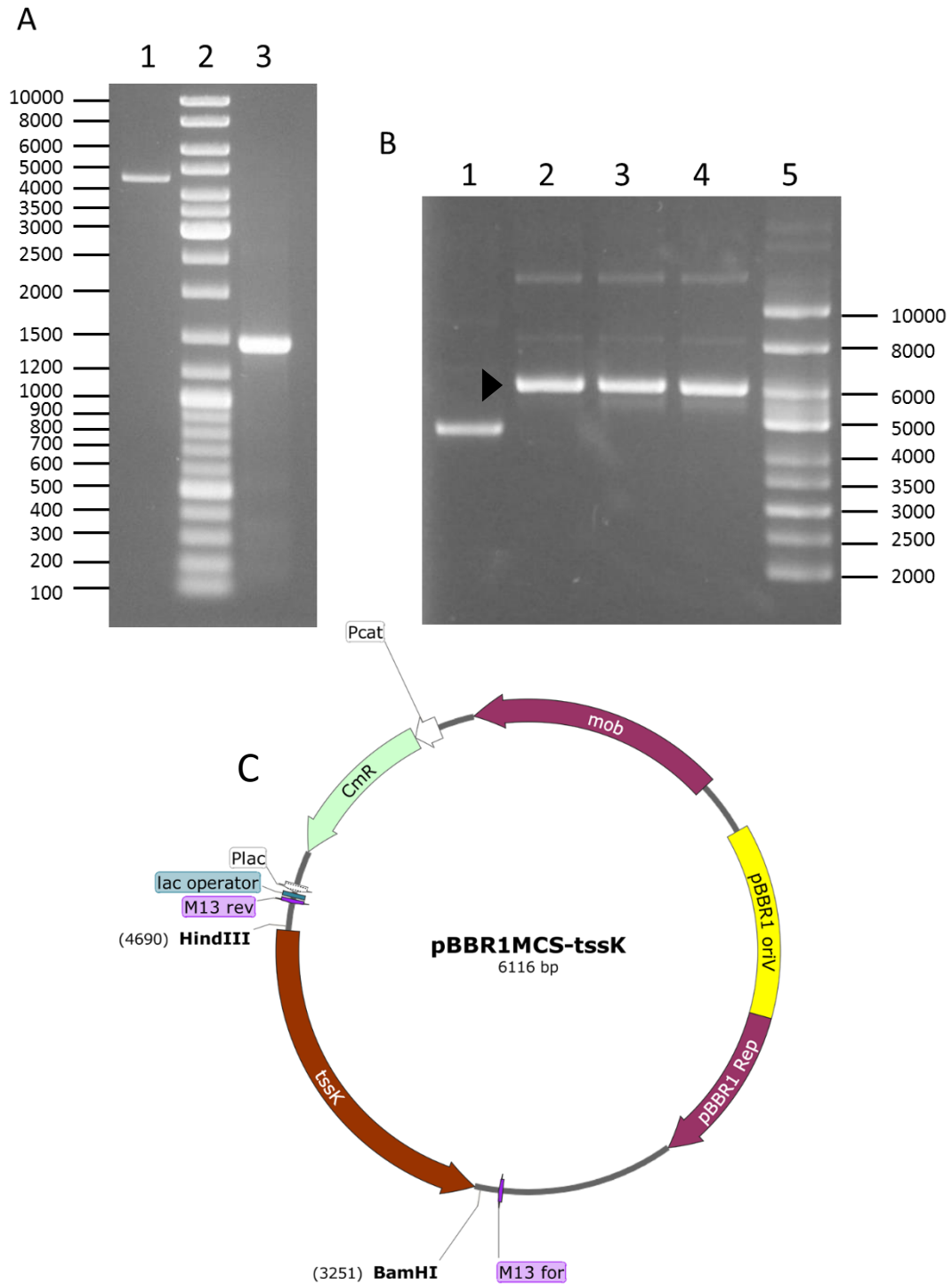


Figure 4.5 Construction of pBBR1MCS-tssK

A) Agarose gel electrophoresis of vector and *tssK* PCR DNA fragment digested with HindIII and BamHI. Lane 1, pBBR1MCS; lane 2, Generuler DNA ladder; lane 3, DNA fragment containing the *tssK* gene. B) Agarose gel electrophoresis of plasmids isolated from overnight cultures of *E. coli* pBBR1MCS transformants which were predicted to contain the desired insertion based on PCR screening of colonies using the M13for and M13rev primers. Lanes 1-4; colonies 1-4; Lane 5, Supercoiled DNA ladder. Black arrowhead indicates the predicted size of pBBR1MCS-tssK. DNA size markers are shown in bp. C) Plasmid map of pBBR1MCS-tssK generated using SnapGene viewer.

transform *E. coli* JM83 cells. These cells were spread on LB agar containing 25 µg/ml chloramphenicol, 100 µM IPTG and 40 µg/ml Xgal. White colonies were screened for the presence of the desired insert using GoTaq polymerase with the M13forward and M13reverse primers. A colony producing the correct sized fragment (1633 bp) was used to inoculate an overnight culture, the 6116 bp plasmid was harvested from these cells by the miniprep method (Figure 4.5 B) and the plasmid sequenced to confirm it contained the correct fragment (Figure 4.5 B).

4.2.5 Re-introduction of the WT *tssK-5* gene into the *tssK-5* mutant restores MNGC formation *in trans*

The pBBR1MCS-*tssK-5* plasmid was used to transform *E. coli* SM10(λpir) cells, following which it was introduced into the *B. thailandensis* Δ*tssK-5* mutant by conjugation. The conjugation mixtures were spread on M9 minimal agar plates containing 250 µg/ml chloramphenicol to select for cells containing the pBBR1MCS-*tssK* plasmid.

RAW 267.4 were grown in 24 well plates 16 hours prior to infection with Δ*tssK-5* pBBR1MCS-*tssK* at a MOI of 10:1 using the procedure outlined previously. 16 hours' post-infection, cells were washed, fixed and stained with Giemsa. When observed under a microscope, giant cells containing three or more nuclei within a single cytoplasmic membrane could be observed (Figure 4.4 D, Figure 4.8), demonstrating that pBBR1MCS-*tssK-5* restores MNGC formation to the Δ*tssK-5* strain. This indicates that the phenotype observed in Δ*tssK* was not a consequence of polar effects on the expression of downstream genes and the pBBR1MCS plasmid can be used for complementation in this assay. Therefore, other genes of interest were deleted using the SOE-PCR and allelic replacement method and any phenotype complemented using the respective WT gene cloned into pBBR1MCS.

4.2.6 Construction of a *B. thailandensis* tagABCD-5 deletion mutant

To determine if one or more of the *tag* genes were required for the formation of giant cells, all four were deleted simultaneously. To create a markerless in-frame deletion of *tagA-5* (BTH_II0862), *tagB-5* (BTH_II0861), *tagC-5* (BTH_II0860), *tagD-5* (BTH_II0859) as a block, the SOE PCR method combined with allelic replacement was employed using the same principle outlined for *tssK-5* in section 4.2.2. First, two PCRs were performed with KOD hot start polymerase, one using tagASOEfor2 and tagABCDmidrev to generate a 634 bp fragment encompassing the 3' end of *tssI-5* (BTH_II0863) and first 69 bp of *tagA* and another using primers tagDSOErev2 and tagABCDmidfor to generate an 869 bp fragment that included the final 78 bp of *tagD* and the first 751 bp of *tssJ-5* (BTH_II0858). These were then used as a template for PCR3, this employed the primers tagASOEfor2 and tagASOErev2 to generate a 1447 bp fragment which was digested with Acc65I and BamHI before ligation into pEX18Tp-

pheS to create the 5934 bp plasmid pEX18Tp-*pheS-tagA-D* which was confirmed by nucleotide sequencing. This plasmid was used to introduce the deletion into the WT *B. thailandensis* strain as described for *tssK* in section 4.2.2 and the *tagA*scrnfor and *tssK*midrev primers were used in a GoTaq PCR which distinguished WT colonies (6459 bp product) from those in which the desired deletion was present (1710 bp product). The deletion left the first 69 bp (23 codons) of *tagA-5* fused to the final 78 bp (26 codons) of *tagD-5* in the resulting $\Delta tagA-D-5$ strain.

4.2.7 The *B. thailandensis tagABCD-5* deletion mutant is incapable of inducing MNGC formation

As with the *tssK-5* mutant, the empty pBBR1MCS vector was delivered into $\Delta tagA-D-5$ via *E. coli* SM10(λ pir) by conjugation. Bacteria containing pBBR1MCS were selected for on M9 containing 250 μ g/ml chloramphenicol. A colony of $\Delta tagA-D-5$ pBBR1MCS was used to inoculate 4 ml of LB containing 250 μ g/ml chloramphenicol which was grown overnight at 37°C with shaking. A 1 ml aliquot of this culture was washed twice by centrifugation and resuspension in PBS before the OD₆₀₀ was measured. This measurement was used to determine the volume of cell suspension to add to DMEM-FCS to obtain a cell density of 1×10^6 CFU/ml. This bacterial cell suspension was used to replace the medium in the wells of a 24 well plate containing RAW cells which had been seeded at 1×10^5 cells/well 16 hours previously (an MOI of 10:1). After two hours at 37°C, 5% CO₂, wells were washed three times with PBS before the culture medium was replaced with DMEM-FCS containing 250 μ g/ml kanamycin to kill extracellular bacteria. After another 14 hours (16 hours after the initial infection), wells were washed three times with PBS before the addition of 100% ethanol for 30 minutes to fix the cells. The ethanol was removed and the wells allowed to air dry before the addition of 100% Giemsa for 5 minutes to stain. Excess stain was removed by rinsing gently with tap water and the wells were imaged using the 10x objective of a Leica DMI4000B inverted microscope.

As shown in Figure 4.6 A, the $\Delta tagA-D-5$ strain of *B. thailandensis* is unable to form multinucleated giant cells, suggesting that one or more of these genes is required for full virulence, consistent with the hypothesis that they are effector substrates of T6SS-5. As the deletion of *tagA-D* removed a large section of DNA (4749 bp) it is possible that this is the result of polar effects on the expression of downstream genes in the T6SS-5 gene cluster.

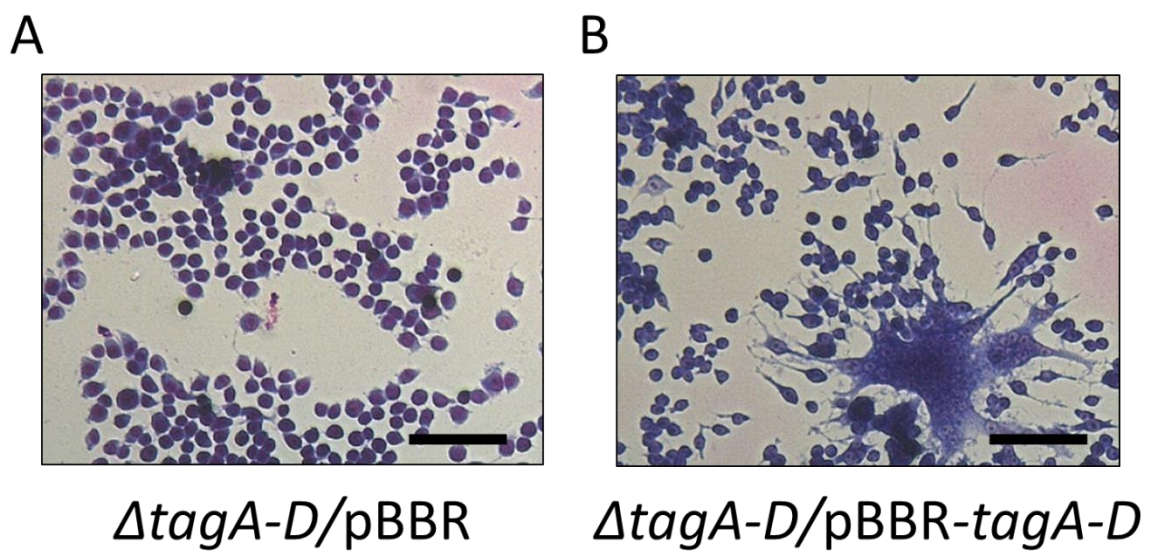


Figure 4.6 Effect of the deletion of all four *tag* genes on MNGC formation by *B. thailandensis*

RAW 264.7 cells infected at a MOI of 10:1 with *B.t* $\Delta tagA-D$ containing pBBR1MCS and *B.t* $\Delta tagA-D$ containing pBBR1MCS-*tagA-D* for 16 hours before fixing with ethanol and staining with Giemsa.. Images acquired using the 10x objective of a Leica DMI4000B inverted microscope. A) $\Delta tagA-D/pBBR$, *B.t* $\Delta tagA-D-5$ containing pBBR1MCS. B) $\Delta tagA-D/pBBR-pBBR-tagA-D$, *B.t* $\Delta tagA-D5$ harbouring pBBR1MCS-*tagA-D-5*. Scale bar = 75 μ m.

4.2.8 Construction of a *tagABCD* complementation plasmid

To ensure that the abolition of MNGC formation observed in Figure 4.6 A was not a consequence of polar effects on downstream genes, it was necessary to re-introduce the WT genes into the $\Delta tagA-D-5$ strain of *B. thailandensis*. The level of expression of *tssK* from pBBR1MCS-*tssK* was demonstrated to be sufficient to restore MNGC formation to a *tssK-5* mutant (Figure 4.4), therefore the pBBR1MCS-*tagA-D* plasmid was constructed using the same procedure outlined in section 4.2.5. The *tagAcompfor* and *tagDcomprev* primers were used in a PCR with Q5 polymerase to amplify a 5135 bp DNA fragment which contained all four of the *tag* genes. This DNA fragment and the pBBR1MCS plasmid were digested with HindIII and BamHI before ligating together to create the 9810 bp plasmid, pBBR1MCS-*tagA-D* which was purified using plasmid miniprep and analysed by nucleotide sequencing.

4.2.9 Re-introduction of the WT *tagA-D-5* genes into the *tagA-D-5* mutant restores MNGC formation *in trans*

Once it had been confirmed that the plasmid contained the correct sequence it was delivered into the *tagA-D* mutant by conjugation, previously described for the *tssK* complementation plasmid. RAW 264.7 cells were infected as described previously and stained with Giemsa to allow the visualisation of membranes and nuclei. As shown in Figure 4.6 B, the *tagA-D* mutant harbouring pBBR1MCS-*tagA-D* was able to form MNGCs. This demonstrates that the loss of MNGC formation observed when cells were infected with *B.t* $\Delta tagA-D$ was not down to polar effects, confirming that at least one of the *tag* genes is required for MNGC formation.

4.3 The Effect of deletion of each *tag* gene on MNGC formation induced by *B. thailandensis*

As the *B. thailandensis* strain lacking all four *tag* genes was incapable of inducing MNGC formation in RAW 264.7 cells, the next step was to determine which of the individual *tag* genes were required for MNGC formation. Therefore, each individual *tag* gene was deleted and the resulting strains used to infect RAW 264.7 cells. If the deletion of any of the *tag* genes had an effect on MNGC formation, then it would be necessary to re-introduce the corresponding WT gene into the mutant on a multicopy plasmid to confirm that the observed phenotype was not a consequence of polar effects.

4.3.1 Construction of a *B. thailandensis* of *tagA-5* mutant

To create the $\Delta tagA-5$ (ΔBTH_II0862) strain of *B. thailandensis*, the primers *tagASOEfor2* and *tagASOEmidrev* were used in PCR1 to generate a 634 bp fragment containing the 3' end of *tssI-5* (BTH_II0863) and first 69 bp of *tagA-5*. The primers *tagASOerev2* and *tagASOEmidfor* were used in PCR2 to generate a 701 bp fragment containing the final 57 bp of *tagA-5* and the first 599 bp of *tagB-*

5. These two fragments were mixed and used as a template in PCR3 with tagASOEfor2 and tagASOErev2 which generated a 1299 bp DNA fragment. Both the PCR product and pEX18Tp-*pheS* were digested with Acc65I and BamHI before ligating the two DNA fragments together to create pEX18Tp-*pheS-ΔtagA* (5766 bp). Once the correct plasmid had been verified by DNA sequencing, it was delivered into WT *B. thailandensis* by conjugation followed by a two-step allelic replacement procedure to yield the *ΔtagA-5* strain. The deletion of the central segment of the *tagA-5* gene to leave the first 69 bp (23 codons) fused to the final 57 bp (19 codons) was confirmed by screening with the tagA_{scrnfor} and tagA_{CSOEmidrev} primers which annealed to genomic sequences either side of the region cloned into pEX18Tp-*pheS-ΔtagA*. This gave rise to a 4413 bp fragment when the WT gene was present and a 1920 bp DNA product when *ΔtagA* was present. Before using in infection assays the pBBR1MCS vector was introduced by conjugation.

4.3.2 *B. thailandensis tagA-5* is required for MNGC formation *in vitro*

The *B.t ΔtagA* mutant containing pBBR1MCS was grown overnight at 37°C in LB containing 250 µg/ml chloramphenicol. The cultures were washed twice with PBS following which the OD₆₀₀ was determined. This was used to inoculate DMEM-FCS with 1 x 10⁶ cells/ml *B.t.* RAW267.4 cells seeded at 1 x 10⁵ cells/well of a 24 well plate 12-16 hours previously were infected by replacing the culture medium with 1 ml of the *B. thailandensis* cell suspension. Two hours post-infection, the wells were washed twice with PBS before the addition of 1 ml DMEM-FCS and 250 µg/ml kanamycin. 16 hours post infection, wells were washed three times with PBS and fixed with ethanol for 30 minutes. After fixing, wells were allowed to dry and cells were stained using undiluted Giemsa (0.4% w/v) for five minutes before rinsing with tap water to achieve the desired staining intensity.

As shown in Figure 4.7 A, RAW 267.4 cells infected with the *tagA* mutant were unable to form MNGCs. To confirm that this phenotype was a result of the mutation introduced, it was necessary to re-introduce a WT copy of *tagA*.

4.3.3 Construction of a *tagA-5* complementation plasmid

To create pBBR1MCS-*tagA*, boiled lysate prepared from WT *B. thailandensis* was used as a template in a PCR with the tagA_{compfor} and tagA_{comprev} primers which introduced a HindIII and BamHI site, respectively. The amplified 2717 bp DNA fragment and pBBR1MCS were digested with HindIII and BamHI before ligating together. This ligation mixture was used to transform JM83 cells which were spread on LB agar plates containing chloramphenicol, Xgal and IPTG which were then placed at 37°C overnight. Selected white colonies on these plates were grown overnight and the plasmids from these cultures extracted by miniprep. The plasmids were run on an agarose gel before a plasmid of the

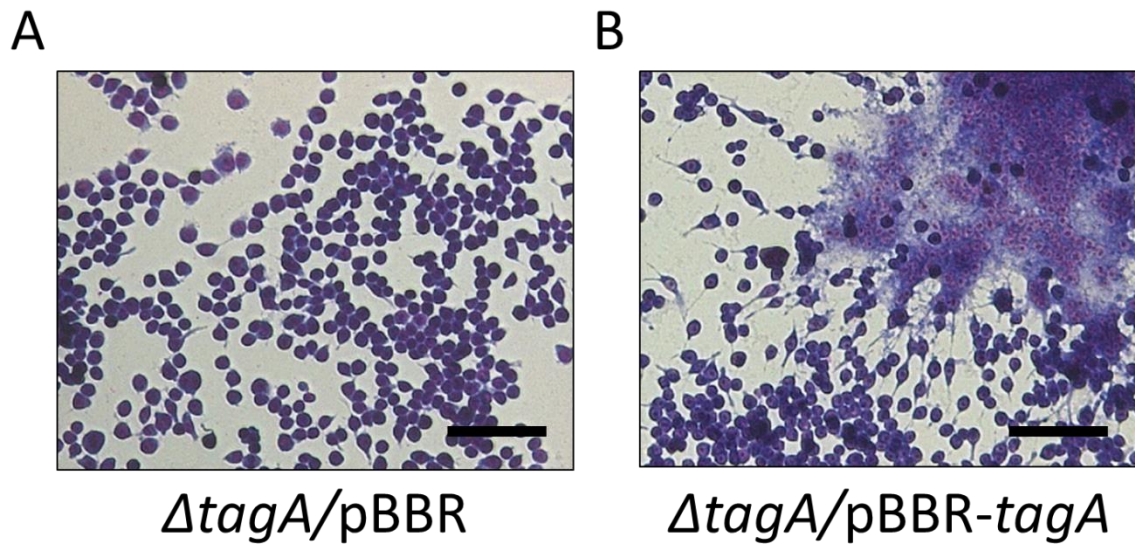


Figure 4.7 Effect of deletion of *tagA-5* on MNGC formation induced by *B. thailandensis*

RAW 264.7 cells infected with *B.t* $\Delta tagA-5$ containing pBBR1MCS and *B.t* $\Delta tagA-5$ containing pBBR1MCS-*tagA-5* at a MOI of 10:1 for 16 hours before fixing with ethanol and staining with Giemsa. Images were acquired using the 10x objective of a Leica DMI4000B inverted microscope. A) $\Delta tagA/pBBR$, *B.t* $\Delta tagA-5$ containing pBBR1MCS. B) $\Delta tagA/pBBR$, *B.t* $\Delta tagA-5$ containing pBBR1MCS-*tagA-5*. Scale bar = 75 μ m.

correct size (7384 bp) was sequenced. The correct pBBR1MCS-*tagA* was introduced into $\Delta tagA$ by conjugation and used in an infection assay as described previously.

4.3.4 Introduction of WT *tagA-5* into the *B.t tagA-5* mutant restores MNGC formation

As demonstrated in Figure 4.7 B, MNGC formation was restored when the *tagA* gene was introduced into the *tagA-5* mutant on the pBBR1MCS plasmid. This indicates that the deletion of the *tagA* gene did not introduce polar effects on the expression of downstream genes in the T6SS-5 gene cluster and therefore *tagA-5* is required for the formation of MNGCs *in vitro*.

4.3.5 Construction of a *B. thailandensis tagB-5* mutant

A markerless in frame deletion of *tagB-5* (BTH_II0861) was created by using the tagBSOEfor2 and tagBSOEmidrev primers in one PCR creating a 520 bp fragment that contained the 3' end of *tagA* and the first 78 bp of the *tagB* ORF and tagBSOErev2 and tagBSOEmidfor primers to create a 582 bp fragment incorporating the final 60 bp of *tagB* and the first 498 bp of *tagC* in another reaction. A third reaction was carried out using the tagBSOEfor2 and tagBSOErev2 primers with the fragments from the previous two reactions acting as a template. This third reaction amplified a 1066 bp DNA fragment which was digested with Acc65I and BamHI, and ligated into pEX18Tp-*pheS* which had been digested with the same enzymes. This generated a 5533 bp plasmid, pEX18Tp-*pheS- $\Delta tagB-5$* , which was used to introduce a version of *tagB-5* possessing only its first 78 bp (23 codons) fused to the final 60 bp (20 codons) of the gene. The ~500 bp of DNA upstream and downstream of the remaining *tagB-5* sequence facilitated the integration of the pEX18Tp-*pheS- $\Delta tagB-5$* plasmid (and hence the trimethoprim resistance and *pheS* genes) into the *B.t* chromosome by a single homologous recombination which was selected for by trimethoprim resistance. Tp^R resistant colonies were restreaked on M9 agar containing cPhe and the plasmid was excised by a second homologous recombination event necessary to allow the bacteria to grow on this agar containing cPhe. The creation of $\Delta tagB-5$ was confirmed using the tagAcompfor and tagDSOEmidrev primers in a GoTaq PCR which produced a 4220 bp fragment when the desired mutation was present on the chromosome, compared to 5175 bp when the WT *tagB* gene was present. The pBBR1MCS plasmid was then introduced into the mutant by conjugation.

4.3.6 *B. thailandensis tagB-5* is required for MNGC formation *in vitro*

RAW 267.4 cells growing in 24 well plates were infected with the *B.t $\Delta tagB-5$* mutant containing pBBR1MCS at an MOI of 10:1 using the procedure outlined previously. 16 hours post-infection, cells were washed, fixed and stained with Giemsa. When observed under a microscope no giant cells containing three or more nuclei within a single cytoplasmic membrane could be observed (Figure 4.8 A), suggesting that *tagB-5* is required for *B.t* to induce MNGC formation in RAW 267.4 cells.

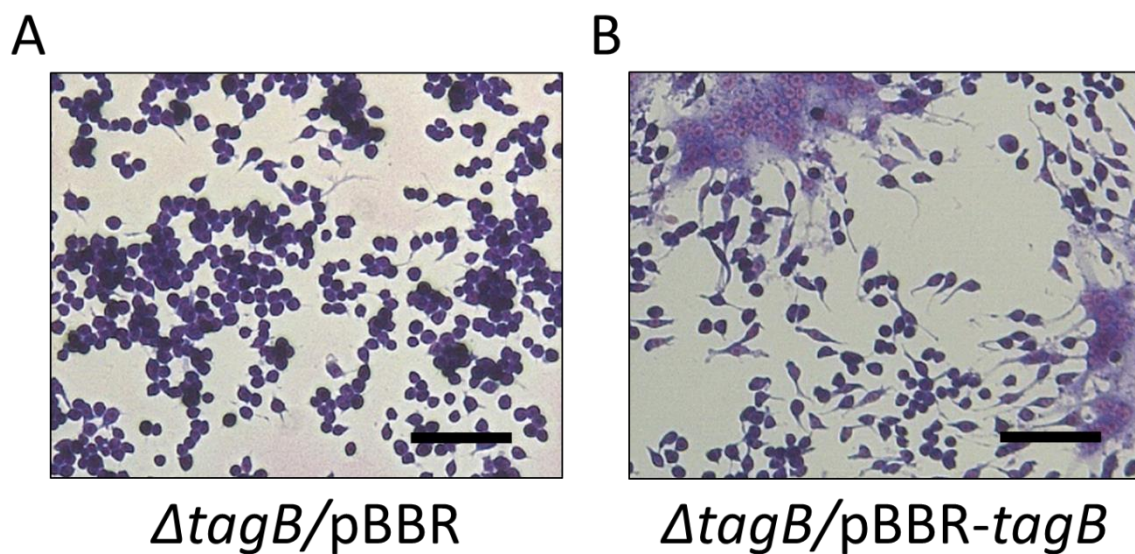


Figure 4.8 Effect of the deletion of *tagB-5* on MNGC formation induced by *B. thailandensis*

RAW 264.7 cells infected with *B.t ΔtagB-5* containing pBBR1MCS and *B.t ΔtagB-5* containing pBBR1MCS-*tagB-5* at a MOI of 10:1 for 16 hours before fixing with ethanol and staining with Giemsa.. Images were acquired using the 10x objective of a Leica DMI4000B inverted microscope. A) *ΔtagB/pBBR*, *B.t ΔtagB-5* containing pBBR1MCS. B) *ΔtagB/pBBR*, *B.t ΔtagB-5* containing pBBR1MCS-*tagB-5*. Scale bar = 75 μm.

4.3.7 Construction of a *tagB-5* complementation plasmid

A PCR with the proofreading Q5 DNA polymerase was performed using tagBcompfor and tagBcomprev to amplify a 1130 bp DNA fragment from a WT *B.t* boiled lysate template. This DNA fragment was digested with HindIII and BamHI which cut the DNA at the sites introduced by the tagBcompfor and tagBcomprev primers, respectively. pBBR1MCS was digested with the same enzymes and ligated with the digested PCR product. Following transformation of JM83 with the ligation mixture, white colonies growing on LB containing chloramphenicol, IPTG and Xgal were selected and grown overnight in liquid medium to facilitate purification of plasmid DNA by the miniprep procedure. A plasmid which migrated with a size corresponding to 5794 bp in an agarose gel was identified and the nucleotide sequence of the insert was determined.

4.3.8 Introduction of WT *tagB-5* into the *B.t tagB-5* mutant restores MNGC formation

The correct pBBR1MCS-*tagB-5* plasmid was introduced into the *B.t tagB-5* mutant by conjugation and a transformant was used in a MNGC formation assay as described previously. Figure 4.8 B shows that introduction of the *tagB-5* complementation plasmid into the *B.t ΔtagB-5* mutant restores the ability of the strain to induce RAW 267.4 cells to fuse resulting in MNGC formation. This result demonstrates that *tagB-5* is indeed required for MNGC formation *in vitro*.

4.3.9 Construction of a *B. thailandensis* of *tagC-5* mutant

To create a markerless in frame deletion of *tagC-5* (BTH_II0860), a splice overlap extension PCR was first performed. The first reaction used the primers tagCSOEfor2 and tagCSOEmidrev to amplify a 531 bp product containing 428 bp of the of the 3' end of *tagB-5* and a short region of the 5' end of *tagC-5*. A second used the primers tagCSOErev2 and tagCSOEmidfor to amplify a 565 bp product containing the final 78 bp of *tagC-5*, all of *tagD-5* and the first 29 bp of *tssJ-5*. These products were gel extracted and combined as templates for a third PCR which used the tagCSOEfor2 and tagCSOErev2 primers to generate a 1060 bp fragment. This PCR product and pEX18Tp-*pheS* were digested with Acc65I and BamHI and then ligated together. The products of the ligation reaction were used to transform JM83 and transformants were selected on M9-glycerol CAA agar containing trimethoprim, Xgal and IPTG at 30°C. Minipreps from white colonies were screened for the presence of presence of plasmids of the expected size (5527 bp). One such plasmid was confirmed as containing the *ΔtagC* DNA fragment by nucleotide sequencing. This plasmid, pEX18Tp-*pheS-ΔtagC*, was introduced into the WT *B.t* chromosome by homologous recombination following conjugation and selected for by acquisition of trimethoprim resistance. Selection for cPhe-resistance was then applied to identify bacteria in which a second recombination event had occurred resulting in the excision of the plasmid leaving behind

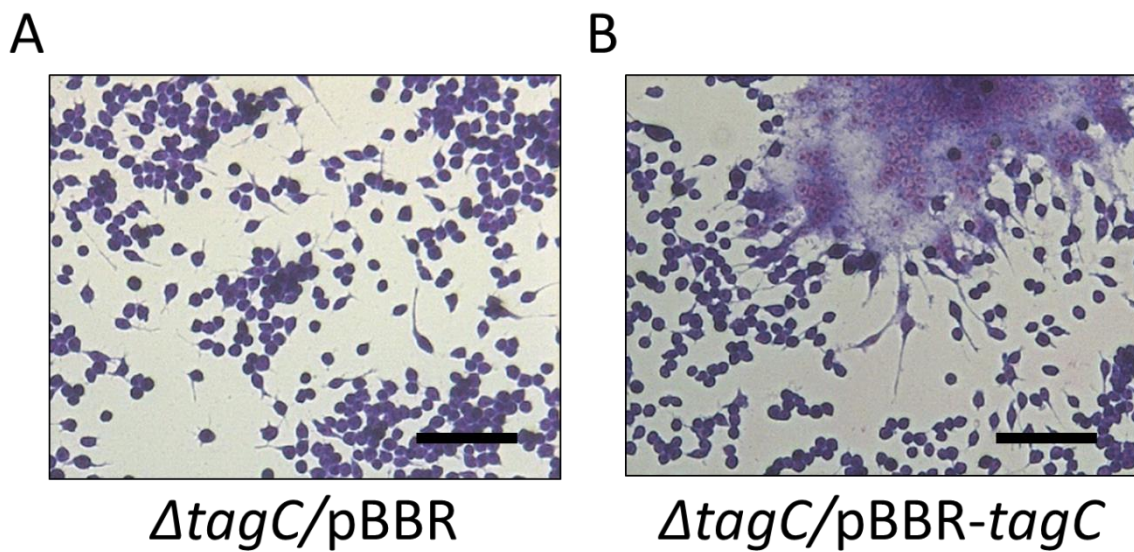


Figure 4.9 Effect of the deletion of *tagC-5* on MNGC formation induced by *B. thailandensis*

RAW 264.7 cells infected with *B.t* $\Delta tagC-5$ containing pBBR1MCS and *B.t* $\Delta tagC-5$ containing pBBR1MCS-*tagC-5* at a MOI of 10:1 for 16 hours before fixing with ethanol and staining with Giemsa.. Images were acquired using the 10x objective of a Leica DMI4000B inverted microscope. A) $\Delta tagC/pBBR$, *B.t* $\Delta tagC-5$ containing pBBR1MCS. B) $\Delta tagC/pBBR$, *B.t* $\Delta tagC-5$ containing pBBR1MCS-*tagC-5*. Scale bar = 75 μ m.

either the WT gene or the $\Delta tagC$ allele. $\Delta tagC$ colonies were identified by PCR using the tagCscrnfor and tagCscrnrev primers which annealed to genomic regions flanking the DNA region that was homologous to the DNA carried by pEX18Tp-*pheS*- $\Delta tagC$. This PCR produced a 1926 bp DNA fragment when the WT gene was present and a 1306 bp DNA fragment when $\Delta tagC$ was present which retained the first 78 bp (26 codons) fused to the final 78 bp (26 codons) of the *tagC-5* gene.

4.3.10 *B. thailandensis tagC-5* is required for MNGC formation *in vitro*

Figure 4.9 A shows a representative image obtained from wells containing RAW 267.4 cells seeded at 2×10^5 cells/ml infected with the *B.t* $\Delta tagC$ mutant containing pBBR1MCS at an MOI of 10:1 for 16 hours prior to fixing and staining with Giemsa. No giant cells could be observed in any field of view. Assuming that polar effects were not responsible for the observed phenotype, this demonstrates that *tagC-5* is required for the *B. thailandensis* induced fusion observed during infection assays.

4.3.11 Construction of a *tagC-5* complementation plasmid

The tagCcompfor and tagCcomprev primers were used to amplify an 835 bp DNA fragment using Q5 polymerase and a WT *B.t* boiled lysate as the template. The resulting DNA fragment and pBBR1MCS were digested with BamHI and HindIII and ligated together. The ligation mixture was used to transform JM83 cells and colonies which potentially contained the desired plasmid construct were identified by blue/white screening. White colonies were used to inoculate in LB containing chloramphenicol and grown overnight whereupon plasmids were isolated from cultures by miniprep procedure. Plasmids were analysed by electrophoresis in an agarose gel and a candidate of the correct size (5499 bp) was confirmed to be pBBR1MCS-*tagC-5* by nucleotide sequencing.

4.3.12 Introduction of WT *tagC-5* into the *B.t tagC-5* mutant restores MNGC formation

pBBR1MCS-*tagC-5* was introduced into the *B.t* $\Delta tagC-5$ mutant by conjugation with SM10(λ pir) and the resulting strain was used to infect RAW 264.7 cells. Figure 4.9 B shows that the *B.t* $\Delta tagC-5$ mutant harbouring pBBR1MCS-*tagC-5* was capable of forming MNGCs. Therefore, *tagC-5* is another *B. thailandensis* virulence factor.

4.3.13 Construction of a *B. thailandensis tagD-5* mutant

As with the other three *tag* genes of the T6SS-5 gene cluster, *tagD-5* (BTH_II0859) was deleted from the *B.t* genome by a splice overlap extension followed by allelic replacement to generate a markerless in frame deletion. The high-fidelity Q5 polymerase was utilised. The first PCR used the tagDSOEfor2 and tagDSOEmidrev primer pair to amplify a 693 bp DNA fragment containing the 3' 529 bp of the *tagC-5* gene and the first 108 bp of the *tagD-5* gene. The second PCR used tagDSOErev2 and tagDSOEmidfor to amplify an 869 bp fragment which contained the final 78 bp of *tagD-5* and the initial 754 bp of *tssJ-5*. These two products were combined and used as a template for a third PCR using the

tagDSOEfor2 and tagDSOErev2 primers which amplified a 1467 bp product. This product, along with the pEX18Tp-*pheS* plasmid, were digested with Acc65I and BamHI and then ligated together. The ligation mixture was used to transform *E. coli* JM83 cells which were spread on M9-glycerol CAA agar containing trimethoprim, Xgal and IPTG and grown at 30°C. After two nights growth, white colonies were grown overnight in IST broth containing trimethoprim and the plasmid DNA isolated by the miniprep procedure. Plasmids were analysed by electrophoresis to identify the correct sized plasmid (5993 bp). The sequence of the cloned DNA in the resulting plasmid, pEX18Tp-*pheS-ΔtagD*, was confirmed by sequencing. pEX18Tp-*pheS-ΔtagD* was used to create a markerless in frame deletion by homologous recombination events as described in section 4.2.2 on the *B.t* chromosome, following selection for loss of the integrated plasmid by cPhe challenge. Candidate mutants were screened by PCR screening using the tagCcompfor and tssKSOEmidrev primers. The size difference between the fragments produced from these reactions was used to distinguish between WT (2156 bp) and *ΔtagD-5* mutants (1949 bp). The *B.t ΔtagD-5* mutant retained the first 108 bp (36 codons) and the final 78 bp (26 codons) of the WT *tagD-5* gene.

4.3.14 *B. thailandensis tagD-5* is required for MNGC formation *in vitro*

To determine if *tagD-5* was required for giant cell formation, the pBBR1MCS plasmid was delivered into the *ΔtagD-5* mutant and the resulting *B.t ΔtagD-5* strain containing pBBR1MCS used to infect monolayers of RAW 264.7 cells as described previously. After fixing and staining, the cells were observed under a light microscope. No cells containing more than two nuclei were visible (Figure 4.10 A), demonstrating that *tagD-5* is required for the formation of MNGCs.

4.3.15 Construction of a *tagD-5* complementation plasmid

To ensure that the inability of the *tagD-5* mutant was not a consequence of polar effects which affected the expression of nearby genes, it was necessary to perform a complementation experiment. To do this, a WT *B. thailandensis* boiled lysate was used as a template for a PCR using the Q5 proofreading DNA polymerase and the tagDcompfor and tagDcomprev primers. The amplified 454 bp DNA fragment containing *tagD-5* was cloned between the HindIII and BamHI sites of the pBBR1MCS plasmid and the ligation product used to transform *E. coli* JM83 cells. Transformants in which the plasmid contained an insert were identified by blue/white screening. Plasmids of the correct sized (5117 bp) isolated from white colonies were sequenced which allowed identification of the correct pBBR1MCS-*tagD-5* construct.

4.3.16 Introduction of WT *tagD-5* into the *B.t tagD-5* mutant restores MNGC formation

E. coli SM10(λ pir) cells were transformed with pBBR1MCS-*tagD-5* before they were used to deliver the plasmid into the *B.t Δ tagD-5* mutant by conjugation. A giant cell formation assay was performed using an MOI of 10:1 with the *B.t Δ tagD-5* mutant harbouring pBBR1MCS-*tagD-5*. As shown in Figure 4.10 B MNGC formation was restored. This demonstrates that the giant cell formation deficient phenotype observed when cells were infected with *B.t Δ tagD-5* was a result of the inactivation of *tagD-5* and not polar effects on downstream genes.

4.4 Quantitative determination of MNGC formation in *tag* mutants and complemented strains.

Having demonstrated that each *tag* gene was required for *B.t* induced MNGC formation in RAW 264.7 cells, the fusion index for each of the complemented strains was determined and compared to that resulting from infection of the WT strain. To do this, three wells of a 24 well plate were infected at a MOI of 10:1 with either a *tag* mutant harbouring empty pBBR1MCS or a *tag* mutant harbouring pBBR1MCS containing the respective WT gene. Two hours post-infection, the culture medium was replaced with culture medium containing 250 μ g/ml kanamycin to kill extracellular bacteria. 16 hours after the initial infection, wells were washed three times with PBS before fixing with 100% ethanol for half an hour. The ethanol was removed and the well allowed to dry before immersing in 100% Giemsa for 5 minutes. The stain was removed before the cells were destained with tap water until the cytoplasm and nuclei of the RAW 265.7 cells could be distinguished.

The 10 x objective of a Leica DMI4000B inverted microscope was used to capture three random fields of view per well. Nuclei within cells containing three or more nuclei (i.e. nuclei within giant cells) were counted, as well as the total number of nuclei in the field of view (typically >1000). Counting was facilitated by the 'cell counter' plugin on ImageJ software. The number of nuclei within giant cells was divided by the total number of nuclei in the field of view and multiplied by 100 to give a percentage fusion index. Three independent repeats were performed for all strains tested. As shown in Figure 4.11 and indicated in previous sections, the *B.t tagA-D-5* mutant and mutants in each individual *tag* gene were unable to induce the formation of giant cells. RAW 264.7 cells infected with each *tag* mutant strain containing the corresponding WT gene on the pBBR1MCS plasmid showed some degree of giant cell formation. Of these, only the complemented Δ *tagA-D-5* (16.8% average fusion index) and Δ *tagD-5* mutants (19.0% average fusion index) showed a statistically significant difference in fusion index compared with the wild type (27.4% average fusion index). This indicates that the complementation was not complete.

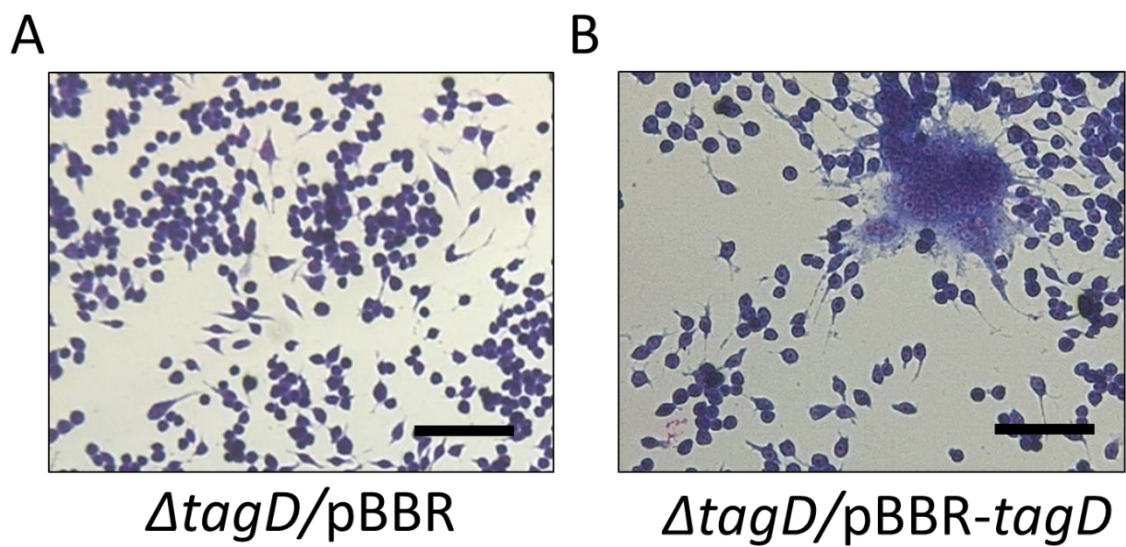


Figure 4.10 Effect of the deletion of *tagD-5* on MNGC formation induced by *B. thailandensis*

RAW 264.7 cells infected with *B.t* $\Delta tagD-5$ containing pBBR1MCS and *B.t* $\Delta tagD-5$ containing pBBR1MCS-*tagD-5* at a MOI of 10:1 for 16 hours before fixing with ethanol and staining with Giemsa. Images were acquired using the 10x objective of a Leica DMI4000B inverted microscope. A) $\Delta tagD/pBBR$, *B.t* $\Delta tagD-5$ containing pBBR1MCS. B) $\Delta tagD/pBBR$, *B.t* $\Delta tagD-5$ containing pBBR1MCS-*tagD-5*. Scale bar = 75 μ m.

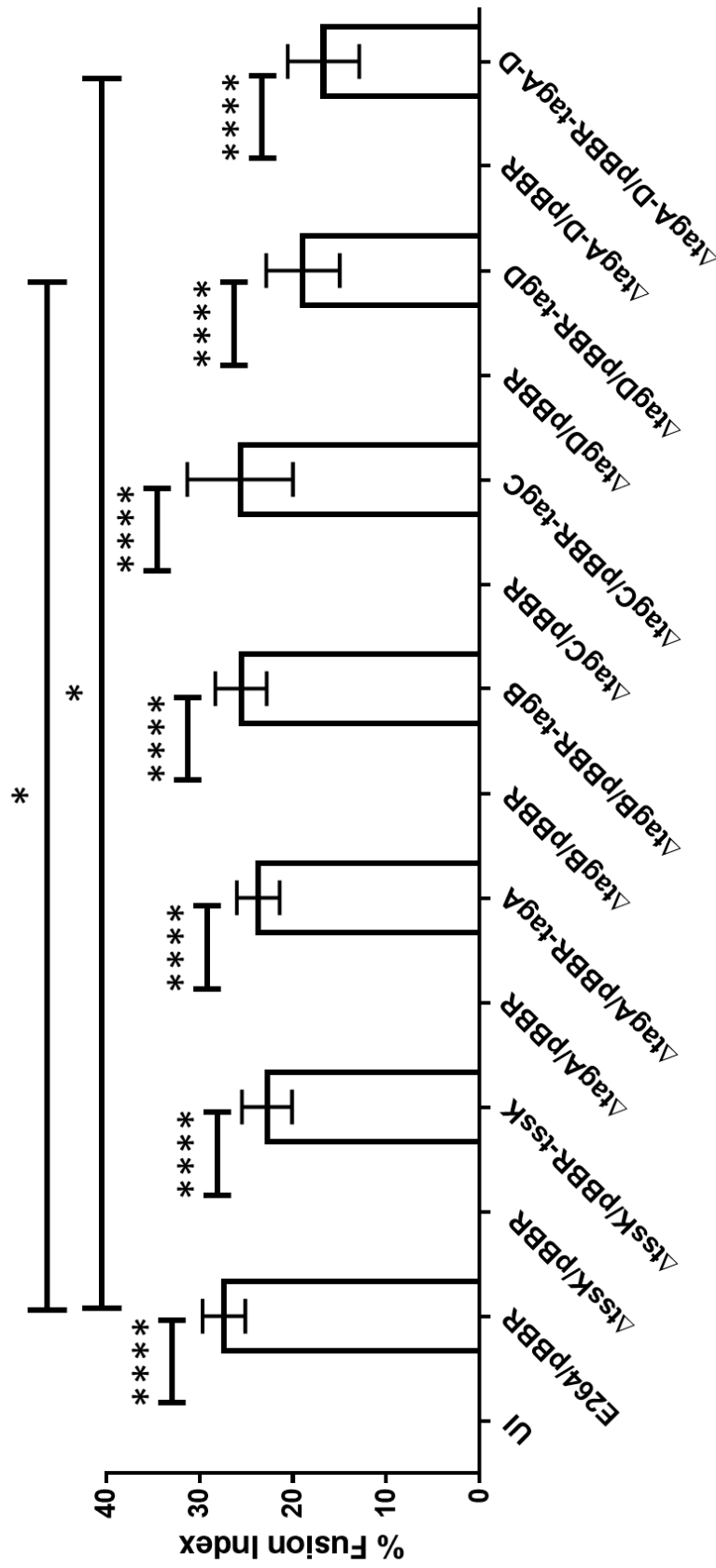


Figure 4.11 Quantitative analysis of MINGC formation induced by *B. thailandensis* tag mutants

RAW 264.7 cells were infected with *B. t.* WT, *tssK* and *tag* mutants containing either pBBR1MCS or a complementing plasmid. The nuclei inside giant cells and the total number of nuclei in three fields of view from three wells were counted. The fusion index was calculated and three independent repeats were performed per strain. UI, Uninfected; E264/pBBR, WT *B. t.* containing pBBR1MCS; Δ*tssK*/pBBR, *B. t.* Δ*tssK* containing pBBR1MCS; Δ*tssK*/pBBR-*tssK*, *B. t.* Δ*tssK* containing pBBR1MCS-*tssK*; Δ*tagA*/pBBR, *B. t.* Δ*tagA* containing pBBR1MCS; Δ*tagA*/pBBR-*tagA*, *B. t.* Δ*tagA* containing pBBR1MCS-*tagA*; Δ*tagB*/pBBR, *B. t.* Δ*tagB* containing pBBR1MCS; Δ*tagB*/pBBR-*tagB*, *B. t.* Δ*tagB* containing pBBR1MCS-*tagB*; Δ*tagC*/pBBR, *B. t.* Δ*tagC* containing pBBR1MCS; Δ*tagC*/pBBR-*tagC*, *B. t.* Δ*tagC* containing pBBR1MCS-*tagC*; Δ*tagD*/pBBR, *B. t.* Δ*tagD* containing pBBR1MCS; Δ*tagD*/pBBR-*tagD*, *B. t.* Δ*tagD* containing pBBR1MCS-*tagD*; Δ*tagA-D*/pBBR, *B. t.* Δ*tagA-D* containing pBBR1MCS; Δ*tagA-D*/pBBR-*tagA-D*, *B. t.* Δ*tagA-D* containing pBBR1MCS-*tagA-D*. Bars on the graph indicate average fusion index. Error bars represent one standard deviation. Statistical significance was tested using ordinary one-way analysis of variance (ANOVA) with Tukeys post-test. * $P < 0.05$, *** $P < 0.001$. Graph created and statistical analysis performed using GraphPad prism.

4.5 Intracellular Replication of *B. thailandensis tag* mutants

It is possible that the loss of MNGC formation observed in the *tag* mutants was due to the mutations having an impact on another virulence characteristic. For example, if the mutants had an effect on the third type three secretion system (T3SS) and were therefore unable to escape from phagosomes then they would no longer be capable of replication in the cytoplasm and would no longer form MNGCs (French et al. 2011). To ensure that the effects observed in MNGC formation were not due to an absence of intracellular bacteria, intracellular replication assays were performed. As in the MNGC formation assays, RAW 264.7 cells were seeded at 2×10^5 cells/well of a 24 well plate and infected at a MOI of 10:1 with WT and mutant strains of *Burkholderia thailandensis* containing the pBBR1MCS plasmid. After two hours wells were washed three times with PBS and the medium replaced with DMEM containing 250 µg/ml kanamycin to kill extracellular bacteria. At indicated time points the wells were washed three times with PBS before lysing by the addition of 250 µl of 1% triton X-100 for 5 minutes. The lysis mixture was serially diluted before 10 µl of each dilution was pipetted onto LB agar plates. After 48 hours' incubation at 37°C colonies were counted and used to calculate colonies per well.

4.5.1 Inactivation of the *tssK* and *tag* genes has no effect on intracellular replication

As shown in Figure 4.12, the *tssK* mutant is capable of intracellular replication and had a similar number of CFU/well at each time point as the WT strain. In both the WT and the *tssK* mutant, the numbers of intracellular bacteria were reduced at six hours compared to two hours but then increased again after twenty-four hours post infection.

The same pattern of a decrease in the number of intracellular bacteria followed by an increase was observed in each of the *tag* mutants. This demonstrates that the lack of giant cell formation induced by the *tag* mutants was not due to an inability of the bacteria to enter the RAW 264.7 cells as they would not be protected from the antibiotic in the medium. The mutations were also unlikely to have had an effect on phagosome escape as mutants that were incapable of phagosome escape would not be able to avoid killing by the host macrophage-like cell.

4.6 Discussion

The results presented in this chapter demonstrate that all four of the *tag* genes located within the T6SS-5 gene cluster are required for MNGC cell formation, but do not appear to be involved in intracellular replication, indicating the mutants are still capable of entering the host cell and escaping from phagosomes. This suggests that the *tag-5* genes are involved in the activity of T6SS-5, as effectors, regulators or auxiliary subunits. When the WT copies of the *tag* genes were re-introduced

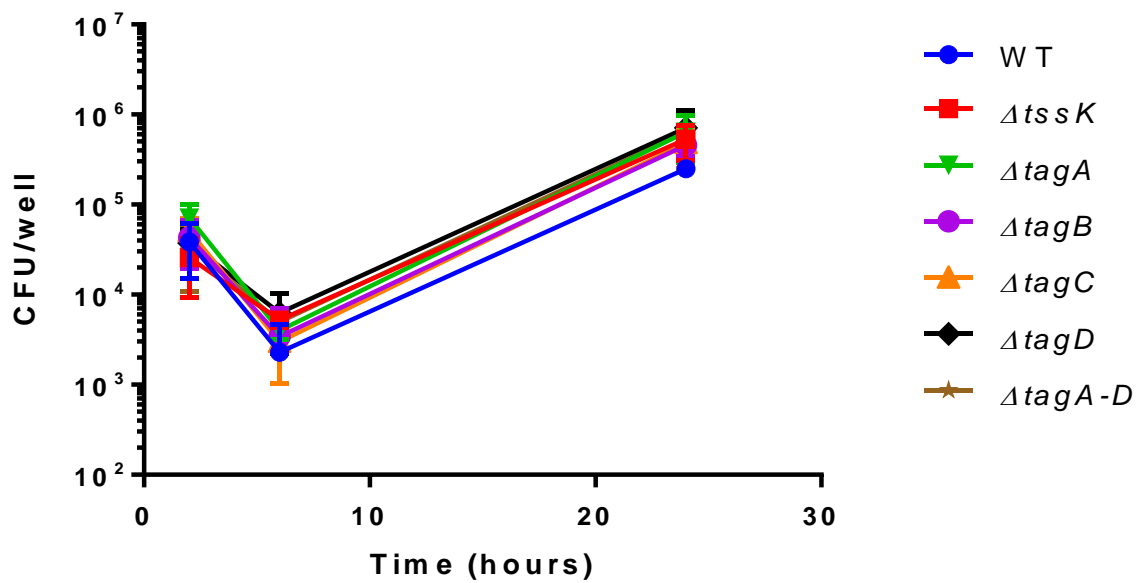


Figure 4.12 Intracellular replication of *B.t* tag mutants

Monolayers of RAW 246.7 macrophage-like cells growing in 24 well plates were infected at a MOI of 10:1 with the indicated strains of *B.t* containing pBBR1MCS. Eukaryotic cells were lysed with PBS containing triton X-100 at 2, 6 and 24 hours post-infecton. Lysates were serially diluted before a 10 μ l drop of each was spotted onto LB agar plates and incubated at 37°C for 48 hours. The number of colonies growing on the plates was used to calculate the CFU/well. Three biological replicates were performed; error bars represent one standard deviation.

into the corresponding mutants *in trans*, MNGC formation was restored. The fusion indexes for the complemented *B.t ΔtagA*, *tagB* and *tagC* mutants were similar to the WT strain. Although they did show a degree on MNGC formation, the fusion indexes for *B.t ΔtagA-D-5* containing pBBR1MCS-*tagA-D-5* and *B.t ΔtagD-5* containing pBBR1MCS-*tagD-5* were significantly reduced when compared with the WT fusion index.

What is not clear, however, is whether the *tag* genes encode effectors delivered by the secretion system which are responsible for cell fusion or auxiliary components required for the function of the system (i.e. in addition to the 13 core components) or regulatory proteins required to activate the system. Based on the observations of Toesca et al. (2014), who found that the TssI-5 C-terminal domain (which is not part of the core region of TssI) is required for cell fusion but dispensable for secretion by T6SS-5 (as determined by the presence of TssD-5 in the supernatant of cultures), it is more likely that the *tag* genes encode auxiliary proteins required for T6SS-5 function. However, it is also possible that one or more of the Tag proteins interact with the CTD of TssI-5 and the combined activity facilitates fusion.

Since the beginning of this work, research was published which demonstrated that *B. pseudomallei tagA-5* (BPSS1504) was required for the formation of MNGCs and virulence in a mouse model of infection (Hopf et al. 2014). This is consistent with the result of the giant cell formation assay performed using the *B.t ΔtagA-5* mutant (and the *ΔtagA-D-5* mutant as it also lacked *tagA-5*). The observation that the *B. thailandensis* and *B. pseudomallei tagA-5* mutants have the same MNGC deficient phenotype further supports the use of *B. thailandensis* as a model for *B. pseudomallei*.

The observation that there is no difference in intracellular replication between WT and *ΔtssK* strains is surprising given that there is a difference when a *B. pseudomallei tssD-5* mutant is used to infect RAW 264.7 cells at 6 hour and 12 hour time points (Burtnick et al. 2011). However, the number of intracellular *B.p* WT cells appeared to be on the decline at 18 hours compared with the same strain at 12 hours, unlike the *ΔtssD-5* mutant cells which were still increasing in number. Conversely, French et al. (2011) found that a *B. thailandensis tssH-5* mutant had similar levels of intracellular replication as its WT counterpart at the 5, 8 and 12-hour time points, but the number of intracellular *B.t tssH-5* mutant cells was increased compared to the WT strain after 16 hours. Another study found that a *B. pseudomallei tssI-5* mutant and a *tssI-5* mutant with the WT gene re-introduced *in trans* exhibited no difference in intracellular replication characteristics at 6, 16 and 22 hours post-infection, but at 28 hours post infection the complemented *B.p tssI-5* mutant showed a reduction in intracellular CFU compared to the mutant. This behaviour was attributed to increased permeability of the membranes of the infected cells over time, resulting in the antibiotics, that were added to the medium to prevent

extracellular growth, being able to enter the host cells and kill the bacteria. In the same study, the replication behaviour of a *B.p tssH-5* mutant was the same as the *tssI-5* mutant, but the characteristics of the WT strain were not tested (Toesca et al. 2014). Although the mutations are not in the same genes, one would expect a *tssK* and *tssH* mutant in *B. thailandensis* to have a similar phenotype as they both result in a T6SS-5-defective phenotype.

The lack of a difference observed in the efficiency of replication between the WT and $\Delta tagA-5$ strains is also inconsistent with results observed in a *B. pseudomallei tagA-5* mutant which showed a reduction in intracellular CFU per well at 24 hours post infection when compared with the WT strain (Hopf et al. 2014). Unlike the replication assay used in this study, the assay performed by Hopf and colleagues used bone marrow derived macrophages prepared from mice. They also found that a *B.p tssD-5* mutant showed decreased intracellular numbers 24 hours post infection.

The other *tag* mutants (i.e. *B.t $\Delta tagB-5$* , *$\Delta tagC-5$* and *$\Delta tagD-5$*) also exhibited the same intracellular replication characteristics in that the numbers of intracellular bacteria were reduced at 6 hours post infection compared to 2 hours, before increasing again at 24 hours. This demonstrates that all the mutant strains investigated are equally capable of intracellular replication as the WT. Further experiments using a different cell line, in particular one which is not used as a model for a professional phagocytic cell (RAW 264.7 cells are used as a model for macrophages), might yield different results. It is also worthwhile noting that other studies use different concentrations of kanamycin (both higher and lower) to kill extracellular bacteria which, if the eukaryotic cell membrane is being damaged (as one would expect given the fusion activity observed), could have an adverse effect on the intracellular bacteria.

It is worth noting that the allelic replacement method using a modified PheS protein as a counter-selectable marker was very time consuming as cPhe takes a long time to dissolve at the concentrations required. In future it would be prudent to use cPhe containing only the L-isomer as this would effectively double the concentration of cPhe. It was also observed that cells were maintaining the plasmid in their chromosome (as determined by trimethoprim resistance) even in the presence of cPhe. I was eventually able to determine that this was due to using agar of insufficient purity. It is probable that this agar contained enough phenylalanine to overcome the effects of cPhe being incorporated into proteins by the mutant *pheS* gene, preventing toxicity. The author of a recent study (Miyazaki 2015) engineered a version of PheS which has a higher cPhe incorporation efficiency and can even be used in LB. Introducing the same modifications into the PheS protein introduced by pEX18Tp-*pheS* could make mutant construction easier.

Chapter 5 Role of the *tagA-tagD* genes in
T6SS-5 activity

5.1 Introduction

The results described in the previous chapter demonstrated that when any of the *tag* genes (*tagA-5*, *tagB-5*, *tagC-5* and *tagD-5*) present in the *B. thailandensis* T6SS-5 gene cluster are deleted, the resulting strains are unable to induce MNGC formation in RAW 264.7 cells. The *B.t tagA-5*, *tagB-5*, *tagC-5* and *tagD-5* mutant strains were still capable of invasion and replication within RAW 264.7 cells. Based on the observations of French et al. (2011), who demonstrated that the fusion of infected host cells was facilitated by T6SS-5 (rather than other virulence factors which prevented internalisation or escape from phagosomes), the results of the previous chapter are consistent with the hypothesis that the four *tag* genes are either secreted effectors or auxiliary components of the T6SS.

Of the 13 core T6SS subunits, previous studies have demonstrated that two of them are universally secreted into culture supernatants: The inner-tube protein, TssD (often called haemolysin co-regulated protein, Hcp), and the tail spike protein, TssI (often called valine-glycine repeat G, VgrG). One of the proteins not originally identified as a core component, the PAAR protein, which 'sharpens' the tip of the TssI spike, is also secreted. Although other proteins can be secreted by T6SSs i.e. effector proteins, the secretion of TssD and TssI is a feature of all active T6SSs and therefore the presence of these two proteins in culture supernatants is considered the hallmark of a functional system.

The presence or the absence of these hallmark secreted proteins in the culture supernatants following deletion of genes of unknown function allows one to determine if the deleted genes are required for T6SS activity. Using this approach, all of the 13 core *tss* genes (including *tssD* and *tssI*) were found to be required for export by the T6SS (Zheng & Leung 2007). In contrast, the deletion of genes encoding T6SS-secreted effectors, such as the antibacterial, *Ssp1* and *Ssp2* proteins of *Serratia marcescens*, results in a phenotype equivalent to a T6SS-deficient mutant in bacterial competition assays, but has no effect on the export of other substrates of this system based on TssD secretion (Murdoch et al. 2011).

Therefore, if the *tag* genes are required for MNGC formation, but are not required for secretion by T6SS-5 as determined by the presence or absence of TssD-5 in the culture supernatants, it would support the suggestion that the Tag proteins are substrates of T6SS-5. It is also possible that, like TssI-5 and TssD-5, the Tag proteins are essential for the activity of T6SS-5 and are also secreted.

To determine whether the Tag proteins are required for T6SS-5 secretion it was necessary to develop a system where the *B.t* T6SS-5 is active under *in vitro* conditions without the need to infect cell lines.

5.1.1 Construction of pSCrhaB2-*virAG* for T6SS-5 induction in *B.t* growing in bacteriological medium

Previous work demonstrated that T6SS-5 in *B.p* was inactive under standard culture conditions but active when induced by the overexpression of the *virAG* genes from a plasmid (Burtnick et al. 2011). Induction of T6SS-5 activity when the *virAG* were overexpressed was also demonstrated in *B.m* (Schell et al. 2007). Therefore, in order to investigate the role of the *tag* genes on T6SS-5 function by monitoring TssD-5 secretion, it was necessary to artificially induce the system *in vitro*. By analogy, expression of the *B.t virA* and *virG* genes on a multicopy plasmid should achieve the same effect. Therefore, it was decided to clone the *B.t virA* and *virG* genes into a rhamnose-inducible expression vector.

The *virA* and *virG* genes were amplified on the same amplicon using the primers BthaiVirAGRhaFor and BthaiVirAGRhaRev in a PCR which used KOD polymerase to generate a 2572 bp product which was digested with the restriction enzymes NdeI and BamHI. The rhamnose-inducible, broad host range pSCrhaB2 plasmid was digested with the same enzymes and the two digested DNA fragments were ligated together. The ligation mixture was used to transform *E. coli* JM83 cells which were spread on IST agar plates containing 25 µg/ml trimethoprim. After incubation at 37°C overnight, colonies growing on this plate were screened to identify those which harboured a plasmid with the correct sized insert. Screening was performed by a colony PCR screen which used the vector-specific pSCrhaB2for and pSCrhaB2rev primers and GoTaq polymerase. When a colony contained the empty pSCrhaB2 vector, a 219 bp DNA fragment was amplified compared to a 2758 bp DNA fragment when the *virAG* genes were cloned into the plasmid. Colonies which appeared positive in the PCR screen were grown overnight and the plasmid extracted by the mini-prep procedure. Plasmid DNA was electrophoresed in an agarose gel to check it was the correct size (10074 bp) and the sequence of the inserted DNA was confirmed by nucleotide sequencing. The pSCrhaB2-*virAG* plasmid was used to transform SM10(λpir) cells and then delivered into WT *B.t* E264 by conjugation. The empty pSCrhaB2 vector was also introduced into WT strain E264 by conjugation, to serve as a non-induced control. The presence of the plasmids in *B. thailandensis* was confirmed by growing overnight cultures of potential plasmid-containing colonies and isolating the plasmid DNA by the mini-prep method. Plasmid DNA was electrophoresed in an agarose gel to confirm the presence of pSCrhaB2-*virAG* (10,074 bp) and pSCrhaB2 (7,519 bp) (Figure 5.1 B). The pSCrhaB2 and pSCrhaB2-*virAG* plasmids were also introduced, by conjugation, into the *B.t Δtssk* mutant which was generated as described in section 4.2.2.

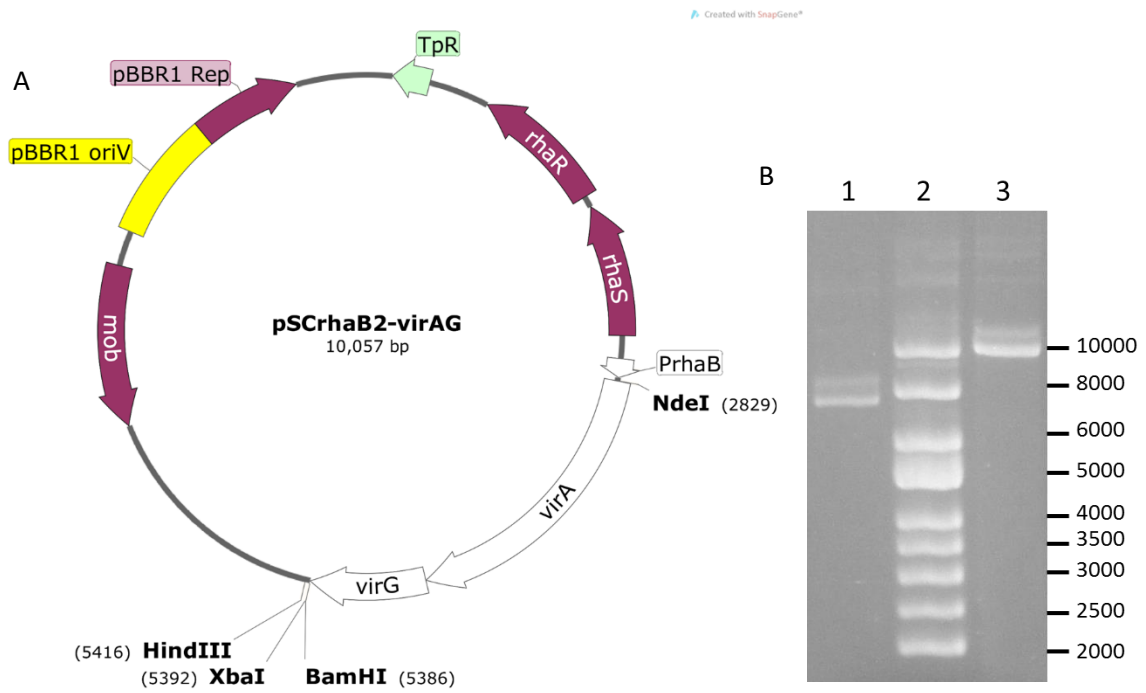


Figure 5.1 pSCrhaB2-*virAG* vector

The pSCrhaB2-*virAG* plasmid was constructed as described in the text and introduced into *B.t* by conjugation. A) Illustration of the pSCrhaB2-*virAG* plasmid drawn with SnapGene. B) Agarose gel electrophoresis of plasmid DNA isolated by miniprep from cultures of *B. thailandensis* containing the indicated plasmids. Lane 1, pSCrhaB2; lane 2, Supercoiled DNA ladder; Lane 3, pSCrhaB2-*virAG*. DNA size markers are shown in bp.

5.1.2 Induction of T6SS-5 activity by the pSCrhaB2-*virAG* plasmid

To perform the secretion assays which would be used to investigate the effect of *tag* gene deletion on T6SS-5 function, it was necessary to grow the bacteria under conditions where the *virA* and *virG* genes were expressed from the pSCrhaB2-*virAG* plasmid to induce the T6SS-5 gene cluster. It was decided to use a broth containing a low protein concentration so as not to interfere with assays using precipitated culture supernatants.

5.1.2.1 Rhamnose Induction of *virAG* expression in dialysed brain heart infusion broth

Initial attempts to induce T6SS-5 by overexpression of the *virA* and *virG* genes used a dialysed brain heart infusion (dBHI) broth prepared by dialysing a concentrated brain heart infusion solution against water overnight at 4°C before the dialysate was sterilised by autoclaving. Colonies of the WT *B.t* strain containing either pSCrhaB2 or pSCrhaB2-*virAG* were grown in dBHI containing 50 µg/ml trimethoprim overnight at 37°C in a shaking incubator. The overnight cultures were used to inoculate fresh 25 ml of the same medium to a starting OD₆₀₀ of 0.05 and the cultures were grown at 37°C in a shaking incubator until the optical density had reached 0.5. At this point, a 10% (w/v) filter sterilised rhamnose solution was added to give a final concentration of either 0.2 or 0.02% (w/v) rhamnose. After three hours of induction, a volume of culture equivalent to 1 ml of OD₆₀₀ 1.0 was taken (i.e. if the OD₆₀₀ was 1.25, a 0.8 ml sample was taken), the cells were collected by centrifugation at 15,000 x g for 1 minute, the supernatant was discarded and the cell pellet was resuspended in 100 µl of 1 x Laemmli buffer to give a 'cell-associated' (CA) sample. The remaining culture was centrifuged at 3,900 x g for 20 minutes following which a volume of the supernatant equivalent to 15 ml of OD₆₀₀ 1.0 culture was filter sterilised. Proteins were precipitated by the addition of 100% (w/v) trichloroacetic acid (TCA) to a final concentration of 10% (w/v), and incubation at -20°C overnight.

The frozen samples were defrosted on ice and centrifuged at 3,900 x g to collect precipitated proteins. Two acetone washes were performed before the pellet was allowed to air dry. The resulting proteins were resuspended in 25 µl of 6 M urea containing 25 mM ammonium bicarbonate, and then mixed 1:1 with 2 x Laemmli buffer to give a 'supernatant' (S) sample. Both the supernatant and cell associated samples were boiled for 10 minutes and centrifuged at 15,000 x g for 10 minutes before 15 µl of each were electrophoresed in a 12% SDS-polyacrylamide gel. As shown in Figure 5.2 this approach did not result in detectable induction of T6SS-5 as judged by the absence of a protein of the expected size of TssD-5 (18.2kDa) in either the supernatant or cell associated samples from *B.t* containing pSCrhaB2-*virAG*. Analysis of the composition of BHI shows that it contains 0.3% (w/v) glucose. As a concentration of 0.2% (w/v) glucose is sufficient to inhibit the *rhaB* promoter activity by catabolite repression in *E. coli* (Cardona & Valvano 2005) it may also be the reason for the absence of secreted TssD-5 in *B.t*.

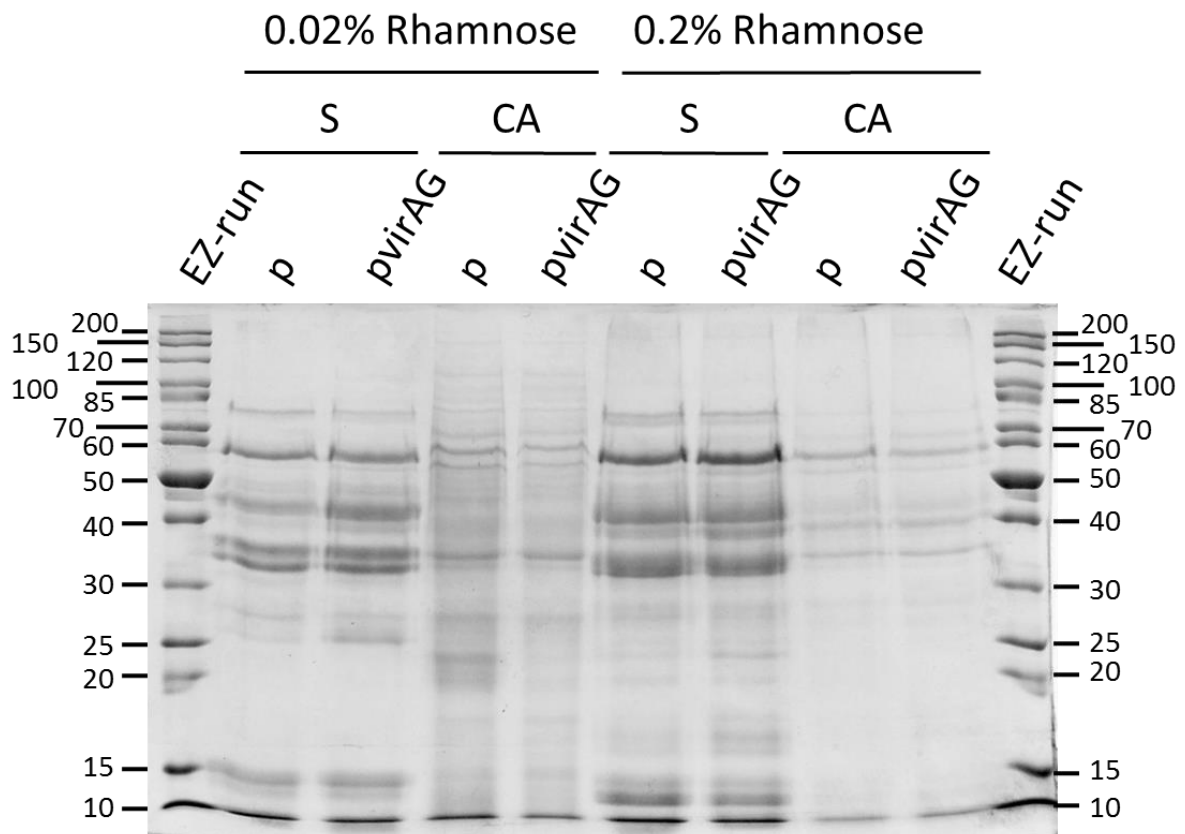


Figure 5.2 Rhamnose induction of cultures of *B. thailandensis* containing pSCrhaB2 or pSCrhaB2-*virAG* grown in dialysed brain heart infusion broth

Coomassie stained 12% polyacrylamide gel of TCA precipitated supernatant (S) and cell associated (CA) samples of *B. thailandensis* containing either pSCrhaB2 (p) or pSCrhaB2-*virAG* (pvirAG) grown in dialysed brain heart infusion induced with either 0.02% or 0.2% (w/v) rhamnose. EZ run, EZrun unstained ladder. Protein markers displayed in kDa.

5.1.2.2 Induction of *virAG* expression in M9 minimal medium

As the presence of glucose in dBHI likely prevented the expression of *virA* and *virG* from pSCrhaB2-*virAG*, a broth using an alternative carbon source was tested. To this end, overnight cultures of WT and $\Delta tssK-5$ *B. thailandensis* harbouring either pSCrhaB2 or pSCrhaB2-*virAG* were grown in M9 minimal medium containing 0.5% glycerol and 0.5% casamino acids with shaking at 37°C. The overnight cultures were used to inoculate 25 ml of the same medium to an OD₆₀₀ of 0.05 and the cultures were grown with shaking at 37°C to an OD₆₀₀ of 2.0 before a CA and S sample was prepared from each culture, 15 µl of each sample was electrophoresed in a 15% SDS polyacrylamide gel. As indicated in Figure 5.3, cell associated samples prepared from cultures of WT *B.t* and the *B.t* $\Delta tssK$ mutant harbouring pSCrhaB2-*virAG* had a prominent band between 15 and 20 kDa which was absent in cell associated samples of cultures containing empty pSCrhaB2. Importantly, a protein band which migrated at roughly the same size was also present in the supernatant obtained from the WT strain containing pSCrhaB2-*virAG*, but absent from all other supernatant samples. These observations are consistent with the idea that the absence of glucose would allow for induction of expression of *virA* and *virG* from pSCrhaB2-*virAG* which in turn induced the expression of the T6SS-5 gene cluster. The band observed is likely to be TssD-5 which has a predicted molecular weight of 18.2 kDa and would be expected to be found in cell associated samples prepared from cultures of the WT strain and $\Delta tssK-5$ mutant samples when the T6SS-5 gene cluster was induced. One would also expect to detect TssD-5 in the supernatant samples prepared from cultures of WT *B.t* harbouring pSCrhaB2-*virAG*, but not those prepared from cultures of the $\Delta tssK-5$ mutant containing pSCrhaB2-*virAG* as the T6SS-5 apparatus is unable to assemble.

These results further imply that the *B.t* $\Delta tssK-5$ mutant is indeed T6SS-5 secretion deficient as suggested by the MNGC formation assays performed previously (section 4.2.3). It is not clear why the pSCrhaB2-*virAG* plasmid is capable of induction of T6SS-5 when there is no rhamnose present in the culture medium. It could be a result of leaky expression from the *rhaB* promoter due to the absence of catabolite repression. Although expression from pSCrhaB2 is tightly regulated in *B. cenocepacia* growing in LB, which has low levels of glucose (Cardona & Valvano 2005), the complete absence of glucose in M9-glycerol may induce expression from the *rhaB* promoter. It is also possible that under these conditions *B. thailandensis* produces a metabolite that could induce expression from pSCrhaB2, for example, a rhamnolipid precursor, although this seems unlikely.

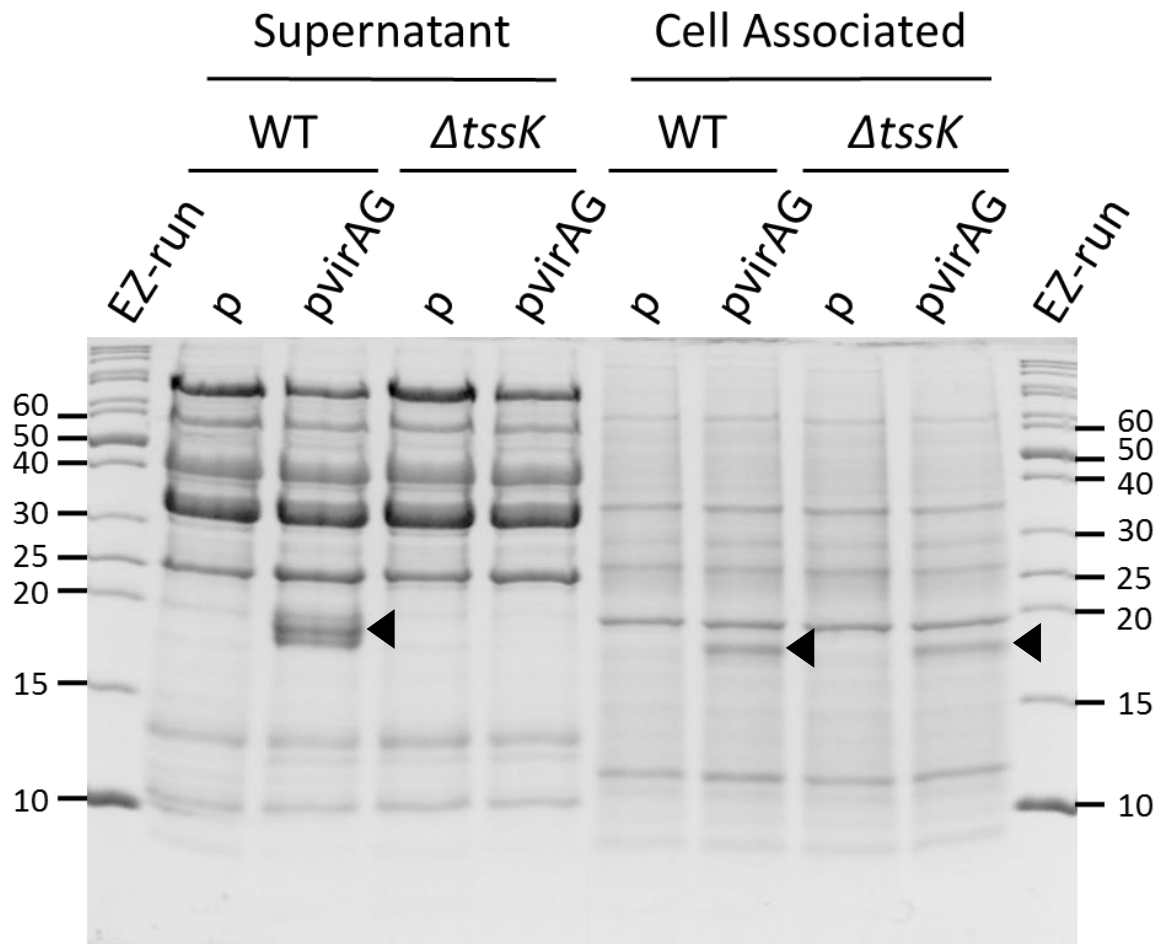


Figure 5.3 Induction of T6SS-5 in *B.t* growing in M9 glycerol

Coomassie blue stained 15% polyacrylamide gel used to fractionate cell associated and supernatant samples prepared from cultures of *B.t* WT and $\Delta tssK$ mutant strains containing either pSCrhaB2 (p) or pSCrhaB2-virAG (pvirAG) grown in M9 containing 0.5% glycerol and 0.5% casamino acids. EZrun, EZrun unstained ladder; black arrowheads, indicate protein bands at approximately 18.2 kDa likely to be TssD-5. Protein markers displayed in kDa.

5.1.3 Identification of potential TssD-5 protein band by mass spectrometry

To confirm that the 18.5 kDa protein band observed in Figure 5.3 was TssD-5, the supernatant sample prepared from a culture of WT *B.t* containing pSCrhaB2-*virAG* was electrophoresed in a 15% SDS polyacrylamide gel and stained using InstantBlue. The prominent band migrating according to a protein with a molecular weight between 15 and 20 kDa was excised, placed in a sterile microcentrifuge tube and sent to the biOMICS facility at the University of Sheffield to be analysed by in-gel tryptic digestion followed by analysis by mass spectrometry. The protein which gave the highest score on the Mascot analysis software was TssD-5 with a coverage of 96.91% (Table 5.1) confirming that the band observed was indeed TssD-5. This also suggests that the pSCrhaB2-*virAG* plasmid is capable of inducing T6SS-5 when present in *B. thailandensis* strains grown in M9 glycerol containing 0.5% (v/v) and 0.5% (w/v) casamino acids without the requirement of adding rhamnose.

5.2 Purification of TssD-5 for antibody generation

Once it had been determined that the prominent protein band observed in M9 culture supernatants of WT *B. thailandensis* containing pSCrhaB2-*virAG* was TssD-5, it was decided to raise antibodies against the protein, which would allow the T6SS-5 secretion phenotype of *B.t* mutant strains to be assayed without relying on mass spectrometry.

5.2.1 Construction of a TssD-5 overexpression vector

To create a plasmid to overproduce the TssD-5 protein in *E. coli*, the *tssD-5* gene was amplified using a *B. thailandensis* boiled lysate as the template with KOD polymerase and primers *tssDpET14bfor* and *tssDpET14brev* which introduced an NdeI site upstream of the *tssD-5* ORF and a BamHI site downstream. The primers were designed so that the start codon encoding the N-terminal methionine of TssD-5 was in frame with the hexa-histidine tag encoded by the pET14b plasmid and would hence express TssD-5 containing an N-terminal hexa-histidine tag. The introduction of the hexa-histidine tag would facilitate purification of TssD-5 by immobilised metal affinity chromatography (IMAC). The cloning of *tssD-5* into pET14b, downstream of the T7 promoter, allowed for overproduction of the protein when the plasmid was introduced into an *E. coli* strain containing the gene encoding the T7 RNA Polymerase (such as BL21(λDE3)).

The 644 bp PCR amplified DNA fragment containing *tssD-5* and the pET14b plasmid were digested with NdeI and BamHI and ligated together. The ligation mixture was used to transform *E. coli* JM83 competent cells which were spread on LB agar plates containing 100 µg/ml ampicillin. Colonies growing on this plate were used as a template for a PCR screen using GoTaq polymerase and the vector specific T7for and T7rev primers which amplified a 212 bp DNA fragment when empty pET14b was present and an 841 bp DNA fragment when pET14b-*tssD-5* (Figure 5.4 A) was present.

Table 5.1 Band identification result with the highest Mascot score

Accession	Description	Score	% Coverage	# Proteins	# Unique Peptides	# Peptides	# AAs	MW [kDa]
83716550*	hcp protein [Burkholderia thailandensis E264]	5805.06	96.91	8	14	21	162	18.2

*Accession number 83716550: TssD-5

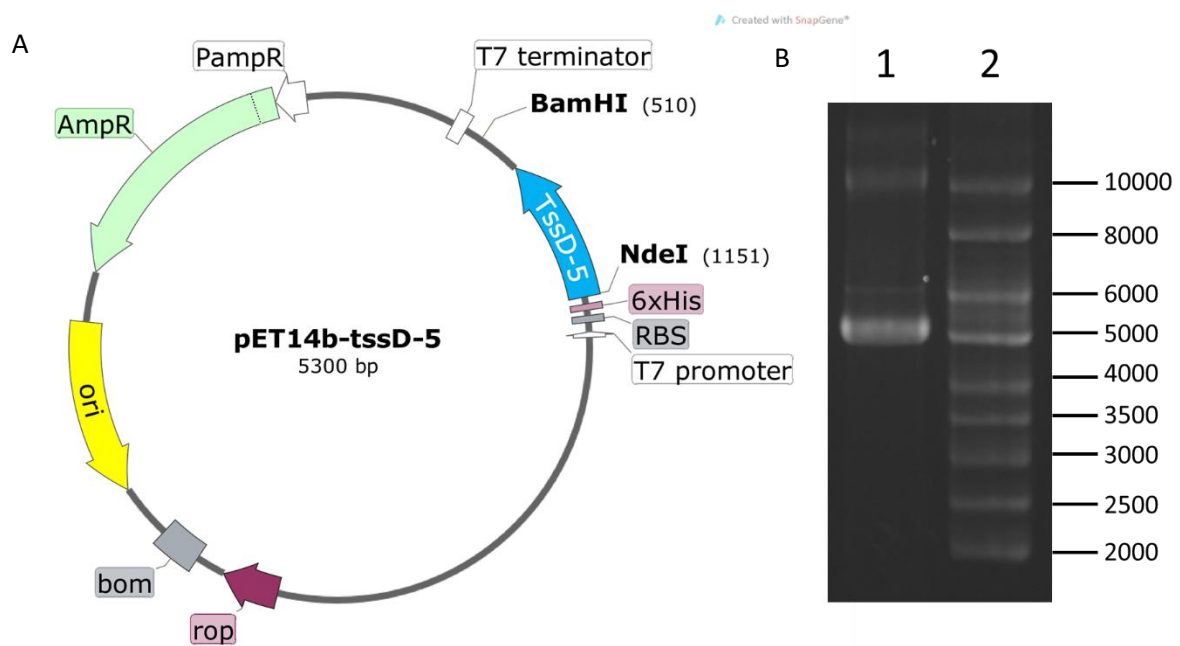


Figure 5.4 pET14b-*tssD-5*

A) Plasmid map of pET14b-*tssD-5* drawn using SnapGene. B) Agarose gel electrophoresis of pET14b-*tssD-5* purified by plasmid mini-prep. Lane 1, pET14b-*tssD-5*; lane 2, supercoiled DNA ladder. DNA size markers are shown in bp.

Colonies which acted as templates for reactions which produced the correct sized fragments as judged by agarose gel electrophoresis were grown overnight in LB containing 100 µg/ml ampicillin whereupon the plasmid DNA was harvested by the miniprep procedure. The prepared plasmid DNA was analysed by agarose gel electrophoresis (Figure 5.4 B) and the sample which contained the correct sized plasmid (5300 bp) analysed by nucleotide sequencing to confirm the integrity of the cloned *tssD-5* gene.

5.2.2 Expression and solubility test of TssD-5

The pET14b-*tssD-5* plasmid was introduced into *E. coli* BL21(λDE3) cells and transformants were selected on LB agar plates containing 100 µg/ml ampicillin following incubation at 37°C overnight. A single colony growing on the plate was then used to inoculate a 4 ml overnight culture in BHI containing 100 µg/ml ampicillin, which in turn was used to inoculate 500 ml of the same medium to a starting OD₆₀₀ of 0.05. Once the culture had reached an OD₆₀₀ of 0.4-0.6, a volume of culture equivalent to 1 ml OD₆₀₀ 1.0 was centrifuged at 15,000 x g and the resulting cell pellet resuspended in 100 µl 1 x Laemmli buffer to give a cell associated pre-induction sample. IPTG was added to the remaining culture at a final concentration of 1 mM to induce production of the TssD-5 protein and incubation was continued for another three hours at which time a volume of culture equivalent to 1 ml at OD₆₀₀ 1.0 was centrifuged at 15,000 x g and the resulting cell pellet resuspended in 100 µl 1 x Laemmli buffer to give a cell associated post-induction sample.

The remaining culture was then centrifuged at 3,900 x g for 10 minutes to collect cells and the supernatant was discarded. The cell pellet was resuspended in wash buffer, recentrifuged and the supernatant removed. The resulting cell pellet was then frozen overnight at -20°C. The following day, the cells were thawed and resuspended in lysis buffer containing 10 mM imidazole supplemented with lysozyme, PMSF and sodium deoxycholate and sonicated to lyse the cells. A sample was taken at this point ('crude lysate') and the remaining lysate was centrifuged to remove the cell debris. The resulting clarified lysate, corresponding to the soluble fraction, along with the other fractions were analysed by SDS-PAGE (Figure 5.5).

SDS-PAGE analysis showed the presence of a high abundance protein of ~20 kDa corresponding to the predicted size of histidine tagged TssD-5 (20.5 kDa) in the induced culture that was absent from the culture prior to induction. Although at least 50% of the protein appeared to be insoluble as the quantity of protein in the band was decreased in the soluble fraction in comparison to the crude fraction, there was enough soluble protein to proceed to purification by IMAC.

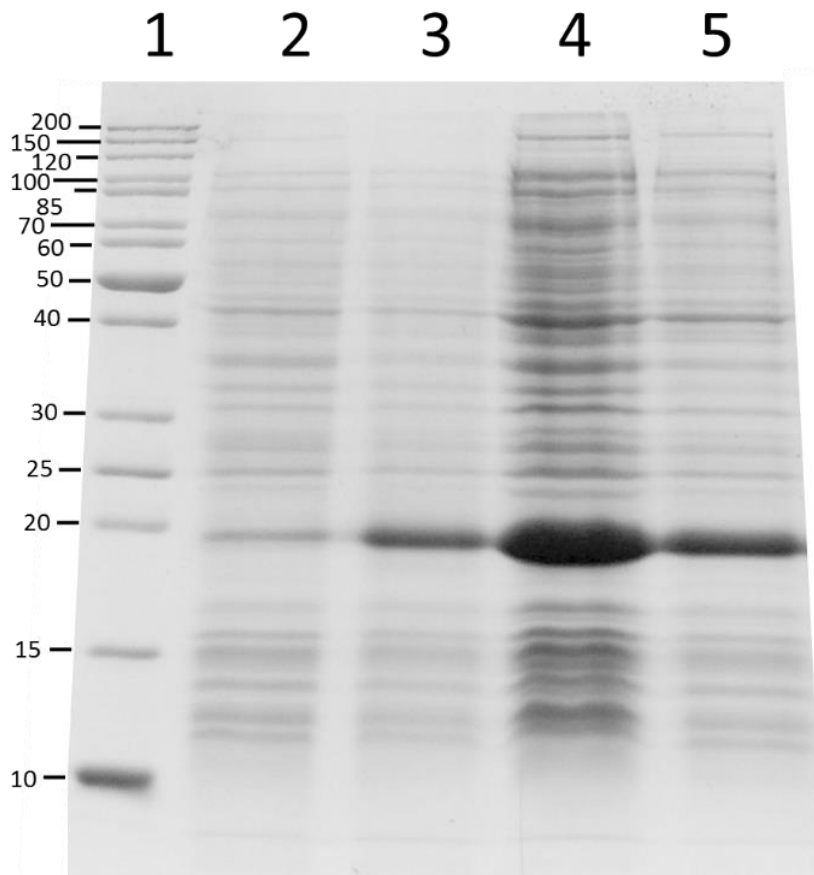


Figure 5.5 Overproduction of TssD-5 in *E. coli*

15% polyacrylamide gel of samples prepared from cultures of *E. coli* BL21(λ DE3) harbouring the pET14b-*tssD-5* plasmid following IPTG induction and solubility testing. Lane 1, EZ-run unstained ladder; lane 2, cell associated sample of culture before induction; lane 3, cell associated sample of culture after 3 hours induction with 1 mM IPTG; lane 4, crude lysate prior to centrifugation; lane 5, soluble fraction. Protein markers displayed in kDa.

5.2.3 Purification of histidine-tagged TssD-5 by IMAC

After filtration through a 0.22 μm syringe filter, 10 ml of the soluble fraction following TssD-5 overexpression was loaded onto a 1 ml HisTrap (GE Healthcare) column using a syringe and the flow through was collected. After loading, the column was connected to an Äkta purifier system (GE Healthcare) running at a flow rate of 1 ml/minute and washed with 10 column volumes of lysis buffer containing 10 mM imidazole. As shown in Figure 5.6 B the vast majority of histidine tagged TssD-5 was adsorbed onto to the column as there was a negligible amount of the 20 kDa protein present in the flow through sample. Using the gradient function of the Äkta system the imidazole concentration was increased from 10 to 500 mM over a period of 30 minutes and 1 ml fractions were collected (Figure 5.6). The protein concentration of the liquid exiting the column was determined by monitoring its absorbance of UV light at 280 nm. As shown in Figure 5.6 A, there is a clear peak in the UV 280 absorbance between elution fractions A15 (255 mM imidazole) to B7 (369.3 mM imidazole) corresponding to the elution of $\text{His}_6\text{TssD-5}$ from the column (Figure 5.6 B).

5.2.4 Generation of antibodies

Before using the protein to immunize a rat, it was necessary to replace the Tris lysis buffer in which the protein was suspended with phosphate buffered saline (PBS) to avoid any potential harmful effects of the lysis buffer on the animal used to generate antibodies. To do this, the three 1 ml elution fractions from the imidazole gradient indicated by the black arrows in Figure 5.6 B were combined and dialysed against 1 L of PBS overnight at 4°C. The concentration of the resulting protein sample in PBS was then adjusted to 1 mg/ml, as determined by the Bradford assay (Bio-Rad), using a 10 kDa molecular weight cut off (MWCO) centrifugal filter device (Amicon) and subjected to SDS-PAGE to assay purity (Figure 5.7 A). Although there were some protein bands present that were not at the expected size of ~20 kDa for $\text{His}_6\text{TssD-5}$, the vast majority of protein present appeared to be the desired protein, and the protein migrating with a size corresponding to ~40 kDa could be a $\text{His}_6\text{TssD-5}$ dimer, although the presence of SDS and β -mercaptoethanol in the Laemmli buffer should prevent this.

All work involving animals was carried out by staff in the University of Sheffield field laboratories in accordance with local ethics committee guidelines. To generate antibodies, a rat was injected with 330 μl of PBS containing 1 mg/ml of purified TssD-5 protein. After 14 days the rat was injected with a second 330 μl dose of antigen and a third 35 days after the initial immunisation. 45 days after the initial injection, a 1 ml sample of blood was taken from the animal and blood cells were removed by centrifugation at 13,000 x G for 1 minute. The supernatant, which contained the serum, was used to probe a western blot to assay the sensitivity of the antibody against a sample known to contain the target protein. Samples of purified $\text{His}_6\text{TssD-5}$ in PBS at 1, 0.1 and 0.01 mg/ml were electrophoresed in a 15% polyacrylamide gel before transferring to a PVDF membrane which was then probed using a

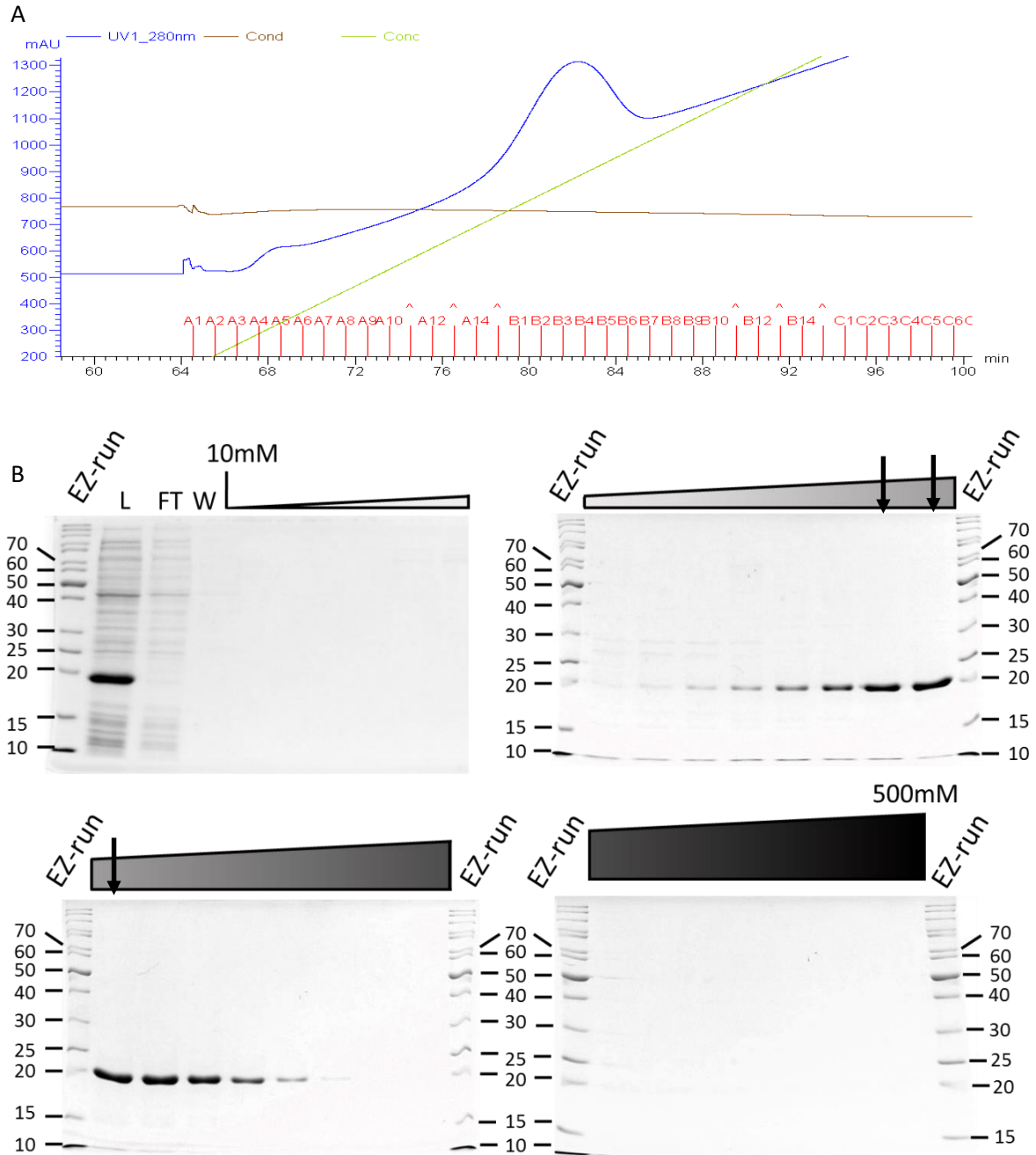


Figure 5.6 IMAC purification of TssD-5

IMAC purification of TssD-5 with elution using a 30 ml imidazole gradient from 10 to 500. A) Trace taken from the Äkta monitoring software. UV1_280nm, absorbance at OD₂₈₀; Cond, conductivity; Conc, Imidazole concentration. B) 15% polyacrylamide gels of sequential samples taken from the indicated samples and the fractions collected. L, load sample taken before application of the crude lysate to the column; FT, flow through (protein that did not bind to the column); W, sample taken from the wash fraction. Bar above gels, representative gradient of the concentration of imidazole in each 1 ml fraction; EZ-run, EZ-run unstained ladder. Protein markers displayed in kDa.

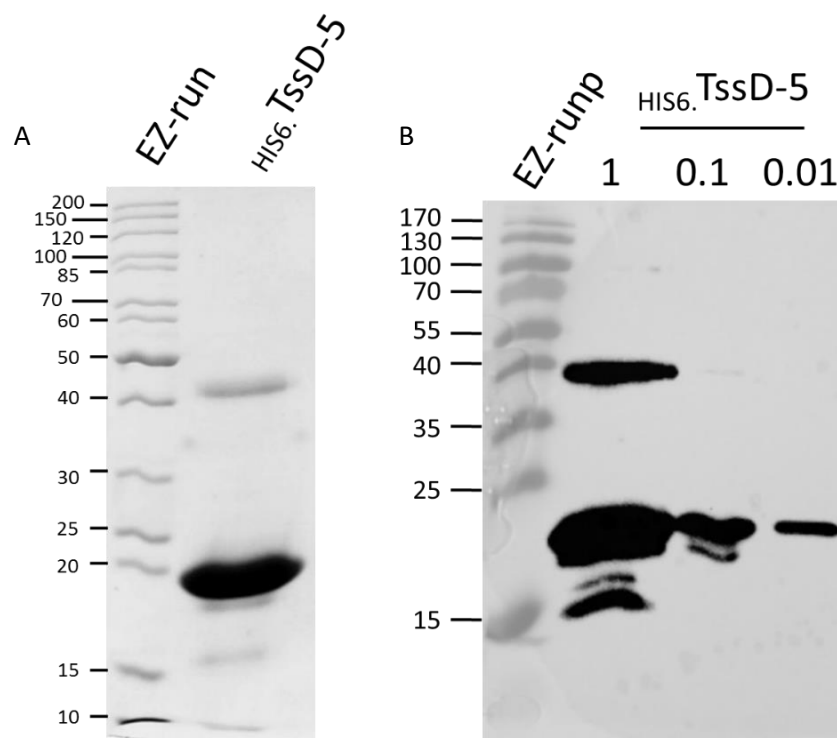


Figure 5.7 Testing of anti-TssD-5 serum taken from the rat 45 days after the initial injection of purified TssD-5

A) Coomassie stained 12% acrylamide gel showing purified protein used to immunise a rat. Samples are indicated above the gel, $_{\text{His6}}$.TssD-5, 1 mg/ml purified TssD-5 containing an N-terminal hexahistidine tag; EZ-run, EZ-run unstained ladder. B) Western blot of SDS-PA gel containing purified $_{\text{His6}}$.TssD-5 at the concentrations indicated in mg/ml following detection with antibody raised against purified $_{\text{His6}}$.TssD-5. EZ-runp, EZ-run prestained ladder. Protein markers displayed in kDa.

1 in 1000 dilution of serum taken from the first bleed in 5% milk powder. The presence of bound antibodies on the membrane was detected by adding 1 in 5000 horse radish peroxidase (HRP)-conjugated secondary antibody raised against rat IgG. Bands were visualised by the addition of chemiluminescent HRP substrate. Emitted light was detected using a ChemiDoc XRS+ system (BioRad). As shown in Figure 5.7 serum from the first bleed bound to the western blot at the location corresponding to the samples used to raise the antibody, as expected.

76 days after immunisation the rat was euthanized and its blood (~ 50 ml) drained. The blood was centrifuged at 3,900 x g for 20 minutes, whereupon pelleted blood cells were discarded. The serum-containing supernatant was separated into 500 µl aliquots and stored at -20°C for long periods or at 4°C for immediate use.

5.2.5 Assaying the antibody raised against TssD-5

To ensure that the antibody raised against purified histidine-tagged TssD-5 can be used to specifically detect native TssD-5 in cell lysate and supernatants and not one of the other four *B.t*-encoded TssD proteins, a *B. thailandensis* *tssD-5* mutant was constructed. The deletion was performed using SOE PCR to generate an in-frame deletion in the *tssD-5* gene which was introduced into the *B.t* chromosome by allelic replacement.

To carry out the SOE-PCR, two pairs of primers were used. Primers *tssDSOEfor2* and *tssDSOEmidrev* were used in a PCR with the proof-reading KOD polymerase and a WT *B.t* boiled lysate template to amplify a 584 bp product which contained the 3' end of the *tssC-5* gene and the first 60 bp of the *tssD-5* gene. The primers *tssDSOErev2* and *tssDSOEmidfor* were used similarly to amplify a 618 bp product which contained the final 60 bp of *tssD-5*, the entire *tssE-5* gene and the first 47 bp of *tssF-5*. The two PCR products were combined and used as a template in a third PCR which employed primers *tssDSOEfor2* and *tssDSOErev2* to amplify a 1168 bp fusion DNA fragment. The product of the third PCR and the pEX18Tp-*pheS* plasmid were digested with XbaI and PstI following which they were ligated together. The products of the ligation reaction were used to transform *E. coli* JM83 cells and transformants were selected on M9 agar containing 25 µg/ml trimethoprim, 1% (w/v) casamino acids, 0.5% (v/v) glycerol, 0.0005% (w/v) thiamine, 40 µg/ml X-gal and 0.1 µg/ml IPTG followed by incubation for two nights at 30°C. White colonies were grown overnight at 37°C in IST broth containing 25 µg/ml trimethoprim and plasmid DNA was harvested by the miniprep procedure. Plasmid DNA was analysed by electrophoresis in an agarose gel and a plasmid which migrated at the expected size for pEX18Tp-*pheS-ΔtssD-5* (i.e. 5632 bp) was checked by nucleotide sequencing.

E. coli SM10(λ pir) cells were transformed with pEX18Tp-*pheS*- Δ *tssD-5* before it was introduced into WT *B. t* by conjugation. Exconjugants were spread on M9 agar plates containing 50 μ g/ml trimethoprim to select for integration of the suicide plasmid into the *B. t* chromosome. Colonies that arose were restreaked on the same medium and following growth at 37°C were then restreaked on an M9 plate containing 0.1 % (w/v) cPhe to select for bacteria in which the *pheS* gene (and therefore the plasmid) had been excised from the chromosome by a second recombination event and hence no longer incorporated cPhe into proteins. Following plasmid excision, it left behind either a WT or mutant *tssD-5* gene which contained only the first 20 codons fused to the final 20 codons. To distinguish between colonies of WT and Δ *tssD-5* *B. t*, they were used as templates for a PCR (GoTaq) which used the primers *tssDscrnfor* and *tssDscrnrev* primers that annealed upstream and downstream of the annealing sites of the *tssDSOEfor2* and *tssDSOErev2* primers, respectively. When the WT *tssD-5* gene was present on chromosome 2, this PCR amplified a 2021 bp product compared with a 1652 bp product when Δ *tssD-5* was present.

To test the effectiveness of the TssD-5 polyclonal antibody the pSCrhaB2-*virAG* plasmid was introduced into the *B. t* Δ *tssD-5* mutant by conjugation. Cultures of WT and Δ *tssD-5* mutant *B. t* harbouring pSCrhaB2-*virAG* were grown in M9 broth containing 0.5% (v/v) glycerol and 0.5% (w/v) casamino acids. A volume of each culture equivalent to 1 ml OD₆₀₀ 1.0 was centrifuged and the cell pellet resuspended in 100 μ l Laemmli buffer to give cell associated (CA) samples. These samples were electrophoresed in a 15% polyacrylamide gel. The gel was subjected to western blotting and the membrane was probed using monoclonal antibody against the *E. coli* RNA polymerase β -subunit (anti-RNAP β). Following this, the bound antibodies were removed using Restore PLUS and the membrane was probed again using a 1 in 1000 dilution of rat serum containing antibody against TssD-5 (anti-TssD-5). As Figure 5.8 demonstrates, anti-TssD-5 binds to a protein of ~18 kDa in WT cells consistent with the predicted molecular weight of untagged TssD-5 (18.2 kDa). In contrast, there was no protein of such a size detected in the Δ *tssD-5* mutant. The anti-RNAP β monoclonal antibody which, although raised against an *E. coli* antigen, recognises a conserved epitope (TPEEKLLRAIFGEKAS) on the RNAP β subunit in a wide range of bacterial species including that of *B. t* (Bergendahl et al. 2003)(Stalder et al. 2011). As expected, probing with this monoclonal antibody as a control for detection of a cell-associated protein, showed the presence of the β subunit of RNAP (153.2 kDa) in the WT and Δ *tssD-5* *B. t* strains (Figure 5.8).

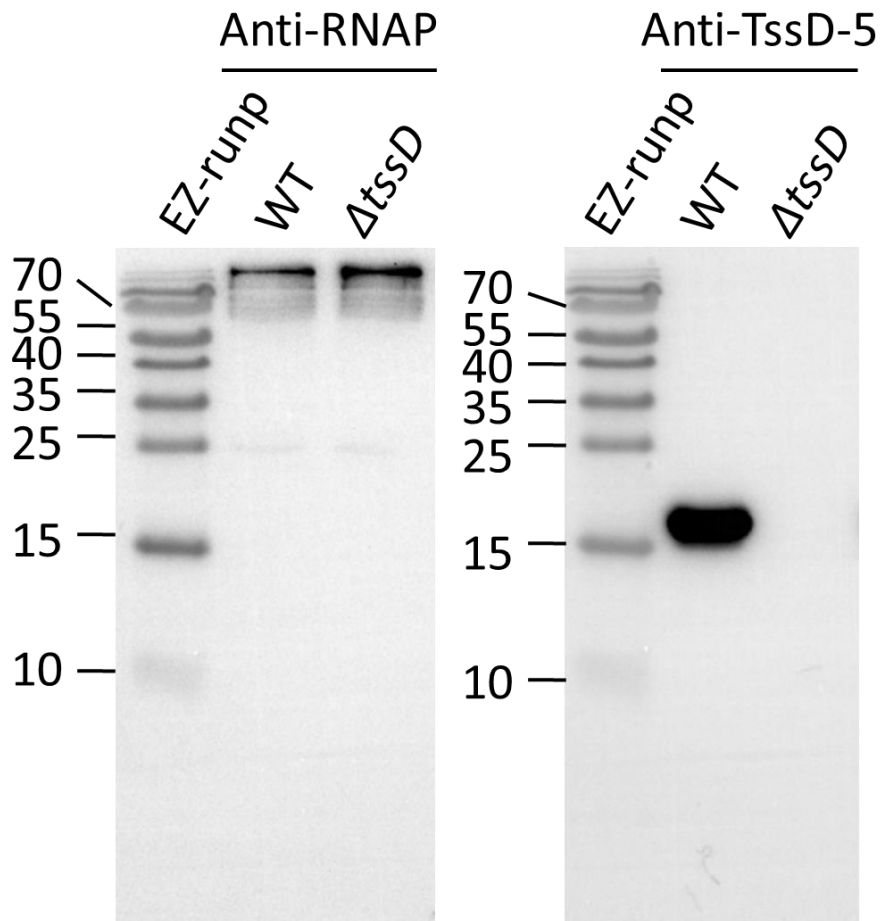


Figure 5.8 Testing of polyclonal antibody raised against TssD-5 in *Burkholderia thailandensis* samples

Western blot of cell-associated samples from *B. thailandensis* cultures grown in conditions where T6SS-5 is expressed. Both images are of the same blot which was probed first with monoclonal antibody raised against the RNAP β subunit followed by anti-TssD-5. WT, WT *B. thailandensis* harbouring pSCRhaB2-*virAG*; $\Delta tssD$, $\Delta tssD$ -5 mutant *B. thailandensis* containing pSCRhaB2-*virAG*; EZ-runp; EZ-run pre-stained ladder. Protein markers indicated in kDa.

The binding of the anti-TssD-5 antibody to a protein present in the WT sample but not to the $\Delta tssD-5$ sample indicates that it only binds to TssD-5 and not to any of the four other *tssD* gene products predicted to be encoded by the *B. thailandensis* genome. In particular, it does not bind to TssD-1 (BTH_I2962) which is expressed when *B.t* is grown in Vogel-Bonner minimal medium (Russell et al. 2012).

5.2.6 Confirmation that the *B.t* $\Delta tssK-5$ mutant lacks a functional T6SS-5

The same samples that were analysed by SDS-PAGE in Figure 5.3 were electrophoresed in a 15% polyacrylamide gel and then transferred to a PVDF membrane. The membrane was probed with a 1 in 1000 dilution of primary anti-TssD-5 antibody and 1 in 5000 anti-Rat IgG secondary antibody. The western blot shown in Figure 5.9 indicates that, as predicted by the observations of the Coomassie stained gel in Figure 5.3, TssD-5 is not present in either strain containing the empty pSCrhaB2 vector, indicating that *tssD-5* is not normally expressed when *B. thailandensis* is grown in the M9 containing 0.5% (v/v) glycerol and 0.5% (w/v) casamino acids. However, as indicated by the cell associated samples prepared from cultures of WT *B.t* cells and $\Delta tssK-5$ mutant cells both harbouring the pSCrhaB2-*virAG* vector, when the *virA* and *virG* genes are present, TssD-5 is expressed. In addition, TssD-5 was also detected in culture supernatants from WT *B.t* cells harbouring pSCrhaB2-*virAG*, whereas despite the presence of TssD-5 in its respective cell associated sample, the supernatant from a culture of the *B.t* $\Delta tssK$ mutant containing pSCrhaB2-*virAG* does not contain any detectable TssD-5. This indicates that the $\Delta tssK$ strain of *B. thailandensis* is defective in secretion by T6SS-5.

5.3 Mass spectrometry analysis of T6SS-5 secretome

In an effort to determine if the Tag proteins (and indeed any other, so far unreported proteins) were secreted by T6SS-5, mass spectrometry was utilised. Cultures of *B. thailandensis* WT and $\Delta tssK$ strains containing pSCrhaB2-*virAG* were grown in 25 ml of M9 containing 0.5% (v/v) glycerol and 0.5% (w/v) casamino acids to an OD₆₀₀ of 1.0. Secreted proteins were isolated by centrifuging the cultures to pellet cells, followed by the filter sterilisation of the resulting supernatant through a 0.22 μ m syringe filter. A volume of this supernatant equivalent to 15 ml of OD₆₀₀ 1.0 of the culture was placed on ice and sodium deoxycholate was added to a concentration of 25 mM. This solution was mixed thoroughly and incubated for 30 mins before adding TCA to a final concentration of 10% (w/v). Proteins were precipitated by incubating the samples at -20°C overnight. The supernatant mixture was defrosted on ice before centrifuging at 3,900 x g at 4°C for 60 minutes. The resulting protein pellet was resuspended in 5 ml 100% ice cold acetone and placed at -20°C for 60 minutes. Proteins were washed a second time by centrifuging at 3,900 x G for 60 minutes at 4°C, discarding the supernatant and again resuspending in 5 ml 100% ice cold acetone and placing at -20°C for 60 minutes. Precipitated proteins were collected

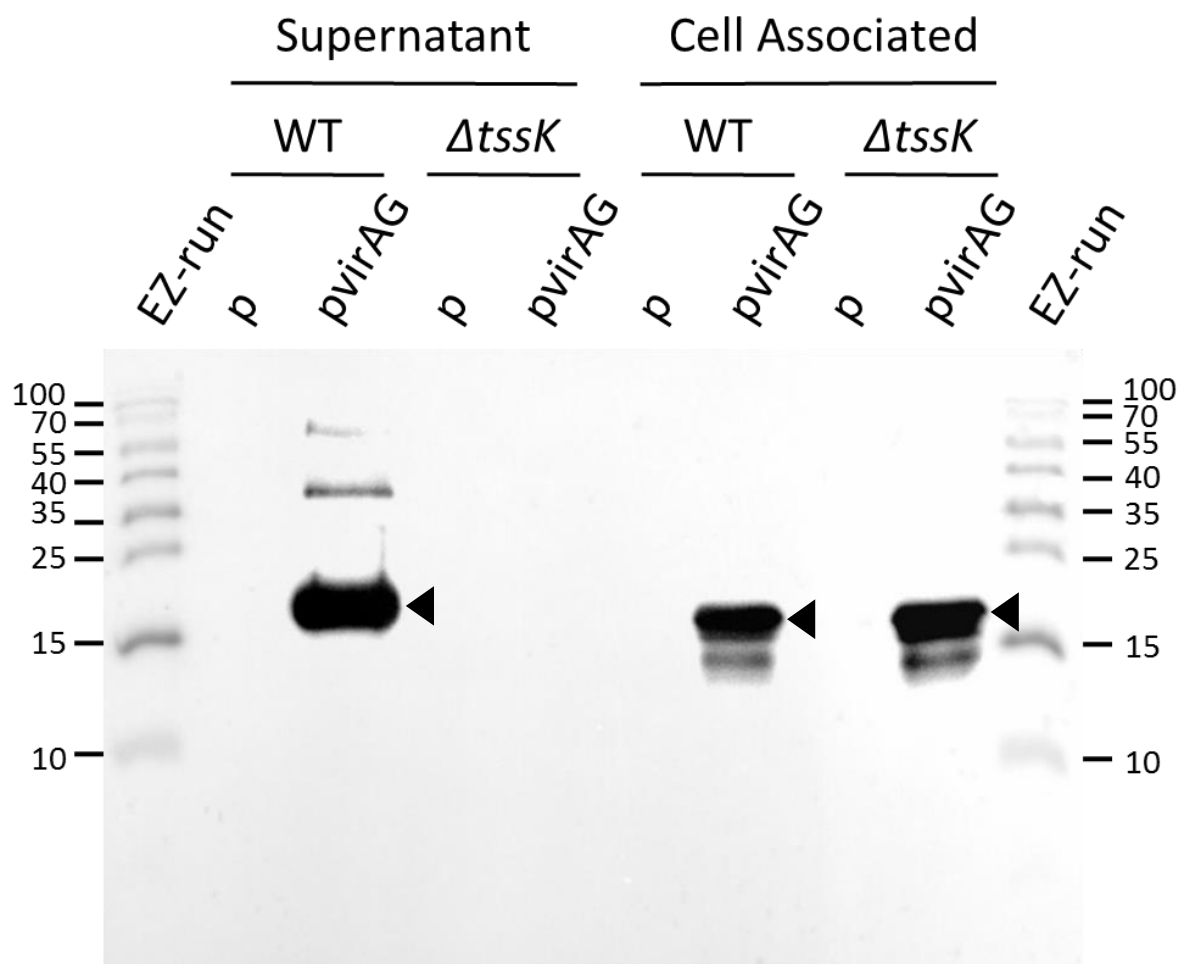


Figure 5.9 Validation of the *B. t* *tssK* mutant

Western blot of cell associated and supernatant samples taken from cultures of WT and $\Delta tssK$ mutant *B. thailandensis* containing either pSCRhaB2 (p) or pSCRhaB2-*virAG* (pvirAG) grown in M9 containing 0.5% glycerol and 0.5% casamino acids. EZrun, EZrun prestained ladder; black arrowheads, protein band migrating at approximately 18.2 kDa likely to be TssD-5. Protein markers displayed in kDa.

by another centrifugation step at 3,900 x g at 4°C for 60 minutes and the supernatant was discarded. Residual acetone was removed by air drying at room temperature for 30 minutes. The resulting protein pellet was resuspended in 50 µl 6 M urea containing 25 mM ammonium bicarbonate. This protein solution was mixed with an equal volume of 2 x Laemmli buffer and a 30 µl sample was electrophoresed in a 15% polyacrylamide gel. The gel was cast using plates which had been cleaned thoroughly to avoid potential contamination from proteins which had been analysed in previous gels which were cast using the same plates. Following electrophoresis, the gel was stained using freshly prepared Coomassie blue stain followed by destaining to obtain the desired colour intensity.

Each lane of the gel was cut into 12 horizontal strips using a sterile scalpel blade. The strips were each placed in an individual sterile microcentrifuge tube, and the proteins were destained, reduced, alkylated and digested using trypsin (described in more detail in section 2.8.6). The resulting peptides were analysed by Trong Khoa Pham of the University of Sheffield Chemical and Biological Engineering department. This was performed in triplicate, from independent samples and a list of proteins identified in each sample was produced, the complete list is shown in the appendix Table 10.4.

A total of 79 proteins were identified in all three samples prepared from culture supernatants of the WT strain, including TssD-5, as one would expect given that previous western blot analysis of samples prepared in the same manner shows that it is present (section 5.2.5). It had also been identified by mass spectrometry performed directly on the protein band predicted to be TssD-5. The only other protein obviously related to the T6SS-5 that was detected in all three samples was TssI-5. Given that the presence of TssD-5 and TssI-5 in culture supernatants are hallmarks of a functional T6SS-5, this further demonstrates that T6SS-5 is expressed and active. Surprisingly, TagA-5, TagB-5, TagC-5 and TagD-5 were not identified in any of the samples. This suggests that they are not secreted.

Although only the TssD-5 and TssI-5 proteins of T6SS-5 were detected in the culture supernatants, the protein product of BTH_II0854 was detected. This gene is found directly adjacent to the T6SS-5 gene cluster, downstream of *tssM-5*. In *B. pseudomallei* and *B. mallei* the genes corresponding to BTH_II0854 (BPSS1512 and BMAA0729, respectively) has been named 'tssM' (Schell et al. 2007). This gene has been shown to be co-regulated with the T6SS-5 gene cluster in *B.m* (Burtnick & Brett 2013). This suggests that 'tssM' would be secreted in *B.t* under the same conditions used to drive T6SS-5 expression. However the protein product of BTH_II0854 is a deubiquitinase that is a substrate for the T2SS, not T6SS (Burtnick et al. 2014).

As would be expected from such preparations, a number of flagella components were also detected including the flagellin proteins BTH_I3196 and BTH_II0113 and the flagellar basal body rod protein FlgB (BTH_I0240). However, there were also some proteins present in all three samples that one would

not expect to observe in a secreted protein preparation. These included the outer membrane porin, OpcP (BTH_I11520) and a number of periplasmic amino acid-binding protein components of ABC transporters (BTH_I3300, BTH_I1783, BTH_I11598). This suggests that although immunoblotting equivalent samples to detect cytoplasmically located RNAP β did not detect any protein, there is probably a degree of cell lysis occurring. It is also possible that there are outer membrane vesicles present in the supernatant preparations.

5.3.1 Comparing the WT secretome to a *tssK* mutant secretome

As the Tag proteins were not detectable in *virAG*-induced WT supernatants when analysed by mass spectrometry, it was decided to attempt to identify any other potential effector proteins that were secreted by T6SS-5. As outlined earlier, the supernatant samples prepared from the *virAG*-induced *tssK-5* mutant were found not to contain TssD-5 when analysed by western blotting (Figure 5.9) indicating that it is deficient in secretion by T6SS-5. Therefore, comparing the secretomes of the WT and $\Delta tssK-5$ mutant should allow the identification of proteins secreted by T6SS-5 as such proteins would be present in WT supernatants but absent from those prepared from a $\Delta tssK$ mutant.

Proteins from supernatants were prepared from 25 ml cultures of the *B.t* $\Delta tssK$ mutant containing pSCrhaB2-*virAG* and analysed in the same way as those prepared from WT *B.t* harbouring pSCrhaB2-*virAG*. A total of 126 proteins could be identified in all three of the samples analysed (Table 10.5). As expected, TssD-5 was not present in all three of the samples, consistent with the western blot observations. However, it was detected in one of the samples, suggesting that there could have been some lysis occurring in one sample. TssI-5 was not detected in any of the samples, consistent with the $\Delta tssK-5$ mutant being defective T6SS-5 function. BTH_I10854 (the ubiquitin-specific proteinase also referred to TssM) was also present in all three samples, further confirming that its secretion is not T6SS-dependent.

Excluding TssD-5 and TssI-5, 20 proteins were present in all three of the WT samples and absent from the *tssK* mutant (Table 5.2). Of these, 13 contained a putative signal peptide, suggesting that they were not T6SS substrates. A further 2 were components of flagella and were therefore unlikely to be secreted by T6SS-5, although it is unclear why they were only found in the WT samples. One of the remaining proteins identified in the supernatant of the WT but not the $\Delta tssK-5$ mutant is TagM-1 (BTH_I2965). The *tagM-1* gene is located in the gene cluster that encodes T6SS-1 and is conserved in T6SS-1 gene clusters in other *Burkholderia* species. Given its genomic location, and the fact that it is predicted to be a periplasmically located lipoprotein that is anchored to the inner face of the outer membrane, it is unlikely to be exported by T6SS-5. BTH_I2965 shares 73.3% sequence identity with *B. cenocepacia tagM* (BCAL0340, also known as *bcsM*) which has been demonstrated to be required for

Table 5.2 Proteins present in the culture supernatant of WT *B.t* samples but absent from those of the T6SS mutant

NCBI Locus Tag	Signal Peptide (UniProt)	Description
BTH_I2965	-	Lipoprotein, putative (TagM-1)
BTH_I2723	-	Filamentous haemagglutinin
BTH_I1431	+	Putative uncharacterized protein
BTH_I1420	+	D-(-)-3-hydroxybutyrate oligomer hydrolase
BTH_I0415	+	Carboxy-terminal protease
BTH_I0353	+	Thiol:disulfide interchange protein
BTH_I0240	-	Flagellar basal body rod protein FlgB
BTH_II2139	+	TonB-dependent heme/hemoglobin receptor family protein
BTH_II2134	-	Lipoprotein
BTH_II1839	+	Leucine-, isoleucine-, valine-, threonine-, and alanine-binding protein
BTH_II1789	+	Ribonuclease T2 family
BTH_II1520	+	Outer membrane porin OpcP
BTH_II1243	+	Putative ABC transporter ATP-binding protein
BTH_II1165	-	Lipoprotein, putative
BTH_II1069	+	Gp28
BTH_II0868	-	Hcp protein (TssD-5)
BTH_II0863	-	Rhs element VgrG protein (TssI-5)
BTH_II0719	+	Streptavidin, putative
BTH_II0606	-	NADH dehydrogenase
BTH_II0228	+	Alpha-1,2-mannosidase family protein
BTH_II0213	+	Probable glucan 1,4- α -glucosidase
BTH_II0151	-	Flagellin D

secretion of the TssD (BCAL0343) in *B. cenocepacia* (Aubert et al. 2015), further suggesting that TagM-1 is probably not secreted by T6SS-5.

BTH_I2723 is predicted to be a filamentous haemagglutinin containing a transmembrane domain and thus is unlikely to be secreted by T6SS-5. Another WT specific protein, BTH_I12134, is predicted to be a D-methionine-binding lipoprotein located in the periplasm and so is unlikely to be a T6SS-5 substrate. BTH_I11165 is another putative lipoprotein and therefore unlikely to be a T6SS-5 substrate. The final potential T6SS-5 secreted protein was BTH_I10606, an FAD-dependent oxidoreductase family protein, which was therefore predicted to be located in the cytoplasmic membrane. Therefore, this approach did not identify any likely T6SS-5 substrates apart from TssD-5 and TssI-5 which had been identified previously.

5.4 Requirement of the Tag proteins for T6SS-5 activity

Given that all four *tag* genes are required for the formation of multinucleated giant cells during infection assays (section 4.2.7) and were not detectable in culture supernatants of WT *B. thailandensis* cells with active T6SS-5, the next logical assumption was that the Tag-5 proteins were required for the operation of T6SS-5. To investigate this hypothesis, the pSCrhaB2-*virAG* plasmid was conjugated into the *B.t* $\Delta tagA-5-tagD-5$, $\Delta tagA-5$, $\Delta tagB$, $\Delta tagC-5$ and $\Delta tagD-5$ mutants and the resulting strains were grown in M9 containing 0.5% (v/v) glycerol and 0.5% (w/v) casamino acids for analysis of T6SS-5 activity by monitoring TssD-5 secretion.

5.4.1 *A. B. thailandensis* strain lacking all four *tag* genes is deficient in TssD-5 secretion

The secretion of TssD-5 by the *B.t* $\Delta tagA-D$ mutant containing pSCrhaB2-*virAG* was assayed by electrophoresing cell associated and supernatant samples in a 15% polyacrylamide gel which were then transferred to a PVDF membrane and probed with antibody raised against *B. thailandensis* TssD-5. As demonstrated by the absence of TssD-5 from the supernatant sample, but presence in the cell associated sample in Figure 5.10, there was no T6SS-5-mediated secretion in a *B. thailandensis* strain in which all four *tag-5* genes had been deleted.

5.4.2 Each individual *tag* gene is required for secretion of TssD-5

Cell associated and supernatant samples of *B.t* $\Delta tagA-5$, $\Delta tagB-5$, $\Delta tagC-5$ and $\Delta tagD-5$ mutants containing pSCrhaB2-*virAG* were assayed for T6SS-5 activity as described previously. Figure 5.11 demonstrates that each individual *tag* gene is required for TssD-5 secretion by T6SS-5. TssD-5 was present in the cell associated samples of all of the cultures demonstrating that the lack of TssD-5 in the culture supernatants was not due to impaired expression of *tssD-5* in the mutants.

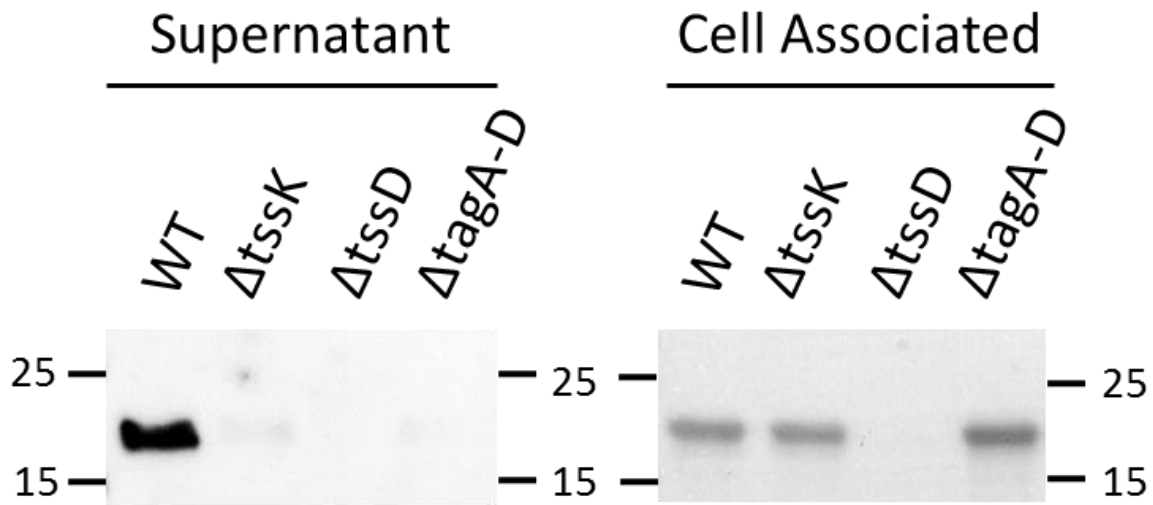


Figure 5.10 TssD-5 secretion by *B. thailandensis* lacking all four *tag* genes

Western blots of TCA precipitated supernatant and cell associated samples taken from cultures of the indicated strains of *B. thailandensis* containing pSCrhaB2-*virAG* grown in M9 containing 0.5% glycerol and 0.5% casamino acids and stained with polyclonal anti-TssD-5 antibody. Numbers indicate molecular weight in kDa.

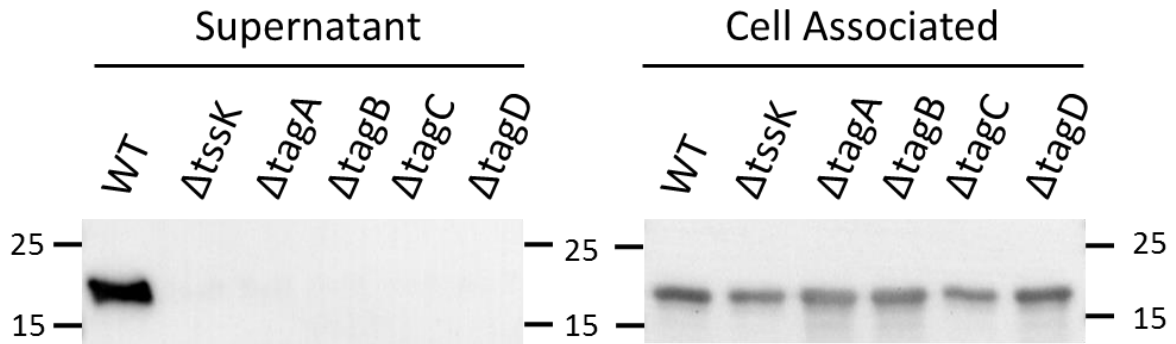


Figure 5.11 TssD-5 secretion by *B. thailandensis* mutants lacking individual *tag* genes

Western blots of TCA precipitated supernatant and cell associated samples taken from cultures of the indicated strains of *B. thailandensis* containing pSCrhaB2-*virAG* grown in M9 containing 0.5% glycerol and 0.5% casamino acids and probing with a polyclonal antibody raised against TssD-5. Protein molecular weights are indicated in kDa.

5.4.3 Generation of pSCrhaB2-virAG plasmid derivatives for complementation of *tssK* and *tag* mutants

To confirm that the T6SS-5-deficient phenotype exhibited by the *B.t tag* mutants in the TssD-5 secretion assays was not a consequence of polar effects on the expression of downstream genes, it was necessary to introduce the respective wild type genes into the mutants *in trans*. Again, it would be necessary to overexpress the *virA* and *virG* genes from the pSCrhaB2-virAG plasmid. However, it was not possible to introduce and maintain the pBBR1MCS plasmids containing the *tag* genes that were used for complementing the defects in MNGC formation (section 4.2). This was because pSCrhaB2 has the same origin of replication as pBBR1MCS, making it unlikely that the two could be stably maintained in a single cell. Initially, an attempt was made to use the kanamycin resistant pCM66 plasmid, a compatible RK2 derivative. This plasmid could be introduced into WT *B.t* devoid of other plasmids on medium containing 250 µg/ml kanamycin. However, following introduction of pCM66 into *B.t* cells already harbouring pSCrhaB2 by conjugation, exconjugants could not be selected on M9 agar plates containing 50 µg/ml trimethoprim and 250 µg/ml kanamycin.

To avoid the problem of supporting two plasmids, it was decided to clone the pertinent *tss* and *tag* genes into pSCrhaB2-virAG, downstream of *virAG*. Previous experiments using the MNGC formation assay had indicated that complementation was achieved when genes of the T6SS-5 cluster were cloned into pBBR1MCS. This indicated that the region of pBBR1MCS upstream of the multiple cloning site, containing the *lac* promoter, gave rise to sufficient expression of the cloned genes when they were introduced into the plasmid with their native ribosome binding site together with a stop codon that was introduced in-frame with the *lacZ* gene segment present on pBBR1MCS.

To utilise the regulatory sequence that was driving the *tss* and *tag* gene expression on pBBR1MCS, it was necessary to transfer the genes from pBBR1MCS using a method which retained the *lac* promoter. However, the introduction of the *virA* and *virG* genes into pSCrhaB2 left few remaining restriction sites in the multiple cloning site. This made it necessary to first transfer the *tss* and *tag* genes from pBBR1MCS to the LITMUS28i vector before using the extra restriction sites present in the multiple cloning site in this plasmid to sub-clone the *tss* and *tag* genes in pSCrhaB2-virAG. An example scheme for transferring genes from pBBR1MCS to pSCrhaB2-virAG via LITMUS28i, using *tssK* as an example, is shown in Figure 5.12.

The pBBR1MCS-*tssK*-5 plasmid was digested with the restriction enzymes NcoI and XbaI (Figure 5.13 A) which generated two linear DNA fragments, one of 1889 bp containing the *tssK* gene and another of 4227 bp, containing the majority of pBBR1MCS. Products of the digestion were ligated with the LITMUS28i plasmid that had been digested with the same enzymes. The ligation mixture was used to

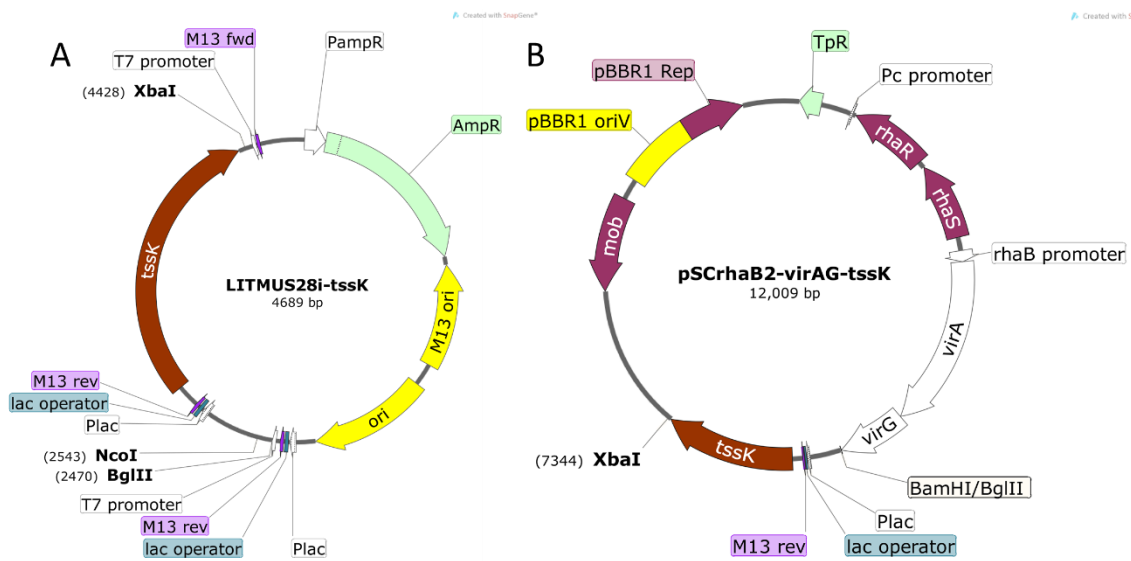


Figure 5.12 Maps of the LITMUS28i-tssK and pSCrhaB2-virAG-tssK plasmids

A) Diagram of the LITMUS28i-tssK plasmid constructed by transferring the smaller fragment generated from the digestion of pBBR1MCS-tssK with NcoI and XbaI into LITMUS28i digested with the same enzymes. B) Diagram of the pSCrhaB2-virAG-tssK plasmid constructed by digesting LITMUS28i-tssK with BglII and XbaI and ligating the fragment containing tssK into pSCrhaB2-virAG digested with BamHI and XbaI. Created using SnapGene viewer.

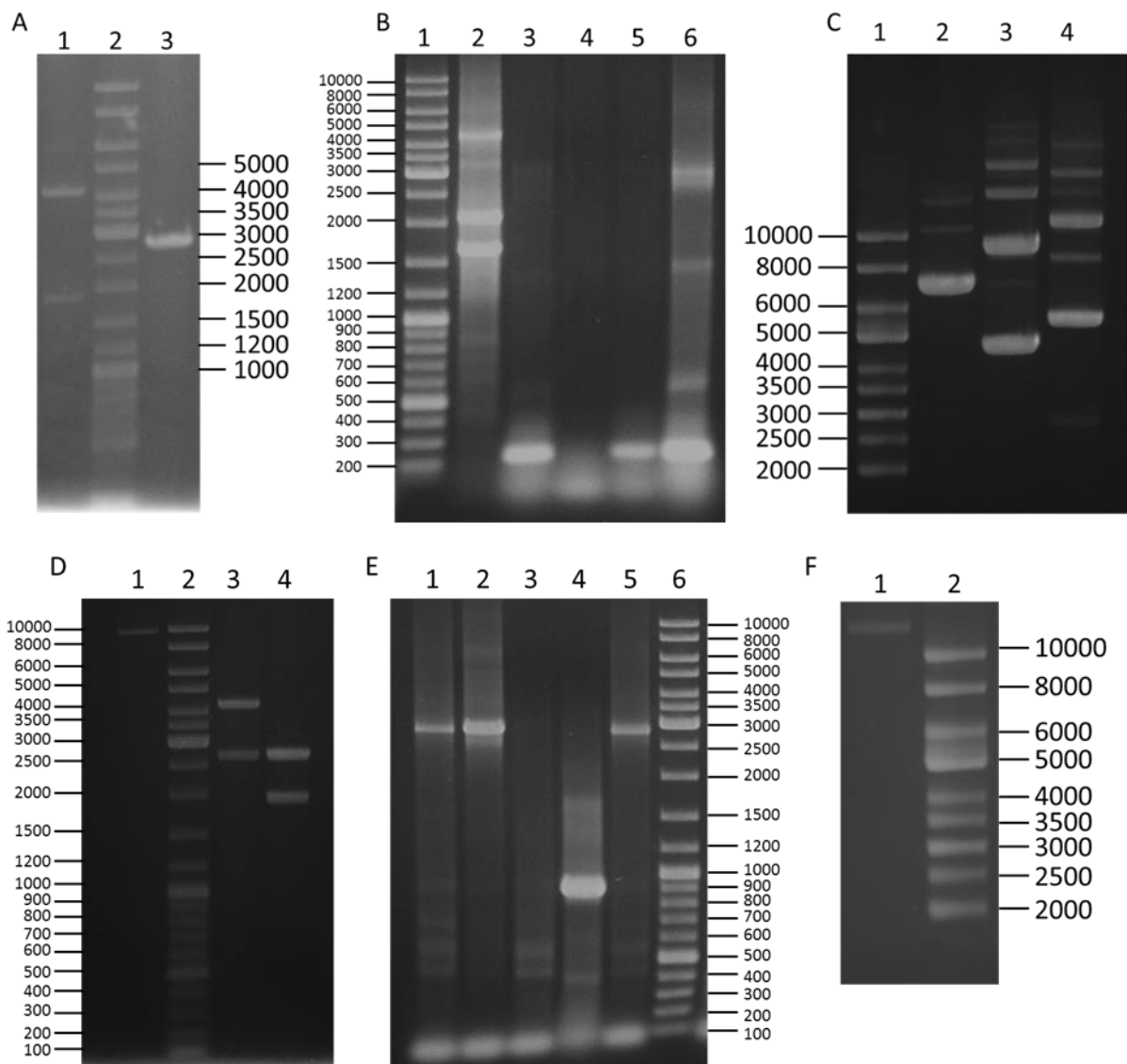


Figure 5.13 Construction of pSCRhaB2-virAG-tssK

Agarose gels showing the transfer of *tssK* together with the *lac* promoter from pBBR1MCS-*tssK*-5 to pSCRhaB2-*virAG* via LITMUS28i as an example for the cloning scheme for transferring genes from pBBR1MCS into pSCRhaB2-*virAG*. A) Lane 1, pBBR1MCS-*tssK* digested with NcoI and XbaI; lane 2, GeneRuler ladder mix; lane 3, LITMUS 28i digested with NcoI and XbaI. B) GoTAQ PCR using M13for and M13rev to screen colonies for insertion of *tssK* into LITMUS 28i. Lane 1, GeneRuler ladder mix; Lanes 2-6, colonies 1-5. C) Plasmid miniprep screen of colonies grown from potential positive colonies identified in the PCR screen. Lane 1, Supercoiled DNA ladder; lane 2, colony 3; lane 3, colony 1 (correct size); lane 4, colony 5. D) Digestion of potential LITMUS 28i-*tssK* plasmids for ligation into pSCRhaB2-*virAG*. Lane 1, pSCRhaB2-*virAG* digested with BamHI and XbaI; lane 2, GeneRuler ladder mix; lane 3, plasmid from colony 3 digested with BglII and XbaI; lane 4, plasmid from colony 1 digested with BglII and XbaI (this contains the correct sized fragment). E) GoTAQ PCR screen using virGfor and pSCRhaB2rev primers to screen for the presence of *tssK* in pSCRhaB2-*virAG*. Lanes 1-5, colonies 1-5; lane 6, GeneRuler ladder mix. F) Plasmid miniprep of an overnight culture grown from colony 1 in the PCR screen. Lane 1, colony 1, appears to be the correct size, was sent for sequencing and proved to contain the correct sequence; lane 2, Supercoiled ladder.

transform *E. coli* JM83 cells which were spread on LB agar plates containing 25 µg/ml kanamycin. Transformants were screened using the M13forward and M13reverse primers in a GoTaq PCR which amplified a 229 bp product when the empty LITMUS28i plasmid was present. When the *tssK* gene was present, two DNA fragments were amplified due to the additional M13reverse primer annealing site which had been transferred from pBBR1MCS with the *tssK* gene, the smaller fragment was 1634 bp and the larger 2095 bp (Figure 5.13 B). Transformants giving rise to fragments of these sizes were grown overnight in LB containing 25 µg/ml and plasmid DNA was harvested by the miniprep method and analysed by agarose gel electrophoresis to identify LITMUS28i-*tssK*-5 (4689 bp, Figure 5.13 C). A plasmid map of LITMUS28i-*tssK*-5 is shown in Figure 5.12 A.

To transfer *Plac-tssK* from LITMUS28i-*tssK*-5 to pSCrhaB2-*virAG*, plasmid DNA from two colonies was digested with XbaI and BglII (although only plasmid DNA from colony 1 migrated at the correct size on the agarose gel, DNA prepared from colony 5 ran at roughly 5500 bp and so was also digested in case of a miscalculation) which was expected to produce a 2727 bp fragment consisting of the remainder of LITMUS28i as well as a 1962 bp fragment when LITMUS28i-*tssK* was present. This showed that the plasmid obtained from clone 1 was indeed the desired plasmid, whereas the larger of the two plasmids appeared to be a fusion of LITMUS28i and pBBR1MCS, as the digestion produced one fragment of 2727 bp corresponding to LITMUS28i and another at roughly 4300 bp corresponding to pBBR1MCS (Figure 5.13 D). pSCrhaB2-*virAG* was also digested with XbaI and BglII. The digestion products of LITMUS28i-*tssK* and pSCrhaB2-*virAG* were ligated together and the ligation mixture was used to transform *E. coli* JM83 cells. Transformants that were selected on IST agar plates containing 25 µg/ml trimethoprim were used as templates for a GoTaq PCR which used the primers *virG*for and pSCrhaB2rev. When the colonies contained pSCrhaB2-*virAG*, an 868 bp product was amplified and when they contained pSCrhaB2-*virAG-tssK*-5 a 2820 bp was amplified (Figure 5.13 E). A colony giving rise to the 2.8 kb amplicon was grown overnight in IST broth containing 25 µg/ml and plasmid DNA was harvested by the miniprep procedure. Plasmid DNA was analysed by agarose gel electrophoresis (Figure 5.13 F) and the integrity of pSCrhaB2-*virAG-tssK*-5 (12009 bp) was confirmed by nucleotide sequencing. A plasmid map of pSCrhaB2-*virAG-tssK*-5 is shown in Figure 5.12 B.

5.4.4 pSCrhaB2-*virAG-tssK* restores T6SS-5 activity to a *tssK* mutant

The pSCrhaB2-*virAG-tssK* plasmid was used to transform *E. coli* SM10(λpir) which in turn was used to deliver pSCrhaB2-*virAG-tssK* into the *B.t tssK* mutant. Cultures of WT *B.t* and the $\Delta tssK$ mutant both harbouring pSCrhaB2-*virAG* and the $\Delta tssK$ mutant containing pSCrhaB2-*virAG-tssK* were grown in M9 minimal medium containing 0.5% (w/v) casamino acids and 0.5% (v/v) glycerol and 50 µg/ml trimethoprim to an OD₆₀₀ of ~1.0. At this point TCA precipitation was performed on the culture supernatants and the protein pellet resuspended in 100 µl 1x Laemmli buffer before electrophoresing

on a 15% polyacrylamide gel, western blotting and probing with anti-RNAP β antibody and anti-TssD-5 antibody. As shown in Figure 5.14 the introduction of the *tssK* gene on pSCrhaB2-*virAG-tssK* restores secretion of TssD-5, validating this approach for the re-introduction of the WT genes into their respective mutants.

5.4.5 pSCrhaB2-*virAG-tagA*, pSCrhaB2-*virAG-tagB*, pSCrhaB2-*virAG-tagC* and pSCrhaB2-*virAG-tagD* restore T6SS-5 activity to their respective mutants

The pSCrhaB2-*virAG-tagA*, pSCrhaB2-*virAG-tagB*, pSCrhaB2-*virAG-tagC* and pSCrhaB2-*virAG-tagD* plasmids were constructed using the same scheme described for pSCrhaB2-*virAG-tssK* above. Once it had been confirmed that the pSCrhaB2-*virAG-tagA*, pSCrhaB2-*virAG-tagB*, pSCrhaB2-*virAG-tagC* and pSCrhaB2-*virAG-tagD* plasmids contained the correct sequence they were delivered into their respective mutants by conjugation. The *B.t* Δ *tagA-5* mutant containing pSCrhaB2-*virAG-tagA*, the Δ *tagB-5* mutant containing pSCrhaB2-*virAG-tagB*, the Δ *tagC-5* mutant containing pSCrhaB2-*virAG-tagC* and Δ *tagD-5* mutant containing pSCrhaB2-*virAG-tagD* were grown in M9 minimal medium containing 0.5% (w/v) casamino acids and 0.5% (v/v) glycerol and 50 mg/ml trimethoprim. Cultures of the *B.t* Δ *tagA-5*, Δ *tagB-5*, Δ *tagC-5* and Δ *tagD-5* mutants, each containing pSCrhaB2-*virAG* (which had both previously been shown to be defective in secretion of TssD-5) were also grown in the same medium. All cultures were grown to an OD₆₀₀ of ~1.0 and the supernatant and cell associated samples prepared as described above. Figure 5.15 shows that when the WT *tagA-5*, *tagB-5*, *tagC-5* and *tagD-5* genes are introduced into their respective mutants and T6SS-5 secretion is induced by the presence of a multicopy plasmid containing *virAG*, TssD-5 export into the supernatant is restored.

5.5 Glutathione induction of the *B. thailandensis* T6SS-5

During the course of this work it was demonstrated that glutathione present in host cells induces T6SS-5 in *B.p* and *B.t* and that addition of glutathione or cysteine to liquid cultures of *B.t* efficiently induces the system (Wong et al. 2015).

5.5.1 Glutathione induces T6SS-5 to a similar level as *virAG*

To test whether this approach produced similar levels of induction and secretion of TssD-5 to those observed when using the pSCrhaB2-*virAG* plasmid, cultures of WT and Δ *tssK* *B.t* strains harbouring pSCrhaB2 were grown in M9 0.5% glycerol, 0.5% casamino acids with or without 200 μ M glutathione. Alongside these, cultures of *B.t* WT Δ *tssK* mutant strains containing pSCrhaB2-*virAG* were grown. A cell associated sample was taken of each and the supernatants were TCA precipitated. As Figure 5.16 demonstrates, when glutathione (GSH) is present in the culture medium TssD-5 can be detected in the cell associated samples of *B. thailandensis* cultures although at a slightly lower level than in cultures

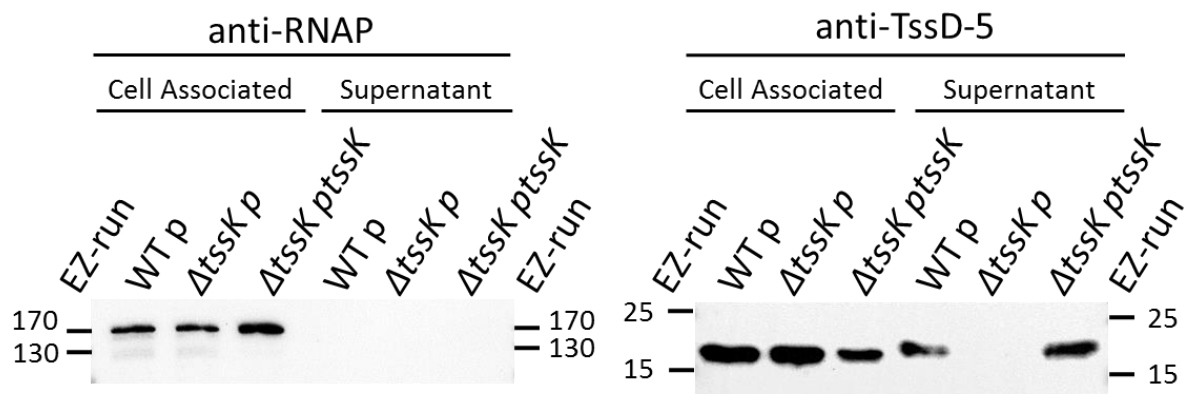


Figure 5.14 Complementation of a *B. t* *tssK* mutant in a T6SS-5 secretion assay

Cell associated and TCA precipitated supernatant samples prepared from the indicated cultures were electrophoresed in a 15% acrylamide gel before transferring to a PVDF membrane and probing with antibody specific to the β subunit of RNAP and TssD-5. WT p, WT *B. t* containing pSCRhaB2-*virAG*; Δ tssK p, Δ tssK-5 mutant containing pSCRhaB2-*virAG*; Δ tssK ptssK; Δ tssK-5 mutant containing pSCRhaB2-*virAG-tssK*; EZ-run, EZ-run prestained ladder. Protein molecular weight markers are indicated in kDa.

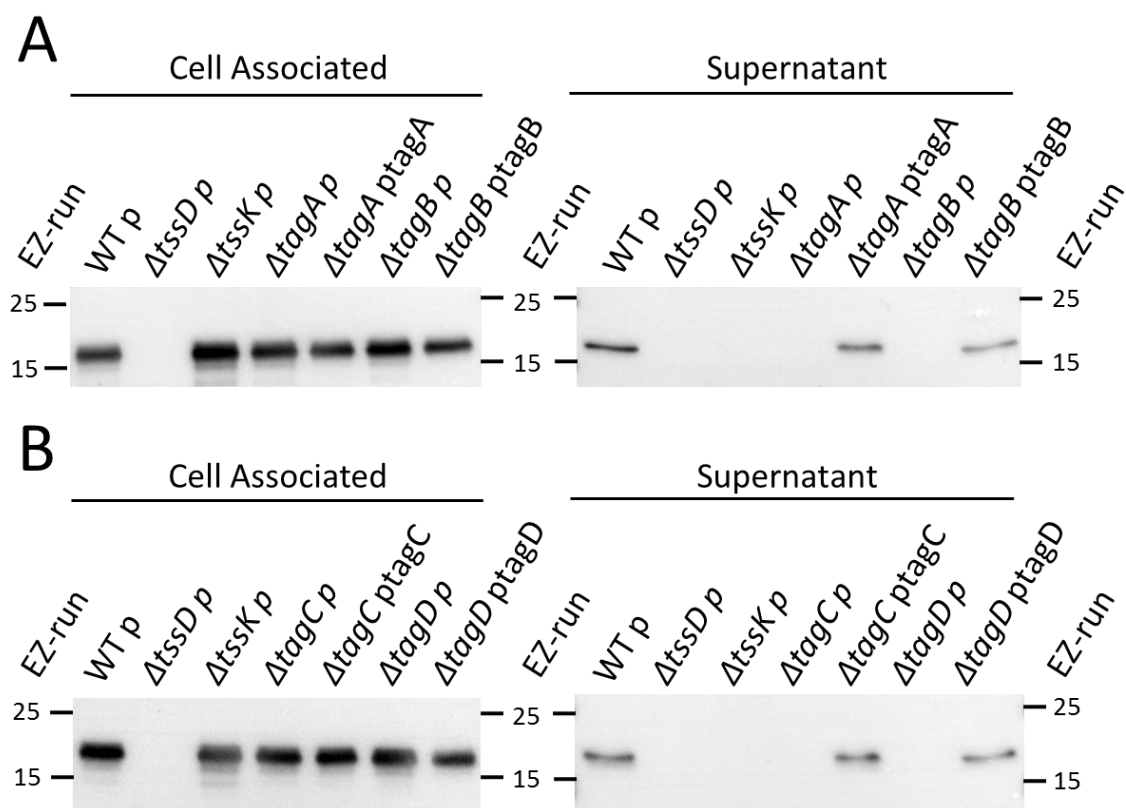


Figure 5.15 Complementation of $\Delta tagA$, $\Delta tagB$, $\Delta tagC$ and $\Delta tagD$ in TssD-5 secretion assays

Cell associated and TCA precipitated supernatant samples prepared from the indicated cultures were electrophoresed on a 15% acrylamide gel before transferring to a PVDF membrane and probing with antibody specific to TssD-5. A) WT p, *B.t* containing pSCrhaB2-*virAG*; $\Delta tssK$ p, *B.t* $\Delta tssK$ -5 mutant containing pSCrhaB2-*virAG*; $\Delta tagA$ p, *B.t* $\Delta tagA$ -5 mutant containing pSCrhaB2-*virAG*; $\Delta tagA$ ptagA, *B.t* $\Delta tagA$ -5 mutant containing pSCrhaB2-*virAG-tagA*; $\Delta tagB$ p, *B.t* $\Delta tagB$ -5 mutant containing pSCrhaB2-*virAG*; $\Delta tagB$ ptagB, *B.t* $\Delta tagB$ -5 mutant containing pSCrhaB2-*virAG-tagB*; EZ-run, EZ-run prestained ladder. B) WT p, WT *B.t* containing pSCrhaB2-*virAG*; $\Delta tssK$ p, *B.t* $\Delta tssK$ -5 mutant containing pSCrhaB2-*virAG*; $\Delta tagC$ p, *B.t* $\Delta tagC$ -5 mutant containing pSCrhaB2-*virAG*; $\Delta tagC$ ptagC, *B.t* $\Delta tagC$ -5 mutant containing pSCrhaB2-*virAG-tagC*; $\Delta tagD$ p, *B.t* $\Delta tagD$ -5 mutant containing pSCrhaB2-*virAG*; $\Delta tagD$ ptagD, *B.t* $\Delta tagD$ -5 mutant containing pSCrhaB2-*virAG-tagD*; EZ-run, EZ-run prestained ladder. Protein markers are displayed in kDa.

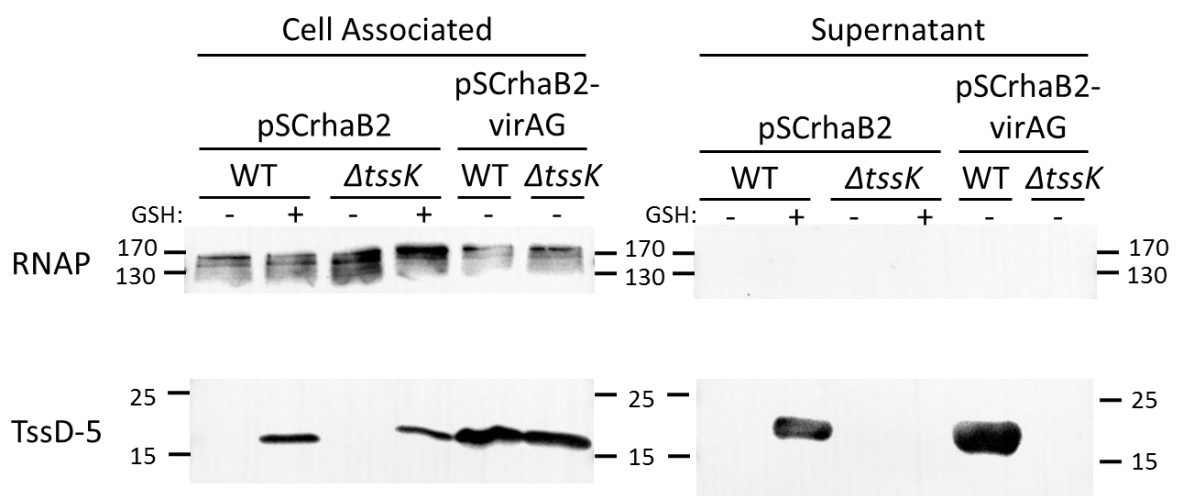


Figure 5.16 Induction of TssD-5 synthesis and secretion in *B.t* when glutathione is added to cultures

Western blots of cell associated and TCA precipitated supernatant samples prepared from cultures of *B. thailandensis* strains containing either pSCrhaB2 or pSCrhaB2-*virAG* grown with and without the addition of glutathione, probed with either antibody against RNAP β or TssD-5. GSH, 200 μ M glutathione; WT, WT *B.t*; $\Delta tssK$, *B.t* $\Delta tssK$ mutant. Protein markers displayed in kDa.

induced by the presence of *virAG* on the pSCrhaB2 plasmid. The culture supernatant of the GSH induced WT strain also contained TssD-5, which was absent from the supernatant of the induced $\Delta tssK$ culture. Like the cell associated samples the level of secreted TssD-5 was slightly lower in the GSH induced cultures than those induced with multi-copy *virAG*. This result demonstrates that the addition of GSH to the culture medium is sufficient to induce TssD-5 secretion by T6SS-5 to levels that are comparable to the *virAG* induction. This removes the requirement of the pSCrhaB2-*virAG* plasmid which restricts the use of other pBBR1-based plasmids that can be introduced into the cell, for example for complementation experiments.

5.6 Discussion

The results in this chapter are consistent with the observations of Burtnick et al. (2011) that when the *virA* and *virG* genes are overexpressed in *B.p*, T6SS-5 is expressed and secreting, as determined by the presence of TssD-5 inside cells and in culture supernatants. This is not surprising given the fact that the *B.t* VirA and VirG proteins are 93.1% and 85.9% identical to their *B.p* homologues, respectively (determined using EMBOSS needle pairwise sequence alignment). One surprising aspect of this experiment was that rhamnose induction of the pSCrhaB2-*virAG* plasmid was not required despite the fact that expression from the pSCrhaB2 plasmid is reported to be tightly controlled, even in the absence of glucose (Cardona & Valvano 2005). The presence of glucose decreases synthesis of cAMP in *E. coli* and therefore the CRP activator protein which is required along with RhaS and RhaR to fully induce the *rha* system, is inactive (Haldimann et al. 1998). It appeared that glucose was still capable of downregulating expression from the plasmid as when the *B.t* WT strain containing pSCrhaB2-*virAG* was grown in dBHI broth which contains sufficient glucose to repress the system supplemented with rhamnose, there was no noticeable induction of TssD-5 expression. It is not clear how glucose exerts catabolic repression on *Burkholderia*, although the *B.t* genome encodes five CRP-like proteins (M. Thomas, personal communication). It would be interesting to see if the addition of glucose to the M9 medium would have restricted expression of *virAG* from the pSCrhaB2-*virAG* vector. Research published after the start of this work also demonstrated that pSCrhaB2-*virAG* induces secretion by T6SS-5 in *B. thailandensis* (Schwarz et al. 2014). However, this study used Vogel-Bonner minimal medium containing 0.05% (w/v) rhamnose and did not comment on whether the system was induced in the absence of rhamnose.

The requirement for *tssK-5* for the activity of T6SS-5 was also demonstrated, consistent with the observations by Schwarz et al. (2010), that a *B. thailandensis* strain possessing a mutation in *tssK-5* is avirulent in a mouse model of infection. Research published after the start of this work also directly

demonstrated that *B.t tssK-5* was required for the activity of T6SS-5 based on secretion of TssD-5 (Schwarz et al. 2014).

The observation that a *B.t* mutant lacking all four of the *tag* genes from the T6SS-5 operon is consistent with research published after the start of this work demonstrating that deletion of *tagA-5* alone was sufficient to abolish the secretion of TssD-5 in a *B.p* infection assay (Hopf et al. 2014). However, it could have been possible that the results observed were just a consequence of there being fewer mutant bacteria present within the infected RAW 264.7 cells. Therefore, the results of this work represent the first time the requirement of *tagA-5* for T6SS-5 activity has been demonstrated in an induction assay using the *virAG* overexpression system. The lack of detectable TagA-5 in the culture supernatants of WT *B.t* in which T6SS-5 is active is further evidence that *tagA-5* encodes a component required for the function of T6SS-5 rather than a secreted effector as hypothesised at the beginning of this work.

The requirement of *tagB-5* for secretion of TssD-5 is something which has not been reported previously and suggests that the results observed in the MNGC formation assays performed previously are a consequence of the loss of T6SS-5 activity. This is contrary to the hypothesis that TagB-5 is a secreted effector protein and suggests that it is another component required for secretion by the system. This is supported by the observation that TagB-5 was not detectable in culture supernatants by mass spectrometry.

It is also clear that a strain containing a mutation in *tagC-5* is completely incapable of secretion of TssD-5 and TagC-5 is not detected in the culture supernatants of a WT *B. thailandensis* strain containing the pSCrhaB2-*virAG* plasmid when examined by mass spectrometry.

The inability of mass spectrometry to detect TagD-5 in culture supernatants was surprising given that it is predicted to be a PAAR protein (Section 3.6). Previous studies have demonstrated that PAAR proteins can interact with TssI facilitating their export via the T6SS (Shneider et al. 2013). However, investigations have thus far been unable to detect PAAR proteins in the supernatant of cultures using mass spectrometry (Altindis et al. 2015) even when it has been demonstrated by other methods that they are secreted (Shneider et al. 2013). Therefore, it remains possible that TagD-5 is secreted but only at very low levels, or some characteristic of the protein, perhaps its small size, makes it difficult to detect by mass spectrometry. Given the previous observations of the effect of the deletion of PAAR proteins on the activity of their respective T6SS, it would have been expected that the deletion of *tagD-5* would attenuate rather than abolish TssD-5 secretion if another PAAR could compensate for its loss as observed in *Vibrio cholerae* and *Acinetobacter baylyi* (Shneider et al. 2013). However, this was not observed and the Δ *tagD-5* mutant proved to be completely deficient in T6SS-5 activity,

indicating that either there are no other T6SS-5 compatible PAAR proteins expressed under these conditions or TagD-5 is not a PAAR protein.

In all of the mutants tested, the re-introduction of the WT version of the gene downstream of *virG* on the pSCrhaB2-*virAG* plasmid was sufficient to restore TssD-5 secretion. In the case of *tagD-5* the level of restoration of TssD-5 activity was surprising given that in the MNGC formation assays the $\Delta tagD$ mutant containing the pBBR1MCS-*tagD* complementation plasmid demonstrated a reduced fusion index compared to the other complemented strains. This was subsequently shown to be due to poor expression of *tagD* from the pBBR1MCS-*tagD* plasmid, as determined by detection of TagD_{FLAG} in cultures of *B.t* containing pBBR1MCS-*tagD*_{FLAG} (identical upstream regulatory domain to pBBR1MCS-*tagD*) using the anti-FLAG antibody. In each instance the *tag* genes were transferred to pSCrhaB2-*virAG* with a section of pBBR1MCS containing the *lac* promoter which had previously been shown to be sufficient for complementation of the same mutants in the MNGC formation assays.

Using genes cloned into pSCrhaB2-*virAG* in this manner it would be possible to introduce modified versions of T6SS-5 genes into *B.t* strains to see what effect the modifications had on T6SS-5 activity. For example, one could re-introduce genes encoding amino acid substitutions into the mutant strains to determine the effect of specific residues. It also presents the opportunity to introduce epitope tags such as the FLAG tag to allow the use of assays which would otherwise require antibodies to be raised against the protein products of the genes in question.

The mass spectrometry results in this chapter are disappointing as they do not reveal any novel T6SS-5 secreted proteins and confirm that the only proteins secreted by this system are TssD-5 and TssI-5. This is consistent with observations by Schwarz et al. (2014) which were released since this work was commenced. They used a very similar system whereby the secretomes of WT and $\Delta tssK-5$ *B.t* strains, induced by the overexpression of *virAG* from the pSCrhaB2 vector, were compared, but instead of M9 minimal medium containing no rhamnose, they used Vogel-Bonner minimal medium supplemented with 0.05% rhamnose. It is of course possible that more proteins are secreted by this system, for example genes encoded elsewhere on the chromosome, but their genes are not expressed when the *virAG* system of induction is used. Wong et al. (2015) demonstrated that the histidine kinase activity of the sensor protein VirA is stimulated by low molecular weight thiols, glutathione in particular, that are present in the host cell resulting in induction of T6SS-5. It is possible that glutathione also induces the expression of other genes on the chromosome which are not induced when the more artificial *virAG* system is used. For that reason, it would be interesting to utilise the glutathione induction method of Wong et al. and analyse the secretome by mass spectrometry to see whether additional T6SS-5-dependent secreted proteins can be detected.

While the results of the TssD-5 secretion assays strongly suggest that the role of the Tag-5 proteins is one that facilitates T6SS-5 activity, it is still possible that they could be secreted. For example, the TssI and TssD proteins are both essential for the operation of type six secretions systems as well as being secreted proteins. Therefore, it would be useful to have antibodies against the Tag proteins to determine if they were secreted despite being undetectable in mass spectrometry analysis of culture supernatants. This would first require purification of the Tag proteins for antibody production. An attempt was made to express and purify the Tag proteins but it was unsuccessful (section 6.4).

Chapter 6 Functional studies on the *B.*
thailandensis T6SS-5 Tag proteins

6.1 Introduction

The bacterial T6SS is a complex nano-machine composed of at least 13 core components which interact in a dynamic way within the host to facilitate the delivery of effectors into target cells. Based on the requirement of each of the *tag* genes encoded within the T6SS-5 gene cluster for secretion by T6SS-5, it is likely that the Tag proteins interact with one or more of the core T6SS-5 proteins. By elucidating the interactions of the Tag proteins, their role could be further determined.

It was also desirable to be able to overproduce the Tag proteins in an *E. coli* host strain. This would allow larger quantities of the Tag proteins to be produced which could be purified and used in structural studies and to generate antibodies.

6.2 Identification of Tag protein interacting partners by co-immunoprecipitation

To determine the interactions of the Tag proteins of T6SS-5, a co-immunoprecipitation was performed. This technique uses an antibody which binds to the protein of interest (or antibody which binds to an epitope engineered into the protein of interest), allowing the protein to be recovered from complex mixtures such as cell lysates. Using the correct conditions, any proteins that interact with this protein are also isolated, allowing their identification by mass spectrometric techniques. As there were no antibodies raised against the Tag proteins available, the Tag proteins were tagged using the FLAG epitope. The FLAG epitope is an 8 amino acid sequence (DYKDDDDK) which is recognised by the commercially available anti-FLAG antibody. Thus when this polypeptide tag is fused to a protein of interest it allows the use of immunological methods to recover the protein.

6.2.1 Construction of plasmids for expression of FLAG-tagged Tag proteins in MNGC assays

One of the problems associated with using an epitope tag to introduce a binding site for an antibody is that it can affect the function of the protein being investigated. In the absence of information regarding the function of the Tag proteins it was decided to place the FLAG epitope at the C-terminus of the Tag proteins. To ensure that the introduction of a C-terminal FLAG epitope did not have a detrimental effect on the function of the proteins, MNGC formation assays were performed using the *B.t tag* mutant strains complemented with C-terminally FLAG-tagged Tag proteins. The *lac* promoter present in the pBBR1MCS plasmid has previously been shown to afford sufficient expression of the *tag* genes during MNGC formation assays. Therefore, it was decided to use this vector again to introduce versions of the genes encoding a C-terminal FLAG epitope tag into the *B.t tag* mutants.

6.2.1.1 Construction of a TagA_{FLAG} complementation plasmid for MNGC analysis

The primers tagAcompfor and tagActermFLAGrev were used in a PCR which used Q5 polymerase with a WT boiled lysate as template to amplify a 2713 bp product. This DNA fragment contained the *tagA*

Shine-Dalgarno sequence and *tagA* ORF with the 24 bp sequence encoding the FLAG epitope introduced between the codon encoding the C-terminal arginine of TagA and the stop codon. The amplified DNA fragment and pBBR1MCS were digested with HindIII and BamHI and ligated together. The ligation mixture was used to transform *E. coli* JM83 cells which were spread on LB agar plates containing 25 µg/ml chloramphenicol, 100 µM IPTG and 40 µg/ml Xgal. White colonies growing on this plate were grown overnight in LB broth containing 25 µg/ml chloramphenicol and plasmid DNA was harvested by the miniprep procedure. Samples of plasmid DNA were analysed by agarose gel electrophoresis to identify the 7376 bp pBBR1MCS-*tagA*_{FLAG} plasmid. The sequence of the insert was confirmed by nucleotide sequencing.

6.2.1.2 Construction of a TagB_{FLAG} complementation plasmid for MNGC analysis

The primers tagBcompfor and tagBctermFLAGrev were used to amplify a 1142 bp amplicon from a WT *B.t* boiled lysate template in a PCR which used the high-fidelity Q5 polymerase. The DNA fragment contained the Shine-Dalgarno sequence and *tagB* ORF with the DNA sequence encoding the FLAG epitope tag engineered after the C-terminal amino acid (arginine) encoding codon of *tagB* and before the stop codon. pBBR1MCS and the PCR product were digested with HindIII and BamHI and the two DNA molecules were ligated together. This ligation was used to transform *E. coli* JM83 cells which were spread on LB agar plates containing 25 µg/ml chloramphenicol, 100 µM IPTG and 40 µg/ml Xgal. After overnight incubation at 37°C, white colonies growing on this plate were used to inoculate LB containing 25 µg/ml chloramphenicol and grown overnight. Plasmid DNA was purified using the miniprep method and analysed by agarose gel electrophoresis. A sample which migrated consistent with a size of 5805 bp, corresponding to the size of pBBR1MCS-*tagB*_{FLAG} was verified as the desired plasmid by nucleotide sequencing.

6.2.1.3 Construction of a TagC_{FLAG} complementation plasmid for MNGC analysis

An 854 bp DNA fragment was amplified from a WT *B.t* boiled lysate template using Q5 polymerase and the primers tagCcompfor and tagCctermFLAGrev. The DNA fragment contained the *tagC* Shine-Dalgarno sequence and *tagB* ORF with the DNA sequence encoding the FLAG epitope tag introduced between the final sense codon and the *tagC* stop codon. The DNA fragment and pBBR1MCS were digested with HindIII and BamHI, then ligated together, and the reaction products were used to transform *E. coli* JM83 cells. Transformants were selected on LB agar plates containing 25 µg/ml chloramphenicol, 100 µM IPTG and 40 µg/ml Xgal following overnight incubation at 37°C. Overnight cultures were prepared from white colonies growing on the plate and plasmid DNA was extracted from these cultures by plasmid miniprep. Plasmid samples were analysed by agarose gel electrophoresis to identify a plasmid of the expected size for pBBR1MCS-*tagC*_{FLAG} (5517 bp). The integrity of the cloned DNA was confirmed by nucleotide sequencing.

6.2.1.4 Construction of a TagD_{FLAG} complementation plasmid for MNGC analysis

The primers tagDcompfor and tagDctermFLAGrev were used in a PCR with Q5 polymerase to amplify a 478 bp product containing the *tagD* Shine-Dalgarno and coding sequences with the DNA sequence encoding the FLAG epitope inserted between the final sense codon and its stop codon. This DNA fragment and pBBR1MCS were digested with HindIII and BamHI and ligated together. *E. coli* JM83 cells were transformed with the ligation mixture and spread on LB agar plates containing 25 µg/ml chloramphenicol, 100 µM IPTG and 40 µg/ml Xgal. After overnight incubation at 37°C, white colonies were grown overnight in LB containing 25 µg/ml chloramphenicol. To isolate plasmid DNA, the miniprep procedure was used and the resulting DNA samples analysed by agarose gel electrophoresis to identify the pBBR1MCS-tagD_{FLAG} plasmid (5141 bp). A plasmid of the expected size was checked by nucleotide sequencing.

6.2.2 Analysis of FLAG-tagged Tag protein production from pBBR1MCS in *B. thailandensis*

The introduction of the C-terminal FLAG epitope allows the detection of proteins in western blots utilising an antibody raised against the FLAG peptide. This is useful as it allows one to determine if the proteins are actually being expressed from the plasmids encoding the FLAG-tagged Tag proteins. Using conjugation, pBBR1MCS-*tagA*_{FLAG}, pBBR1MCS-*tagB*_{FLAG}, pBBR1MCS-*tagC*_{FLAG} and pBBR1MCS-*tagD*_{FLAG} were introduced into the respective *B.t tag* mutants by conjugation using *E. coli* SM10(λpir). Each *B.t tag* mutant harbouring pBBR1MCS expressing the corresponding native or FLAG-tagged Tag protein was used to inoculate a 4 ml culture in LB containing 250 µg/ml chloramphenicol and grown at 37°C. Once the cultures had reached an OD₆₀₀ of 1.0, the cells were collected by centrifugation at 15,000 x g and the supernatant discarded. The resulting cell pellet was resuspended in 100 µl 1 x Laemmli buffer and boiled before separating the proteins in the samples by SDS-PAGE in a 15% gel and transferring the proteins to a PVDF membrane which was probed using antibody against the FLAG epitope.

As shown in Figure 6.1, all of the FLAG-tagged proteins were present to some extent in the *B.t* cell lysates, with no anti-FLAG cross-reactive proteins being detected in the controls containing plasmids expressing the native Tag proteins (i.e. without the FLAG tag), indicating that there is no non-specific binding of the antibody. Although a 15% gel is not ideal for separating proteins of the size of TagA_{FLAG}

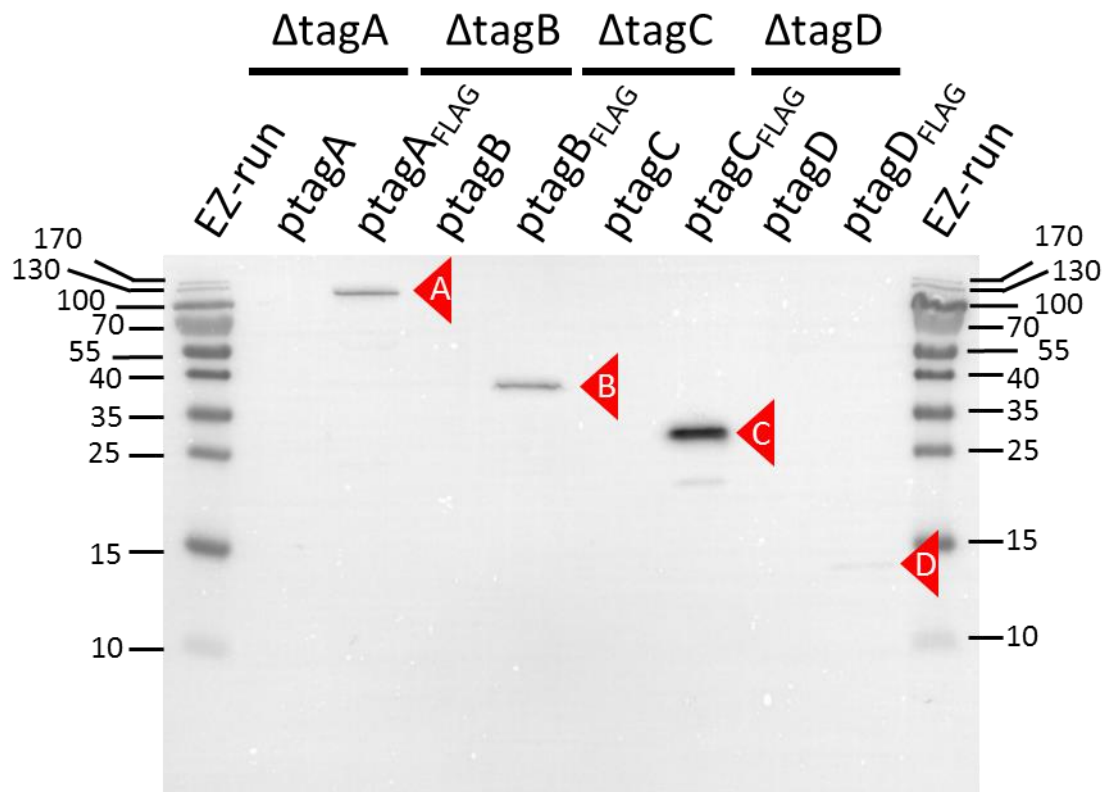


Figure 6.1 Expression of FLAG-tagged Tag proteins in *B. thailandensis*

Western blot of cell associated protein samples prepared from the indicated cultures of *B. thailandensis* probed with anti-FLAG antibody. $\Delta tagA$, *B.t* $\Delta tagA$ mutant containing *ptagA* (pBBR1MCS-*tagA*) or *ptagA*_{FLAG} (pBBR1MCS-*tagA*_{FLAG}); $\Delta tagB$, *B.t* $\Delta tagB$ mutant containing *ptagB* (pBBR1MCS-*tagB*) or *ptagB*_{FLAG} (pBBR1MCS-*tagB*_{FLAG}); $\Delta tagC$, *B.t* $\Delta tagC$ mutant containing *ptagC* (pBBR1MCS-*tagC*) or *ptagC*_{FLAG} (pBBR1MCS-*tagC*_{FLAG}); $\Delta tagD$, *B.t* $\Delta tagD$ mutant containing *ptagD* (pBBR1MCS-*tagD*) or *ptagD*_{FLAG} (pBBR1MCS-*tagD*_{FLAG}). Red arrow A, protein band corresponding to TagA_{FLAG}; red arrow B, protein band corresponding to TagB_{FLAG}; red arrow C, protein band corresponding to TagC_{FLAG}; red arrow D, protein band corresponding to TagD_{FLAG}; EZ-run, EZ-run prestained ladder, sizes shown in kDa.

it is clear that there is a protein band present in this sample that could correspond to the size of TagA_{FLAG} (92.2 kDa). A protein is present in the TagB_{FLAG} sample at around 40 kDa which was estimated to be 38.5 kDa based on the molecular weight determination tool in Image Lab software (Bio-Rad), almost identical to the predicted MW of TagB_{FLAG} (38.6 kDa). TagC_{FLAG} was also present in its respective culture based on the presence of a protein band with an estimated MW of 29.8 kDa, which is slightly larger than its predicted MW of 28.9 kDa. A protein band which appears to be a degradation product is also visible at around 20 kDa. Finally, there was a very faint cross-reactive protein present in the TagD_{FLAG} sample that was estimated to be 13.7 kDa, i.e. similar to the predicted MW for TagD_{FLAG} (13.0 kDa), suggesting that TagD_{FLAG} is not expressed efficiently from pBBR1MCS.

As the regulatory DNA sequences present upstream of *tagD* and *tagD_{FLAG}* cloned in pBBR1MCS are identical, it would be reasonable to suspect that the expression of *tagD* would be broadly similar to that of *tagD_{FLAG}*. If this is the case, then it could explain why pBBR1MCS-*tagD* did not complement its respective mutant as fully as the other pBBR1MCS-*tag* constructs in MNGC formation assays.

6.2.3 Assessment of ability of FLAG-tagged Tag proteins to participate in T6SS-5 dependent stimulation of MNGC formation

After it was confirmed that the FLAG-tagged proteins were expressed in *B.t* cells, cultures of each of the four *B.t tag* mutants harbouring pBBR1MCS expressing the corresponding native or FLAG-tagged Tag proteins were grown overnight in LB before being used to infect RAW 264.7 cells at an MOI of 10:1. After 16 hours, wells were stained for 5 minutes with 0.4% (w/v) Giemsa before rinsing with tap water until the stain intensity was appropriate for nuclei counting. The fusion index was calculated and plotted on a graph. As shown in Figure 6.2 A, pBBR1MCS-*tagA_{FLAG}* restored the ability of the *B.t ΔtagA-5* mutant to induce the formation of MNGCs in RAW 264.7 cells, suggesting that the addition of the FLAG tag did not have a detrimental effect on TagA. Figure 6.2 B shows that the *B.t ΔtagB* mutant containing pBBR1MCS-*tagB_{FLAG}* was capable of inducing MNGC formation in RAW 264.7 cells. In fact, the fusion index for these two complemented *B.t* strains was significantly higher than those complemented with plasmids containing the respective WT genes (Figure 6.3). Although the fusion indexes for the FLAG complemented strains were higher than the WT strain, it was not statistically significant. The reasons for this are unclear. These results suggest that TagA_{FLAG} and TagB_{FLAG} are suitable for studies using an antibody to the FLAG epitope to elucidate the role of TagA and TagB in experiments where an antibody raised against these proteins would otherwise be necessary.

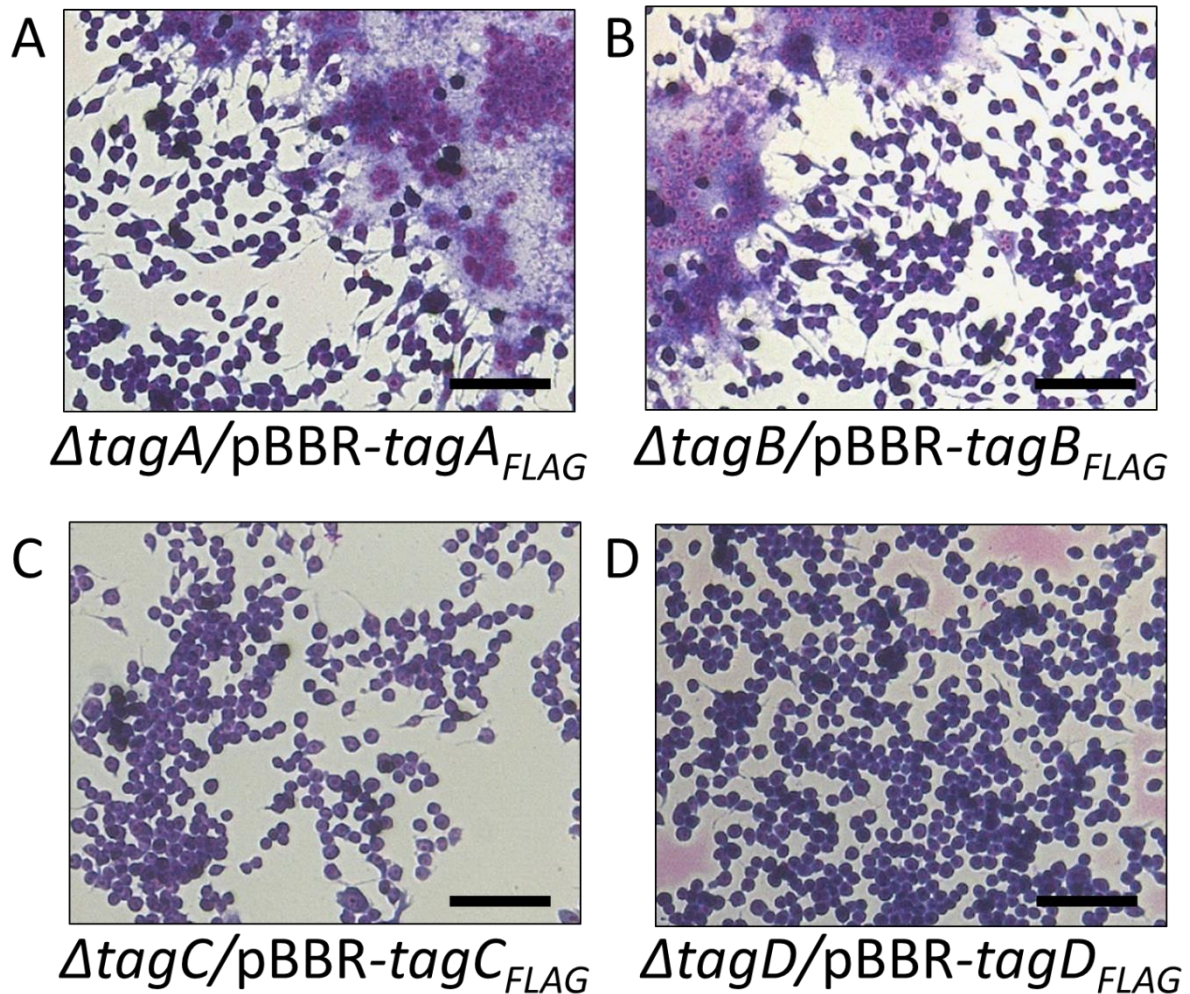


Figure 6.2 Induction of MNGC formation by *B.t* mutants complemented by genes encoding FLAG-tagged Tag proteins

Light microscope images of Giemsa stained RAW 267.4 cells infected with the indicated strains of *B. thailandensis*. A) $\Delta tagA/pBBR-tagA_{FLAG}$, *B.t* $\Delta tagA$ mutant containing pBBR1MCS- $tagA_{FLAG}$. B) $\Delta tagB/pBBR-tagB_{FLAG}$, *B.t* $\Delta tagB$ mutant containing pBBR1MCS- $tagB_{FLAG}$. C) $\Delta tagC/pBBR-tagC_{FLAG}$, *B.t* $\Delta tagC$ mutant containing pBBR1MCS- $tagC_{FLAG}$. D) $\Delta tagD/pBBR-tagD_{FLAG}$, *B.t* $\Delta tagD$ mutant containing pBBR1MCS- $tagD_{FLAG}$. Scale bar = 75 μm .

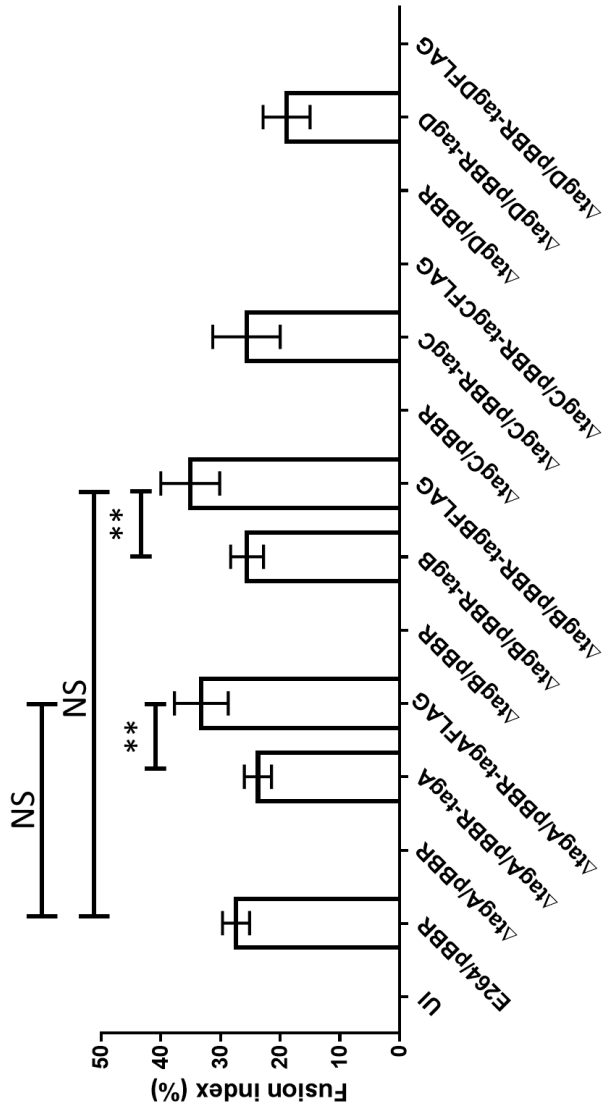


Figure 6.3 Fusion Indexes calculated from RAW 264.7 cells infected with *B. thailandensis* tag mutants complemented with genes encoding FLAG-tagged proteins

RAW 264.7 cells were infected with WT *B. t* or *B. t* tag mutants containing either pBBR1MCS or a complementing plasmid. The nuclei inside giant cells and the total number of nuclei in three fields of view from three wells were counted. The fusion index was calculated and three independent repeats were performed per strain. UI, uninfected; E264/pBBR, WT *B. t* containing pBBR1MCS; ΔtagA/pBBR, *B. t* ΔtagA mutant containing pBBR1MCS; ΔtagA/pBBR-tagA, *B. t* ΔtagA mutant containing pBBR1MCS-tagA_{FLAG}; ΔtagB/pBBR, *B. t* ΔtagB mutant containing pBBR1MCS; ΔtagB/pBBR-tagB, *B. t* ΔtagB mutant containing pBBR1MCS-tagB_{FLAG}; ΔtagC/pBBR, *B. t* ΔtagC mutant containing pBBR1MCS; ΔtagC/pBBR-tagC, ΔtagC/pBBR-tagCFLAG, *B. t* ΔtagC mutant containing pBBR1MCS-tagC_{FLAG}; ΔtagD/pBBR, *B. t* ΔtagD mutant containing pBBR1MCS; ΔtagD/pBBR-tagD, *B. t* ΔtagD mutant containing pBBR1MCS-tagD; ΔtagD/pBBR-tagDFLAG, *B. t* ΔtagD mutant containing pBBR1MCS-tagD_{FLAG}. Error bars = standard deviation. Statistical significance was tested using ordinary one-way analysis of variance (ANOVA) with Tukeys post-test. NS, not significant; **, $P < 0.01$. Graph created and statistical analysis performed using GraphPad prism.

The *B.t* $\Delta tagC$ mutant containing pBBR1MCS-*tagC*_{FLAG} did not induce MNGC formation in RAW 264.7 cells (Figure 6.2 C), despite the observation that the WT version of the gene restored MNGC formation and the TagC_{FLAG} protein was efficiently expressed in the *B.t* $\Delta tagC$ mutant containing pBBR1MCS-*tagC*_{FLAG} (Figure 6.1). Therefore, it is likely that the introduction of the FLAG epitope tag has modified the protein in such a way as to make it non-functional and therefore it could not be used in further studies. Similarly, the *B.t* $\Delta tagD$ mutant containing pBBR1MCS-*tagD*_{FLAG} did not induce the formation of giant cells during infection assays despite the fact that the *B.t* $\Delta tagD$ mutant expressing untagged TagD was capable of inducing the formation of giant cells, albeit at a reduced level compared to other strains (with the exception of the *B.t* $\Delta tagA-D$ mutant containing pBBR1MCS-*tagA-D*). This could be due to a low level of TagD_{FLAG} as determined in the western blot in Figure 6.1. However, as mentioned earlier, the expression of *tagD*_{FLAG} should not be different to that of *tagD*. This result suggests that the addition of a C-terminal FLAG tag renders TagD non-functional.

6.2.4 Construction of plasmids for expression of FLAG-tagged Tag proteins in secretion assays

Based on the observation that pBBR1MCS-*tagA*_{FLAG} and pBBR1MCS-*tagB*_{FLAG} restored MNGC formation to their respective mutants (unlike the corresponding *tagC* and *tagD* plasmids), indicating that TagA_{FLAG} and TagB_{FLAG} were functional, it was decided to attempt a co-immunoprecipitation using these proteins. As the most probable interaction partners are products of genes in the T6SS-5 gene cluster, it was necessary to induce the expression of this cluster using the *virAG* system outlined earlier in section 5.1.2.

Based on the successful restoration of T6SS-5 secretion to the *tag* mutants using their respective native *tag* genes cloned into pSCrhaB2-*virAG*, it was decided to clone *tagA*_{FLAG} and *tagB*_{FLAG} into this plasmid. This would allow pull down assays to be carried out in the corresponding *B.t* *tag* mutant strains under conditions in which the T6SS-5 gene cluster is expressed.

To introduce the *tagA*_{FLAG} and *tagB*_{FLAG} genes into pSCrhaB2-*virAG*, it was first necessary to transfer the genes from pBBR1MCS-*tagA*_{FLAG} and pBBR1MCS-*tagB*_{FLAG} into LITMUS28i. The LITMUS28i intermediates were then digested and ligated with pSCrhaB2-*virAG* to generate pSCrhaB2-*virAG*-*tagA*_{FLAG} and pSCrhaB2-*virAG*-*tagB*_{FLAG}. This process is described in more detail in section 5.4.3.

6.2.5 Assessment of the ability of TagA_{FLAG} and TagB_{FLAG} to restore T6SS-5 activity in *B.t* *tagA* and *tagB* mutants

The pSCrhaB2-*virAG*-*tagA*_{FLAG} and pSCrhaB2-*virAG*-*tagB*_{FLAG} plasmids were delivered into the *B.t* *tagA* and *tagB* mutants, respectively, by conjugation using *E. coli* SM10(λ pir). Colonies of WT *B.t* containing

pSCrhaB2-*virAG*, the *B.t tssK* mutant containing pSCrhaB2-*virAG* and the *B.t tagA* mutant containing pSCrhaB2-*virAG*, pSCrhaB2-*virAG-tagA* or pSCrhaB2-*virAG_{FLAG}* were used to inoculate overnight cultures in M9 minimal medium. These overnight cultures were used to inoculate 25 ml cultures in the same medium and incubated at 37°C. Once the cultures had reached an OD₆₀₀ of 1.0, cell-associated and TCA precipitated supernatant samples were prepared. The same process was repeated for cultures of the *B.t tagB* mutant harbouring pSCrhaB2-*virAG*, pSCrhaB2-*virAG-tagB* or pSCrhaB2-*virAG-tagB_{FLAG}*. The proteins in the samples were resolved by SDS-PAGE before transferring to PVDF membranes by western blotting. Blots were probed with antibodies against the RNAP β-subunit, the FLAG epitope and the *B.t TssD-5* protein.

6.2.5.1 pSCrhaB2-*virAG-tagA_{FLAG}* restores T6SS-5 activity to a *B.t tagA* mutant

As shown in Figure 6.4, the anti-FLAG antibody bound to a protein of the expected size for TagA_{FLAG} in the cell associated samples of the *B.t ΔtagA* mutant containing pSCrhaB2-*virAG-tagA_{FLAG}*. This demonstrates that TagA_{FLAG} is present in the cells. As shown previously, the *B.t tssK* and *tagA* mutants did not secrete TssD-5, as indicated by the absence of a TssD-5 cross-reacting protein in supernatant samples of these cultures, whereas TssD-5 was present in all of the cell associated samples. The presence of either pSCrhaB2-*virAG-tagA* or pSCrhaB2-*virAG-tagA_{FLAG}* was capable of restoring T6SS-5 function to the *B.t tagA* mutant as demonstrated by the presence of TssD-5 in the culture supernatants of these two cultures. This result demonstrates that TagA_{FLAG} is functionally the same as native TagA with respect to its role in T6SS-5 activity, making it a suitable 'bait' protein for use in co-immunoprecipitation assays using anti-FLAG antibody to recover TagA_{FLAG}. The anti-FLAG antibody did not bind to proteins in the culture supernatant from the strain which contained pSCrhaB2-*virAG-tagA_{FLAG}*, indicating that TagA_{FLAG} is not secreted.

6.2.5.2 pSCrhaB2-*virAG-tagB_{FLAG}* restores T6SS-5 activity to a *B.t tagB* mutant

Figure 6.5 demonstrates that TagB_{FLAG} was expressed in cultures of the *B.t ΔtagB* mutant containing pSCrhaB2-*virAG-tagB_{FLAG}* and could be detected in cell associated samples by probing with anti-FLAG antibody. However, TagB_{FLAG} could not be detected in the supernatants, consistent with the suggestion that it is an integral component or regulator of the T6SS-5 rather than a secreted effector. As observed previously, TssD-5 was absent from the supernatants of the *tagB* mutant containing multiple copies of *virAG* but present when *tagB* was added *in trans*. There appeared to be no detrimental effect of the addition of the FLAG epitope to the C-terminus of TagB as the culture supernatant of the *ΔtagB* mutant harbouring pSCrhaB2-*virAG-tagB_{FLAG}* contained TssD-5. Cultures of the *ΔtagB* mutant harbouring pSCrhaB2-*virAG-tagB_{FLAG}* would therefore be suitable for use in co-immunoprecipitation experiments using anti-FLAG antibody to bind to TagB_{FLAG}.

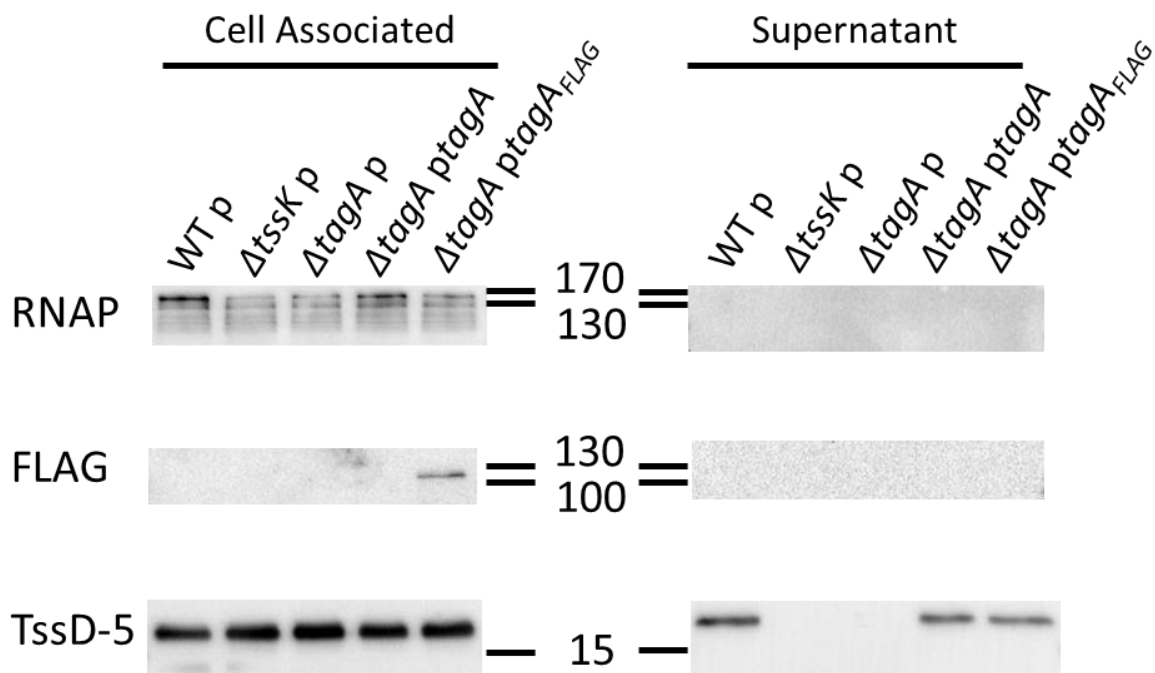


Figure 6.4 pSCrhaB2-*virAG*-*tagA*_{FLAG} restores T6SS-5 function to a *B.t tagA* mutant

Cultures of *B. thailandensis* were grown in M9 medium containing 0.5% glycerol and 0.5% casamino acids to an OD₆₀₀ of 1.0 before a cell associated sample was taken and the supernatants were TCA precipitated and electrophoresed in a 15% SDS polyacrylamide gels before transfer of the proteins to a PVDF membrane and probing with antibodies against the β subunit of RNAP, the FLAG epitope and TssD-5 as indicated on the left. WT p, sample prepared from WT *B.t* containing pSCrhaB2-*virAG*; $\Delta tssK$ p, sample prepared from the *B.t* $\Delta tssK$ mutant containing pSCrhaB2-*virAG*; $\Delta tagA$ p, sample prepared from the *B.t* $\Delta tagA$ mutant containing pSCrhaB2-*virAG*; $\Delta tagA$ *ptagA*, sample prepared from the *B.t* $\Delta tagA$ mutant containing pSCrhaB2-*virAG*-*tagA*; $\Delta tagA$ *ptagA*_{FLAG} sample prepared from the *B.t* $\Delta tagA$ mutant containing pSCrhaB2-*virAG*-*tagA*_{FLAG}. Location of pertinent protein size markers indicated by horizontal lines. Sizes are given in kDa.

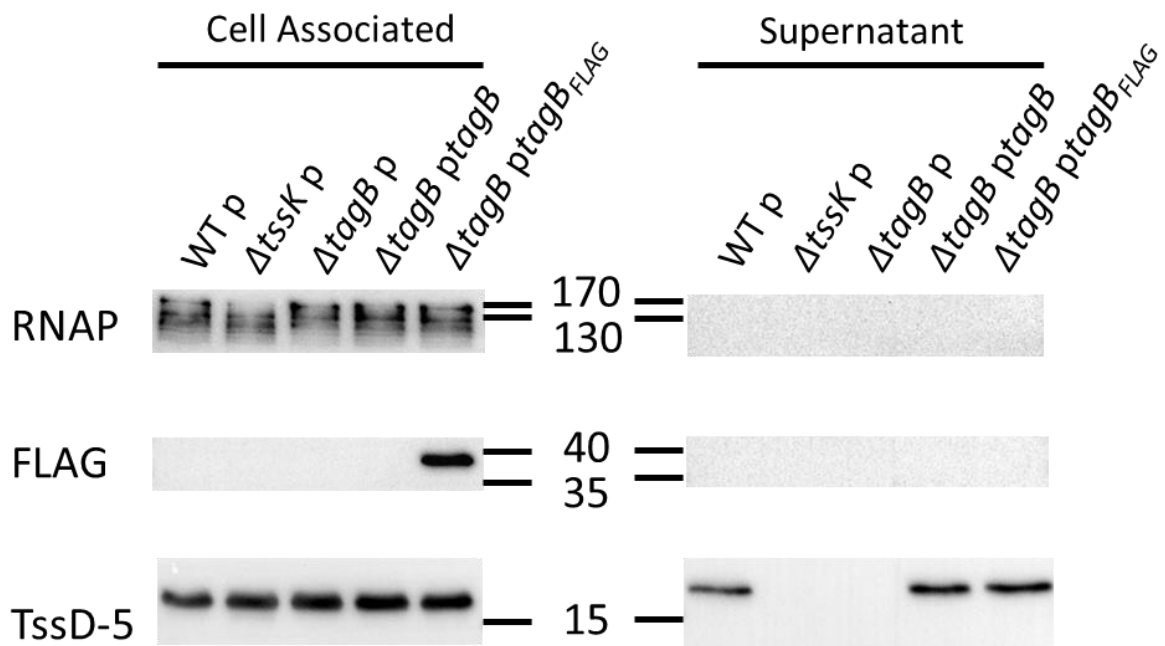


Figure 6.5 pSCrhaB2-*virAG*-*tagB*_{FLAG} restores T6SS-5 function to a *tagB* mutant

Cultures of *B. thailandensis* were grown in M9 medium containing 0.5% glycerol and 0.5% casamino acids to an OD₆₀₀ of 1.0 before a cell associated sample was taken and the supernatants were TCA precipitated and electrophoresed in a 15% SDS polyacrylamide gels before transfer of the proteins to a PVDF membrane and probing with antibodies against the β subunit of RNAP, the FLAG epitope and TssD-5 as indicated on the left. WT p, sample prepared from WT *B.t* containing pSCrhaB2-*virAG*; $\Delta tssK$ p, sample prepared from the *B.t* $\Delta tssK$ mutant containing pSCrhaB2-*virAG*; $\Delta tagB$ p, sample prepared from the *B.t* $\Delta tagB$ mutant containing pSCrhaB2-*virAG*; $\Delta tagB$ ptagB, sample prepared from the *B.t* $\Delta tagB$ mutant containing pSCrhaB2-*virAG*-*tagB*; $\Delta tagB$ ptagB_{FLAG} sample prepared from the *B.t* $\Delta tagB$ mutant containing pSCrhaB2-*virAG*-*tagB*_{FLAG}. Location of pertinent protein size markers indicated by horizontal lines. Sizes are given in kDa.

6.2.5.3 Expression of *tagC_{FLAG}* and *tagD_{FLAG}* does not restore T6SS-5 activity to *B.t tagC* and *tagD* mutants

Due to the inability of pBBR1MCS-*tagC_{FLAG}* and pBBR1MCS-*tagD_{FLAG}* to complement their respective mutants in MNGC assays, it was decided not to transfer *tagC_{FLAG}* and *tagD_{FLAG}* to pSCrhaB2-*virAG*, as the encoded epitope tagged proteins were unlikely to be representative of their wild type counterparts. However, using the natural inducer of T6SS-5, glutathione (section 5.5), there is potential for directly assessing the ability of the *tagC_{FLAG}* and *tagD_{FLAG}* alleles to restore T6SS-5 function in a complementation assay without the need to transfer the genes to pSCrhaB2-*virAG*. Cultures of WT *B. thailandensis* containing pBBR1MCS, the *B.t ΔtagC* mutant containing pBBR1MCS, pBBR1MCS-*tagC* or pBBR1MCS-*tagC_{FLAG}*, and the *B.t ΔtagD* mutant containing pBBR1MCS, pBBR1MCS-*tagD*, or pBBR1MCS-*tagD_{FLAG}*, were grown in M9 medium containing 0.5% glycerol, 0.5% casamino acids and 200 μM glutathione (GSH). As shown in Figure 6.6, both TagC_{FLAG} and TagD_{FLAG} could be detected in cell associated samples from strains harbouring pBBR1MCS-*tagC_{FLAG}* and pBBR1MCS-*tagD_{FLAG}*, respectively, at their respective predicted sizes of 28.9 and 13.9 kDa, although TagD_{FLAG} was only detectable following a longer exposure time suggesting that it was present at a lower level than TagC_{FLAG}. TssD-5 was present in all of the cell associated samples indicating that GSH had induced the expression of T6SS-5. The only strains in which TssD-5 was identified in the culture supernatants were WT *B.t* containing pBBR1MCS, the *B.t ΔtagC* mutant containing pBBR1MCS-*tagC* and the *B.t ΔtagD* mutant containing pBBR1MCS-*tagD*. This is consistent with the observation that these strains are capable of inducing MNGC formation and that TagC_{FLAG} and TagD_{FLAG} are not functional. Therefore, cultures containing C-terminal FLAG epitope-tagged TagC and TagD are not suitable for co-immunoprecipitation assays.

6.2.6 Co-immunoprecipitation using TagA_{FLAG} as bait

Once it had been established that TagA_{FLAG} was capable of restoring T6SS-5 function to the *B.t ΔtagA* mutant, a co-immunoprecipitation using TagA_{FLAG} as bait was attempted. An overnight culture was used to inoculate 25 ml cultures of the *B.t ΔtagA* mutant containing pSCrhaB2-*virAG-tagA_{FLAG}* and pSCrhaB2-*virAG-tagA*. The latter served as a control which lacked the FLAG epitope but was otherwise isogenic. The cultures were grown in M9 medium containing 0.5% (v/v) glycerol and 0.5% (w/v) casamino acids to an OD₆₀₀ of ~1.0 whereupon the cells were collected by centrifugation and washed by resuspending in 5 ml TBS. The cell suspensions were centrifuged again and the supernatants discarded before the pellet was frozen at -20°C. The cells were lysed by sonication, the insoluble material was removed by centrifugation and the soluble proteins added to washed M2 Anti-FLAG gel.

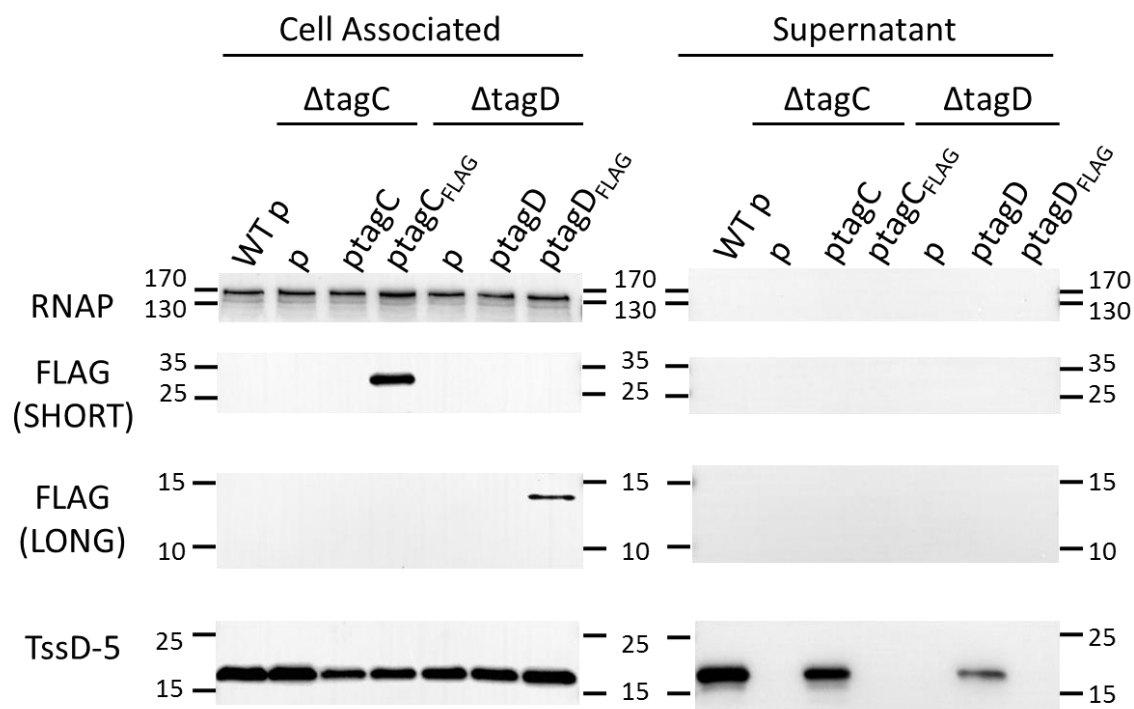


Figure 6.6 T6SS-5 activity in glutathione-induced *B.t tagC* and *tagD* mutants complemented with Tag_{FLAG} and TagD_{FLAG}

Western blot stained with antibody against RNAP, TssD-5 and the FLAG epitope at long and short exposure times as indicated. Cell associated and TCA precipitated supernatant samples were prepared from cultures of the indicated strains in which T6SS-5 had been induced by the addition of GSH. WT p, WT *B.t* containing pBBR1MCS; $\Delta tagC$ p, *B.t* $\Delta tagC$ mutant containing pBBR1MCS; $\Delta tagC$ ptagC, *B.t* $\Delta tagC$ mutant containing pBBR1MCS-*tagC*; $\Delta tagC$ ptagC_{FLAG}, *B.t* $\Delta tagC$ mutant containing pBBR1MCS-*tagC*_{FLAG}; $\Delta tagD$ p, *B.t* $\Delta tagD$ mutant containing pBBR1MCS; $\Delta tagD$ ptagD, *B.t* $\Delta tagD$ mutant containing pBBR1MCS-*tagD*; $\Delta tagD$ ptagD_{FLAG}, *B.t* $\Delta tagD$ mutant containing pBBR1MCS-*tagD*_{FLAG}. Location of pertinent protein size markers indicated by horizontal lines. Sizes are given in kDa.

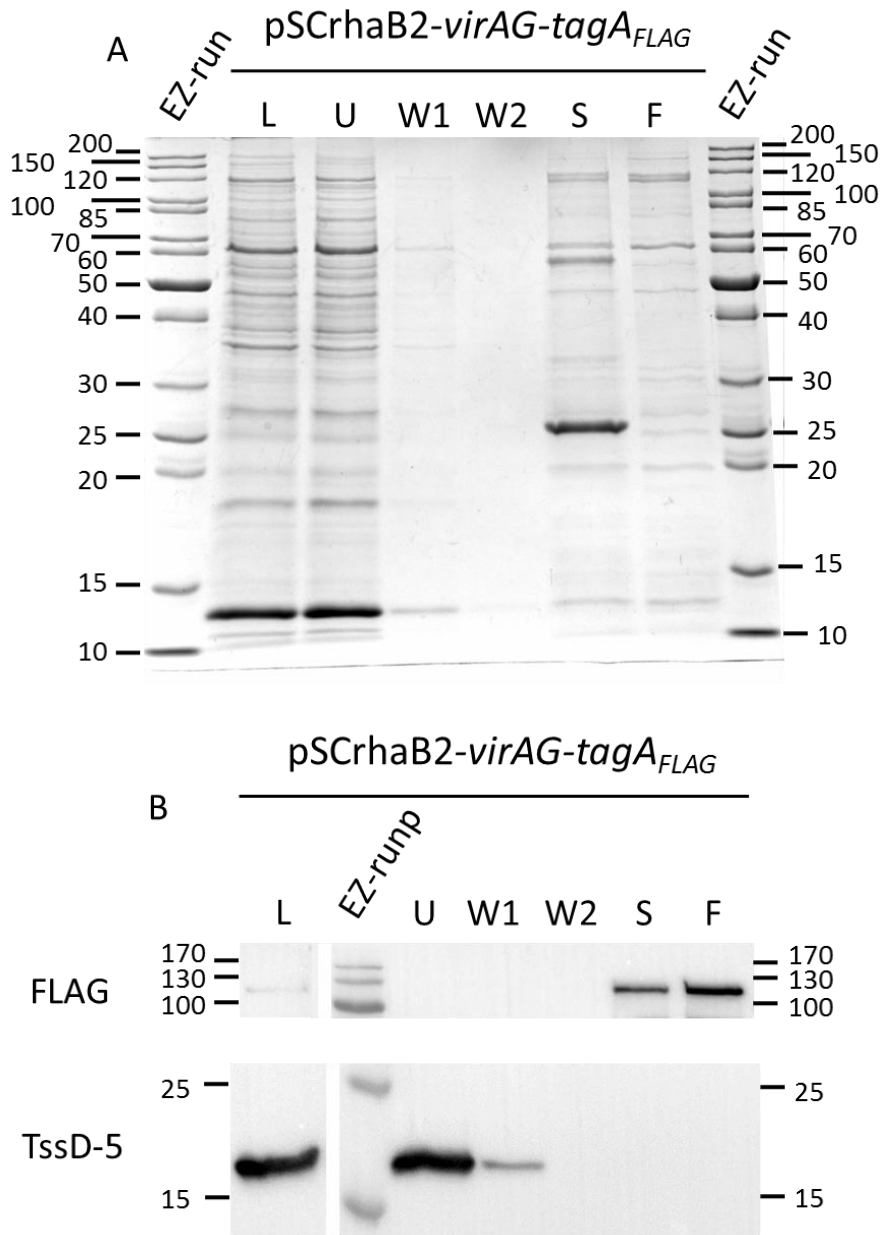


Figure 6.7 Co-immunoprecipitation using TagA_{FLAG} as bait

A) Coomassie blue stained SDS polyacrylamide gel to separate proteins taken from a co-immunoprecipitation using anti-FLAG M2 affinity gel to recover TagA_{FLAG} present in cell lysates prepared from a culture of the *B.t* $\Delta tagA$ mutant containing pSCrhaB2-*virAG-tagA*_{FLAG}. L, Soluble fraction of cell lysate applied to the washed M2 affinity gel; U, unbound material; W1, wash 1; W2, wash 2; S, material eluted using Laemmli buffer; F, material eluted using a FLAG peptide solution; EZ-run, EZrun ladder (sizes shown in kDa). B) Western blot of the same samples in the SDS polyacrylamide gel stained with antibody against the FLAG epitope or TssD-5. EZ-runp, EZrun pre-stained ladder (sizes shown in kDa).

After a two-hour incubation at 4°C the gel was washed with TBS four times and the bound protein eluted by either boiling in 2 x Laemmli buffer or addition of competing FLAG peptide in TBS. Samples were analysed by SDS-PAGE and western blotting.

Analysis of the Coomassie blue stained gel in Figure 6.7 A shows a large number of proteins in the fraction of the cell lysate that was applied to the affinity gel and they were largely present in the unbound fraction. This indicated that the majority of the proteins did not bind to the affinity gel. The first wash eluted small amounts of some proteins, while there were no proteins present in the second wash, indicating that most of the unbound protein had been removed in the first step. Both the Laemmli and FLAG peptide elution samples contained visible protein bands, although not as many as were present in the cell lysate applied to the gel or in the unbound material suggesting that enrichment of some of the proteins had taken place. While the Laemmli and FLAG peptide elution samples appeared similar in their content there were two distinct proteins of approximately 55 and 25 kDa present in the Laemmli eluted samples that were not present in the FLAG peptide eluted samples. These proteins are likely to be the heavy and light chain of the M2 anti-FLAG IgG present in the affinity gel which have a predicted molecular weight of 50 and 23 kDa, respectively.

As Figure 6.7 B demonstrates, when a western blot of the same samples was probed with antibody against the FLAG peptide, a faint band was observed in the soluble fraction of the cell lysate which approximately corresponded to the predicted size of TagA_{FLAG} (92.2 kDa) indicating that the protein is soluble. Following incubation of the lysate with the affinity gel and recovery of the gel, the unbound and wash fractions were found not to contain any detectable TagA_{FLAG} indicating that the majority of the protein has been immobilised onto the affinity gel. When the bound peptides were eluted from the anti-FLAG gel, either by the addition of Laemmli buffer or FLAG peptide, a band at the predicted molecular weight of TagA_{FLAG} was detected, confirming that TagA_{FLAG} is bound to, and then eluted from the affinity gel. When looking at the pattern of staining with the antibody raised against TssD-5, it is clear that soluble TssD-5 was also present in the sample applied to the affinity gel as well as the unbound fraction. TssD-5 was also present in the first wash but not the second. As TssD-5 seems to be present at very high concentrations in the cell and is absent from the second wash it represents a useful control of the effectiveness of the wash steps. TssD-5 is not detectable in either the Laemmli or FLAG peptide eluted samples, indicating that it probably does not interact with TagA or the resin.

Among the proteins that were eluted from the agarose-based affinity gel, it is likely that many bound non-specifically. To identify the proteins on the gel which were present as a result of specific binding to TagA_{FLAG}, the Laemmli and FLAG peptide elutions from an experiment performed using the soluble

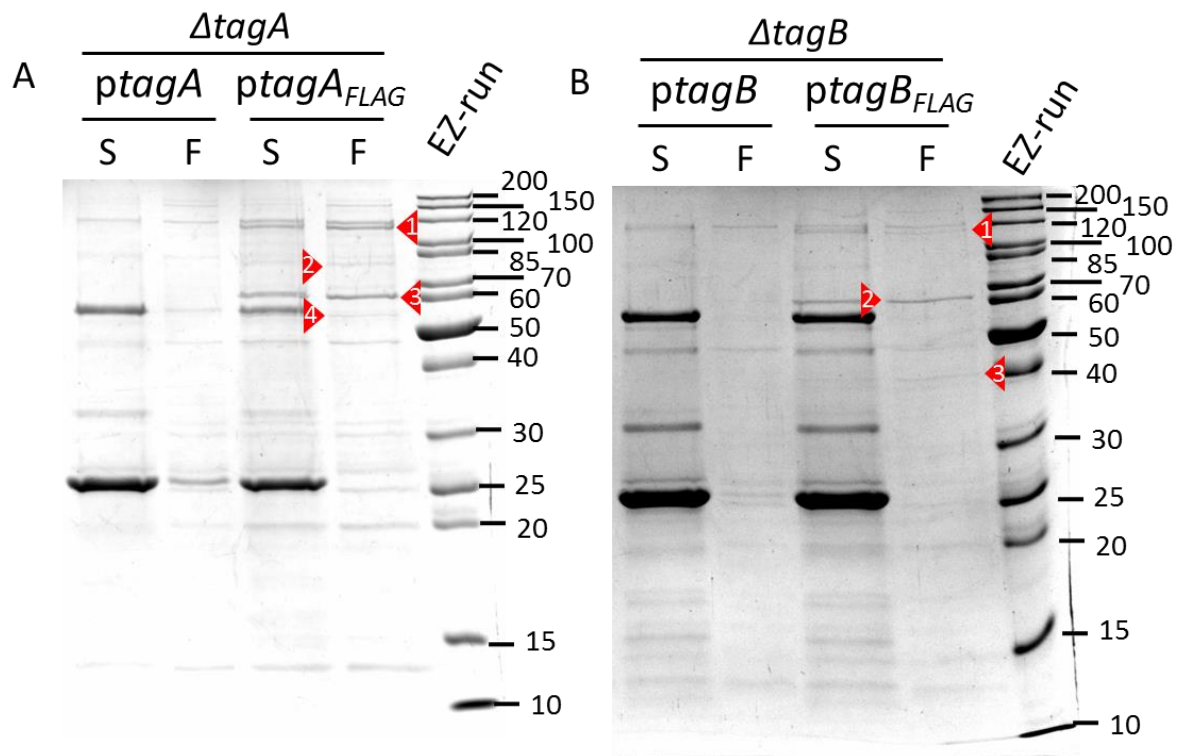


Figure 6.8 Eluted proteins from co-immunoprecipitation assays

Coomassie blue stained polyacrylamide gels of S, Laemmli eluted samples and F, FLAG eluted samples taken from pull down assays using lysates from cultures of A) *B.t* $\Delta tagA$ -5 mutant containing either pSCrhaB2-*virAG-tagA* (*ptagA*) or pSCrhaB2-*virAG-tagA*_{FLAG} (*ptagA*_{FLAG}) and B) *B.t* $\Delta tagB$ -5 mutant containing either pSCrhaB2-*virAG-tagB* (*ptagB*) or pSCrhaB2-*virAG-tagB*_{FLAG} (*ptagB*_{FLAG}). Numbered red arrows indicate bands present in the elution samples taken from cultures expressing FLAG-tagged proteins that are absent from the respective controls which express the respective protein without a FLAG tag. The molecular weights of the proteins indicated by each arrow are shown in Table 6.1. EZrun, EZrun unstained ladder (sizes shown in kDa).

Table 6.1 Predicted molecular weight of protein bands marked by red arrows in Figure 6.8

Arrow Indicated on gel		Estimated MW (kDa) ^a		Potential T6SS-5 Proteins	MW (kDa) Of Potential Proteins
TagA _{FLAG}	TagB _{FLAG}	TagA _{FLAG}	TagB _{FLAG}		
1	1	113.2	109.4	TssI-5/TssH-5 /TagA-5	108.8/101.2/91.2
2	-	79.4	-	N/A	N/A
3	2	60.3	58.7	TssC-5	57.3
-	3	-	38.5	TagB-5	37.6
4	-	54.6	-	TssK-5	51.6

^a Molecular weight predicted using ImageLab

fraction of a lysate prepared from cultures of the *B.t ΔtagA* mutant containing pSCrhaB2-*virAG-tagA* were electrophoresed in a gel alongside elutions from the *B.t ΔtagA* mutant containing pSCrhaB2-*virAG-tagA_{FLAG}* (Figure 6.8 A). It was clear that several of the proteins in the elution samples were specific to lysates applied to the affinity gel that contained TagA_{FLAG}, suggesting that they could be interaction partners. The molecular weights of these TagA_{FLAG}-specific proteins was calculated using the molecular weight estimation tool found in the ImageLab software (BioRad) and used to make a prediction of the T6SS-5 proteins TagA might be interacting with (Table 6.1). To identify any interaction partners specific to TagA_{FLAG}, the FLAG elution sample from the affinity gel incubated with cell lysates containing TagA_{FLAG} and native TagA were analysed by mass spectrometry. The results are presented in section 6.2.8.

6.2.7 Co-immunoprecipitation using TagB_{FLAG} as bait

The same procedure that was used for the TagA_{FLAG} co-immunoprecipitation described in section 6.2.6 was used on lysates prepared from cultures of the *B.t ΔtagB* mutant containing pSCrhaB2-*virAG-tagB_{FLAG}* and pSCrhaB2-*virAG-tagB*. Again, samples from the lysate, unbound material, first and second wash, as well as the Laemmli buffer and FLAG peptide elutions were analysed by electrophoresis in a 12% polyacrylamide gel which was stained with Coomassie blue (Figure 6.8A). As expected for a cell lysate there was an abundance of protein bands in the material loaded on the affinity gel and the protein profile remained similar in the unbound samples. A few proteins were present in low amounts in the first wash but no proteins were present in the second wash. There appeared to be fewer proteins present in the samples eluted from the affinity gel in this experiment in comparison to the eluted material in the TagA_{FLAG} co-immunoprecipitation. Protein bands corresponding to the light (23 kDa) and heavy (50 kDa) chains of the anti-FLAG antibody were visible in the samples eluted by Laemmli buffer, but not those eluted using the FLAG peptide. The same samples, but with the addition of a sample taken from the FLAG peptide elution were also analysed by western blotting (Figure 6.9 B). When the blot was probed with the monoclonal antibody against the FLAG epitope, a protein of approximately the same MW as the calculated molecular weight of TagB_{FLAG} (38.6 kDa) was present in the cell lysate which was applied to the affinity gel. A very low abundance protein at this molecular weight was also detectable in the unbound fraction but not observed in the wash fractions suggesting that the majority of TagB_{FLAG} had been adsorbed onto the affinity gel. TagB_{FLAG} appeared to be present in the Laemmli buffer eluted fraction, indicating that TagB_{FLAG} had been liberated from the affinity gel to which it had previously bound. As with TagA_{FLAG}, the blot was also probed with polyclonal antibody raised against TssD-5 which detected a protein at the approximate size of TssD-5 in the soluble fraction of the lysate as well as in the unbound protein and first wash sample, but not in the second wash or elution samples. This suggests that like TagA_{FLAG}, TssD-5 does not bind to TagB_{FLAG}.

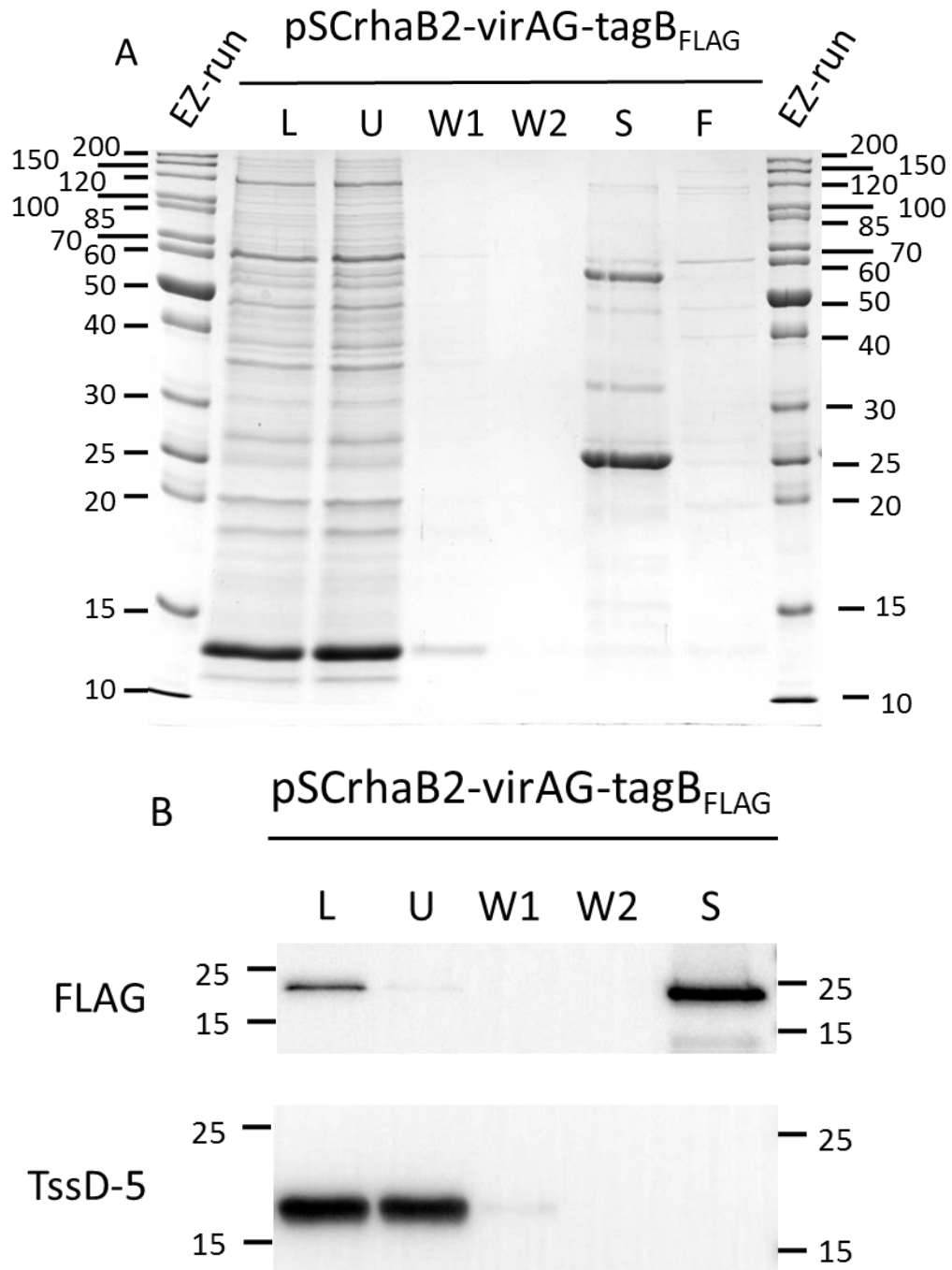


Figure 6.9 Co-immunoprecipitation using TagB_{FLAG} as bait

A) Coomassie stained SDS polyacrylamide gel of samples taken from a co-immunoprecipitation using anti-FLAG M2 affinity gel to recover TagB_{FLAG} present in cell lysates prepared from a culture of the *B.t* $\Delta tagB$ mutant containing pScRhaB2-virAG-tagB_{FLAG}. L, Soluble fraction of cell lysate applied to the washed M2 affinity gel; U, unbound material; W1, wash 1; W2, wash 2; S, material eluted using Laemmli buffer; F, material eluted using a FLAG peptide solution; EZ-run, EZrun ladder (sizes shown in kDa). B) Western blot of the same samples in the Coomassie stained SDS polyacrylamide gel. EZ-run, EZrun pre-stained ladder (sizes shown in kDa).

To distinguish between proteins that had bound non-specifically to the affinity gel and those which had bound via TagB_{FLAG}, the Laemmli buffer and FLAG peptide elutions from the co-immunoprecipitation prepared using the lysate prepared from the *B.t ΔtagB* mutant containing pSCrhaB2-*virAG-tagB_{FLAG}* were analysed by SDS-PAGE alongside those from the *B.t ΔtagB* mutant containing pSCrhaB2-*virAG-tagB*. As indicated by the arrows in Figure 6.8 B, there were three proteins which were present in the elution samples containing TagB_{FLAG} that were not present in those which contained untagged-TagB. The estimated MW and predicted identity (assuming they are T6SS-5 proteins) of these proteins is indicated in Table 6.1.

6.2.8 Mass spectrometry analysis of FLAG eluted samples

Based on the observations of samples analysed by SDS-PAGE, it was determined that the FLAG peptide eluted samples contained fewer contaminating proteins that could interfere with downstream analysis techniques than the Laemmli buffer eluted samples. To identify any proteins that interacted with TagA and TagB, the FLAG peptide elution samples from the TagA_{FLAG} and TagB_{FLAG} co-immunoprecipitations were analysed by mass spectrometry at the biOMICS facility (University of Sheffield). The solutions were reduced, alkylated and then subjected to in gel tryptic digestion before detection. The TagA and TagB samples were also sent for MS analysis.

6.2.8.1 TagA interaction partners

The total of the label free quantification (LFQ) intensity for TagA_{FLAG} was combined for each protein detected across the three repeats. This value was divided by the total LFQ intensity for proteins identified in all three native TagA samples to give a ratio of the LFQ intensity of proteins in the TagA_{FLAG} samples to the LFQ intensity of the native TagA-5 samples. Proteins with a ratio of 3 and above are shown in Table 6.2. Unsurprisingly, TagA-5 was enriched in the TagA_{FLAG} pulldown with a high ratio, consistent with the detection of TagA_{FLAG} in the eluted samples by western blotting. The chaperone proteins GroL1 (also known as GroEL), DnaK and GrpE were also enriched, these proteins are involved in protein folding and are therefore likely to be non-specifically interacting with TagA-5. Interestingly the T6SS-5 tail spike protein, TssI-5 also appears to be an interaction partner. Another T6SS-5 protein detected in higher quantities in the TagA_{FLAG} samples is the base plate protein, TssF-5. There were also a number of proteins which were only identified in the TagA_{FLAG} samples, making it impossible to determine a ratio. Amongst these proteins was TagD-5, although this could be present due to an interaction with TssI-5 (which itself appeared to interact with TagA-5).

Table 6.2 TagA interaction partners identified by mass spec

UniProt Protein ID	Protein name and description	Gene name	Ratio LFQ intensity TagA _{FLAG} /TagA (average)	t-test Significant?	t-test p value	t-test Difference
Q2T6Z0	TagA-5	<i>tagA-5</i>	35.453	+	0.002	5.409
Q2SYJ5	60 kDa chaperonin 1	<i>groL1</i>	38.978	+	0.005	5.079
Q2T6Y9	TssI-5	<i>tssI-5</i>	9.561	+	0.072	4.184
Q2SYZ6	Protein GrpE	<i>grpE</i>	9.332	+	0.072	2.945
Q2T6Y6	TssF-5	<i>tssF-5</i>	9.154	+	0.041	3.034
Q2SZ78	Glutamate dehydrogenase	BTH_I1224	8.019	-	1.000	0.772
Q2T5Z2	Polyketide synthase	BTH_II1211	7.433	+	0.035	2.704
Q2T295	Cell shape determining, MreB/Mrl family protein	BTH_I0146	6.956	+	0.007	2.871
Q2SZ67	Putative iron-sulfur cluster insertion protein ErpA	<i>erpA</i>	6.181	-	1.000	2.475
Q2T748	Acyl-homoserine-lactone synthase	BTH_II0804	6.082	-	1.000	2.537
Q2SYZ4	Chaperone protein DnaK	<i>dnaK</i>	5.937	+	0.047	3.098
Q2SYH5	Putative O-antigen methyl transferase	BTH_I1478	5.536	+	0.004	2.496
Q2T0V0	Protein RecA	<i>recA</i>	5.209	-	1.000	2.367
Q2SZE0	Acetyl-CoA carboxylase, biotin carboxylase	<i>accC</i>	4.669	-	1.000	1.044
Q2SVV9	Cyclic peptide ABC transporter, ATP-binding protein	BTH_I2419	4.168	-	1.000	1.873
Q2SZH8	Cell division protein FtsZ	<i>ftsZ</i>	4.094	-	0.030	2.192
Q2T5S7	Uncharacterized protein	BTH_II1276	3.996	-	0.036	2.222
Q2T6Z1	TagB-5	<i>tagB-5</i>	3.801	-	0.053	1.829
Q2SYH6	Putative glycosyl transferase	BTH_I1477	3.725	-	0.014	1.975
Q2T2C4	PglY	BTH_I0115	3.454	-	0.130	2.367
Q2T7G0	GDP-mannose 4,6-dehydratase	<i>gmd-2</i>	3.414	-	0.097	1.679
Q2T7V2	Capsular exopolysaccharide family domain protein	BTH_II0547	3.217	-	1.000	1.550
Q2SW97	Lycopene cyclase family protein	BTH_I2281	3.205	-	0.027	1.620
Q2T9B1	Universal stress family protein	BTH_II0036	3.108	-	0.022	1.753
Q2SZZ0	Chaperone protein HtpG	<i>htpG</i>	3.095	-	1.000	1.529
Q2STE9	ATP synthase subunit beta 1	<i>atpD1</i>	3.020	-	0.177	1.377

Table 6.3 TagB interaction partners identified by mass spec

UniProt Protein ID	Protein name and description	Gene name	Ratio LFQ intensity TagB _{FLAG} /TagB (average)	t-test Significant?	t-test p value	t-test Difference
Q2T6Z1	TagB-5	<i>tagB-5</i>	34.47	+	0.005	5.580
Q2T6Y9	TssI-5	<i>tssI-5</i>	10.92	-	0.066	3.278
Q2SYJ5	60 kDa chaperonin 1	<i>groL1</i>	7.75	+	0.009	3.037
Q2SZE0	Acetyl-CoA carboxylase, biotin carboxylase	<i>accC</i>	7.44	-	1.000	1.017
Q2T838	Acetoacetyl-CoA reductase	<i>phbB</i>	6.62	+	0.011	2.830
Q2SUD8	TssM-1	<i>tssM-1</i>	6.39	-	1.000	2.654
Q2T6Z3	TagD-5	<i>tagD-5</i>	5.52	-	0.074	2.501
Q2T4Y8	Universal stress family protein	BTH_II1566	5.49	+	0.007	2.455
Q2SUJ2	Phenylacetic acid degradation protein paaN	<i>paaN</i>	4.25	-	0.404	1.888
Q2SYZ6	Protein GrpE	<i>grpE</i>	3.75	-	0.552	1.422
Q2T5Z2	Polyketide synthase	BTH_II1211	3.73	-	0.392	1.393
Q2T0F4	Uncharacterized protein	BTH_I0789	3.58	-	0.209	1.779
Q2T784	Twitching motility protein PilT, putative	BTH_II0768	3.49	-	0.149	1.595
Q2T295	Cell shape determining, MreB/Mrl family protein	BTH_I0146	3.29	-	0.018	1.787
Q2T5W5	Metallo-beta-lactamase superfamily protein	BTH_II1238	3.24	-	0.016	1.685
Q2SW97	Lycopene cyclase family protein	BTH_I2281	3.23	-	0.004	1.717
Q2SUS8	Heat shock protein, Hsp20 family	BTH_I2809	3.20	-	1.000	1.662
Q2T5W6	Thio-template mechanism natural product synthetase	BTH_II1237	3.10	-	0.062	1.548

6.2.8.2 TagB interaction partners

Proteins which interacted with TagB-5 were determined using the same methods as TagA and a list of proteins with an LFQ intensity ratio of 3 and above is shown in Table 6.3. As expected, TagB-5 is enriched in the TagB_{FLAG} sample. Like TagA-5, TagB-5 also demonstrates an interaction with GroL1, which is presumably non-specific. There were also statistically significant enrichments for an Acetoacetyl-CoA reductase, PhbB, and a universal stress family protein, encoded by BTH_II1566. Neither of these proteins are likely to interact specifically with TagB-5. Interestingly TssI-5 is also enriched, but not to a statistically significant level. Another protein found at a higher intensity in the TagB_{FLAG} samples was TagD-5, again this was not statistically significant but merits further investigation given that both proteins are encoded by genes of the T6SS-5 gene cluster.

6.3 Identification of Tag protein-interacting partners by two-hybrid analysis

As an alternative approach to study the interactions of the *B. thailandensis* T6SS-5 Tag proteins with other components of the T6SS, the bacterial adenylate cyclase two-hybrid (BACTH) assay was utilised.

The system utilises the catalytic activity of the *Bordetella pertussis* adenylate cyclase (CyaA) which synthesises cyclic adenosine monophosphate (cAMP). CyaA is separated into two inactive fragments; T25 and T18, when these fragments are in close proximity cAMP is generated, which in turn binds to the catabolite activator protein (CAP). The resulting cAMP/CAP complex can then turn on the expression of the *mal* operon and the expressed gene products enable the fermentation of maltose when it is present in the growth medium. The fermentation of the maltose generates acidic end products which can be detected using appropriate indicator medium such as MacConkey agar base which turns a pink colour in the presence of acid. The genes encoding the proteins whose interaction is to be investigated are cloned into one of the two kanamycin resistant plasmids to create a fusion of the C-terminal end of the T25 fragment to the N-terminal end of the protein of interest (pKT25) or the N-terminal end of the T25 fragment to the C-terminal end of the protein of interest (pKNT25). To test interactions a potential binding partner is cloned into one of the two ampicillin resistant plasmids to create a fusion of the C-terminal end of the T18 fragment to the N-terminal end of the protein of interest (pUT18C), or the N-terminal end of the T18 fragment to the C-terminal end of the protein of interest (pUT18). The *E. coli* BTH101 strain is then transformed with a combination of a kanamycin and ampicillin resistant plasmid containing the genes of interest and plated on MacConkey agar base medium (BD) containing 1% (w/v) maltose, 100 µg/ml ampicillin and 50 µg/ml kanamycin and grown at 30°C. Over a time period of three to five nights the colour of the colonies growing on the plates is assessed. If there is an interaction between the proteins of interest, then the T25 and T18 fragments

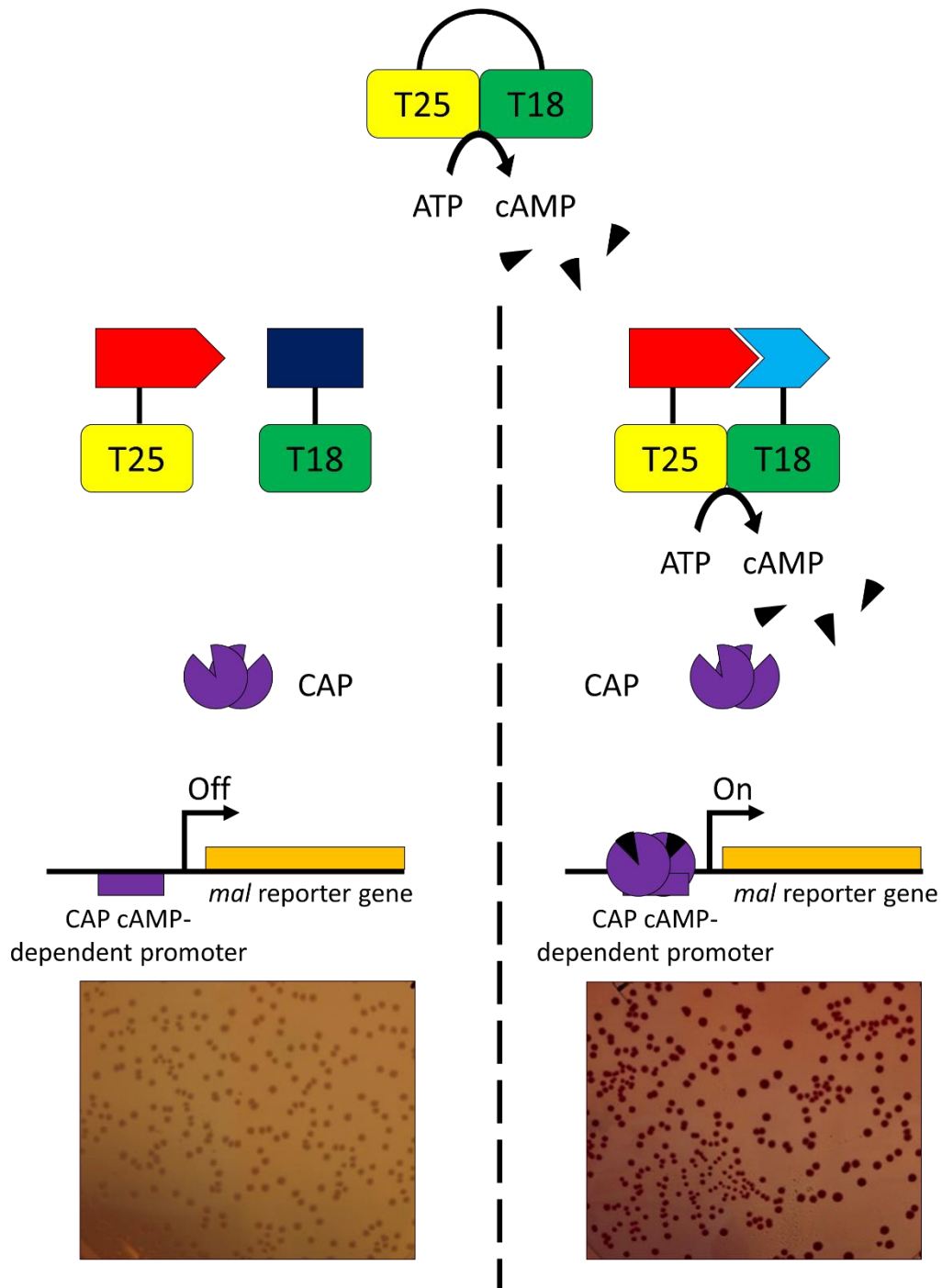


Figure 6.10 Principle of the bacterial two hybrid system

Outline of the BACTH assay showing the catalytic domain of adenylate cyclase (CyaA) top, with adenylate cyclase activity. When the T25 and T18 domains are separated and fused with proteins that do not interact (left) adenylate cyclase is non-functional and cAMP is not synthesised. There is no cAMP to bind to catabolite activator protein (CAP) and therefore the expression of the *mal* gene is not induced. When the cells are plated on MacConkey agar containing maltose, the cells do not metabolise the sugar and there is a negative phenotype (bottom left). When the T25 and T18 domains are fused with proteins that interact, they are brought into close proximity, creating a functional adenylate cyclase, resulting in high levels of cellular cAMP. cAMP binds to CAP which induces expression of the *mal* gene. When the cells are plated on MacConkey agar containing maltose, the cells are able to metabolise the sugar and there is a positive phenotype (bottom right).

are brought into close proximity creating a functional adenylate cyclase enzyme resulting in a pink colouration around the colonies. However, if there is no interaction then an off-white or pale pink colony phenotype is observed. This process is outlined in Figure 6.10.

Given that this is a directed approach which requires predicted interaction partners to be identified and cloned into the BACTH vectors, it was necessary to choose a set of candidate interaction partner proteins. As this study focusses on the Tag-5 proteins, the genes encoding all four of them were cloned into BACTH vectors. However, it was also necessary to decide which particular two-hybrid plasmids to use, as cloning the genes into pKNT25 and pUT18 results in the expression of a hybrid protein with its C-terminus fused to the N-terminus of T25 and T18, respectively. When using these two vectors, it is important to remove the stop codon of the gene encoding the test protein to allow the T25 and T18 fragments to be translated. Cloning the genes into pKT25 and pUT18C results in the expression of a hybrid protein in which the N-terminus of the test protein is fused to the C-terminus of T25 and T18, respectively. It is important to ensure that the genes are inserted into the plasmids in such a manner that they are in-frame with the T25 or T18 ORF. The gene encoding the test protein should be cloned into the vectors which are least likely to create a fusion protein with altered behaviour as a result of the presence of the T25 or T18 fragment. The activity of the C-terminal FLAG-tagged Tag proteins informed this decision.

6.3.1 Cloning of *tagA-5* into pKNT25 and pUT18

As MNGC formation and TssD-5 secretion assays had shown that TagA engineered to contain a C-terminal FLAG epitope was fully functional, it was decided to clone *tagA* into the BACTH vectors pKNT25 and pUT18. When primers are designed appropriately, these vectors allow the construction of a hybrid protein with its C-terminus fused to the N-terminus of T25 and T18, respectively. The primers tagApUT18for and tagApUT18rev were used in a Q5 PCR with a boiled lysate of WT *B.t* as a template which amplified a 2636 bp DNA fragment that included the entire TagA-5 ORF but not its stop codon. This fragment, as well as the pKNT25 plasmid were digested with PstI and BamHI and ligated together. The ligation mixture was used to transform *E. coli* JM83 cells which were spread on LB agar containing 25 µg/ml kanamycin and incubated at 37°C overnight. 18 colonies were used as templates for a GoTaq PCR screen which used the pKNT+pUT.seq.for.RJ and pKNT.rev.seq.RJ primers. These reactions were analysed by agarose gel electrophoresis, which amplified a 2832 bp fragment when the insert was present, whereas when the empty vector was present a 228 bp fragment was generated. A colony which appeared to contain the correct plasmid based on the PCR screen was grown overnight in LB containing 25 µg/ml kanamycin and the plasmid harvested by miniprep before the correct pKNT25-*tagA-5* construct was confirmed by sequencing.

The pUT18-*tagA-5* construct was engineered using the same amplicon and same pair of restriction enzymes used to generate pKNT25-*tagA-5*. *E. coli* JM83 cells were transformed with the ligation mixture before plating on LB containing 100 µg/ml ampicillin and growing overnight at 37°C. The presence of the correct plasmid was screened for by picking 18 colonies which were used as a template for a GoTaq PCR screen using the pKNT+pUT.seq.for.RJ and pUT.seq.rev.RJ primers which amplified a 195 bp DNA fragment when the empty pUT18 vector was present and a 2799 bp DNA fragment when the *tagA-5* gene was present. A positive colony was used to inoculate an overnight culture of LB containing 100 µg/ml ampicillin. Plasmid DNA was isolated by miniprep and the sequence of the 5627 bp pUT18-*tagA-5* plasmid was confirmed by sequencing.

6.3.2 Cloning of *tagB-5* into pKNT25 and pUT18

Like *tagA-5*, *B. thailandensis tagB-5* mutants harbouring pBBR1MCS-*tagB_{FLAG}* or pSCrhaB2-*virAG-tagB_{FLAG}* were fully functional with respect to inducing MNGC formation and TssD-5 secretion activity, respectively. This demonstrated that appending a tag to the C-terminus of TagB did not impair its function. Therefore, the pKNT25 and pUT18 plasmids were used for generating TagB-CyaA hybrid proteins for the BACTH assay.

A 1080 bp amplicon containing the *tagB-5* gene lacking its stop codon was generated using a PCR with the tagBpKNTfor and tagBpKNTrev primers, Q5 polymerase and a WT boiled lysate template. pKNT25, pUT18 and the amplified *tagB* DNA, were digested with PstI and BamHI restriction enzymes following which two ligations were prepared; one to clone the digested PCR product into the linearised pKNT25 vector and the other to clone the digested PCR product into pUT18. The completed ligation reactions containing pKNT25 and pUT18 were used to transform *E. coli* JM83 cells which were spread on LB agar plates containing 25 µg/ml kanamycin and 100 µg/ml ampicillin, respectively.

Eighteen colonies growing on kanamycin plates were used as a template in a GoTaq PCR which used the pKNT+pUT.seq.for.RJ and pKNT.rev.seq.RJ primers to screen for the presence of pKNT25-*tagB-5*. Colonies containing the empty vector (228 bp) were distinguished from those containing the desired construct (1258 bp) based on the size of the PCR product when electrophoresed in agarose gel. A colony which appeared to harbour plasmid containing the correct sized insert was used to inoculate 4 ml of LB containing 25 µg/ml kanamycin and grown overnight at 37°C with shaking. The plasmid DNA was isolated by plasmid miniprep and the 4507 bp pKNT25-*tagB-5* confirmed by DNA sequencing.

To screen for pUT18-*tagB-5*, 18 colonies were used as templates for GoTaq PCRs with the pKNT+pUT.seq.for.RJ and pUT.seq.rev.RJ primers to amplify a 195 bp DNA fragment when the colony contained the empty vector and a 1068 bp DNA fragment when the *tagB-5* gene was present. A colony which appeared to contain the desired plasmid according to the amplified PCR product was grown

overnight from which a plasmid of 4061 bp was recovered consistent with the predicted size of pUT18-*tagB-5*. The integrity of the construct was confirmed by sequencing.

6.3.3 Cloning of *tagC-5* into pKT25 and pUT18C

Unlike TagA and TagB, C-terminally FLAG-tagged TagC did not function like its WT counterpart. Thus, In MNGC formation assays pBBR1MCS-*tagC_{FLAG}* did not restore the ability to induce giant cell formation to the Δ *tagC-5* mutant despite the *tagC_{FLAG}* gene being expressed and did not complement the mutant in the TssD secretion assay. Since the addition of a short peptide at the C-terminus of TagC interfered with its activity, it was reasoned that a TagC fusion protein with the much larger T25 or T18 fragment at its C-terminus would almost definitely impair its function. Therefore, *tagC-5* was cloned into pKT25 and pUT18C to create a fusion in which the T25 and T18 segments of CyaA were fused to the N-terminus of TagC.

To clone *tagC-5* into pKT25, WT *B. thailandensis* boiled lysate and the primers tagCpKT25for2 and tagCcomprev were used in a PCR with Q5 polymerase which amplified an 817 bp *tagC-5* DNA fragment that included its stop codon. This DNA fragment was digested with PstI and BamHI and ligated to pKT25 that was cut with the same enzymes. The ligation reaction was used to transform *E. coli* JM83 cells which were spread on LB agar plates containing 25 μ g/ml kanamycin. Eighteen colonies were screened for the presence of the *tagC-5* gene in the pKT25 plasmid using the pKT.for.seq.RJ and pKT.rev.seq.RJ primers in a GoTaq PCR. This amplified a 198 bp DNA fragment when the empty vector was present and a 982 bp fragment when *tagC-5* was present. A colony giving rise to an amplicon of the correct size was grown overnight in LB containing 25 μ g/ml kanamycin. Plasmid DNA was extracted from the culture by miniprep and the sequencing of the insert confirmed that the 4226 bp plasmid was indeed pKT25-*tagC-5*.

To create pUT18C-*tagC-5*, the pUT18CtagCfor and tagCcomprev primers were used to amplify an 801 bp PCR product with Q5. The pUT18C plasmid and the amplicon containing *tagC-5* were digested with XbaI and BamHI and ligated together. *E. coli* JM83 cells were transformed with the ligation mixture and spread on LB agar plates containing 100 μ g/ml ampicillin. GoTaq PCRs used to screen 18 transformant colonies taken from this LB agar plate as a template with the pUTC.for.seq.RJ and pUTC.rev.seq.RJ primers which amplified a 197 bp fragment when the empty vector was present and a 978 bp fragment when *tagC-5* was cloned between the XbaI and BamHI sites. A colony which served as the template for a PCR which yielded a 978 bp product was used to inoculate an overnight culture. The plasmid DNA was harvested by the miniprep procedure and subjected to nucleotide sequencing to confirm that the correct insert was present resulting in pUT18C-*tagC-5* (3798 bp).

6.3.4 Cloning of *tagD-5* into pKT25 and pUT18C

Like TagC-5, the presence of a C-terminal FLAG epitope-tagged TagD-5 was unable to complement the defect in the activity of T6SS-5 in the *B.t tagD-5* mutant. Although this could be a consequence of poor expression of *tagD_{FLAG}* it was decided to use the pKT25 and pUT18C vectors to determine specific interactions.

A PCR product containing the *tagD-5* gene including its stop codon was amplified from a WT boiled lysate template using Q5 polymerase and the pKT25tagDfor2 and tagDcomprev primers. The resulting 313 bp DNA fragment was digested with XbaI and BamHI and ligated into pKT25 digested with the same enzymes. The ligation mixture was used to transform JM83 competent cells which were spread on LB agar plates containing 25 µg/ml kanamycin. 18 colonies were screened for the presence of pKT25-*tagD-5* using the pKT.for.seq.RJ and pKT.rev.seq.RJ primers and GoTaq polymerase in a colony PCR. This either amplified a 197 bp fragment indicating that the empty pKT25 vector was present, or a 585 bp fragment indicating that pKT25-*tagD-5* was present. A colony predicted to contain pKT25-*tagD-5* based on the PCR screen was grown overnight in LB containing 25 µg/ml kanamycin. The 3829 bp plasmid was isolated from the culture by the miniprep procedure and subjected to nucleotide sequencing to confirm the correct sequence of the insert in pKT25-*tagD-5*.

The plasmid encoding the T18-TagD fusion was created by amplifying a 313 bp DNA PCR product using the tagDpKTfor and tagDcomprev primers and Q5 polymerase. This DNA fragment was ligated into pUT18C after both were digested with Sall and BamHI. *E. coli* JM83 cells were transformed with the ligation mixture and spread on LB agar plates containing 100 µg/ml ampicillin which were grown overnight at 37°C. 18 colonies were screened for the presence of *tagD-5* using the pUTC.for.seq.RJ and pUTC.rev.seq.RJ primers and GoTaq polymerase which amplified a 197 bp PCR product when the empty vector was present and 3404 bp when pUT18C-*tagD-5* was present. A colony which harboured a plasmid giving rise to the desired amplicon was grown overnight in LB containing 100 µg/ml ampicillin whereupon the pUT18C-*tagD-5* plasmid was isolated by miniprep and confirmed by sequencing.

6.3.5 Cloning of *tssl-5* into pKT25, pKNT25, pUT18 and pUT18C

Previous work has shown that a TssI (BCAM0148) encoded by the genome of *B. cenocepacia* J2315 interacts with the *B. cenocepacia* TagA protein encoded by BCAL1295 when analysed by BACTH assay. Published research has demonstrated that the C-terminal region of TssI-5 is required for the formation of multinucleated giant cells, but not the secretion of TssD-5. This demonstrates that this region of TssI-5 is dispensable for T6SS-5 activity, but is essential for giant cell formation, indicating that it either performs the fusion, or interacts with a protein which does. Therefore, it is likely that the fusion of

T25 or T18 to the C-terminal end of TssI-5 could prevent such an interaction and would consequently show up as a false negative in the BACTH assay. Moreover, it was predicted that TagD-5 corresponded to a PAAR protein, which function by interacting with and 'sharpening' the C-terminal end of the T6SS spike protein, TssI. For this reason, the pKT25 and pUT18C vectors were used to create a fusion of the N-terminus of TssI-5 with the C-terminus of the T25 and T18 fragments, respectively.

The *tssI-5* gene was amplified from a WT boiled lysate using the pKT25-*tssI*for and pKT25-*tssI*rev primers and Q5 polymerase. The amplified 3067 bp DNA fragment was digested with XbaI and Acc65I and then ligated into pKT25 and pUT18C digested with the same enzymes. The resulting ligation reaction products were used to transform *E. coli* JM83 cells and transformants were selected on LB agar containing 25 µg/ml kanamycin and 100 µg/ml ampicillin as appropriate. After overnight incubation at 37°C, 18 individual colonies from each transformation were used as the template for a GoTaq PCR screen with the pKT.for.seq.RJ and pKT.rev.seq.RJ primers for the pKT25 clones and pUTC.for.seq.RJ and pUTC.rev.seq.RJ for the pUT18C clones. Analysis of the PCR products by agarose gel electrophoresis allowed the distinction between colonies harbouring pKT25-*tssI-5* (3236 bp) and pUT18C-*tssI-5* (3235 bp) on the one hand and the empty vectors on the other (197 bp). A colony which appeared positive from each PCR screen was grown overnight following which plasmid DNA was isolated by the miniprep procedure and the correct sequence of the *tssI-5* insert in pKT25-*tssI-5* and pUT18C-*tssI-5* was confirmed by sequencing.

In case any of the Tag proteins interact with the N-terminal domain of TssI-5, it was decided to also create plasmids that would express fusions of T25 or T18 to the C-terminus of TssI-5. The *tssI-5* gene was amplified, excluding its stop codon using the pKNT25-*tssI*for and pKNT25-*tssI*rev primers in a Q5 PCR which generated a 3053 bp product. This product was digested with XbaI and Acc65I and ligated into pKNT25 and pUT18C digested with the same enzymes. The ligation mixture was then used to transform *E. coli* JM83 cells which were spread on LB agar containing 25 µg/ml kanamycin or 100 µg/ml ampicillin as appropriate. A number of colonies (18) which had grown on each plate were used as templates for a GoTaq PCR which used the pKNT+pUT.seq.for.RJ primer in combination with the pKNT.rev.seq.RJ or pUT.seq.rev primers for screening pKNT25 and pUT18 clones, respectively. When the empty vector was present a 228 or 195 bp product was amplified for pKNT25 and pUT18, respectively, but when the colonies contained pKNT25-*tssI-5* or pUT18-*tssI-5*, a 3244 or 3211 bp fragment was amplified. Based on the size of the DNA fragment amplified, colonies predicted to contain pKNT25-*tssI-5* and pUT18-*tssI-5* were used to inoculate 4 ml of LB broth containing 25 µg/ml kanamycin or 100 µg/ml ampicillin which were grown overnight. The plasmids were purified from the overnight cultures by miniprep and the sequences of the inserts were checked by sequencing.

6.3.6 Cloning of other selected *tss* genes into two hybrid vectors

When the eluted fractions from the pull down assays were analysed by SDS-PAGE, there was a relatively prominent protein of ~60 kDa present when either Tag_AFLAG or Tag_BFLAG were used as bait that was absent from the control samples. Based on the molecular weight of the T6SS-5 proteins, this could be TssC-5 (57.3 kDa), VirA (59.6 kDa), TssA-5 (62.6 kDa) or TssF-5 (63.2 kDa) or indeed another, non-T6SS-5 protein.

6.3.6.1 Cloning *tssA* into pKT25 and pUT18C

As other work in this study was aimed at investigating the role of TssA-5, this protein was also included in the BACTH assay as a candidate interaction partner of the Tag proteins. Based on studies in *B. cenocepacia* which found that the C-terminus of the TssA protein encoded by BCAL0348 was critical for protein interactions in the BACTH assay (Ahmad, 2013), the pKT25 and pUT18C plasmids were used.

To create pKT25-*tssA*-5 and pUT18C-*tssA*-5, the pUT18C-*tssA*for and *tssA*comprev primers were used in a Q5 PCR which amplified an 1823 bp DNA fragment from a boiled lysate template. The PCR product containing the *tssA* coding sequence and stop codon, was digested with XbaI and BamHI and ligated into either pKT25 or pUT18C which had been digested with the same enzymes. The ligation mixtures were used to transform JM83 cells. Those transformed with a ligation mixture containing pKT25 were spread on LB plates containing 25 µg/ml kanamycin, while those transformed with a ligation mixture containing pUT18C were spread on LB plates containing 100 µg/ml ampicillin. To screen for pKT25-*tssA*-5 in colonies growing on plates containing kanamycin, 18 colonies were used as a template for a GoTaq PCR screen which used the pUTC.for.seq.RJ and pUTC.rev.seq.RJ primers. The presence of the empty pKT25 vector in the colony resulted in a 198 bp product when the reactions were run on a gel, while the presence of pKT25-*tssA*-5 resulted in a 2001 bp DNA fragment. Colonies predicted to contain the correct insert were grown overnight in LB containing 25 µg/ml kanamycin, plasmid DNA was isolated by miniprep and the insert in the 5425 bp plasmid sequenced to verify it as pKT25-*tssA*-5.

To screen for the presence of pUT18C-*tssA*-5, 18 colonies were picked from the ampicillin plate and used as a template for a GoTaq PCR screen which amplified a 197 bp product when pUT18C was present and a 1998 bp product when pUT18C-*tssA*-5 was present. Colonies which appeared to contain the desired construct based on the PCR screen were grown overnight in LB containing 100 µg/ml ampicillin and the plasmid DNA harvested by miniprep. The cloned DNA in a plasmid with an approximate size of 4800 bp based on agarose gel electrophoresis was subjected to DNA sequencing to confirm that it was pUT18C-*tssA*-5.

6.3.6.2 Cloning of *tssC-5* into all four two-hybrid vectors

TssC-5 was detected in all of the pull down elution samples analysed by mass spectrometry in the first repeat of the experiment (the remaining two had not been performed at this point). There was a ratio of 12.53:1 in the LFQ intensity of Tag_A^{FLAG}: TagA and 4.09 Tag_B^{FLAG}: TagB, indicating that *TssC* might be binding to these two Tag proteins. Plasmids expressing fusions of both the N- and C-terminus of *TssC-5* to the T25 and T18 *CyaA* fragments were constructed.

To clone *tssC-5* into pKT25 and pUT18C, it was amplified from a WT boiled lysate template using the pKT25*tssC*for and pKT25*tssC*rev in a Q5 PCR which generated a 1529 bp amplicon. This was digested with PstI and XbaI and ligated into pKT25 and pUT18C digested with the same enzymes. *E. coli* JM83 cells were transformed with the products of the ligation reactions and spread on LB containing 25 µg/ml kanamycin or 100 µg/ml ampicillin as appropriate before incubating at 37°C overnight. Eighteen colonies from each transformation were used as templates for a GoTaq PCR screen employing the pKT.for.seq.RJ and pKT.rev.seq.RJ primers for the pKT25 clones and the pUTC.for.seq.RJ and pUTC.rev.seq.RJ primers for the pUT18C clones. This amplified a 198 bp fragment when either empty vector was present and a 1690 or 1689 bp fragment when pKT25-*tssC-5* or pUT18C-*tssC-5* was present. A colony generating a fragment of the correct size was grown overnight and the plasmid DNA isolated by miniprep and sent for sequencing to check the 4934 bp and 4509 bp pKT25-*tssC-5* and pUT18C-*tssC* plasmids were correct.

pKNT25-*tssC-5* and pUT18-*tssC-5* were constructed by ligating the 1517 bp product amplified in a PCR using Q5 and the pKNT25*tssC*for and pKNT*tssC*rev primers into the PstI and XbaI sites of pKNT25 and pUT18, respectively. The ligation mixtures were used to transform *E. coli* JM83 cells and spread on LB agar plates containing 25 µg/ml kanamycin or 100 µg/ml ampicillin, as appropriate. Colonies growing on each of these plates were used as templates for 18 PCRs in which the pKNT+pUT.seq.for.RJ and pKNT.rev.seq.RJ primers were employed. This amplified a 228 bp product when the empty pKNT25 vector was present and a 1711 bp product when the *tssC-5* gene was inserted. Or in the case of pUT18 the pKNT+pUT.seq.for.RJ and pUT.seq.rev.RJ primers amplified a 187 bp product when the empty vector was present and a 1678 bp product when pUT18-*tssC-5* was present. A positive colony from each screen was grown overnight and the resulting 4960 and 5514 bp plasmids were harvested by the miniprep procedure. The sequence of the insert in both plasmids was confirmed by sequencing.

6.3.7 BACTH analysis of Tag protein interactions

To test interactions of the Tag proteins, compatible pairs of kanamycin resistant (pKT25 and pKNT25) and ampicillin resistant (pUT18 and pUT18C) plasmids in the combinations shown in Table 6.4 were used to co-transform *E. coli* indicator strain BTH101. As well as the plasmids which were constructed

as described above, empty vectors were also included to ensure that any interactions observed were not a consequence of inherent adenylate cyclase activity of the proteins being tested or direct interaction of the test proteins with the T25 or T18 proteins which would result in a Mal⁺ phenotype. *E. coli* BTH101 cells were also co-transformed with the pKT25-*zip* and pUT18C-*zip* plasmids. These plasmids encode fusions of a 35 amino acid leucine zipper region of the yeast transcriptional activator protein, GCN4, with the C-terminus of the T25 and T18 fragments. This leucine zipper interacts with itself, bringing the T25 and T18 fragments into close proximity to create a functional adenylate cyclase, which results in a Mal⁺ phenotype. Therefore, colonies of BTH101 cells containing pKT25-*zip* and pUT18C-*zip* act as a positive control. The transformed cells were spread on MacConkey agar plates containing 1% (w/v) maltose, 100 µg/ml ampicillin and 50 µg/ml kanamycin and incubated at 30°C. After three nights and then five nights incubation, the colour of the colonies growing on these plates was assessed to determine whether they were capable or incapable of fermenting maltose (Mal⁺ or Mal⁻, respectively) and therefore whether or not the pair of hybrid proteins present were interacting. Colonies in which proteins were not interacting (such as those containing two empty vectors) had an off-white colour, while colonies in which proteins were interacting (such as those containing pKT25-*zip* and pUT18C-*zip*) had a vivid red/purple colouration. Combinations were recorded as having a Mal⁻ phenotype (-), a weak Mal⁺ phenotype (+), a strong Mal⁺ phenotype (++) or a very strong Mal⁺ phenotype (+++). Three repeats of each plasmid combination were performed.

As shown in Table 6.4, none of the negative control combinations tested demonstrated a Mal⁺ phenotype. This indicated that the Tss and Tag proteins being tested did not interact with the T25 or T18 protein fragments and did not have endogenous adenylate cyclase activity. The Mal⁻ phenotype observed in colonies of BTH101 cells which had been co-transformed with two empty vectors also confirmed that the *E. coli* BTH101 cells were adenylate cyclase deficient. As expected, colonies containing the pKT25-*zip* and pUT18C-*zip* plasmids had a vivid red/purple colouration indicating a strong Mal⁺ phenotype (+++). This positive control confirmed that the assay gave a Mal⁺ phenotype when proteins fused to the T25 or T18 fragments were interacting. The combination of pKT25-*tssA* with pUT18C-*tssA* also gave rise to a strongly positive Mal phenotype. This was also expected as the TssA proteins of *B. cenocepacia* and *Aeromonas hydrophila* give rise to a strong Mal⁺ phenotype in this assay (Ahmad 2013).

As shown in Table 6.4, none of the Tag proteins appeared to interact with themselves or with any of the other Tag proteins as demonstrated by the Mal⁻ phenotype observed when *E. coli* BTH101 cells were transformed with the plasmids expressing the indicated combinations of Tag hybrid proteins and grown on MacConkey agar containing maltose, ampicillin and kanamycin.

Additionally, the Tag proteins did not appear to interact with TssA, TssC, or TssI according to the BACTH assay using the combinations of plasmids shown in Table 6.4. This was not a consequence of the agar plates or *E. coli* cells being inappropriate as colonies of cells containing pKT25-*zip* and pUT18C-*zip* demonstrated a strong Mal⁺ phenotype. As well as not interacting with any of the Tag proteins, TssI did not interact with itself or TssA as shown previously for *B. cenocepacia* TssI and TssA (Ahmad 2013). The only plasmid combination tested which displayed a Mal⁺ was pKT25-*tssA* and pUT18C-*tssA*. The implications of this are discussed in section 7.8.

6.4 Overexpression of the Tag proteins for structure analysis

To further investigate the role of the Tag proteins, an attempt was made to overexpress them in an *E. coli* host strain. This would potentially allow the purification of the proteins for use in investigations into their structures or in pull down experiments to determine their interactions. The 'Duet' vector system (Novagen) was utilised for this purpose. pETDuet contains a ColE1 origin of replication and confers resistance to ampicillin while pACYCDuet contains a p15A origin of replication and confers chloramphenicol resistance. These features allow the two plasmids to be introduced and maintained in the same *E. coli* cell. pETDuet and pACYCDuet each contain two multiple cloning sites with upstream T7 promoter sequences, allowing the expression of up to four genes in a single *E. coli* cell to be induced by the addition of IPTG. Although these plasmids enable proteins to be produced as histidine-tagged derivatives, here they were expressed as mutant (i.e. untagged) proteins.

6.4.1 Construction of a TagA expression vector

The *tagA-5* gene was amplified from a WT *B.t* boiled lysate template using the primers tagAMCS1for and tagAMCS1rev in a PCR with Q5 polymerase. The 2640 bp DNA product was digested with BspHI and HindIII and ligated with pETDuet-1 which had been digested with NcoI and HindIII. The ligation mixture was used to transform JM83 cells which were spread on LB agar plates containing 100 µg/ml ampicillin. After incubation at 37°C overnight, colonies which grew on this plate were screened for the presence of pETDuet-*tagA-5*. This screen was performed using the colonies as templates for PCRs which used GoTaq and the vector-specific primers pETDuet-T7-1for and pACYCDuet-T7-1rev to amplify a 271 bp DNA fragment when they contained empty pETDuet and a 2823 bp DNA fragment when they contained pETDuet-*tagA*. Colonies that appeared to contain the correct sized insert according to the screen were grown overnight in LB containing 100 µg/ml. Plasmid DNA was harvested from these cultures by the miniprep procedure and analysed by agarose gel electrophoresis. Plasmid DNA that migrated in an agarose gel at around the expected size of 7972 bp was analysed by nucleotide sequencing to confirm that *tagA* was cloned into the first multiple cloning site (MCS-1) of pETDuet.

6.4.2 Construction of a TagB expression vector and a TagA and TagB dual expression vector

To clone the *tagB-5* gene into the second multiple cloning site (MCS-2) of pETDuet, a PCR was performed using Q5 polymerase and the primers tagBMCS2for and tagBMCS2rev to amplify a 1130 bp DNA fragment which was digested with NdeI and BamHI. This DNA fragment was ligated into pETDuet digested with NdeI and BglII and the products of this ligation were used to transform *E. coli* JM83 cells which were spread on an LB agar plate containing 100 µg/ml ampicillin and incubated at 37°C overnight. Colonies growing on this plate were used as templates for a GoTaq PCR using the pACYC-T7-2for and T7rev primers which amplified a 278 bp product when the empty vector was present and a 1386 bp product when pETDuet-*tagB-5* was present. Plasmids were purified from colonies which gave rise to an amplicon of the expected size and analysed by agarose gel electrophoresis. The cloned DNA in plasmids of the predicted size of pETDuet-*tagB* (6528 bp) was analysed by nucleotide sequencing. To create pETDuet containing *tagA* cloned into MCS-1 and *tagB* cloned into MCS-2 (pETDuet-*tagAB*), the same procedure was used for the construction of pETDuet-*tagB* but instead of using pETDuet as the target vector, pETDuet-*tagA* was used. The pETDuet-*tagAB* plasmid was 9079 bp in size.

6.4.3 Construction of a TagC expression vector

The primers tagCMCS1for and tagCcomprev were used in a Q5 PCR to amplify an 801 bp DNA fragment from a WT *B.t* boiled lysate template. This PCR product and pACYCDuet were digested with NcoI and BamHI and ligated together. The ligation mixture was used to transform JM83 cells which were spread on an LB agar plate containing 25 µg/ml chloramphenicol. After overnight incubation at 37°C, transformant colonies were used as a template for a GoTaq PCR which employed the pACYC-T7-1for and pACYC-T7-1rev primers to screen for the presence of pACYCDuet-*tagC*. When the empty vector was present in the colonies, a 225 bp product was amplified compared to a 1034 bp product when *tagC* was cloned into MCS-1. Colonies likely to contain a plasmid with the desired insert were grown overnight in LB containing 25 µg/ml chloramphenicol before plasmid DNA was harvested by the miniprep method. A plasmid sample that ran at the correct size (4774 bp) when analysed by agarose gel electrophoresis was checked by nucleotide sequencing.

6.4.4 Construction of a TagD expression vector and a TagC and TagD dual expression vector

The *tagD* gene was cloned into MCS-2 of pACYCDuet. The primers tagDMCS2for2 and tagDcomprev were used in a PCR with Q5 polymerase and a WT *B.t* boiled lysate template to amplify a 412 bp product. This was digested with NdeI and BamHI and ligated into pACYCDuet digested with NdeI and BglII. The ligation mixture was used to transform *E. coli* JM83 cells which were spread on LB agar plates containing 25 µg/ml chloramphenicol and grown at 37°C overnight. Colonies growing on this plate

were screened by a GoTaq PCR which used the primers pACYC-T7-2for and T7rev to amplify a 278 bp DNA fragment when the empty vector was present and a 635 bp fragment when the *tagD* gene was present in MCS-2. Plasmid DNA was prepared from colonies giving rise to a correct sized amplicon in the PCR screen and electrophoresed to identify a plasmid of roughly the correct size (4398 bp). The insert sequence was confirmed by nucleotide sequencing. The *tagD* gene was also cloned into MCS-2 of pACYCDuet-*tagC* in an analogous fashion to create pACYCDuet-*tagCD*.

6.4.5 Induction of Tag protein production

The plasmid constructs described in sections 6.4.1 to 6.4.4 were used to transform *E. coli* BL21(λDE3) cells. Individual colonies of BL21(λDE3) harbouring pETDuet, pETDuet-*tagA*, pETDuet-*tagB*, pETDuet-*tagAB*, pACYCDuet, pACYCDuet-*tagC*, pACYCDuet-*tagD* and pACYCDuet-*tagCD* were used to inoculate 4 ml of BHI broth containing the appropriate antibiotic and cultures were grown overnight at 37°C with aeration. Overnight cultures were used to inoculate 8 ml of BHI broth to an OD₆₀₀ of 0.05 and grown at 37°C with aeration until the cultures reached an OD₆₀₀ of 0.4-0.6, at which point 4 ml of the culture was transferred to a new culture vessel and expression of proteins was induced by the addition 1 mM IPTG. Induction was continued for a further 3 hours at which point the OD₆₀₀ of the cultures was determined and a volume of culture equivalent to 1 ml OD₆₀₀ 1.0 was transferred to a microcentrifuge tube which was centrifuged at 13,000 x g for 1 minute. The supernatant was discarded and the cell pellet was resuspended in 100 µl Laemmli buffer and boiled for 10 minutes, following which the cell lysates were electrophoresed in a polyacrylamide gel and stained with Coomassie blue to visualise protein bands.

As shown in Figure 6.11 A, the addition of IPTG to cultures of BL21(λDE3) cells harbouring pETDuet-*tagA* resulted in the expression of a protein at approximately the same molecular weight as TagA (91.2 kDa) that was not observed in the non-induced samples, or those containing the empty vector. The addition of IPTG also resulted in the presence of an additional band in the samples prepared from cells harbouring pETDuet-*tagB* compared to those prepared from samples where no IPTG was added. However, the induced protein was much smaller than the 37.6 kDa expected for TagB. This could be a TagB degradation product. Unfortunately, as it was not tagged it was not possible to verify this by western blotting. When BL21(λDE3) cells containing pETDuet-*tagAB* a relatively low abundance protein was observed migrating with an estimated molecular weight similar to that of TagA, but no protein similar in size to TagB was present. A protein likely to be TagC (27.9 kDa) was visible in samples prepared from the IPTG-induced culture of BL21(λDE3) harbouring pETDuet-*tagC*, but not in the sample prepared from the uninduced culture or from induced samples prepared from cultures of cells

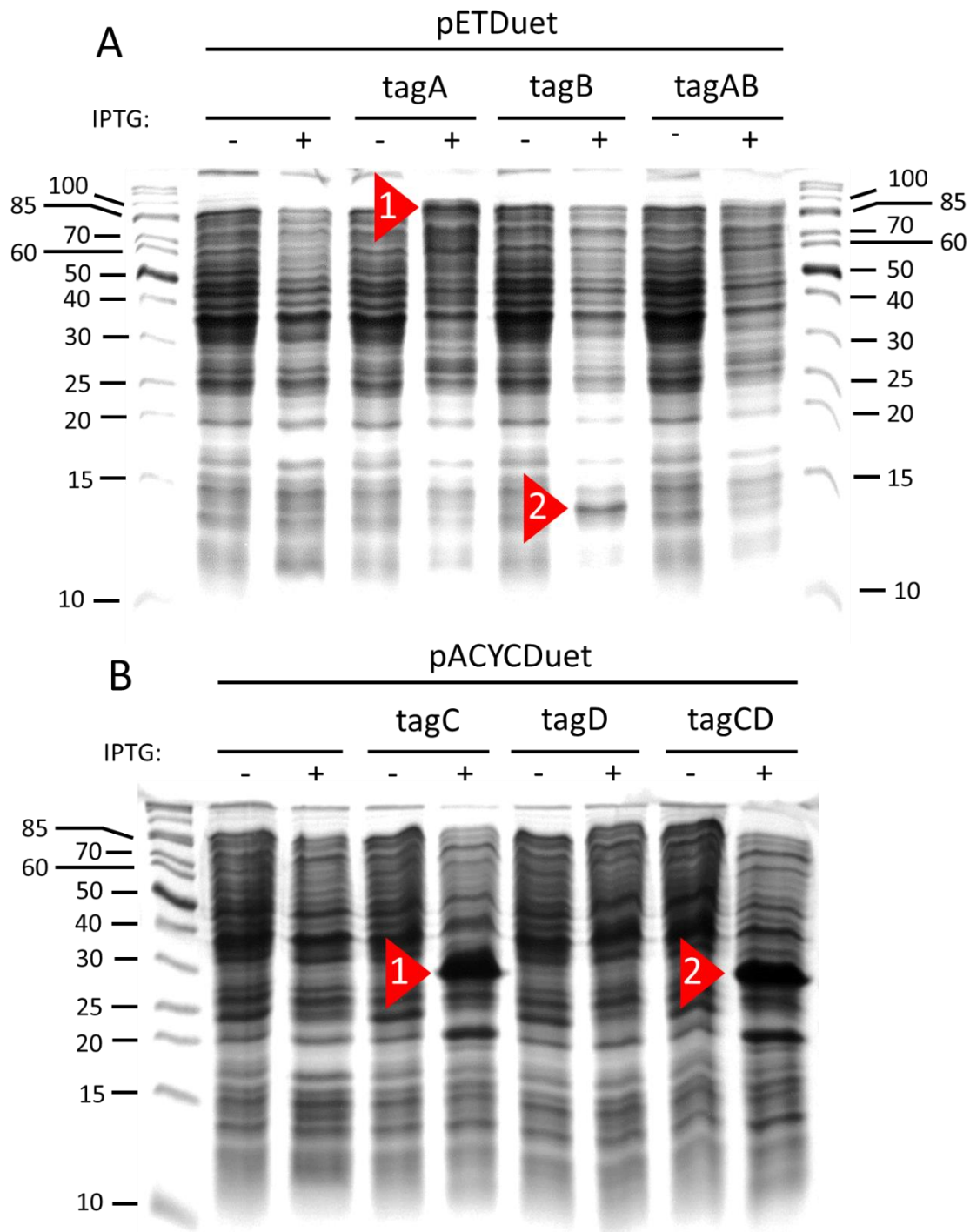


Figure 6.11 IPTG induction of BL21(λDE3) cells harbouring the tag expression vectors

SDS-PAGE analysis of samples prepared from cultures of *E. coli* BL21(λDE3) cells harbouring pETDuet (A) or pACYCDuet (B) plasmids containing the indicated genes. Cultures were incubated at 37°C and either uninduced (-) or induced by the addition of 1 mM IPTG (+) for 3 hours. A) tagA, *E. coli* BL21(λDE3) containing pETDuet-tagA; tagB, *E. coli* BL21(λDE3) containing pETDuet-tagB; tagAB, *E. coli* BL21(λDE3) containing pETDuet-tagAB; red arrows 1, protein at the expected MW of TagA (91.2 kDa); 2, protein of 13-14 kDa, possibly corresponding to TagB degradation product. B) tagC, *E. coli* BL21(λDE3) containing pACYCDuet-tagC; tagD, *E. coli* BL21(λDE3) containing pACYCDuet-tagD; tagCD, *E. coli* BL21(λDE3) containing pACYCDuet-tagCD; red arrows 1 and 2, proteins migrating at the expected MW of TagC (27.9 kDa). Gels stained with Coomassie blue. Protein markers displayed in kDa.

harbouring the empty pACYCDuet vector (Figure 6.11 B). In contrast, a protein corresponding to TagD (13.1 kDa) was not observed in the samples prepared from an induced culture of BL21(λ DE3) harbouring the pACYCDuet-*tagD* plasmid (Figure 6.11 B). In samples prepared from cultures of BL21(λ DE3) containing pACYCDuet-*tagCD*, the only protein present in the induced sample compared to the non-induced sample was the one corresponding in size with TagC.

6.4.6 Analysis of TagA and TagC solubility

The only plasmids which expressed proteins of the expected size when they were delivered into BL21(λ DE3) cells and induced with IPTG were pETDuet-*tagA* and pACYCDuet-*tagC*. Biochemical and structural analysis of these proteins would be possible if they were soluble. Therefore, to test this cultures of BL21(λ DE3) containing pETDuet-*tagA* or pACYCDuet-*tagC* were grown overnight in BHI containing 100 μ g/ml ampicillin or 25 μ g/ml chloramphenicol, respectively. The overnight cultures were each used to inoculate two 50 ml cultures of BHI containing the appropriate antibiotic to an OD₆₀₀ of 0.05. These cultures were grown in a shaking incubator at 37°C until the OD₆₀₀ reached 0.5-0.7 whereupon IPTG was added to a final concentration of 1 mM to one of the 50 ml cultures to induce expression of the plasmid borne genes. After 3 hours induction cells were collected by centrifugation at 3,900 x g for 20 minutes and the supernatant was discarded. The weight of the resulting pellet was determined before it was gently resuspended in a volume of BugBuster (Novagen) equivalent to 5 ml per g of pellet. The cell suspension was incubated on a shaker at room temperature for 20 minutes and transferred to a microcentrifuge tube which was centrifuged at 16,000 x g to remove insoluble cell debris. Samples of the cleared lysates were mixed 1:1 with 2 x Laemmli buffer prior to analysis by polyacrylamide gel electrophoresis. The gel was stained with Coomassie blue to visualise protein bands.

As shown in Figure 6.12 A, a low abundance protein corresponding in size to TagA (91.2 kDa), was present in the crude lysate prepared from an induced culture of BL21(λ DE3) containing pETDuet-*tagA*. However, when the insoluble material was removed by centrifugation, TagA was not present in the soluble fraction. This suggests that the TagA protein is insoluble when expressed under these conditions. A more abundant protein at the size of TagC (27.9 kDa) was present in the induced crude lysate sample. However, this protein also proved to be insoluble as there was no protein visible corresponding to TagC in the sample prepared from the soluble lysate.

Although interaction between the Tag proteins were not detected by two-hybrid assay, it might be possible that all four of them are required for formation of a complex that would enhance their stability and solubility. To investigate whether this is the case, *E. coli* BL21(λ DE3) cells were co-

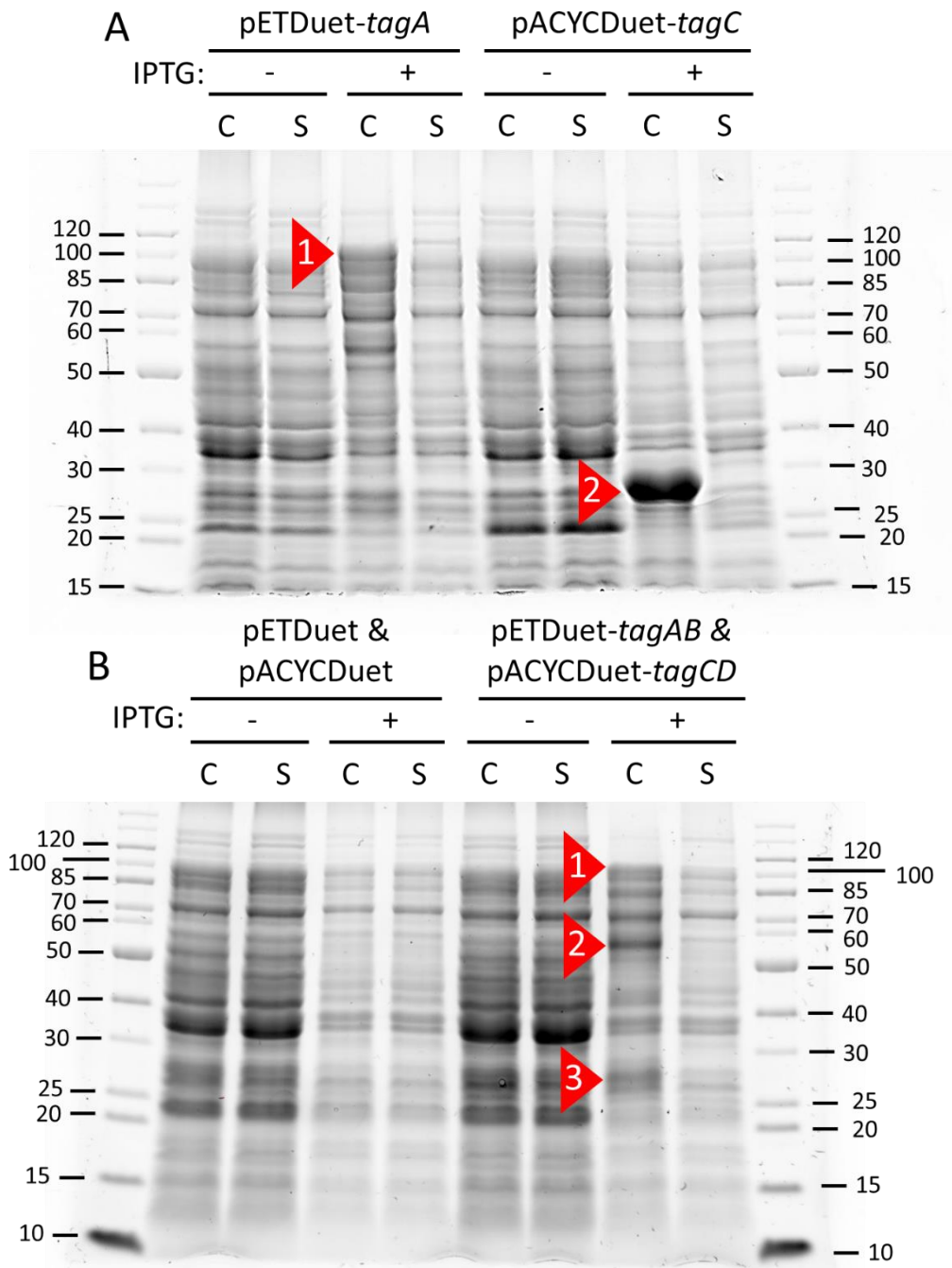


Figure 6.12 TagA and TagC solubility test

SDS-PAGE analysis of crude (C) and soluble (S) cell lysate prepared from cultures of *E. coli* BL21(λ DE3) cells harbouring the indicated plasmid(s). Cells containing the plasmids were grown at 37°C to logarithmic phase before inducing with IPTG (+) or allowing growth to continue in the absence of IPTG (-) for a further three hours. A) pETDuet-*tagA*, *E. coli* BL21(λ DE3) containing pETDuet-*tagA*; pACYCDuet-*tagC*, *E. coli* BL21(λ DE3) containing pACYCDuet-*tagC*; arrowhead 1, protein at the expected MW of TagA (91.2 kDa); arrowhead 2, protein at the expected MW of TagC (27.9 kDa). B) pETDuet & pACYCDuet, *E. coli* BL21(λ DE3) containing both pETDuet and pACYCDuet; pETDuet-*tagAB* & pACYCDuet-*tagCD*, *E. coli* BL21(λ DE3) containing pETDuet-*tagAB* and pACYCDuet-*tagCD*; arrowhead 1, protein at the expected MW of TagA (91.2 kDa); arrowhead 2, unexpected protein at ~58 kDa; arrowhead 3 protein at the expected MW of TagC (27.9 kDa). Gels were stained with Coomassie blue. Protein markers displayed in kDa.

transformed with pETDuet-*tagAB* and pACYCDuet-*tagCD* and spread on LB agar plates containing 100 µg/ml ampicillin and 25 µg/ml.

An individual colony of BL21(λDE3) containing pETDuet-*tagAB* and pACYCDuet-*tagCD* were used to inoculate 4 ml of BHI containing 100 µg/ml ampicillin and 25 µg/ml chloramphenicol and grown overnight at 37°C. The overnight culture was used to inoculate two flasks, each containing 50 ml of BHI containing 100 µg/ml ampicillin and 25 µg/ml chloramphenicol to a starting OD₆₀₀ of 0.05. One of the cultures was induced by the addition of 1 mM IPTG for three hours before the solubility test was performed. The same procedure was used to analyse BL21(λDE3) cells containing the pair of empty pETDuet and pACYCDuet plasmids.

As shown in Figure 6.12 B, a low abundance protein migrating at the size of TagA was present as well as one corresponding in size to TagC in the crude lysates of induced samples prepared from cultures of BL21(λDE3) containing pETDuet-*tagAB* and pACYCDuet-*tagCD* which were absent from samples prepared from BL21(λDE3) cells harbouring the empty vectors. There was also a protein present at ~58 kDa that was absent from the non-induced sample, and the samples prepared from BL21(λDE3) cells harbouring the empty vectors. It is unclear what this protein is, as it does not correspond to the predicted molecular weight of either of the remaining Tag proteins; TagB is predicted to be 37.6 kDa, while TagD is 13.1 kDa. None of the proteins induced by the addition of IPTG were soluble demonstrating that TagA and TagC were not soluble even when the other Tag proteins encoded by the T6SS-5 gene cluster were present.

6.5 Discussion

The addition of the relatively small FLAG epitope tag (1 kDa) at the C-terminal end of TagA and TagB did not have an observable effect on MNGC formation or T6SS-5 activity, suggesting they behaved in the same way as their native counterparts. Therefore, it was decided that TagA_{FLAG} and TagB_{FLAG} were suitable bait proteins for co-immunoprecipitations using the anti-FLAG antibody. This identified a number of potential TagA-5 interaction partners, although many were chaperones and unlikely to be specific to TagA-5, the T6SS-5 proteins TssF-5 and TssI-5 were enriched. TssI-5 was also enriched in the TagB_{FLAG} pull down, although not to a statistically significant level. Despite these observations, TssI-5 did not appear to interact with TagA-5 or TagB-5 in the BACTH assays.

The *tagA* and *tagB* genes were cloned into the pKNT25 and pUT18 vectors because the addition of the small C-terminal FLAG epitope did not have a detrimental effect on the TagA and TagB proteins. However, the introduction of the much larger T25 (21.2 kDa) and T18 (19.2 kDa) fragments to the C-terminus of these proteins is more likely to exert an effect on the ability of the protein to interact with other proteins or on the ability of the protein to correctly fold. It is also possible that the hybrid

proteins are insoluble when produced in the absence of other T6SS components, as TagA was observed to be insoluble when overexpressed in *E. coli* or not expressed/degraded (TagB could not be detected when its expression was induced in *E. coli* BL21(λ DE3) cells).

The decision to clone *tagC* and *tagD* into the pKT25 and pUT18C vectors (which would express TagC and TagD fused at their N-termini to the T25 and T18 fragments) was made based on the observation that the introduction of a FLAG epitope tag to the C-terminus of TagC and TagD had a detrimental effect on their function as determined by MNGC formation and T6SS-5 activity assays. Bioinformatic analysis of TagC proteins indicates that a C-terminal glycine residue is almost absolutely conserved (section 3.5.4), the FLAG epitope is probably interfering with whatever role it plays. Similarly, the C-terminal residues of TagD are predicted to facilitate interaction with TssI-5 (section 3.6.5). It is possible that the fusion of the large T25 and T18 fragments to the N-termini of these proteins had an impact on the activity of TagC and TagD. TagD in particular has a MW of 13.1 kDa, which is smaller than the T25 and T18 fragments. Of the Tag proteins, TagC was overproduced the most efficiently in *E. coli* BL21(λ DE3) cells, but was insoluble. Therefore, it is possible that the T25-TagC and T18-TagC fusion proteins are insoluble in *E. coli* cells which could prevent interactions from occurring. It is also possible that the T25-TagD and T18-TagD are not expressed, as TagD did not appear to be expressed in *E. coli* BL21(λ DE3) cells.

TssI proteins from a number of species have been shown to self-interact to form a homotrimeric structure (Pukatzi et al. 2007, Leiman et al. 2009) and previous work in the Thomas group has also demonstrated an interaction between *B. cenocepacia* TssI and itself in BACTH assays (Ahmad 2013). Therefore, it is surprising that *B.t* TssI-5 did not give rise to a positive result in any of the two-hybrid combinations tested. As with the Tag proteins, it is possible that these particular TssI fusion proteins are not expressed or are insoluble in *E. coli*.

It would be useful to include more T6SS proteins that are known to interact with TssA, TssC and TssI to act as positive controls to ensure that the proteins tested in this work were interacting as expected. For example, it would be useful to have constructs expressing fusions of the T25 and T18 fragments with TssB, which has previously been shown to interact with TssC, to check the TssC functionality of the fusions. This would also increase the repertoire of potential interaction partners that could be investigated.

As there is uncertainty over whether or not a number of the fusion proteins are expressed, it would be useful to check if they were present in *E. coli* BTH101 cells. This could be done by culturing *E. coli* BTH101 cells harbouring the BACTH plasmids containing the *tag* genes and analysing whole cell lysates by SDS-PAGE. Western blot analysis of these lysates using antibodies raised against the T25 and T18

fragments of *Bordetella pertussis* CyaA would then demonstrate whether or not the fusion proteins were expressed based on the presence or absence of proteins of the appropriate sizes. There was insufficient time to perform these checks.

A protein corresponding in size to TagA was specifically produced in *E. coli* cells containing pETDuet-*tagA* (and pETDuet-*tagAB*), although it was not present in large amounts. However, this protein was insoluble. In contrast, TagA_{FLAG} was shown to be soluble when cultures of *B.t* containing pBBR1MCS-*tagA*_{FLAG} were lysed by sonication to be used in co-immunoprecipitation studies. There are a number of explanations for this discrepancy, it is possible that presence of the C-terminal FLAG epitope in TagA_{FLAG} aids in solubility, although this is unlikely as *tagA*_{FLAG} complements the *B.t* Δ *tagA* mutant to the same extent as *tagA*. There is also a chance that there are other proteins present in *B.t* that increase the solubility of TagA that are absent from *E. coli* BL21(λ DE3), although the expression of the other *tag* genes alongside *tagA* did not increase its solubility. It is also possible that the lysis of *E. coli* cells using BugBuster was not as effective as the sonication method used for lysing *B.t* cells.

There was a high level of expression of TagC in *E. coli* BTH101 cells containing pACYCDuet-*tagC*, however TagC was still not detectable in the soluble fraction of the cell lysate indicating that, like TagA, TagC is insoluble in *E. coli*. Given that *B.t* TagC was predicted to contain a lipoprotein signal peptide (although TagC proteins are not thought to be lipoproteins in general, see section 3.5.3) it is possible that TagC is exported to the periplasm and embedded in the inner or outer membrane in *E. coli* and would therefore be insoluble in these experiments. The expression of TagD or TagA, TagB and TagD alongside TagC did not increase its solubility. It would be useful to attempt to purify these proteins using the inclusion body method which would use the insolubility of TagA and TagC as an advantage, however the proteins would have to be re-solubilised after purification. It may also be worthwhile modifying the induction conditions to achieve production of the TagB and TagD proteins. For example, lowering the temperature the cultures were grown at or changing the IPTG concentration. These approaches might also render the TagA and TagC proteins soluble. It would also have been useful to engineer the proteins to contain an affinity tag (for example hexa-Histidine or Strep-tag) to facilitate their purification and make any interactions easier to detect.

Chapter 7 Investigation into the *tssA-5*
gene of *B. thailandensis*

7.1 Introduction

One of the observations in Schell et al. (2007) was that *tssA-5* (BMAA0747) of *B. mallei* was not required for T6SS-5 activity. The authors of the study predicted that *tssA-5* was a component of the *Burkholderia* Intracellular Motility (BIM) gene cluster located adjacent to the T6SS-5 gene cluster and therefore designated it *bimE*. The *bimE* mutant was constructed by transposon insertion which prevented actin tail formation in macrophage-like J774.2 cells, but did not attenuate the strain during a Syrian hamster model of infection. This observation is consistent with the loss of actin tail motility, but full virulence observed when hamsters are infected with *B.m bimA*, *bimB* and *bimC* mutants. This result is surprising given that the orthologues of *bimE* in *B.p* and *B.t* are considered to encode core components of T6SS-5. Bioinformatic analysis of BimE indicates that it belongs to protein family (Pfam) 06812. Another protein belonging to this Pfam is *Edwardsiella tarda* EvpK (TssA), the *E. tarda evpK* mutant is T6SS-5 deficient. An alignment of BimE with selected proteins belonging to pfam06812 is shown in Figure 7.1.

Therefore, it was decided to determine whether *tssA-5* (BTH_II0873) was required for MNGC formation and T6SS-5 activity in *B. thailandensis* by constructing a *tssA-5* mutant. As the previous experiments in this study in which markerless in-frame deletions were introduced into genes to generate mutants did not result in undesired polar effects (for example, as demonstrated by restoration of T6SS-5 activity to the *tssA-5* mutant when the wild type gene was reintroduced *in trans*), this technique was used for the deletion of *tssA-5*.

7.2 Construction of a *B. thailandensis tssA-5* mutant

The procedure outlined in further detail in section 4.2.2 was used to delete *tssA-5*. The primers *tssASOEfor2* and *tssASOEmidrev* were used in a Q5 polymerase PCR with a WT *B.t* boiled lysate template to amplify a 551 bp fragment containing the final 464 bp of *virG* and the first 69 bp of *tssA*. A second PCR was performed using *tssASOEREv2* and *tssASOEmidfor* to amplify a 517 bp fragment containing the final 57 bp of *tssA-5* and the final 142 bp of BTH_II0874 (this gene is transcribed in the opposite orientation to *tssA*). The resulting DNA fragments were gel extracted and mixed. This mixture was then used as a template for a third PCR which used the primers *tssASOEfor2* and *tssASOEREv2* to amplify a 1032 bp DNA fragment. This PCR product and the pEX18Tp-*pheS* plasmid were both digested with KpnI and BamHI before ligating them together. *E. coli* JM83 cells were transformed with this ligation mixture and spread on M9 agar plates containing 25 µg/ml trimethoprim, 1% (w/v) casamino acids, 0.5% (v/v) glycerol, 0.0005% (w/v) thiamine, 40 µg/ml X-gal and 0.1 µg/ml IPTG. This plate was incubated at 30°C for two nights. White colonies growing on this plate were grown overnight in IST

EtTssA 1 MGTLPNLIAACQVDEVQLRQQAQALTESWHPWLA-----PVSDSRPTGHDPGYDDD
 AhTssA 1 -----MSYQ-----HPWCARLIT-----SLPDEQIRGAVLADEPR
 BmTssA-5 1 -----MSERRPPGGAARARMPLDQALAVLGRTDIDSAMPAGADVRRADAR
 BtTssA-5 1 -----MGMNERRQPGGAASGALLPELFDALGALGRADIDPAAAPAGADVRRADAR
 YpTssA 1 -----MILKRMDNNM-----SDIFPQAL--FGVEYDPA
 AfTssA 1 -----MDTQHV-----KRDIEFLGNCGNIRNDSR
 BcTssA 1 -----MPINLPEL-----LTFISEASPSGDDLLFSNE
 BtTssA-1 1 -----M-----LTFISEASPCGDDLLFSAE
 PaTssA 1 -----MLDVPVL-----LAAVSPDSPCGDDLEYDAA
 BbTssA 1 -----MPRMTTMEFADL-----LKTLPSPSPCGDDLEYDAD

EtTssA 52 FQRITREEDRIS-----GWDTGLICQLAERLLTRTAQDIRVATYYCW
 AhTssA 31 WDYVETEIVKLGSL-----LA-HSQVDLNAVAEACLGLESRIKDMRVLAQLLR
 BmTssA-5 47 FDALHAELAKLAS-----PGASGQVDWRAATHLAELLRERKGDLLVGCYLAG
 BtTssA-5 49 FDALHAELAKLAS-----PGASGHVDWRAAMSLAAGLLRDRGKDLLVGCYLAG
 YpTssA 27 YGETESIISQLDESADPLSR-----PHEPPQINWHHISEQANKL-LEQCFDLRVMLWFIR
 AfTssA 26 TREIYYRKDERNQARAEEAASPODNLKISSWDSVSNLCLQIYSESKDMEHLAWLAE
 BcTssA 28 FDAIQDARR----YDDPTLD-QGEWVTEIKEADWGFVVDHAGELLRTRTKDLRLAVWLTE
 BtTssA-1 21 FDAIQHARK----FDDPSLD-QGEWITDIKEADWGFVVEQSSTLRERTKDLRLAVWLTE
 PaTssA 27 FLELERIAQ----GQPERQ-MGDAVLPAPPEWPRVRALESEL-FGRSKDLRVANLLQ
 BbTssA 33 ELQIQAAV-----GRSEQQ-FGATIIIPAQAFDWRRAVERLALGL-LERTRDLRIAYLTR

EtTssA 94 ARIHRDGEAGFAEGLALLAGLLQRYGAQLHPQR--ERS---RKSALWLAGP-----
 AhTssA 78 CLQHPAKATEFGAAISLEAWIQAYWLLAWPGNASQKQ--R-----LMVQVVKRFEG--
 BmTssA-5 95 ALLQQTGGAAGLRGGLVGVGLMERHWDAMSEPPVSRMRA---RRGALQWLVRVDAMHD--
 BtTssA-5 97 ALLQIGGAAGLRGGLVGVGLMERHWAAMSEPPVSRMRA---RRGALQWLDRVDATRD--
 YpTssA 81 ANIHIKGTSLYDGFMRINLQTDQTDVVIYQSEEPPLNSGHAAALGWLSTA---QCIA
 AfTssA 86 ASLRIRGFHGLREIYELCGLDFYNHWDSLRSISDDNDEEK--FAPFAGLNGIGSEGTLVQ
 BcTssA 83 ALALEDGVTGLTEGYALTECLREFWDTFPLPEDDDIEH-RLGNVAWLSGRTAELLR--
 BtTssA-1 76 ALALEDGVTGLTQGYELTNLCRFQWDHVEPLPDGDDAEY-RLGNVAWLAGRTVALLR--
 PaTssA 80 SNVALDGDGLADGILLVRELLGQYWDGYPLLDADDDND-PTFRINALTGLVAEPLQL
 BbTssA 86 AWTEMRGLPGYAEVTLAAGTLEQYWDVAHPMLASGGED-PMPRVNALASLGDPQGCVR

EtTssA 141 ---RVLDGLSRW-PEV-VR--DEALRTVGVLL---LIRDSLEA--EPEASREPSALY--
 AhTssA 128 ALPRICESASAA--EL-AQLLAQAQELERVWL---AQCPD-----K-----
 BmTssA-5 150 AGAAACGGACSA--EL-VAQLRAAARRIDALL---AERDD-----DAEPTMRAVH--
 BtTssA-5 152 AGAAACGACSV--EL-VEQLRAAARRIDALL---AERDD-----EAETMRAVTV--
 YpTssA 137 ELKTRARLTFEHPYI---IQDLIT-----TEALPNCQ---ERYFVT
 AfTssA 144 PIRLASLIPGKFGESLWDFQLAQRPNESKR-----R-----EELYRI
 BcTssA 140 AVPLTDG-ASNAFSTL---DWEVAQHVAQSTK----RDPEHA-DDIARGRPSTEQIDAS
 BtTssA-1 133 AVPLTDG-ASNAFSEL---DWDVAQHVAQATR----RDPEQA-NEIARGRPSTEQIEAS
 PaTssA 139 VWAIPLV-RSRAFGPV---NLRAALNAAGLQRFASSETLSPEQIAGAFADAD--ADALAAT
 BbTssA 145 GMRSAACL-LDDVHGRL---SLRDAEAL-----LDGGRSEADYPGER--TRLIENL

EtTssA 187 -----RA---LESRLMKAGG-----
 AhTssA 163 -----GELLDPLVM-LKRAQRQQL
 BmTssA-5 193 -----AFAERLPVEVVEVVEVADEADVAEAAEAALAA
 BtTssA-5 195 -----AFAARLPVESGESGEPGEPGEPGE-----
 YpTssA 171 SSTLFLTVNNYFQONGLPDKDQLTKVDMLEQIESYANQS-----TESYQLH---CEQ
 AfTssA 183 ASE--AGVA--AMSSHLAAVNTCLSSFDAITAVLSERCGQA---PPSSNIRNTLIBAA
 BcTssA 190 RRV--TSIA--FYTALLANLKAFEFALDAFEERLIVERAGDS-----APSFQRADFETV
 BtTssA-1 183 KRM--TPVA--FYARLLGELKTFQAALDAEQELDQRAGDA-----APSFQRADAYETV
 PaTssA 193 RRA--LDGA--QEHAL-----AESGVAERVGSAQ---GLDLGSPRLRQLLRQA
 BbTssA 189 RQA--RLRR--DDAAL--AVGAAAGALRRVQQQATQRLGSAW-----CPDYAQLRALDAL

EtTssA 199 -----VDAVVPQNA-----HQAPPEP--L-----
 AhTssA 182 -----AQAEANAACQPQSSG-----AAAASFPASVASTA---
 BmTssA-5 225 EAAEAAEAAEAAEAAEAAEAAEAAEADVDVADVAETAADAHGSTGCPAAEIAIAAE
 BtTssA-5 219 -----PGEPEGESNSTHAHGSVCAAPAERAALSFAE
 YpTssA 222 -----LRIFLKNNISQ-----LAQLNAPE
 AfTssA 235 -----AARTLGRDQ-----EPAPVEQTPAJA
 BcTssA 241 -----YRLAERFAREQ-----GYTCSAPHTQ---AVQ
 BtTssA-1 234 -----YRLAERFAKEQ-----GYSIDAQPRGVAPNAQ
 PaTssA 233 -----LQVFDLYG-PQ-----GAGESIAPGAEAVADE
 BbTssA 239 -----LRTWSDLD-ET-----AAAPAAAMPAEA

EtTssA 218 -----HTAEP-----D---AP---RLS---RITSGQDLIAQARTLAELYLR
 AhTssA 211 --SCAGAMVLSGSAGVDVDS--SS-----NDRAWRQT--Q-LKVAELLI
 BmTssA-5 285 QALIDPAGRAAPSAGTDTNANAD---AARQPARDLDEAACRDRALADALQOLHCVATAFA
 BtTssA-5 251 HASIEPAGRAAPRA-----NAD---AARHPASLDDAACRERALADALQOLHRIATAFA
 YpTssA 241 HDDP---E---TVY-QKIDSHES-----LDTQSFNSNDKSIKRSRQELIMMLDRILEYFQ
 AfTssA 258 A-----GTDESGQ-----SAARTSPASPEGISSRDLAFETILLSVARYFR
 BcTssA 265 QAQP---ERIEPVFGQPIQTEETHVQQQTASRPPVTQTIAAGIQNRAQAVDQLRAVARYFR
 BtTssA-1 261 DASR---ERAEPFRTPHSEEPVQRHAHAPSAPAPIVIAAGIQNRAQAVQOLRAVARYFR
 PaTssA 259 Q-----VGAAPVAAVAAPAPRASGEIANREDVLRQLDRILEYLV
 BbTssA 261 H-----HAAPAPEPQPAPASWHDARIATREDALAMLAKVSAEYF

EtTssA 249 EQPAGWLAHRLMKSRLRHDTLISA-----IPAPDAE-GKTRIEPPRADQRAMLKRLYLQ
 AhTssA 247 ERQPEVAVGYRLRRHAWAGITA-----VPMSGAGNKT-PLAPMSADMVDEYRAMNA
 BmTssA-5 341 QADWADARGFRLRRVACWSSVCA-----LPETDAENGRTRIAAPSASIVGAAKNIDED
 BtTssA-5 301 QADWADTRGFRLLRRIACWSSVHA-----MPDTEADSGRTRIAAPNAQVVDVAKGIDAQ
 YpTssA 288 HYEPSHEPAPIFIRRTKEMIGMDFYSIVVEEILPEAVI--TL-----KQFTGKT--
 AfTssA 297 RTEPHSPISLSIETLVRRGRMDFSELIAELLPEIQARNV-----LTAAGIK--
 BcTssA 322 QTEPHSPVAYLADKAEWADMPHLKWEVSVVKDDGSLSHI-----RELLGVR--
 BtTssA-1 318 GTEPHSPVAYLADKAEWADMPHLQWLASVVKDDGSLAHI-----RELLGK--
 PaTssA 298 RHEPSSPMPVLLKRAKTLVTADFAEIVRNLIIPDGI--SQF-----ETLRGPE--
 BbTssA 300 THEPSHEPAPYLIRRVQQLIPIIDFHDIRNLIAPQGL--AQF-----EAWTARE--

EtTssA 301 QSWPEMLAQVDSTFSGRANHLWLDLQWYTHQALVKSGQEV--LAEIITADLKGLLRRLSG
 AhTssA 299 PD--QGLWQ-RIEQSLTLAPYWFEGHRLSAEVAEKLGFGA--VAQAI AEELGTFLQRLPA
 BmTssA-5 394 GE-PVAAVR-FAEHAQAFFPLWLDLQRIAARALARAGGDGADARREVETAVRALLARLPG
 BtTssA-5 354 GD-PAAAVR-FAEEHAQAFFPLWLDLQRIAARALARAGGDCTGAQREVETAVRALLMRLPG
 YpTssA 333 -----
 AfTssA 344 -----
 BcTssA 369 -----
 BtTssA-1 365 -----
 PaTssA 343 -----
 BbTssA 345 -----

EtTssA 359 LETLAFNDGTPFADEITLNWINQSVLDGISGWREAPVSAVSETDNDILALEPEA-----
 AhTssA 354 LRELAFSDGSPFLSPECSRWLQPAKGG-SAGIGEA-----GL-----
 BmTssA-5 452 LDALTFADGTPFADDATRAWLGELGAP-VVAADAV-----SPSSLPLSPRPSPPERS
 BtTssA-5 412 LDALKEFADGTPFADAATRAWLAELCTP-IGAANAA-----LTSPPPPSPAPS
 YpTssA 333 --NLPER-----
 AfTssA 344 --PGDNNCK-----
 BcTssA 369 --PDEQS-----
 BtTssA-1 365 --PDDNA-----
 PaTssA 343 --SE-----
 BbTssA 345 --AASQS-----

```

EtTssA      413  ----LEK-----ADTEGLDATLHWLQTRPG---ADSTKGKWLL
AhTssA      390  ---AEEVAQRHGEQG-----IA-----AALALLDERIAQLKEPRDRFHALLVQAEELLA
BmTssA-5    503  SPMAGEPARAPGDACGASADDAVDRACAFASGQLDLALHAIQHAI DRAT--SAEQRLRA
BtTssA-5    459  LPMTGESDRARGDARDANADDAHARARALAASGRDLALGAIQQAIDRAP--SAERRLRA
YpTssA
AfTssA
BcTssA
BtTssA-1
PaTssA
BbTssA

EtTssA      444  RLLMARVAEQRGRNELALHLLGELESTAQAITLTQWIPALLFEVKSRRLRLLRMKATRSE
AhTssA      435  QEGMEALARQH YQHLWQE-----ASRLGLSHWEPGLVNRLES LAAPLSK-----
BmTssA-5    561  RVRLCE LARDHWPHEVPEAFARGVIEPIRRHDLLAWNPELALDGLSAA YALLIRRDRESA
BtTssA-5    517  RIRLCE FARDHWEHEIPDAFARGVIEPIRRHDLLAWEPELALDGLSAA YALLIRRDGDSA
YpTssA
AfTssA
BcTssA
BtTssA-1
PaTssA
BbTssA

```

Figure 7.1 Amino acid sequence alignment of selected TssA proteins

Alignment performed using Clustal Omega and shaded using BoxShade. EtTssA, *Edwardsiella tarda* EvpK (ETEE_4095); AhTssA, *Aeromonas hydrophila subsp. hydrophila* AHA_1844; BmTssA-5, *B.m* TssA-5 (also known as 'BimE' BMAA0747); BtTssA-5, *B.t* TssA-5 (BTH_I10873); YpTssA, *Yersinia pseudotuberculosis* YPTB0640; AfTssA, *Agrobacterium fabrum* ImpA (Atu4343); BcTssA, *B. cenocepacia* TssA (BCAL0348); BtTssA-1, *B.t* TssA-1 (BTH_I2957); PaTssA, *Pseudomonas aeruginosa* PA0082; BbTssA, *Bordetella bronchiseptica* BB0799. Accession numbers of proteins are listed in Table 10.1

containing 25 µg/ml trimethoprim following which plasmid DNA was harvested by the miniprep method. Plasmid DNA samples were analysed by agarose gel electrophoresis to identify a 5499 bp plasmid. The sequence of the pEX18Tp-*pheS*- Δ *tssA* insert was confirmed by nucleotide sequencing before it was introduced into *E. coli* SM10(λ pir) which was used to deliver the plasmid into WT *B. t.* The suicide plasmid, and hence the trimethoprim resistance gene, was integrated into the chromosome by homologous recombination, between cloned sequences, present on the plasmid and the corresponding genomic locus. This allowed the growth of merodiploid *B. t.* colonies on M9 agar containing 50 µg/ml trimethoprim. Colonies were streaked onto plates containing chlorophenylalanine which is toxic to cells containing the mutant *pheS* gene and therefore only allowed the growth of colonies that had excised the pEX18Tp-*pheS* plasmid leaving behind either the WT *tssA-5* gene or Δ *tssA-5*. Boiled lysate was prepared from a number of colonies and used as a template for a GoTaq PCR using the *tssA*scrnfor and *tssA*scrnrev primers. When WT *tssA-5* was present in the colony used to prepare the boiled lysate the reaction amplified a 2949 bp fragment, but when Δ *tssA-5* was present lacking the central sequence of the gene but retaining the first 69 bp (23 codons) including the start codon fused to the last 57 bp (19 codons), a 1278 bp fragment was amplified.

7.3 MNGC formation in a *B. thailandensis tssA-5* mutant

RAW 267.4 cells seeded the previous day at 2×10^5 cell per well of a 24 well plate were infected at an MOI of 10:1 with WT *B. t.* containing pBBR1MCS, the *B. t.* Δ *tssA-5* mutant containing pBBR1MCS, or left uninfected but otherwise treated in an identical fashion to the infected cells. Two hours post infection wells were washed three times with PBS before replacing the culture medium (DMEM containing 10% FCS) with culture medium supplemented with 250 µg/ml kanamycin to kill extracellular bacteria. 16 hours after the initial infection, wells were washed three times with PBS before fixing for thirty minutes with 100% ethanol. The ethanol was removed and the wells allowed to dry before staining with 100% Giemsa for 5 minutes. Wells were washed gently with tap water until the desired staining intensity was obtained. Images were obtained using the 10x objective of a Leica DMI4000B inverted light microscope and nuclei within giant cells (defined as having three or more nuclei contained within a single cytoplasmic membrane) and outside of giant cells counted using the cell counter plugin on ImageJ. The number of nuclei within giant cells was divided by the total number of nuclei and multiplied by 100 to give the fusion index. Fusion indexes were obtained from three fields of view from three independent experiments. As shown in Figure 7.2 C, no giant cell formation could be observed in RAW cells infected with the *B. t.* Δ *tssA-5* mutant containing pBBR1MCS, suggesting that this mutation had an effect on T6SS-5 activity.

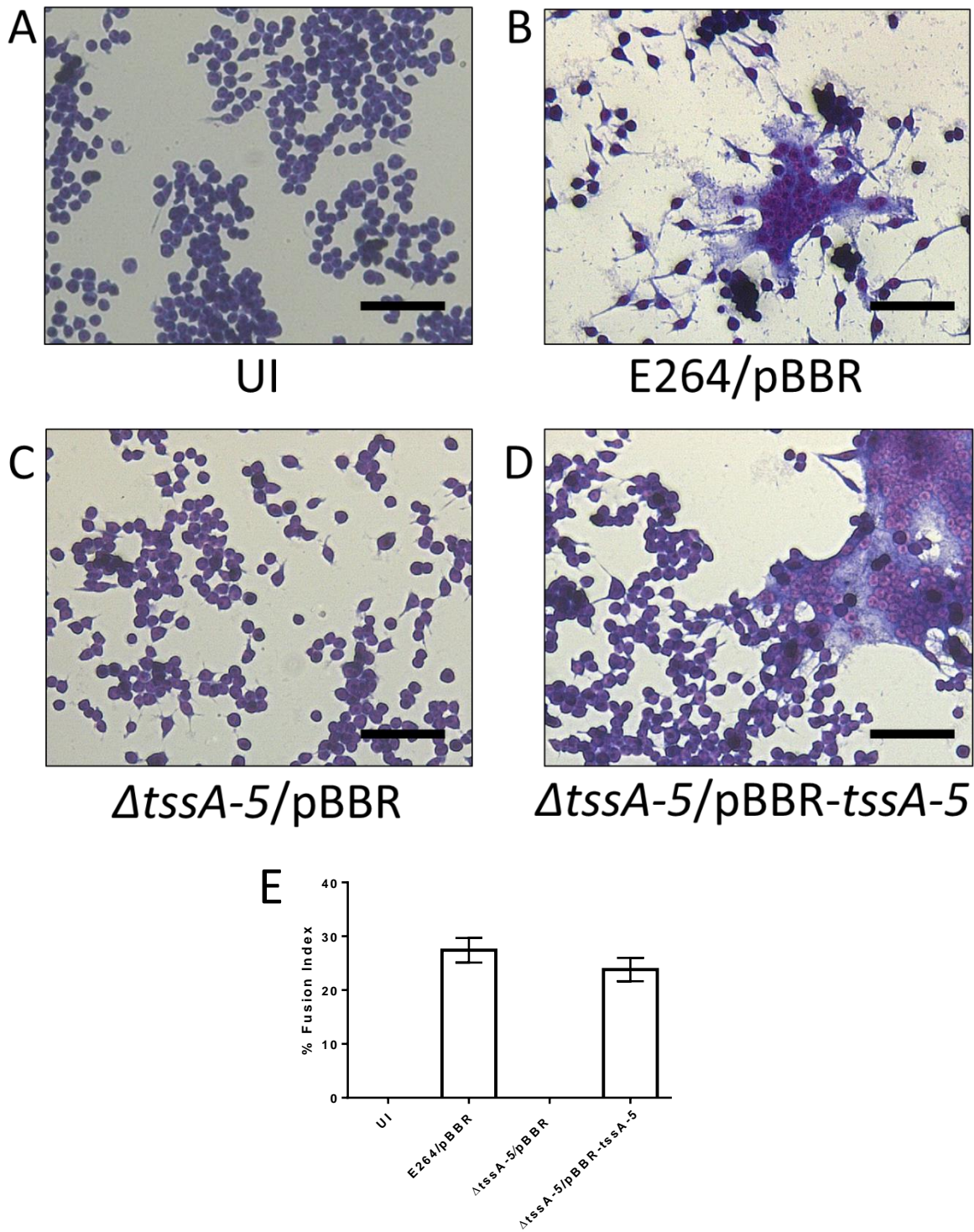


Figure 7.2 Effect of deleting *tssA-5* on MNGC formation *in vitro*

RAW 264.7 cells seeded at 2×10^5 cells/well and grown overnight were infected with the indicated strains of *B. thailandensis* at an MOI of 10:1 for 2 hours following which the growth medium was replaced with fresh growth medium containing kanamycin and incubation for a further 14 hours at 37°C. A-D) Representative images of infected RAW cells stained with Giemsa, scale bar = 75 μ m A) UI, uninfected. B) E264/pBBR, WT *B.t* containing pBBR1MCS. C) $\Delta tssA-5$ /pBBR, *B.t* $\Delta tssA-5$ mutant containing pBBR1MCS. D) $\Delta tssA-5$ /pBBR-*tssA-5*, *B.t* $\Delta tssA-5$ containing pBBR1MCS-*tssA-5*. E) Graph of fusion indexes taken from three independent experiments, error bars = one standard deviation.

7.4 Construction of a *tssA-5* complementation plasmid

To confirm that polar effects on the expression of downstream genes were not responsible for the inability of the *B.t* $\Delta tssA-5$ mutant to induce the formation of MNGCs, it was necessary to restore MNGC inducing activity by introducing the WT gene *in trans*. Previous experiments have demonstrated that expression of WT genes from pBBR1MCS was sufficient to restore MNGC formation to mutants that were unable to form MNGCs during infection assays. Primers were designed to include a stop codon in frame with the *lacZ α* peptide coding sequence on the vector and the native ribosome binding site upstream of the *tssA-5* gene. The primers *tssAcompfor* and *tssAcomprev* were used in a Q5 PCR which amplified an 1837 bp DNA fragment containing *tssA-5* flanked by an upstream HindIII site and a downstream BamHI site. pBBR1MCS and the DNA fragment containing *tssA-5* were digested with HindIII and BamHI before they were ligated together in a reaction mixture which was used to transform competent JM83 cells. Transformants were selected on LB containing 25 μ g/ml chloramphenicol, 100 μ M IPTG and 40 μ g/ml Xgal. This allowed colonies harbouring plasmids which contained an insert that disrupts the *lacZ* gene to be identified by a white colony colour compared with a blue colour seen in colonies harbouring the empty pBBR1MCS plasmid with its *lacZ α* peptide coding sequence intact. Plasmids were isolated from overnight cultures of selected colonies by plasmid miniprep and those that migrated at the correct size (6500 bp) in an agarose gel were analysed by nucleotide sequencing. The confirmed pBBR1MCS-*tssA-5* plasmid was then used to transform *E. coli* SM10 and cultures of the resulting colonies used as donors for conjugation with *B.t* $\Delta tssA-5$.

The *B.t* $\Delta tssA$ mutant containing pBBR1MCS-*tssA-5* was used to infect RAW 264.7 cells at a MOI of 10:1 in 24 well plates for 16 hours following which the wells were stained with Giemsa. As shown in Figure 7.2 D, when the WT *tssA-5* gene was reintroduced *in trans* using the pBBR1MCS-*tssA-5* plasmid, MNGC formation was restored at a fusion index similar to the WT strain. This result demonstrated that the inability of the $\Delta tssA-5$ strain to form giant cells was a consequence of the deletion introduced and not due to polar or adventitious effects.

7.5 Secretion of TssD-5 by a *tssA-5* mutant

The observations that the deletion of *tssA-5* resulted in a strain which was unable to induce the formation MNGCs in RAW cells and re-introduction of the WT *tssA-5* gene on the pBBR1MCS vector restored the ability to induce giant cell formation was consistent with the hypothesis that *tssA-5* was required for T6SS-5 activity. To confirm this, it was necessary to analyse TssD-5 secretion by a $\Delta tssA-5$ strain in which T6SS-5 had been induced by the presence of the pSCrhaB2-*virAG* vector. To facilitate this, the pSCrhaB2-*virAG* plasmid was delivered to the *B.t* $\Delta tssA-5$ mutant by conjugation. It was also desirable to have a strain in which the WT *tssA-5* gene had been re-introduced into the induced *tssA-*

5 mutant. The pBBR1MCS-*tssA-5* construct would be unsuitable for this as it has the same origin of replication as the pSCrhaB2-*virAG* plasmid used to induce T6SS-5. Therefore, in an analogous approach described earlier for *tssK-5*, the *tssA-5* gene was transferred from pBBR1MCS-*tssA-5* to pSCrhaB2-*virAG* via the LITMUS28i plasmid. pBBR1MCS-*tssA-5* was digested with NcoI and XbaI, resulting in a 2275 bp DNA fragment containing the *tssA-5* gene located downstream of the *lac* promoter and operator. The fragment was ligated into LITMUS28i which had been digested with NcoI and XbaI to create the intermediate plasmid LITMUS28i-*tssA-5*. The ligation mixture was used to transform *E. coli* JM83 cells which were spread on LB agar plates containing 25 µg/ml kanamycin. Colonies growing on this plate were screened by PCR using GoTaq and the primers M13for and M13rev to amplify a 230 bp product when colonies contained LITMUS28i and two products at 2019 bp and 2642 bp when the colonies contained LITMUS28i-*tssA-5*.

LITMUS28i-*tssA-5* was digested with BamHI and XbaI, generating a 2453 bp DNA fragment which was ligated into pSCrhaB2-*virAG* that had been digested with BglII and XbaI. The ligation mixture was used to transform *E. coli* JM83 cells which were spread on IST agar plates containing 25 µg/ml trimethoprim. Colonies growing on this plate were used as a template for GoTaq PCRs which used the primers *virG*for and pSCrhaB2rev to amplify an 868 bp DNA fragment when the colonies contained pSCrhaB2-*virAG* and a 3366 bp DNA fragment when pSCrhaB2-*virAG-tssA-5* was present. pSCrhaB2-*virAG-tssA-5* was confirmed by nucleotide sequencing and then delivered into the *B. t. ΔtssA-5* mutant by conjugation.

WT *B. t.* containing pSCrhaB2-*virAG*, *B. t. ΔtssD-5* mutant containing pSCrhaB2-*virAG*, *B. t. ΔtssK-5* mutant containing pSCrhaB2-*virAG*, *B. t. ΔtssK-5* mutant containing pSCrhaB2-*virAG-tssK-5*, *B. t. ΔtssA-5* mutant containing pSCrhaB2-*virAG* and *B. t. ΔtssA-5* mutant containing pSCrhaB2-*virAG-tssA-5* were grown overnight in M9 containing 0.5% (v/v) glycerol, 0.5% (w/v) casamino acids and 50 µg/ml trimethoprim. The cultures were used to inoculate 25 ml of the same medium and grown at 37°C with shaking to an OD₆₀₀ of ~1.0. At this point a volume of the culture equivalent to 1 ml of OD₆₀₀ 1.0 was centrifuged at 13,000 x g for one minute whereupon the supernatant was discarded. The resulting cell pellet was resuspended in 100 µl of 1 x Laemmli buffer to yield a cell associated sample. The remainder of the 25 ml culture was centrifuged at 3,900 x g and the resulting supernatant was filter sterilised using a 0.22 µm syringe driven filter. Proteins were precipitated by taking a volume of this filter sterilised supernatant equivalent to 15 ml of OD₆₀₀ 1.0 and adding sodium deoxycholate to a final concentration of 200 µg/ml and incubating on ice for 30 minutes followed by the addition of trichloroacetic acid (TCA) to a final concentration of 10% (v/v) and incubating at -20°C overnight. Precipitated proteins were isolated by centrifugation at 3,900 x g for one hour at 4°C, the supernatant was discarded and the pellet resuspended in 5 ml of acetone and incubated at -20°C for one hour. Insoluble protein was collected by centrifugation at 3,900 x g for one hour at 4°C and the supernatant discarded. Again, the

pellet was resuspended in 5 ml of acetone and incubated at -20°C for one hour before centrifuging at 3,900 x g for one hour at 4°C. The supernatant was discarded and residual acetone was removed by evaporation at room temperature. The washed protein pellet was resuspended in 200 µl of 1 x Laemmli buffer to give a supernatant sample.

The cell associated and supernatant samples were boiled for 10 minutes and centrifuged for 10 minutes at 13,000 x g. The samples were electrophoresed in a 15% SDS polyacrylamide gel and transferred to a PVDF membrane which was stained with antibody against RNAP and then stripped and reprobbed with antibody against TssD-5. As shown in Figure 7.3, the *B.t ΔtssA-5* mutant had a reduced level of TssD-5 secretion compared to the WT strain although there were similar levels of TssD-5 in the respective cell associated samples. However, TssD-5 secretion was not completely abolished as a small amount of TssD was detected by the antibody. This is in contrast to the supernatant sample prepared from the culture of *B.t ΔtssK-5* shown on the same blot which had no detectable TssD-5. A level of TssD-5 secretion similar to that observed in the WT and complemented *tssK-5* mutant samples can be detected in the complemented *tssA-5* mutant samples confirming that the phenotype observed was not a consequence of polar or adventitious effects.

7.6 Creation of a *B. thailandensis ΔtssA-1* and *ΔtssA-5* double mutant

Following the surprising observation that the *ΔtssA-5* mutant still secreted low, but detectable amounts of TssD-5 when induced by the pScRhaB2-*virAG* plasmid in T6SS-5 activity assays, it was speculated that one of the other four TssA proteins encoded by the *B. thailandensis* genome was partially compensating for the lack of *tssA-5*. Of the six T6SSs present in *B. pseudomallei*, only T6SS-1 is constitutively expressed, based on the presence of TssD-1 in the cell lysates of cultures grown under laboratory conditions (Burtnick et al. 2011). Given that if another *tssA* was compensating for a loss of *tssA-5* it would have to be expressed, *tssA-1* represented the most likely candidate and therefore to test this hypothesis, it was decided to delete *tssA-1* in the *B.t ΔtssA-5* mutant strain.

To perform the deletion of *tssA-1*, the markerless in frame deletion method was utilised again. The primers *tssA1SOEfor* and *tssA1SOEmidrev* were used in a Q5 PCR which amplified a 740 bp DNA fragment which contained the final 535 bp of *tssH-1* and the first 93 bp of *tssA-1*. A second PCR used *tssA1SOEmidfor* and *tssA1SOErev* to amplify a 625 bp DNA fragment containing the final 323 bp of *tagN-1* (transcribed in an opposite orientation to *tssA-1* in the T6SS-1 gene cluster) and the final 75 bp of *tssA-1*. A third PCR using the combined, gel extracted products of the previous reactions as a template with the *tssA1SOEfor* and *tssA1SOErev* primers amplified a 1320 bp DNA fragment. This PCR product was digested with *Acc65I* and *BamHI* before ligating into pEX18Tp-*pheS* which had been

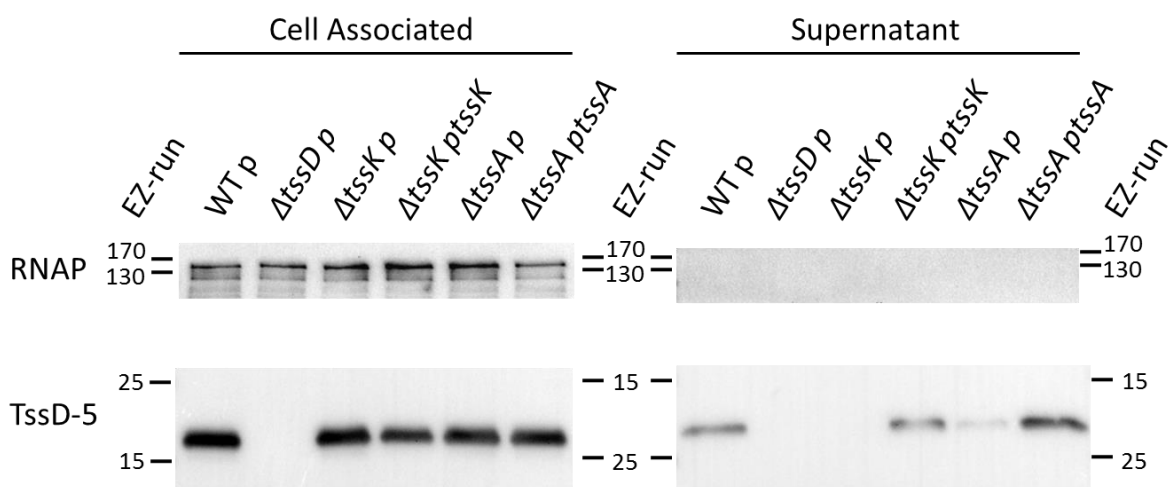


Figure 7.3 Analysis of TssD-5 secretion by the *B. thailandensis* $\Delta tssA-5$ mutant

Western blots of cell associated and TCA precipitated supernatant samples prepared from cultures of the indicated strains grown in M9 containing 0.5% glycerol and 0.5% casamino acids. WT p, WT *B.t* containing pSCrhaB2-*virAG*; $\Delta tssD$ p, *B.t* $\Delta tssD-5$ containing pSCrhaB2-*virAG*; $\Delta tssK$ p, *B.t* $\Delta tssK-5$ containing pSCrhaB2-*virAG*; $\Delta tssK$ ptssK, *B.t* $\Delta tssK-5$ containing pSCrhaB2-*virAG-tssK-5*; $\Delta tssA$ p, *B.t* $\Delta tssA-5$ containing pSCrhaB2-*virAG*; $\Delta tssA$ ptssA, *B.t* $\Delta tssA-5$ pSCrhaB2-*virAG-tssA-5*. RNAP, blot probed with anti RNAP antibody; TssD-5, blot probed with anti TssD-5 antibody. EZ-run, EZrun prestained protein ladder. Protein molecular weight markers are given in kDa.

digested with the same enzymes. The ligation mixture was used to transform *E. coli* JM83 cells which were spread on M9 agar plates containing 25 µg/ml trimethoprim, 1% (w/v) casamino acids, 0.5% (v/v) glycerol, 0.0005% (w/v) thiamine, 40 µg/ml X-gal and 0.1 µg/ml IPTG. After two nights incubation at 30°C, white colonies growing on this plate were inoculated into IST broth containing 25 µg/ml trimethoprim and grown overnight. Plasmid DNA was harvested by the miniprep method and analysed by agarose gel electrophoresis to identify a plasmid at the correct size to be pEX18Tp-*pheS-ΔtssA-1* (5797 bp).

pEX18Tp-*pheS-ΔtssA-1* was confirmed by DNA sequencing before introduction into *B. thailandensis ΔtssA-5* by conjugation via the *E. coli* SM10(λpir) conjugal donor strain. The conjugations were spread on M9 agar plates containing 50 µg/ml trimethoprim which only allowed the growth of colonies in which the pEX18Tp-*pheS* plasmid had integrated into the chromosome. This was followed by streaking these colonies onto M9 agar plates containing 0.1% (w/v) chlorophenylalanine which prevented the growth of pEX18Tp-*pheS* co-integrates, thereby selecting for colonies in which a second homologous recombination event had occurred to excise the vector. A GoTaq PCR screen was performed using boiled lysates prepared from selected colonies using the *tssA1scrnfor* and *tssA1scrnrev* primers which amplified a 2546 bp DNA fragment when the WT *tssA-1* gene was present on the *B.t* chromosome and a 1583 bp DNA fragment when the *ΔtssA-1* mutant was present which retained the first 93 bp (31 codons) fused to the final 75 bp (25 codons) of *tssA-1* resulting in a *B.t ΔtssA-1* and *ΔtssA-5* double mutant.

7.7 Secretion of TssD-5 by a *B. thailandensis tssA-1* and *tssA-5* double mutant

The pSCRhaB2-*virAG* plasmid was introduced into the *B.t ΔtssA-1* and *ΔtssA-5* double mutant strain by conjugation and the secretion of TssD-5 was assayed as described previously using 25 ml cultures of WT *B.t* containing pSCRhaB2-*virAG*, *B.t ΔtssD-5* mutant containing pSCRhaB2-*virAG*, *B.t ΔtssK-5* mutant containing pSCRhaB2-*virAG*, *B.t ΔtssA-5* mutant containing pSCRhaB2-*virAG* and *B.t ΔtssA-1 ΔtssA-5* mutant containing pSCRhaB2-*virAG*. Figure 7.4 demonstrates that there is no observable effect of the deletion of the *tssA-1* gene on secretion of TssD-5 in a *ΔtssA-5* background, as the supernatant prepared from the *B.t ΔtssA-1* and *ΔtssA-5* double mutant showed a similar level of TssD-5 in the TCA precipitated culture supernatant to that present in the *tssA-5* mutant. This indicates that the *tssA-1* gene product was not compensating for the loss of *tssA-5*.

7.8 Interaction of TssA-5 with itself

Previous studies by members of the Thomas group have shown that *Burkholderia cenocepacia* TssA interacts with itself (and a number of other proteins of the *B. cenocepacia* T6SS) (Ahmad 2013). To test whether the *B.t* TssA-5 interacts with itself, the bacterial two hybrid (BACTH) assay was used. Self-

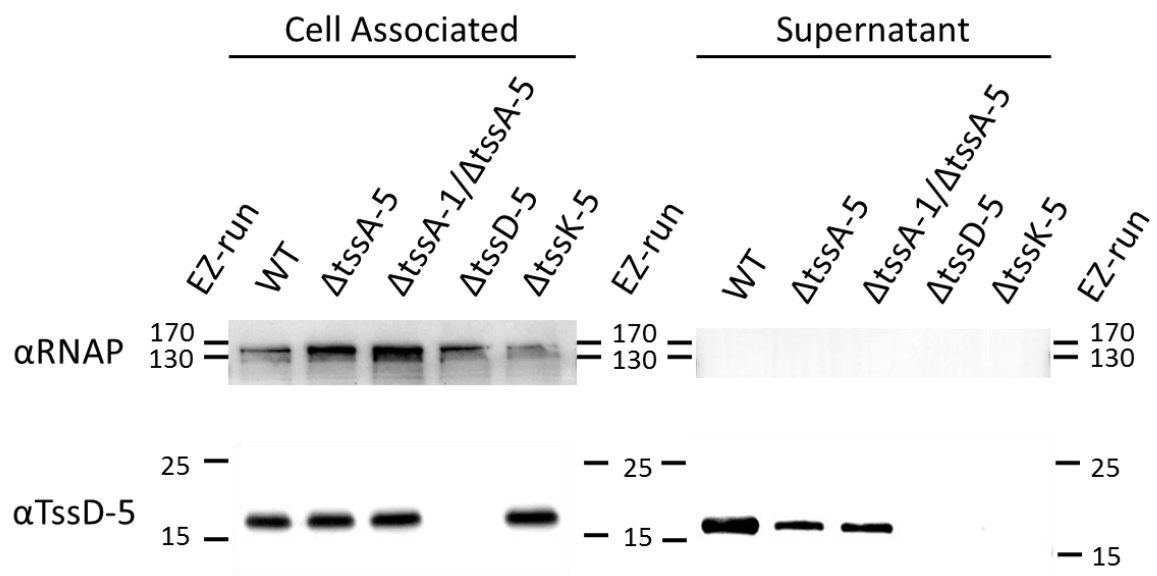


Figure 7.4 Secretion of TssD-5 by a *B. thailandensis* *tssA-1* and *tssA-5* double mutant

Western blots of cell associated and TCA precipitated supernatant samples prepared from cultures of the indicated strains of *B. thailandensis* M9 containing 0.5% glycerol and 0.5% casamino acids. Blots stained with antibody against RNAP (α RNAP) and TssD-5 (α TssD-5). WT, WT *B.t* containing pSCrhaB2-*virAG*; $\Delta tssA-5$, *B.t* $\Delta tssA-5$ mutant containing pSCrhaB2-*virAG*; $\Delta tssA-1/\Delta tssA-5$, *B.t* $\Delta tssA-1$ and $\Delta tssA-5$ mutant containing pSCrhaB2-*virAG*; $\Delta tssD-5$, *B.t* $\Delta tssD-5$ mutant containing pSCrhaB2-*virAG*; $\Delta tssK-5$, *B.t* $\Delta tssK-5$ mutant containing pSCrhaB2-*virAG*; EZ-run, EZ-run prestained ladder. Protein molecular weight markers given in kDa.

interaction of the *B. cenocepacia* TssA was observed when plasmids expressing fusions of the N-terminus of TssA to the C-terminus of T25 or T18 were used. Therefore, equivalent constructs were made for expression of *B. t* TssA-5 BACTH fusion proteins. The pKT25-*tssA* and pUT18C-*tssA* plasmids were created as described in section 6.3.6.1. *E. coli* BTH101 cells were co-transformed with pKT25-*tssA* and pUT18C-*tssA* and spread on MacConkey agar plates containing 1% (w/v) maltose, 100 µg/ml ampicillin and 50 µg/ml kanamycin. Plates were incubated at 30°C for 48 hours and the strength of the self-interaction was determined based on the colour of colonies growing on the plates. *E. coli* BTH101 cells were also co-transformed with pKT25-*zip* and pUT18C-*zip* which express fusion proteins which interact via leucine zipper motifs to act as a positive control. *E. coli* BTH101 cells were also transformed with pKT25-*tssA* and pUT18C, pKT25 and pUT18C-*tssA*, and pKT25 and pUT18C plasmid combinations to ensure any phenotype observed was not the result of non-specific interactions or a direct ability of *tssA* to induce a Cya⁺ phenotype.

As shown in Figure 7.5 BTH101 colonies containing pKT25-*tssA* and pUT18C-*tssA* were able to ferment maltose, indicating that the T25 and T18 protein fragments are in close proximity and hence TssA interacts with itself. The colour of the colonies on the control plates indicate that they are Cya⁻, indicating that TssA does not interact with either the T25 or T18 fragments and cannot induce a Cya⁺ phenotype on its own. The colour of the colonies of BTH101 containing pKT25-*tssA* and pUT18C-*tssA* is of a similar intensity to the colour of the *zip* control, suggesting the interaction of TssA with itself is strong.

7.9 Secretion of TssD-1 by a *B. thailandensis tssA-1* and *tssA-5* double mutant

For future work, a mutant that is incapable of secretion by T6SS-1 might be of use, therefore the secretion of TssD-1 by the *B. t* $\Delta tssA-1$ and $\Delta tssA-5$ double mutant was assessed. Although an antibody to TssD-1 was not available, a polyclonal antibody against purified hexa-histidine tagged BCAL0343, a TssD protein of *B. cenocepacia* J2315 corresponding to TssD-1 (*B. cenocepacia* encodes T6SS-1) was available. The EMBOSS needle tool was used to quantify the identical amino acids shared by the BCAL0343 protein with each of the four TssD proteins of *B. thailandensis*. As shown in Table 7.1, BCAL0343 shares 92.8% identity with the TssD-1 (BTH_I2962) protein of *B. thailandensis*, but no more than 27% identity with any of the other *B. thailandensis* TssD proteins. Therefore, the antibody raised against BCAL0343 may also bind specifically to TssD-1.

To test this hypothesis, cultures of WT *B. t*, the *B. t* $\Delta tssA-1$ and $\Delta tssA-5$ double mutant and *B. t* $\Delta tssD-5$ all containing pSCrhaB2-*virAG* were grown in 25 ml of M9 containing 0.5% (v/v) glycerol, 0.5% (w/v) casamino acids and 50 µg/ml to an OD₆₀₀ of 1.0 at which point cell associated samples and TCA precipitated supernatant samples were prepared. These were analysed by electrophoresis in a 15%

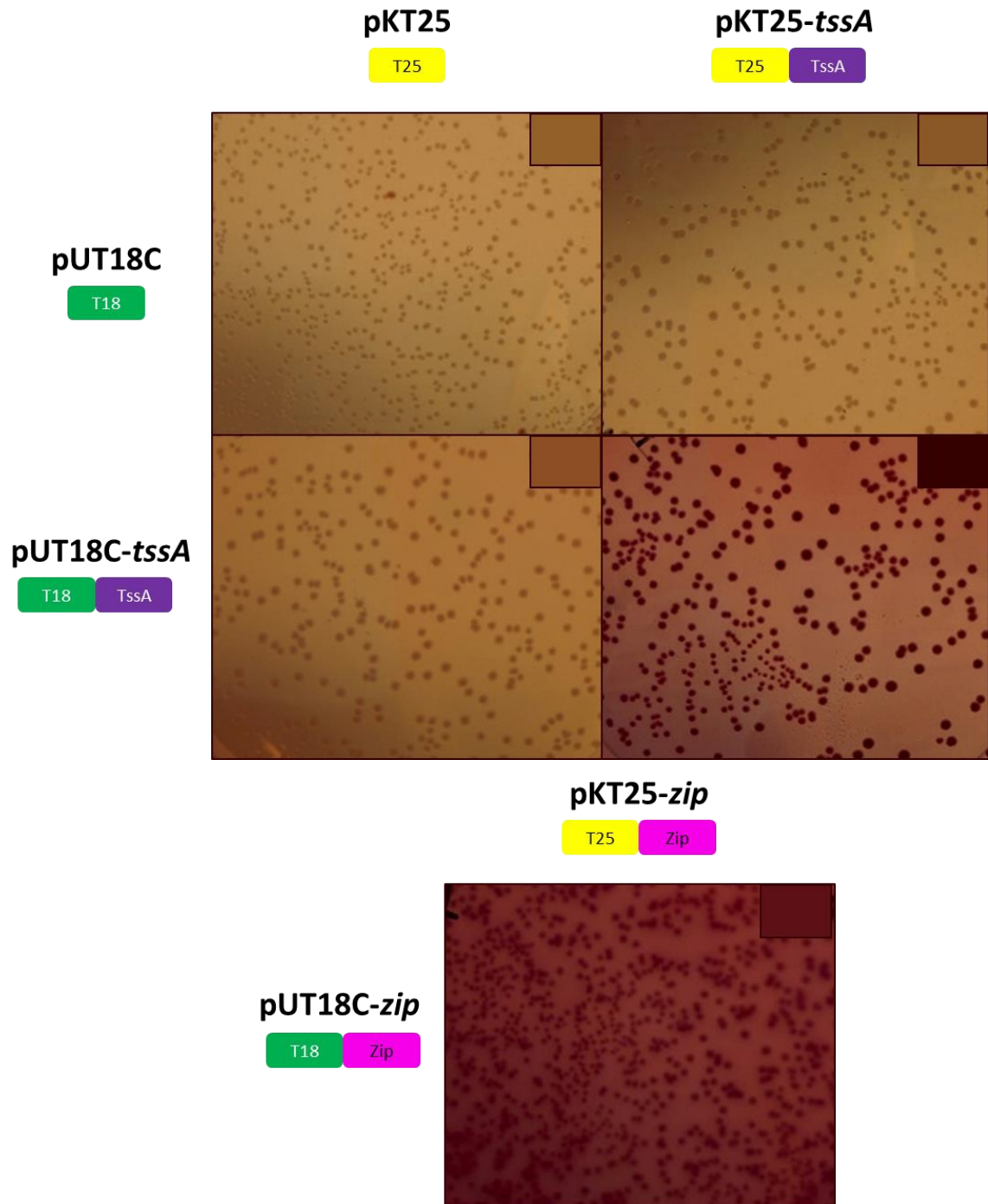


Figure 7.5 Self-interaction of TssA determined by BACTH assay

Maltose phenotypes of *E. coli* BTH101 colonies harbouring the indicated plasmid pairs growing on MacConkey agar plates containing 1% (w/v) maltose, 100 µg/ml and 50 µg/ml kanamycin after three nights incubation at 30°C. Boxes inset coloured using the 'eyedropper' tool over the centre of a colony from the middle of the plates.

Table 7.1 Identities of the five TssD-5 proteins of *B. thailandensis* with *B. cenocepacia* BCAL0343

	TssD-1	TssD-2	TssD-4	TssD-5	TssD-6
Identity with BCAL0343^a	92.8%	24.1%	19.6%	26.9%	21.8%

^a determined by EMBOSS Needle

polyacrylamide gel which was transferred to a PVDF membrane by western blotting. This blot was sequentially probed with antibody against the RNAP β subunit, BCAL0343 and TssD-5. As shown in Figure 7.6 the antibody against BCAL0343 binds to a protein at approximately the same molecular weight as TssD-1 (18.4 kDa) in all of the cell associated samples. This staining was not a result of an interaction with TssD-5 (the other TssD expressed under these conditions) as the same protein was detected in the $\Delta tssD-5$ cell associated sample. No proteins were detected in any of the supernatant samples when stained with antibody against BCAL0343 suggesting that the protein in the cell associated samples assumed to be TssD-1 is not being secreted under these growth conditions. This means that it was not possible to determine if the mutation in *tssA-1* had an effect on secretion by T6SS-1. When the blot was stained with antibody against TssD-5 the staining pattern was the same as demonstrated previously for samples prepared from the strains grown under T6SS-5-inducing conditions. These results suggest that the anti-BCAL0343 antibody binds to TssD-1 specifically and that under the conditions tested, the apparent TssD-1 protein was expressed but not secreted by T6SS-1.

7.10 Discussion

The observation that the *B.t tssA-5* mutant was incapable of inducing MNGC formation was not surprising given that TssA has previously been shown to be a core component of the T6SS. However this is in contrast to the results of Schell et al. (2007) who found that a *B.m tssA-5* (referred to by the authors as '*bimE*') mutant was still virulent in an *in vivo* infection model. Schell and colleagues also tested the virulence of the T6SS-5 deficient (based on TssD-5 secretion) *B.m tssG-5* (BMAA0739, referred to as '*tssE*') mutant and found that it was non-virulent in this hamster model of infection, indicating that T6SS-5 deficient mutants were avirulent. Later work demonstrated that this mutant was also incapable of inducing the formation of MNGCs in RAW 267.4 cells (Burtnick et al. 2010). Assuming that the formation of MNGCs is required for full virulence by *B.m*, it would have been expected that the *B.t tssA-5* mutant would be capable of MNGC formation. It might be the case that the relationship between intracellular motility in *B.t* is different in *B.m*. This is certainly possible as *B.p tssD-5* and *tagA-5* (and hence T6SS-5 deficient) mutants are capable of forming actin tails to the same extent as the WT strain, whereas a *B.m tssG-5* (T6SS-5 deficient) mutant has impaired actin tail formation (Burtnick et al. 2010). It would therefore be interesting to use phalloidin staining to determine whether or not the *B.t tssA-5* mutant (as well as other T6SS-5 defective strains) demonstrated the same actin polymerisation defect as the *B.m tssA-5* mutant. As a predicted subunit of T6SS-5, it is unclear why the *B.t tssA-5* mutant demonstrated low levels of TssD-5 secretion compared with the *tssK-5* mutant which demonstrated no TssD-5 secretion even though

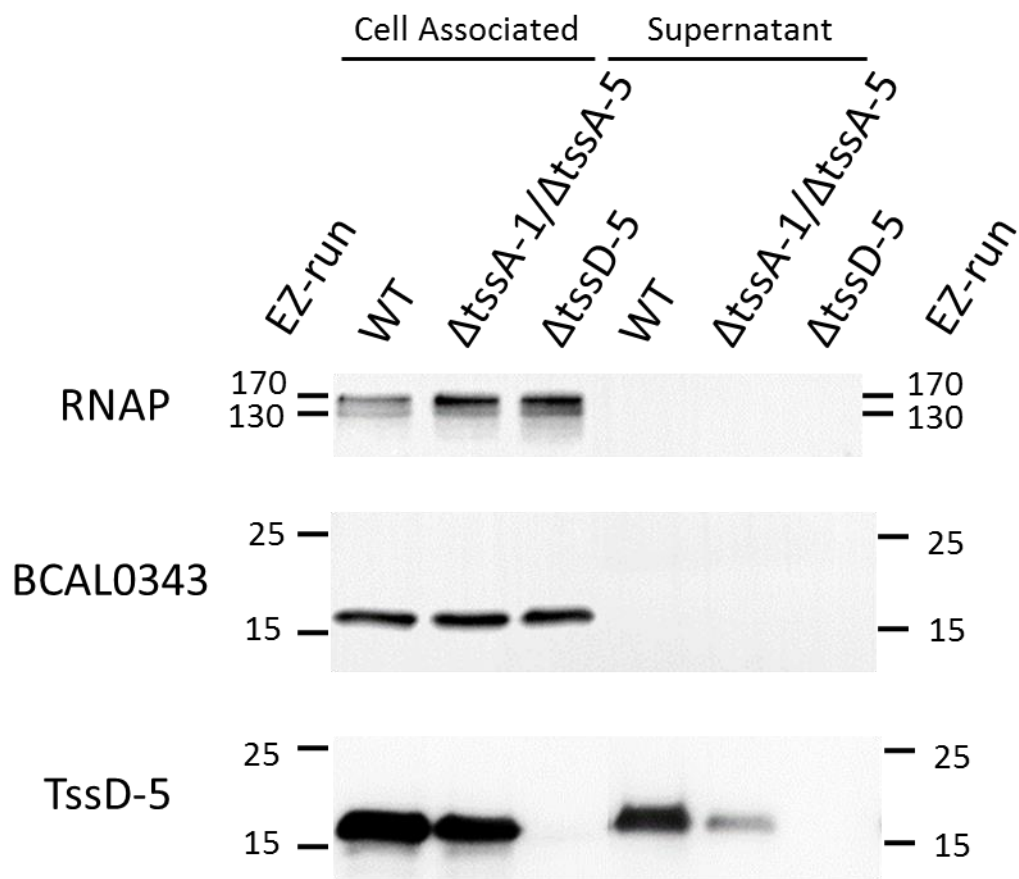


Figure 7.6 Cross reactivity of BCAL0343 with *B. thailandensis* TssD-1

Western blots of cell associated and TCA precipitated supernatant samples prepared from cultures of the indicated strains grown in M9 containing 0.5% glycerol and 0.5% casamino acids and probed with the indicated antibodies. WT, WT *B. thailandensis* containing pSCrhaB2-*virAG*; Δ tssA-1/ Δ tssA-5, *B. t* Δ tssA-1 and Δ tssA-5 double mutant containing pSCrhaB2-*virAG*; Δ tssD-5, *B. t* Δ tssD-5 mutant containing pSCrhaB2-*virAG*. EZ-run, EZrun prestained protein ladder. Protein molecular weight markers given in kDa.

both showed a total inability to induce the formation of MNGCs. It did not appear to be a result of partial complementation by the *tssA-1* gene, as a *B.t tssA-1* and *tssA-5* double mutant demonstrated the same level of TssD-5 secretion as the *B.t tssA-5* single mutant. Further evidence that BTH_II0873 encodes a T6SS TssA protein was provided by the interaction of TssA with itself in the BACTH assay, a characteristic that is shared with *B. cenocepacia* TssA.

The cross reactivity of the antibody against *B. cenocepacia* BCAL0343 with *B.t* TssD-1 observed in section 7.9 is not surprising, given the high level of sequence identity between *B. thailandensis* TssD-1 and *B. cenocepacia* BCAL0343. Thus, it is likely that one of the epitopes that the polyclonal antibody against BCAL0343 binds to is present in TssD-1. Furthermore, the antibody to BCAL0343 does not bind to the only other *B.t* TssD known to be expressed under the conditions tested, TssD-5, as it still binds to proteins in samples prepared from the *B.t ΔtssD-5* mutant strain. While it is still possible that the antibody against BCAL0343 binds to one of the other three TssD proteins encoded by the *B. thailandensis* chromosome, this is unlikely given the low level of sequence similarity between each of TssD-2, TssD-4, TssD-6 and BCAL0343. To confirm that the antibody against BCAL0343 was only binding to TssD-1, it would be useful to construct a *tssD-1* mutant. If the antibody against BCAL0343 did not bind to cell associated samples prepared from this strain under conditions where the T6SS gene cluster is expressed, then it could be confirmed that this antibody is specific to TssD-1.

Although TssD-1 appears to be present in cell associated samples, it is absent from secreted samples. This is consistent with the observations of Burtnick et al. (2011) who demonstrated that an antibody against *B. pseudomallei* TssD-1 bound to protein in cell associated samples of *B. pseudomallei* cultures grown in LB, but not supernatants when analysed by western blotting. However, when *B. thailandensis* cells were grown in Vogel-Bonner synthetic CF sputum minimal medium containing 19 mM amino acids, 1% (v/v) Tween 80 and 0.5% (v/v) glucose, TssD-1 was detectable by mass spectrometry in culture supernatants (Russell et al. 2012), although this was not investigated by immunoblotting. Therefore, it would be desirable to repeat the experiments in this synthetic sputum medium to see if TssD-1 can be detected in *B.t* culture supernatants by western blotting. Another potential way to induce the bacteria-targeting T6SS-1 to secrete could be to introduce another bacterial species which possesses an antibacterial T6SS into the culture of *B. thailandensis*. This is based on a study in *Pseudomonas aeruginosa* that demonstrated that T6SS activity is stimulated in response to attack from other bacteria possessing a T6SS (Basler et al. 2013). Alternatively, the effect of the *tssA-1* mutation could be determined indirectly using bacterial competition assays, as T6SS-1 defective *B.t* mutant is displaced by *Pseudomonas putida* in mixed biofilm assays, whereas *B.t* containing a functional T6SS-1 gene cluster persists (Schwarz et al. 2010).

Chapter 8 General discussion

8.1 Findings

The results of this study highlights four *B.t* genes which are critical for the induction of the formation of MNGCs in a macrophage-like cell line. The results were not a consequence of polar effects on neighbouring genes as the re-introduction of the native genes on a multi-copy plasmid restored the capability of the *B.t tag* mutants to induce the formation of MNGCs. The inability of the *B.t tag* mutant strains to induce MNGC formation in RAW cells was determined to be a result of inactivation of the T6SS as determined by the severely reduced level of TssD-5 secretion in T6SS-5-induced cultures. Research conducted by Hopf et al. (2014) published after the start of the work presented in this thesis demonstrated that *B.p tagA-5* was critical for the induction of MNGC formation and secretion by T6SS-5. This correlates with the observations made in this study in *B.t*, further supporting the use of *B.t* as a model for the study of T6SS-5 in *B.p*.

Although the TagA-TagD proteins were predicted to be type VI secreted effector proteins, a mass spectrometry screen of the T6SS-5 secretome was unable to facilitate their identification in culture supernatants. This was particularly surprising given the predicted role of TagD as a secreted PAAR protein. Although the PAAR proteins can be detected by western blotting of supernatant samples when fused to an epitope tag (Shneider et al. 2013), mass spectrometric analysis was unable to detect them in culture supernatant samples (Altindis et al. 2015). This indicates that TagD might be secreted but not readily detectable by mass spectrometry.

As there were no antibodies available which recognised the Tag proteins, FLAG epitope tagging was performed. *B. thailandensis* $\Delta tagA$ and $\Delta tagB$ mutants complemented with plasmids encoding TagA and TagB containing a C-terminal FLAG tag demonstrated the same properties as their native equivalents in MNGC and secretion assays. The anti-FLAG antibody was able to detect TagA_{FLAG} and TagB_{FLAG} in cell associated samples prepared from cultures of *B.t* expressing *tagA_{FLAG}* and *tagB_{FLAG}*, respectively. However, the antibody did not detect TagA_{FLAG} or TagB_{FLAG} in the supernatants of the same cultures, further suggesting that these two proteins are not secreted. Unfortunately, the C-terminal FLAG-tagged TagC and TagD proteins appeared to be non-functional, limiting their use in further assays.

TagA_{FLAG} and TagB_{FLAG} were subsequently used in co-immunoprecipitation assays to determine potential interaction partners of the two proteins. These assays suggested TagA and TagB might interact with TssI-5. However, this could not be confirmed by BACTH assay. TssF was enriched in the TagA pull down, but further investigation was not performed due to time constraints.

The results obtained from the investigation into TssA-5 are intriguing; although the *B.t tssA-5* mutant was unable to induce the formation of MNGCs, TssD-5 was still detected in the supernatant of a *virAG* induced culture, albeit at a much lower level. While it is possible that T6SS-5 was inactive and the deletion of *tssA* had an impact on the integrity of the *B.t* cell envelope, this seems unlikely given that the RNAP β -subunit (a lysis control) could not be detected in the supernatants. Although deletion of *tssA* in other T6SSs abolished TssD secretion (Zheng & Leung 2007; Zoued et al. 2016), it is possible that T6SS-5 is still partially active in the *B.t Δ tssA-5* mutant. Given that the other *tssA* deletion mutants studied to date have been T6SS-deficient (Zheng & Leung 2007; Aubert et al. 2015; Zoued et al. 2016), it is also possible that TssA-5 plays a different role in T6SS-5. It is also possible that another TssA protein partially compensates for a lack of TssA-5. However, deletion of the most likely candidate, *tssA-1*, did not abolish secretion. Plasmids were constructed for the deletion of the other *tssA* genes (not shown), however there was insufficient time to attempt to make the deletions in *B.t*.

8.2 Limitations

Of course, the primary limitation to this work is the fact that it was performed in *B.t* rather than the clinically relevant *B.p*. Although there are differences, to date, lessons learnt about T6SS-5 of individual pseudomallei group species have generally held true for all members of the group suggesting that the role of the Tag proteins is likely to be conserved in *B.p* and *B.m*. Indeed, with some exceptions, information gained on components in the T6SS of one organism generally hold true for others, suggesting that the Tag proteins are likely to play a similar role in T6SSs of other species too.

The BACTH assays also tested a limited number of potential interaction partners and it is possible that the Tag proteins interact with other T6SS-5 subunits that were not tested. It was particularly disappointing that there was not time to validate the potential TagA-5-TssF-5 interaction observed in the co-immunoprecipitation assay.

8.3 Future work

In the absence of specific antibodies which recognised the Tag proteins, the C-terminal FLAG epitope-tagged TagA_{FLAG} and TagB_{FLAG} proteins proved a useful alternative as they were able to functionally substitute for the corresponding WT proteins in TssD secretion assays. However, TagC_{FLAG} and TagD_{FLAG} did not restore TssD secretion to *B.t tagC* and *tagD* mutants indicating that the addition of the FLAG epitope to the C-terminus of these proteins had a detrimental effect on their function. The use of an alternative epitope tag (such as the HA tag) or placing the epitope tag at the N-termini of TagC and TagD might not have the same detrimental effect and could be investigated in future.

This study only used FLAG epitope-tagged Tag proteins, which limits their potential use in combination for assays such as pull downs. Therefore, it would also be desirable to have a strain in which the Tag proteins were fused to different epitope tags, facilitating the study of their interactions *in vivo*. Given that these epitope-tagged proteins might behave differently to their native versions, it might be more productive to focus on optimising the overproduction and purification of the native Tag proteins from *E. coli*. This would allow antibodies to be generated against the native proteins for use in antibody-based analytical techniques such as pull downs. Although it might be more convenient to have antibodies raised against epitopes of the Tag proteins (which would remove the necessity of Tag protein purification) the purified Tag proteins could also be used in structural analysis.

Although it was determined that it was unlikely that TagA and TagB are secreted, it is disappointing there was no time in this study to investigate the sub-cellular location of the Tag proteins. Using the FLAG specific antibody to probe samples prepared by membrane fractionation of cultures expressing *tagA_{FLAG}* or *tagB_{FLAG}* it should be possible to determine if they are membrane-associated. If the addition of an N-terminal FLAG epitope or the use of an alternative epitope tag does not have a detrimental effect on the function of TagC and TagD then their cellular (or perhaps extracellular) location could also be determined.

Although it is clear that the Tag proteins are required for secretion by the T6SS, their precise role is not known. It would be interesting to determine whether the T6SS is completely assembled in *tag* mutants or whether it assembles aberrantly. One way to determine this would be to utilise an assay which uses fluorescently labelled TssB subunits to monitor the conformation of the contractile sheath in the *tag* mutants (Basler et al. 2012). For example, if the Tag proteins are required for the assembly of the sheath (or any component which must be assembled first) then one would expect to see diffuse fluorescence throughout the cell. However, if the Tag proteins are required for the initiation of firing then long extended sheaths would be observed. If the Tag proteins are required for disassembly, then contracted sheaths would be observed.

Schwarz et al. (2014) demonstrated that, unlike other T6SSs which seem to be randomly distributed around the cell, *B.t* T6SS-5 predominantly localises to the poles. This was determined by the localisation of GFP-labelled TssH-5, although the localisation phenotype could also be investigated using fluorescently labelled TssB. Using these experiments, it could be determined whether the Tag proteins were required for the apparently unique polar localisation of T6SS-5.

Another informative experiment to perform with the *B.t tag* mutants would be the *in vivo* TssD assembly assay outlined by Brunet et al. (2014). This uses an engineered TssD which has had its cysteine residues removed. Specific cysteine residues were then introduced to the modified TssD

protein which allowed determination of whether the TssD hexamers have stacked in the correct head-to-tail fashion or randomly (as observed in a mutant lacking all other T6SS components) when cells were oxidised. Using this approach, the same research group were able to determine which T6SS proteins were required for the correct assembly of the TssD inner-tube in *E. coli* EAEC cells (Brunet et al. 2015). Use of a modified version of this assay in *B.t* cells could determine if the Tag proteins are required for correct formation of the TssD inner tube.

Given the fact that genes encoding Tag proteins are often found together (either as a block of all four, or just *tagA* and *tagD*) in T6SS gene clusters, it was surprising that they did not interact in the BACTH assays in the combinations tested. It is possible that the addition of the T25 and T18 domains of the *Bordetella pertussis* adenylate cyclase had a detrimental effect on protein folding. It would therefore be useful to alter the location of the fusions. It might also be necessary to express additional proteins in the *E. coli* reporter strain as the interaction of some T6SS proteins can only be observed in the presence of other proteins, for example, TssF and TssK only interact in the presence of TssG (Brunet et al. 2015).

References

- Abby, S.S. & Rocha, E.P.C., 2012. The non-flagellar type III secretion system evolved from the bacterial flagellum and diversified into host-cell adapted systems. M. Achtman, ed. *PLoS genetics*, 8(9), p.e1002983.
- Abdallah, A.M. et al., 2007. Type VII secretion--mycobacteria show the way. *Nature reviews. Microbiology*, 5(11), pp.883–891.
- Ahmad, A., 2013. *Protein-protein interactions in the bacterial type VI secretion system*. The University of Sheffield.
- Alibek, K. & Handelman, S., 1999. *Biohazard: The Chilling True Story of the Largest Covert Biological Weapons Program in the World: Told from the inside by the Man Who Ran It*, New York: Random House.
- Altindis, E. et al., 2015. Secretome analysis of *Vibrio cholerae* type VI secretion system reveals a new effector-immunity pair. *mBio*, 6(2), p.e00075.
- Alvarez-Martinez, C.E. & Christie, P.J., 2009. Biological diversity of prokaryotic type IV secretion systems. *Microbiology and molecular biology reviews : MMBR*, 73(4), pp.775–808.
- Aschtgen, M.-S. et al., 2008. SciN is an outer membrane lipoprotein required for type VI secretion in enteroaggregative *Escherichia coli*. *Journal of bacteriology*, 190(22), pp.7523–31.
- Aschtgen, M.-S., Thomas, M.S. & Cascales, E., 2010. Anchoring the type VI secretion system to the peptidoglycan: TssL, TagL, TagP... what else? *Virulence*, 1(6), pp.535–540.
- Atkins, T. et al., 2002. Characterisation of an acapsular mutant of *Burkholderia pseudomallei* identified by signature tagged mutagenesis. *Journal of Medical Microbiology*, 51(7), pp.539–547.
- Aubert, D.F., Valvano, M.A. & Hu, S., 2015. Quantification of type VI secretion system activity in macrophages infected with *Burkholderia cenocepacia*. *Microbiology*, 161(11), pp.2161–2173.
- Barnes, J.L. & Ketheesan, N., 2007. Development of protective immunity in a murine model of melioidosis is influenced by the source of *Burkholderia pseudomallei* antigens. *Immunology and cell biology*, 85(7), pp.551–7.
- Barnhart, M.M. & Chapman, M.R., 2006. Curli Biogenesis and Function. *Annual Review of Microbiology*, 60(1), pp.131–147.

- Barrett, A.R. et al., 2008. Genetic tools for allelic replacement in *Burkholderia* species. *Applied and environmental microbiology*, 74(14), pp.4498–508.
- Basler, M. et al., 2012. Type VI secretion requires a dynamic contractile phage tail-like structure. *Nature*, 483(7388), pp.182–186.
- Basler, M., Ho, B.T. & Mekalanos, J.J., 2013. Tit-for-tat: type VI secretion system counterattack during bacterial cell-cell interactions. *Cell*, 152(4), pp.884–94.
- Benanti, E.L., Nguyen, C.M. & Welch, M.D., 2015. Virulent *Burkholderia* species mimic host actin polymerases to drive actin-based motility. *Cell*, 161(2), pp.348–60.
- Bergendahl, V. et al., 2003. A cross-reactive polyol-responsive monoclonal antibody useful for isolation of core RNA polymerase from many bacterial species. *Protein Expression and Purification*, 31(1), pp.155–160.
- Berger, K.H. & Isberg, R.R., 1993. Two distinct defects in intracellular growth complemented by a single genetic locus in *Legionella pneumophila*. *Molecular Microbiology*, 7(1), pp.7–19.
- Bingle, L.E., Bailey, C.M. & Pallen, M.J., 2008. Type VI secretion: a beginner's guide. *Current Opinion in Microbiology*, 11(1), pp.3–8.
- Blondel, C.J. et al., 2009. Comparative genomic analysis uncovers 3 novel loci encoding type six secretion systems differentially distributed in *Salmonella* serotypes. *BMC Genomics*, 10(1), p.354.
- Boddey, J.A. et al., 2007. The bacterial gene *lfpA* influences the potent induction of calcitonin receptor and osteoclast-related genes in *Burkholderia pseudomallei*-induced TRAP-positive multinucleated giant cells. *Cellular Microbiology*, 9(2), pp.514–531.
- Bodilsen, J., Langgaard, H. & Nielsen, H.L., 2015. Cutaneous melioidosis in a healthy Danish man after travelling to South-East Asia. *BMJ Case Reports*, Published .
- Bönemann, G. et al., 2009. Remodelling of *VipA/VipB* tubules by *ClpV*-mediated threading is crucial for type VI protein secretion. *The EMBO Journal*, 28(4), pp.315–325.
- Boyer, F. et al., 2009. Dissecting the bacterial type VI secretion system by a genome wide in silico analysis: what can be learned from available microbial genomic resources? *BMC Genomics*, 10(1), p.104.
- Breitbach, K. et al., 2003. Actin-based motility of *Burkholderia pseudomallei* involves the Arp 2/3 complex, but not N-WASP and Ena/VASP proteins. *Cellular Microbiology*, 5(6), pp.385–393.

- Breitbach, K., Kähler, J. & Steinmetz, I., 2008. Induction of protective immunity against *Burkholderia pseudomallei* using attenuated mutants with defects in the intracellular life cycle. *Transactions of the Royal Society of Tropical Medicine and Hygiene*, 102(SUPPL. 1), pp.4–9.
- Brett, P.J., Deshazer, D. & Woods, D.E., 1997. Characterization of *Burkholderia pseudomallei* and *Burkholderia pseudomallei*-like strains. *Epidemiology and Infection*, 118(2), pp.137–48.
- Brett, P.J., DeShazer, D. & Woods, D.E., 1998. Note: *Burkholderia thailandensis* sp. nov., a *Burkholderia pseudomallei*-like species. *International Journal of Systematic Bacteriology*, 48(1), pp.317–320.
- Brooks, T.M. et al., 2013. Lytic activity of the *Vibrio cholerae* type VI secretion toxin VgrG-3 is inhibited by the antitoxin TsaB. *The Journal of biological chemistry*, 288(11), pp.7618–25.
- Brown, N.F. et al., 2002. Adherence of *Burkholderia pseudomallei* cells to cultured human epithelial cell lines is regulated by growth temperature. *Infection and Immunity*, 70(2), pp.974–980.
- Brunet, Y.R. et al., 2015. The type VI secretion TssEFGK-VgrG phage-like baseplate is recruited to the TssJLM membrane complex via multiple contacts and serves as assembly platform for tail tube/sheath polymerization. P. H. Viollier, ed. *PLoS genetics*, 11(10), p.e1005545.
- Brunet, Y.R. et al., 2014. Type VI secretion and bacteriophage tail tubes share a common assembly pathway. *EMBO Reports*, 15(3), pp.315–321.
- Buchan, D.W.A. et al., 2013. Scalable web services for the PSIPRED Protein Analysis Workbench. *Nucleic Acids Research*, 41(W1), pp.W349–W357.
- Burkinshaw, B.J. & Strynadka, N.C.J., 2014. Assembly and structure of the T3SS. *Biochimica et Biophysica Acta (BBA) - Molecular Cell Research*, 1843(8), pp.1649–1663.
- Burnick, M.N. et al., 2010. *Burkholderia mallei* cluster 1 type VI secretion mutants exhibit growth and actin polymerization defects in RAW 264.7 murine macrophages. *Infection and immunity*, 78(1), pp.88–99.
- Burnick, M.N. et al., 2011. The cluster 1 type VI secretion system is a major virulence determinant in *Burkholderia pseudomallei*. *Infection and Immunity*, 79(4), pp.1512–1525.
- Burnick, M.N. & Brett, P.J., 2013. *Burkholderia mallei* and *Burkholderia pseudomallei* cluster 1 type VI secretion system gene expression is negatively regulated by iron and zinc. *PloS one*, 8(10), p.e76767.

- Burtneck, M.N., Brett, P.J. & DeShazer, D., 2014. Proteomic analysis of the *Burkholderia pseudomallei* type II secretome reveals hydrolytic enzymes, novel proteins, and the deubiquitinase TssM. *Infection and immunity*, 82(8), pp.3214–26.
- Cardona, S.T. & Valvano, M.A., 2005. An expression vector containing a rhamnose-inducible promoter provides tightly regulated gene expression in *Burkholderia cenocepacia*. *Plasmid*, 54(3), pp.219–228.
- de Castro, E. et al., 2006. ScanProsite: detection of PROSITE signature matches and ProRule-associated functional and structural residues in proteins. *Nucleic Acids Research*, 34(Web Server), pp.W362–W365.
- Chanchamroen, S. et al., 2009. Human polymorphonuclear neutrophil responses to *Burkholderia pseudomallei* in healthy and diabetic subjects. *Infection and Immunity*, 77(1), pp.456–463.
- Chen, Y. et al., 2011. Regulation of type VI secretion system during *Burkholderia pseudomallei* infection. *Infection and immunity*, 79(8), pp.3064–73.
- Cheng, A.C. & Currie, B.J., 2005. Melioidosis: Epidemiology, Pathophysiology, and Management. *Clinical Microbiology Reviews*, 18(2), pp.383–416.
- Choy, J.L. et al., 2000. Animal melioidosis in Australia. *Acta Tropica*, 74(2-3), pp.153–158.
- Chua, K.L., Chan, Y.Y. & Gan, Y.H., 2003. Flagella are virulence determinants of *Burkholderia pseudomallei*. *Infection and immunity*, 71(4), pp.1622–9.
- Costa, T.R.D. et al., 2015. Secretion systems in Gram-negative bacteria: structural and mechanistic insights. *Nature Reviews Microbiology*, 13(6), pp.343–359.
- Craig, L., Pique, M.E. & Tainer, J.A., 2004. Type IV pilus structure and bacterial pathogenicity. *Nature Reviews Microbiology*, 2(5), pp.363–378.
- Cruz-Migoni, A. et al., 2011. A *Burkholderia pseudomallei* toxin inhibits helicase activity of translation factor eIF4A. *Science (New York, N.Y.)*, 334(6057), pp.821–4.
- Currie, B.J. et al., 2000. Endemic melioidosis in tropical northern Australia: a 10-year prospective study and review of the literature. *Clinical infectious diseases : an official publication of the Infectious Diseases Society of America*, 31(4), pp.981–6.
- Currie, B.J., Dance, D.A.B. & Cheng, A.C., 2008. The global distribution of *Burkholderia pseudomallei* and melioidosis: an update. *Transactions of the Royal Society of Tropical Medicine and Hygiene*, 102(SUPPL. 1), pp.S1–S4.

- Dance, D., 2014. Treatment and prophylaxis of melioidosis. *International Journal of Antimicrobial Agents*, 43(4), pp.310–318.
- Dance, D.A. et al., 1989. Acute suppurative parotitis caused by *Pseudomonas pseudomallei* in children. *The Journal of infectious diseases*, 159(4), pp.654–60.
- Deitchman, S. & Sokas, R., 2001. Glanders in a military research microbiologist. *The New England journal of medicine*, 345(22), p.1644.
- DeShazer, D. et al., 1997. Mutagenesis of *Burkholderia pseudomallei* with Tn5-OT182: isolation of motility mutants and molecular characterization of the flagellin structural gene. *Journal of bacteriology*, 179(7), pp.2116–25.
- DeShazer, D., 2007. Virulence of clinical and environmental isolates of *Burkholderia oklahomensis* and *Burkholderia thailandensis* in hamsters and mice. *FEMS Microbiology Letters*, 277(1), pp.64–69.
- DeShazer, D., Brett, P.J. & Woods, D.E., 1998. The type II O-antigenic polysaccharide moiety of *Burkholderia pseudomallei* lipopolysaccharide is required for serum resistance and virulence. *Molecular Microbiology*, 30(5), pp.1081–1100.
- Dong, T.G. et al., 2013. Identification of T6SS-dependent effector and immunity proteins by Tn-seq in *Vibrio cholerae*. *Proceedings of the National Academy of Sciences*, 110(7), pp.2623–2628.
- Druar, C. et al., 2008. Evaluating *Burkholderia pseudomallei* Bip proteins as vaccines and Bip antibodies as detection agents. *FEMS Immunology and Medical Microbiology*, 52(1), pp.78–87.
- Durand, E. et al., 2015. Biogenesis and structure of a type VI secretion membrane core complex. *Nature*, 523(7562), pp.555–560.
- Durand, E. et al., 2012. Structural characterization and oligomerization of the TssL protein, a component shared by bacterial type VI and type IVb secretion systems. *The Journal of biological chemistry*, 287(17), pp.14157–68.
- Durand, E. et al., 2014. VgrG, Tae, Tle, and beyond: the versatile arsenal of Type VI secretion effectors. *Trends in Microbiology*, 22(9), pp.498–507.
- Ekpo, P. et al., 2007. Use of protein-specific monoclonal antibody-based latex agglutination for rapid diagnosis of *Burkholderia pseudomallei* infection in patients with community-acquired septicemia. *Clinical and Vaccine Immunology*, 14(6), pp.811–812.

- English, G. et al., 2014. Biochemical analysis of TssK, a core component of the bacterial Type VI secretion system, reveals distinct oligomeric states of TssK and identifies a TssK–TssFG subcomplex. *Biochemical Journal*, 461(2), pp.291–304.
- English, G. et al., 2012. New secreted toxins and immunity proteins encoded within the Type VI secretion system gene cluster of *Serratia marcescens*. *Molecular Microbiology*, 86(4), pp.921–936.
- Essex-Lopresti, A.E. et al., 2005. A type IV pilin, PilA, Contributes To Adherence of *Burkholderia pseudomallei* and virulence in vivo. *Infection and immunity*, 73(2), pp.1260–4.
- Evans, M.L. & Chapman, M.R., 2014. Curli biogenesis: order out of disorder. *Biochimica et biophysica acta*, 1843(8), pp.1551–8.
- Ezzedine, K., Heenen, M. & Malvy, D., 2007. Imported cutaneous melioidosis in traveler, Belgium. *Emerging infectious diseases*, 13(6), pp.946–7.
- Felisberto-Rodrigues, C. et al., 2011. Towards a structural comprehension of bacterial type VI secretion systems: characterization of the TssJ–TssM complex of an *Escherichia coli* pathovar. *PLoS pathogens*, 7(11), p.e1002386.
- Fisher, N.A. et al., 2012. The Madagascar hissing cockroach as a novel surrogate host for *Burkholderia pseudomallei*, *B. mallei* and *B. thailandensis*. *BMC Microbiology*, 12(1), p.117.
- Förster, A. et al., 2014. Coevolution of the ATPase ClpV, the sheath proteins TssB and TssC, and the accessory protein TagJ/HsiE1 distinguishes type VI secretion classes. *The Journal of biological chemistry*, 289(47), pp.33032–43.
- French, C.T. et al., 2011. Dissection of the *Burkholderia* intracellular life cycle using a photothermal nanoblade. *Proceedings of the National Academy of Sciences*, 108(29), pp.12095–12100.
- Galán, J.E. & Wolf-Watz, H., 2006. Protein delivery into eukaryotic cells by type III secretion machines. *Nature*, 444(7119), pp.567–573.
- German, N., Doyscher, D. & Rensing, C., 2013. Bacterial killing in macrophages and amoeba: do they all use a brass dagger? *Future Microbiology*, 8(10), pp.1257–1264.
- Gibney, K.B., Cheng, A.C. & Currie, B.J., 2008. Cutaneous melioidosis in the tropical top end of Australia: a prospective study and review of the literature. *Clinical infectious diseases : an official publication of the Infectious Diseases Society of America*, 47(5), pp.603–9.

- Glass, M.B., Steigerwalt, A.G., et al., 2006. *Burkholderia oklahomensis* sp. nov., a *Burkholderia pseudomallei*-like species formerly known as the Oklahoma strain of *Pseudomonas pseudomallei*. *International Journal of Systematic and Evolutionary Microbiology*, 56(9), pp.2171–2176.
- Glass, M.B., Gee, J.E., et al., 2006. Pneumonia and septicemia caused by *Burkholderia thailandensis* in the United States. *Journal of clinical microbiology*, 44(12), pp.4601–4.
- Godoy, D. et al., 2003. Multilocus sequence typing and evolutionary relationships among the causative agents of melioidosis and glanders, *Burkholderia pseudomallei* and *Burkholderia mallei*. *Journal of clinical microbiology*, 41(5), pp.2068–79.
- Goujon, M. et al., 2010. A new bioinformatics analysis tools framework at EMBL-EBI. *Nucleic Acids Research*, 38(Web Server), pp.W695–W699.
- Green, R.N. & Tuffnell, P.G., 1968. Laboratory acquired melioidosis. *The American journal of medicine*, 44(4), pp.599–605.
- Guglielmini, J., de la Cruz, F. & Rocha, E.P.C., 2013. Evolution of conjugation and type IV secretion systems. *Molecular biology and evolution*, 30(2), pp.315–31.
- Haldimann, A., Daniels, L.L. & Wanner, B.L., 1998. Use of new methods for construction of tightly regulated arabinose and rhamnose promoter fusions in studies of the *Escherichia coli* phosphate regulon. *Journal of bacteriology*, 180(5), pp.1277–86.
- Hanahan, D., 1983. Studies on transformation of *Escherichia coli* with plasmids. *Journal of Molecular Biology*, 166(4), pp.557–580.
- Harley, V.S. et al., 1998. Effects of *Burkholderia pseudomallei* and other *Burkholderia* species on eukaryotic cells in tissue culture. *Microbios*, 96(384), pp.71–93.
- Heckman, K.L. & Pease, L.R., 2007. Gene splicing and mutagenesis by PCR-driven overlap extension. *Nature Protocols*, 2(4), pp.924–932.
- Henderson, I.R. & Nataro, J.P., 2001. Virulence functions of autotransporter proteins. *Infection and immunity*, 69(3), pp.1231–43.
- Henry, T. et al., 2006. The *Salmonella* effector protein PipB2 is a linker for kinesin-1. *Proceedings of the National Academy of Sciences*, 103(36), pp.13497–13502.
- Higgins, C.F., 1992. ABC transporters: from microorganisms to man. *Annual review of cell biology*, 8(1), pp.67–113.

- Holden, M.T.G. et al., 2004. Genomic plasticity of the causative agent of melioidosis, *Burkholderia pseudomallei*. *Proceedings of the National Academy of Sciences*, 101(39), pp.14240–14245.
- Hopf, V. et al., 2014. BPSS1504, a cluster 1 type VI secretion gene, is involved in intracellular survival and virulence of *Burkholderia pseudomallei*. *Infection and immunity*, 82(5), pp.2006–15.
- Horton, R.M. et al., 1989. Engineering hybrid genes without the use of restriction enzymes: gene splicing by overlap extension. *Gene*, 77(1), pp.61–68.
- Houghton, R.L. et al., 2014. Development of a prototype lateral flow immunoassay (LFI) for the rapid diagnosis of melioidosis. *PLoS neglected tropical diseases*, 8(3), p.e2727.
- Inglis, T.J.J. et al., 2003. Flagellum-mediated adhesion by *Burkholderia pseudomallei* precedes invasion of *Acanthamoeba astronyxis*. *Infection and immunity*, 71(4), pp.2280–2.
- Jiang, F. et al., 2014. A *Pseudomonas aeruginosa* type VI secretion phospholipase D effector targets both prokaryotic and eukaryotic cells. *Cell Host and Microbe*, 15(5), pp.600–610.
- Jilani, M.S.A. et al., 2016. *Burkholderia pseudomallei*: Its detection in soil and seroprevalence in Bangladesh. P. L. C. Small, ed. *PLoS neglected tropical diseases*, 10(1), p.e0004301.
- Jobichen, C. et al., 2010. Structural basis for the secretion of EvpC: a key type VI secretion system protein from *Edwardsiella tarda*. *PloS one*, 5(9), p.e12910.
- Jones, P. et al., 2014. InterProScan 5: genome-scale protein function classification. *Bioinformatics*, 30(9), pp.1236–1240.
- Kanamaru, S. et al., 2002. Structure of the cell-puncturing device of bacteriophage T4. *Nature*, 415(6871), pp.553–557.
- Kanonenberg, K., Schwarz, C.K.W. & Schmitt, L., 2013. Type I secretion systems – a story of appendices. *Research in Microbiology*, 164(6), pp.596–604.
- Karimova, G. et al., 1998. A bacterial two-hybrid system based on a reconstituted signal transduction pathway. *Proceedings of the National Academy of Sciences*, 95(10), pp.5752–5756.
- Katangwe, T. et al., 2013. Human melioidosis, Malawi, 2011. *Emerging infectious diseases*, 19(6), pp.981–4.
- Kelley, L.A. et al., 2015. The Phyre2 web portal for protein modeling, prediction and analysis. *Nature Protocols*, 10(6), pp.845–858.

- Kespichayawattana, W. et al., 2000. *Burkholderia pseudomallei* induces cell fusion and actin-associated membrane protrusion: a possible mechanism for cell-to-cell spreading. *Infection and immunity*, 68(9), pp.5377–84.
- Kespichayawattana, W. et al., 2004. Virulent *Burkholderia pseudomallei* is more efficient than avirulent *Burkholderia thailandensis* in invasion of and adherence to cultured human epithelial cells. *Microbial Pathogenesis*, 36(5), pp.287–292.
- Khan, I. et al., 2013. Glanders in animals: a review on epidemiology, clinical presentation, diagnosis and countermeasures. *Transboundary and emerging diseases*, 60(3), pp.204–21.
- Knodler, L. a. et al., 2004. *Salmonella* type III effectors PipB and PipB2 are targeted to detergent-resistant microdomains on internal host cell membranes. *Molecular Microbiology*, 49(3), pp.685–704.
- Knodler, L.A. et al., 2002. *Salmonella* effectors within a single pathogenicity island are differentially expressed and translocated by separate type III secretion systems. *Molecular Microbiology*, 43(5), pp.1089–1103.
- Korotkov, K. V, Sandkvist, M. & Hol, W.G.J., 2012. The type II secretion system: biogenesis, molecular architecture and mechanism. *Nature reviews. Microbiology*, 10(5), pp.336–51.
- Kovach, M.E. et al., 1995. Four new derivatives of the broad-host-range cloning vector pBBR1MCS, carrying different antibiotic-resistance cassettes. *Gene*, 166(1), pp.175–176.
- Kube, S. et al., 2014. Structure of the VipA/B type VI secretion complex suggests a contraction-state-specific recycling mechanism. *Cell reports*, 8(1), pp.20–30.
- Lazar Adler, N.R. et al., 2015. Systematic mutagenesis of genes encoding predicted autotransported proteins of *Burkholderia pseudomallei* identifies factors mediating virulence in mice, net intracellular replication and a novel protein conferring serum resistance. *PloS one*, 10(4), p.e0121271.
- Leiman, P.G. et al., 2009. Type VI secretion apparatus and phage tail-associated protein complexes share a common evolutionary origin. *Proceedings of the National Academy of Sciences*, 106(11), pp.4154–4159.
- Leiman, P.G. & Shneider, M.M., 2012. Contractile tail machines of bacteriophages. *Advances in experimental medicine and biology*, 726, pp.93–114.

- Leo, J.C., Grin, I. & Linke, D., 2012. Type V secretion: mechanism(s) of autotransport through the bacterial outer membrane. *Philosophical Transactions of the Royal Society B: Biological Sciences*, 367(1592), pp.1088–1101.
- Lertpatanasuwan, N. et al., 1999. Arabinose-positive *Burkholderia pseudomallei* infection in humans: case report. *Clinical infectious ...*, 28(4), pp.927–928.
- Lery, L.M.S. et al., 2014. Comparative analysis of *Klebsiella pneumoniae* genomes identifies a phospholipase D family protein as a novel virulence factor. *BMC biology*, 12(1), p.41.
- Leyton, D.L., Rossiter, A.E. & Henderson, I.R., 2012. From self sufficiency to dependence: mechanisms and factors important for autotransporter biogenesis. *Nature Reviews Microbiology*, 10(3), pp.213–225.
- Li, W. et al., 2015. The EMBL-EBI bioinformatics web and programmatic tools framework. *Nucleic Acids Research*, 43(W1), pp.W580–W584.
- Limmathurotsakul, D., Jansen, K., et al., 2010. Defining the true sensitivity of culture for the diagnosis of melioidosis using Bayesian latent class models. *PloS one*, 5(8), p.e12485.
- Limmathurotsakul, D., Wongratanacheewin, S., et al., 2010. Increasing incidence of Human Melioidosis in Northeast Thailand. *American Journal of Tropical Medicine and Hygiene*, 82(6), pp.1113–1117.
- Limmathurotsakul, D. et al., 2014. Melioidosis caused by *Burkholderia pseudomallei* in drinking water, Thailand, 2012. *Emerging infectious diseases*, 20(2), pp.265–8.
- Limmathurotsakul, D. et al., 2016. Predicted global distribution of *Burkholderia pseudomallei* and burden of melioidosis. *Nature Microbiology*, 1(1), p.15008.
- Limmathurotsakul, D. & Peacock, S.J., 2011. Melioidosis: a clinical overview. *British Medical Bulletin*, 99(1), pp.125–139.
- Lin, J.-S., Ma, L.-S. & Lai, E.-M., 2013. Systematic dissection of the *Agrobacterium* type VI secretion system reveals machinery and secreted components for subcomplex formation. A. Roujeinikova, ed. *PloS one*, 8(7), p.e67647.
- Lossi, N.S. et al., 2013. The HsiB1C1 (TssB-TssC) complex of the *Pseudomonas aeruginosa* type VI secretion system forms a bacteriophage tail sheathlike structure. *The Journal of biological chemistry*, 288(11), pp.7536–48.

- Lycklama a Nijeholt, J. a. & Driessen, a. J.M., 2012. The bacterial Sec-translocase: structure and mechanism. *Philosophical Transactions of the Royal Society B: Biological Sciences*, 367(1592), pp.1016–1028.
- Ma, A.T. & Mekalanos, J.J., 2010. In vivo actin cross-linking induced by *Vibrio cholerae* type VI secretion system is associated with intestinal inflammation. *Proceedings of the National Academy of Sciences*, 107(9), pp.4365–4370.
- Ma, L.-S. et al., 2014. *Agrobacterium tumefaciens* deploys a superfamily of type VI secretion DNase effectors as weapons for interbacterial competition in planta. *Cell host & microbe*, 16(1), pp.94–104.
- Ma, L.-S., Lin, J.-S. & Lai, E.-M., 2009. An IcmF family protein, ImpLM, is an integral inner membrane protein interacting with ImpKL, and its walker a motif is required for type VI secretion system-mediated Hcp secretion in *Agrobacterium tumefaciens*. *Journal of bacteriology*, 191(13), pp.4316–29.
- Mahan, M.J., Slauch, J.M. & Mekalanos, J.J., 1993. Selection of bacterial virulence genes that are specifically induced in host tissues. *Science*, 259(5095), pp.686–688.
- Marlovits, T.C. & Stebbins, C.E., 2010. Type III secretion systems shape up as they ship out. *Current Opinion in Microbiology*, 13(1), pp.47–52.
- Mays, E.E.E. & Ricketts, E.A., 1975. Melioidosis: recrudescence associated with bronchogenic carcinoma twenty-six years following initial geographic exposure. *Chest*, 68(2), pp.261–263.
- McBride, M.J. & Zhu, Y., 2013. Gliding motility and Por secretion system genes are widespread among members of the phylum *Bacteroidetes*. *Journal of bacteriology*, 195(2), pp.270–8.
- McCormick, J.B. et al., 1977. Wound Infection by an Indigenous *Pseudomonas pseudomallei*-Like Organism Isolated from the Soil: Case Report and Epidemiologic Study. *Journal of Infectious Diseases*, 135(1), pp.103–107.
- Meumann, E.M. et al., 2006. Clinical evaluation of a type III secretion system real-time PCR assay for diagnosing melioidosis. *Journal of Clinical Microbiology*, 44(8), pp.3028–3030.
- Meumann, E.M. et al., 2012. Clinical features and epidemiology of melioidosis pneumonia: results from a 21-year study and review of the literature. *Clinical infectious diseases: an official publication of the Infectious Diseases Society of America*, 54(3), pp.362–9.

- Miyata, S.T. et al., 2013. Dual expression profile of type VI secretion system immunity genes protects pandemic *Vibrio cholerae*. J. D. Mougous, ed. *PLoS pathogens*, 9(12), p.e1003752.
- Miyazaki, K., 2015. Molecular engineering of a PheS counterselection marker for improved operating efficiency in *Escherichia coli*. *BioTechniques*, 58(2), pp.86–88.
- Moore, R. a et al., 1999. Efflux-mediated aminoglycoside and macrolide resistance in *Burkholderia pseudomallei*. *Antimicrobial agents and chemotherapy*, 43(3), pp.465–70.
- Morrison, R.E. et al., 1988. Melioidosis: a reminder. *The American journal of medicine*, 84(5), pp.965–7.
- Mougous, J.D., 2006. A virulence locus of *Pseudomonas aeruginosa* encodes a protein secretion apparatus intergovernmental panel on climate change, ed. *Science*, 312(5779), pp.1526–1530.
- Murdoch, S.L. et al., 2011. The opportunistic pathogen *Serratia marcescens* utilizes type VI secretion to target bacterial competitors. *Journal of Bacteriology*, 193(21), pp.6057–6069.
- Natale, P., Brüser, T. & Driessen, A.J.M., 2008. Sec- and Tat-mediated protein secretion across the bacterial cytoplasmic membrane—Distinct translocases and mechanisms. *Biochimica et Biophysica Acta (BBA) - Biomembranes*, 1778(9), pp.1735–1756.
- Ngauy, V. et al., 2005. Cutaneous melioidosis in a man who was taken as a prisoner of war by the Japanese during World War II. *Journal of clinical microbiology*, 43(2), pp.970–2.
- Nierman, W.C. et al., 2004. Structural flexibility in the *Burkholderia mallei* genome. *Proceedings of the National Academy of Sciences*, 101(39), pp.14246–14251.
- Nivaskumar, M. & Francetic, O., 2014. Type II secretion system: A magic beanstalk or a protein escalator. *Biochimica et Biophysica Acta (BBA) - Molecular Cell Research*, 1843(8), pp.1568–1577.
- Nussbaum, J.J., Hull, D.S. & Carter, M.J., 1980. *Pseudomonas pseudomallei* in an anophthalmic orbit. *Archives of ophthalmology (Chicago, Ill. : 1960)*, 98(7), pp.1224–5.
- Osipiuk, J. et al., 2011. Crystal structure of secretory protein Hcp3 from *Pseudomonas aeruginosa*. *Journal of Structural and Functional Genomics*, 12(1), pp.21–26.
- Patterson, M.C., 1967. Acute melioidosis in a soldier home from South Vietnam. *JAMA: The Journal of the American Medical Association*, 200(6), pp.447–451.
- Perry, M.B. et al., 1995. Structural characterization of the lipopolysaccharide O antigens of *Burkholderia pseudomallei*. *Infection and Immunity*, 63(9), pp.3348–3352.

- Pieper, R. et al., 2009. Temperature and growth phase influence the outer-membrane proteome and the expression of a type VI secretion system in *Yersinia pestis*. *Microbiology*, 155(2), pp.498–512.
- Podnecky, N.L. et al., 2013. The BpeEF-OprC efflux pump is responsible for widespread trimethoprim resistance in clinical and environmental *Burkholderia pseudomallei* isolates. *Antimicrobial Agents and Chemotherapy*, 57(9), pp.4381–4386.
- Pukatzki, S. et al., 2006. Identification of a conserved bacterial protein secretion system in *Vibrio cholerae* using the *Dictyostelium* host model system. *Proceedings of the National Academy of Sciences*, 103(5), pp.1528–1533.
- Pukatzki, S. et al., 2007. Type VI secretion system translocates a phage tail spike-like protein into target cells where it cross-links actin. *Proceedings of the National Academy of Sciences*, 104(39), pp.15508–15513.
- Pumpuang, A. et al., 2011. Survival of *Burkholderia pseudomallei* in distilled water for 16 years. *Transactions of the Royal Society of Tropical Medicine and Hygiene*, 105(10), pp.598–600.
- Radics, J., Königsmaier, L. & Marlovits, T.C., 2013. Structure of a pathogenic type 3 secretion system in action. *Nature Structural & Molecular Biology*, 21(1), pp.82–87.
- Reckseidler, S.L. et al., 2001. Detection of bacterial virulence genes by subtractive hybridization: identification of capsular polysaccharide of *Burkholderia pseudomallei* as a major virulence determinant. *Infection and immunity*, 69(1), pp.34–44.
- Reckseidler-Zenteno, S.L., DeVinney, R. & Woods, D.E., 2005. The capsular polysaccharide of *Burkholderia pseudomallei* contributes to survival in serum by reducing complement factor C3b deposition. *Infection and immunity*, 73(2), pp.1106–15.
- Rhomberg, T.A. et al., 2009. A translocated protein of *Bartonella henselae* interferes with endocytic uptake of individual bacteria and triggers uptake of large bacterial aggregates via the invasome. *Cellular Microbiology*, 11(6), pp.927–945.
- Richardson, L.J. et al., 2012. Towards a rapid molecular diagnostic for melioidosis: Comparison of DNA extraction methods from clinical specimens. *Journal of Microbiological Methods*, 88(1), pp.179–181.
- Robertson, G. et al., 2015. Rapid diagnostics for melioidosis: A comparative study of a novel lateral flow antigen detection assay. *Journal of Medical Microbiology*, 64(8), pp.845–848.

- Rotz, L.D. et al., 2002. Public health assessment of potential biological terrorism agents. *Emerging infectious diseases*, 8(2), pp.225–30.
- Russell, A.B. et al., 2012. A widespread bacterial type VI secretion effector superfamily identified using a heuristic approach. *Cell host & microbe*, 11(5), pp.538–49.
- Russell, A.B. et al., 2013. Diverse type VI secretion phospholipases are functionally plastic antibacterial effectors. *Nature*, 496(7446), pp.508–512.
- Russell, A.B. et al., 2011. Type VI secretion delivers bacteriolytic effectors to target cells. *Nature*, 475(7356), pp.343–347.
- Saiki, K. & Konishi, K., 2007. Identification of a *Porphyromonas gingivalis* novel protein sov required for the secretion of gingipains. *Microbiology and immunology*, 51(5), pp.483–91.
- Sánchez, J. & Holmgren, J., 2008. Cholera toxin structure, gene regulation and pathophysiological and immunological aspects. *Cellular and Molecular Life Sciences*, 65(9), pp.1347–1360.
- Sato, H. & Frank, D.W., 2011. Multi-functional characteristics of the *Pseudomonas aeruginosa* type III needle-tip protein, PcrV; comparison to orthologs in other Gram-negative bacteria. *Frontiers in Microbiology*, 2, p.142.
- Sato, K. et al., 2010. A protein secretion system linked to bacteroidete gliding motility and pathogenesis. *Proceedings of the National Academy of Sciences*, 107(1), pp.276–281.
- Schell, M.A. et al., 2007. Type VI secretion is a major virulence determinant in *Burkholderia mallei*. *Molecular Microbiology*, 64(6), pp.1466–1485.
- Schlech, W.F. et al., 1981. Laboratory-acquired infection with *Pseudomonas pseudomallei* (melioidosis). *The New England journal of medicine*, 305(19), pp.1133–5.
- Schraidt, O. & Marlovits, T.C., 2011. Three-dimensional model of *Salmonella*'s needle complex at subnanometer resolution. *Science (New York, N.Y.)*, 331(6021), pp.1192–5.
- Schrodinger LLC, 2015. The PyMOL Molecular Graphics System, Version 1.8.
- Schwarz, S. et al., 2010. *Burkholderia* type VI secretion systems have distinct roles in eukaryotic and bacterial cell interactions. P. J. Christie, ed. *PLoS pathogens*, 6(8), p.e1001068.
- Schwarz, S. et al., 2014. VgrG-5 is a *Burkholderia* type VI secretion system-exported protein required for multinucleated giant cell formation and virulence. *Infection and immunity*, 82(4), pp.1445–52.

- Schweizer, H.P., 2012. Mechanisms of antibiotic resistance in *Burkholderia pseudomallei* : implications for treatment of melioidosis. *Future Microbiology*, 7(12), pp.1389–1399.
- Shalom, G., Shaw, J.G. & Thomas, M.S., 2007. In vivo expression technology identifies a type VI secretion system locus in *Burkholderia pseudomallei* that is induced upon invasion of macrophages. *Microbiology*, 153(8), pp.2689–2699.
- Sharrer, G.T., 1995. The great glanders epizootic, 1861-1866: a Civil War legacy. *Agricultural history*, 69(1), pp.79–97.
- Shneider, M.M. et al., 2013. PAAR-repeat proteins sharpen and diversify the type VI secretion system spike. *Nature*, 500(7462), pp.350–353.
- Sievers, F. et al., 2014. Fast, scalable generation of high-quality protein multiple sequence alignments using Clustal Omega. *Molecular Systems Biology*, 7(1), pp.539–539.
- Sikora, A.E. et al., 2011. Proteomic analysis of the *Vibrio cholerae* type II secretome reveals new proteins, including three related serine proteases. *The Journal of biological chemistry*, 286(19), pp.16555–66.
- Silva, E.B. & Dow, S.W., 2013. Development of *Burkholderia mallei* and *pseudomallei* vaccines. *Frontiers in cellular and infection microbiology*, 3(March), p.10.
- Silverman, J.M. et al., 2013. Haemolysin coregulated protein is an exported receptor and chaperone of type VI secretion substrates. *Molecular cell*, 51(5), pp.584–93.
- Simon, R., Priefer, U. & Pühler, A., 1983. A Broad Host Range Mobilization System for In Vivo Genetic Engineering: Transposon Mutagenesis in Gram Negative Bacteria. *Bio/Technology*, 1(9), pp.784–791.
- Simpson, A.J.H., 2000. Interaction of insulin with *Burkholderia pseudomallei* may be caused by a preservative. *Journal of Clinical Pathology*, 53(2), pp.159–160.
- Sitthidet, C. et al., 2011. Identification of motifs of *Burkholderia pseudomallei* BimA required for intracellular motility, actin binding, and actin polymerization. *Journal of bacteriology*, 193(8), pp.1901–10.
- Smith, M.D. et al., 1997. Arabinose assimilation defines a nonvirulent biotype of *Burkholderia pseudomallei*. *Infection and Immunity*, 65(10), pp.4319–4321.
- Spiewak, H.L., 2016. *Identifying novel secreted effectors of the type VI protein secretion system in Burkholderia cenocepacia*. The University of Sheffield.

- Spínola-Amilibia, M. et al., 2016. The structure of VgrG1 from *Pseudomonas aeruginosa*, the needle tip of the bacterial type VI secretion system. *Acta Crystallographica Section D Structural Biology*, 72(1), pp.22–33.
- Sprague, L.D. & Neubauer, H., 2004. Melioidosis in animals: a review on epizootiology, diagnosis and clinical presentation. *Journal of veterinary medicine. B, Infectious diseases and veterinary public health*, 51(7), pp.305–20.
- Srikannathasan, V. et al., 2013. Structural basis for type VI secreted peptidoglycan DL-endopeptidase function, specificity and neutralization in *Serratia marcescens*. *Acta Crystallographica Section D Biological Crystallography*, 69(12), pp.2468–2482.
- Stalder, E.S. et al., 2011. The epitope for the polyol-responsive monoclonal antibody 8RB13 is in the flap-domain of the beta-subunit of bacterial RNA polymerase and can be used as an epitope tag for immunoaffinity chromatography. *Protein Expression and Purification*, 77(1), pp.26–33.
- Stevens, J.M. et al., 2005. Actin-binding proteins from *Burkholderia mallei* and *Burkholderia thailandensis* can functionally compensate for the actin-based motility defect of a *Burkholderia pseudomallei* *bimA* mutant. *Journal of Bacteriology*, 187(22), pp.7857–7862.
- Stevens, M.P. et al., 2002. An Inv/Mxi-Spa-like type III protein secretion system in *Burkholderia pseudomallei* modulates intracellular behaviour of the pathogen. *Molecular Microbiology*, 46(3), pp.649–659.
- Stevens, M.P., 2004. Attenuated virulence and protective efficacy of a *Burkholderia pseudomallei* bsa type III secretion mutant in murine models of melioidosis. *Microbiology*, 150(8), pp.2669–2676.
- Stevens, M.P. et al., 2005. Identification of a bacterial factor required for actin-based motility of *Burkholderia pseudomallei*. *Molecular microbiology*, 56(1), pp.40–53.
- Studier, F.W. & Moffatt, B. a, 1986. Use of bacteriophage T7 RNA polymerase to direct selective high-level expression of cloned genes. *Journal of Molecular Biology*, 189(1), pp.113–130.
- Suarez, G. et al., 2010. A type VI secretion system effector protein, VgrG1, from *Aeromonas hydrophila* that induces host cell toxicity by ADP ribosylation of actin. *Journal of bacteriology*, 192(1), pp.155–68.
- Suparak, S. et al., 2005. Multinucleated giant cell formation and apoptosis in infected host cells is mediated by *Burkholderia pseudomallei* type III secretion protein BipB. *Journal of bacteriology*, 187(18), pp.6556–60.

- Suputtamongkol, Y. et al., 1999. Risk factors for melioidosis and bacteremic melioidosis. *Clinical infectious diseases : an official publication of the Infectious Diseases Society of America*, 29(2), pp.408–13.
- Tandhavanant, S. et al., 2013. Monoclonal antibody-based immunofluorescence microscopy for the rapid identification of *Burkholderia pseudomallei* in clinical specimens. *The American journal of tropical medicine and hygiene*, 89(1), pp.165–8.
- Thomas, S., Holland, I.B. & Schmitt, L., 2014. The Type 1 secretion pathway — The hemolysin system and beyond. *Biochimica et Biophysica Acta (BBA) - Molecular Cell Research*, 1843(8), pp.1629–1641.
- Toesca, I.J., French, C.T. & Miller, J.F., 2014. The type VI secretion system spike protein VgrG5 mediates membrane fusion during intercellular spread by pseudomallei group *Burkholderia* species. *Infection and immunity*, 82(4), pp.1436–1444.
- Tuanyok, A. et al., 2007. A horizontal gene transfer event defines two distinct groups within *Burkholderia pseudomallei* that have dissimilar geographic distributions. *Journal of bacteriology*, 189(24), pp.9044–9.
- Utaisincharoen, P. et al., 2006. *Burkholderia pseudomallei* RpoS regulates multinucleated giant cell formation and inducible nitric oxide synthase expression in mouse macrophage cell line (RAW 264.7). *Microbial Pathogenesis*, 40(4), pp.184–189.
- Utaisincharoen, P. et al., 2003. Involvement of beta interferon in enhancing inducible nitric oxide synthase production and antimicrobial activity of *Burkholderia pseudomallei*-infected macrophages. *Infection and immunity*, 71(6), pp.3053–7.
- Vetting, M.M.W. et al., 2006. Pentapeptide repeat proteins. *Biochemistry*, 45(1), pp.1–10.
- Vetting, M.W. et al., 2011. Structure of QnrB1, a plasmid-mediated fluoroquinolone resistance factor. *Journal of Biological Chemistry*, 286(28), pp.25265–25273.
- Wand, M.E. et al., 2011. Macrophage and *Galleria mellonella* infection models reflect the virulence of naturally occurring isolates of *B. pseudomallei*, *B. thailandensis* and *B. oklahomensis*. *BMC Microbiology*, 11(1), p.11.
- Wheelis, M., 1998. First shots fired in biological warfare. *Nature*, 395(6699), p.213.
- Whitmore, A., 1913. An Account of a Glanders-like Disease occurring in Rangoon. *The Journal of hygiene*, 13(1), pp.1–34.1.

- Whitmore, A. & Krishnaswami, C., 1912. An account of the discovery of a hitherto undescribed infective disease occurring among the population of Rangoon. *Indian Medical Gazette*, 47, pp.262–267.
- Whitney, J.C. et al., 2013. Identification, structure, and function of a novel type VI secretion peptidoglycan glycoside hydrolase effector-immunity pair. *The Journal of biological chemistry*, 288(37), pp.26616–24.
- Wiersinga, W.J. et al., 2006. Melioidosis: insights into the pathogenicity of *Burkholderia pseudomallei*. *Nature Reviews Microbiology*, 4(4), pp.272–282.
- Wiersinga, W.J., Currie, B.J. & Peacock, S.J., 2012. Melioidosis. *New England Journal of Medicine*, 367(11), pp.1035–1044.
- Wikraiphat, C. et al., 2009. Comparative in vivo and in vitro analyses of putative virulence factors of *Burkholderia pseudomallei* using lipopolysaccharide, capsule and flagellin mutants. *FEMS Immunology and Medical Microbiology*, 56(3), pp.253–259.
- Williams, N.L. et al., 2014. Migration of dendritic cells facilitates systemic dissemination of *Burkholderia pseudomallei*. *Infection and immunity*, 82(10), pp.4233–40.
- Williams, S.G. et al., 1996. *Vibrio cholerae* Hcp, a secreted protein coregulated with HlyA. *Infection and immunity*, 64(1), pp.283–289.
- Winsor, G.L. et al., 2008. The *Burkholderia* Genome Database: facilitating flexible queries and comparative analyses. *Bioinformatics*, 24(23), pp.2803–2804.
- Wong, J., Chen, Y. & Gan, Y.H., 2015. Host cytosolic glutathione sensing by a membrane histidine kinase activates the type VI secretion system in an intracellular bacterium. *Cell Host and Microbe*, 18(1), pp.38–48.
- Wong, K.T., Puthuchery, S.D. & Vadivelu, J., 1995. The histopathology of human melioidosis. *Histopathology*, 26(1), pp.51–55.
- Woods, D.E., Jones, A.L. & Hill, P.J., 1993. Interaction of insulin with *Pseudomonas pseudomallei*. *Infection and Immunity*, 61(10), pp.4045–4050.
- Wright, K.J., Seed, P.C. & Hultgren, S.J., 2007. Development of intracellular bacterial communities of uropathogenic *Escherichia coli* depends on type 1 pili. *Cellular Microbiology*, 9(9), pp.2230–2241.

- Wuthiekanun, V. et al., 2011. Survey of antimicrobial resistance in clinical *Burkholderia pseudomallei* isolates over two decades in Northeast Thailand. *Antimicrobial Agents and Chemotherapy*, 55(11), pp.5388–5391.
- Yabuuchi, E. et al., 1992. Proposal of *Burkholderia* gen. nov. and transfer of seven species of the genus *Pseudomonas* homology group II to the new genus, with the type species *Burkholderia cepacia* (Palleroni and Holmes 1981) comb. nov. *Microbiology and Immunology*, 36(12), pp.1251–1275.
- Yanisch-Perron, C., Vieira, J. & Messing, J., 1985. Improved M13 phage cloning vectors and host strains: nucleotide sequences of the M13mpl8 and pUC19 vectors. *Gene*, 33(1), pp.103–119.
- Yu, N.Y. et al., 2010. PSORTb 3.0: improved protein subcellular localization prediction with refined localization subcategories and predictive capabilities for all prokaryotes. *Bioinformatics*, 26(13), pp.1608–1615.
- Van Zandt, K.E., Greer, M.T. & Gelhaus, H., 2013. Glanders: an overview of infection in humans. *Orphanet Journal of Rare Diseases*, 8(1), p.131.
- Zheng, J. & Leung, K.Y., 2007. Dissection of a type VI secretion system in *Edwardsiella tarda*. *Molecular Microbiology*, 66(5), pp.1192–1206.
- Zoued, A. et al., 2016. Priming and polymerization of a bacterial contractile tail structure. *Nature*, 531(7592), pp.59–63.
- Zoued, A. et al., 2013. TssK is a trimeric cytoplasmic protein interacting with components of both phage-like and membrane anchoring complexes of the Type VI secretion system. *The Journal of biological chemistry*, 288(38), pp.27031–27041.

Appendix

10.1 Accession numbers

Table 10.1 Accession numbers of proteins used in alignments

Abbreviation	Accession Number	Abbreviation	Accession Number
AfGpV	AAK86272	BtTssA-1	ABC36834
AfTagA	AAK89756	BtTssA-5	ABC34267
AfTagD	AAK89757	EcPAAR	AAN80342
AfTssA	AAK89097	EcTagA	ABE05757
AhTssA	ABK39115	EcTagD	ABE05758
AvTagA	ACO78834	EpGpV	AAD03282
AvTagB	ACO78833	EpPAAR	AEM00814
AvTagC	ACO78832	EtTssA	AIJ10501
AvTagD	ACO78831	LfTagA	BAM07954
BbTagA	CAE31294	LfTagB	BAM07955
BbTagB	CAE31295	LfTagC	BAM07956
BbTagC	CAE31305	LfTagD	BAM07957
BbTagD	CAE31296	PaGpV	AAG04005
BbTssA	CAE31298	PaTagA	AAG03487
BcTagA	CAR51595	PaTagD	AAG03489
BcTagD	CAR51596	PaTssA	AAG03472
BcTssA	CAR50658	RITagA	CAK12190
BmTssA-5	AAU46916	RITagD	CAK12191
BpTagA-3	CAH37627	SePAAR	CAX67965
BpTagB-3	CAH37628	SmmTagA	CDG12822
BpTagC-3	CAH37629	SmmTagB	CDG12823
BpTagD-3	CAH37630	SmmTagC	CDG12824
BtGpV	ABC35841	SmmTagD	CDG12825
BtTagA-4	ABC35410	VcPAAR	AAF96019
BtTagA-5	ABC35832	VpTagA	BAC59661
BtTagB-4	ABC34591	VpTagD	BAC59678
BtTagB-5	ABC35356	YpTagA	CAH19889
BtTagC-4	ABC33959	YpTagB	CAH19890
BtTagC-5	ABC34658	YpTagC	CAH19891
BtTagD-4	ABC35777	YpTagD	CAH19892
BtTagD-5	ABC34315	YpTssA	CAH19880

10.2 Ladders

10.2.1 DNA ladders

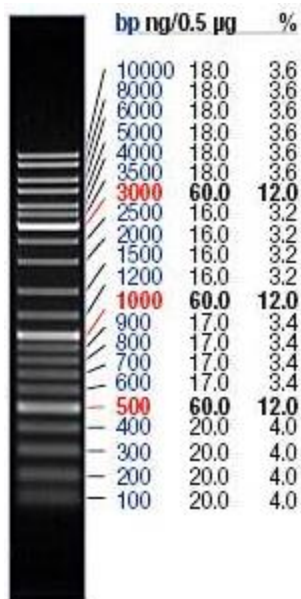


Figure 10.1 GeneRuler DNA ladder mix

DNA ladder used for size estimation and rough quantification of linear DNA run on agarose gels, supplied by Fisher Scientific.

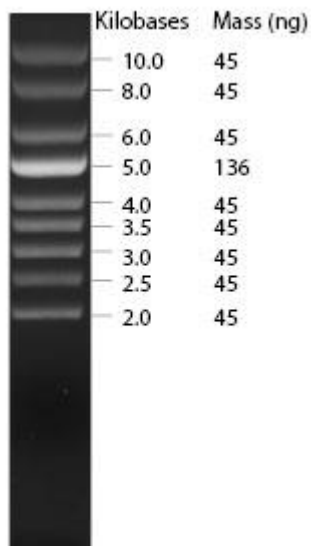


Figure 10.2 Supercoiled DNA ladder

DNA ladder used for size estimation and rough quantification of supercoiled plasmid DNA run on agarose gels, supplied by New England Biolabs.

10.2.2 Protein ladders

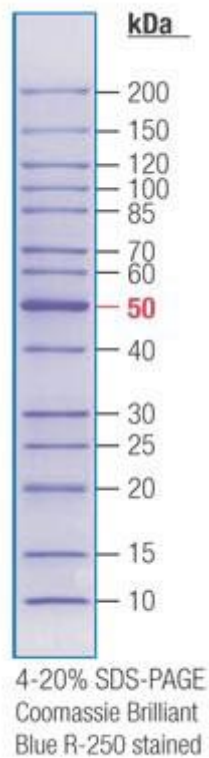


Figure 10.3 EZ-Run Rec protein ladder.

Protein ladder used for the size estimation of proteins run by SDS-PAGE and stained with Coomassie blue, supplied by Fisher scientific.

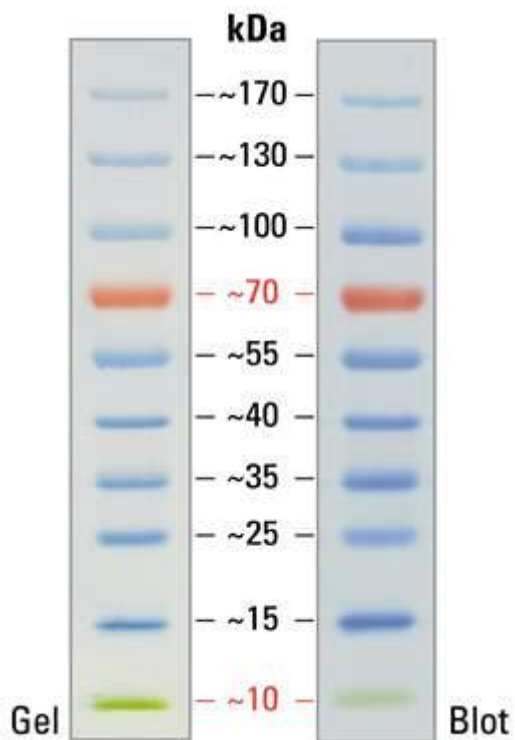


Figure 10.4 EZ-Run Rec prestained ladder

Protein ladder used for the size estimation of proteins run by SDS-PAGE and western blotted, supplied by Fisher scientific.

Table 10.2 Locus tags of T6SS-5 genes in *B.p*, *B.t* and *B.m*

Gene name	Locus tag		
	<i>B. pseudomallei</i> K96243	<i>B. thailandensis</i> E264	<i>B. mallei</i> ATCC 23344
<i>tssA-5</i>	BPSS1493	BTH_II0873	BMAA0747
<i>virG</i>	BPSS1494	BTH_II0872	BMAA0746
<i>virA</i>	BPSS1495	BTH_II0871	BMAA0745
<i>tssB-5</i>	BPSS1496	BTH_II0870	BMAA0744
<i>tssC-5</i>	BPSS1497	BTH_II0869	BMAA0743
<i>tssD-5</i>	BPSS1498	BTH_II0868	BMAA0742
<i>tssE-5</i>	BPSS1499	BTH_II0867	BMAA0741
<i>tssF-5</i>	BPSS1500	BTH_II0866	BMAA0740
<i>tssG-5</i>	BPSS1501	BTH_II0865	BMAA0739
<i>tssH-5</i>	BPSS1502	BTH_II0864	BMAA0738
<i>tssI-5</i>	BPSS1503	BTH_II0863	BMAA0737
<i>tagA-5</i>	BPSS1504	BTH_II0862	BMAA0736B ^a
<i>tagB-5</i>	BPSS1505	BTH_II0861	BMAA0736A ^a
<i>tagC-5</i>	BPSS1506	BTH_II0860	BMAA0735
<i>tagD-5</i>	BPSS1507	BTH_II0859	BMAA0734
<i>tssJ-5</i>	BPSS1508	BTH_II0858	BMAA0733
<i>tssK-5</i>	BPSS1509	BTH_II0857	BMAA0732
<i>tssL-5</i>	BPSS1510	BTH_II0856	BMAA0731
<i>tssM-5</i>	BPSS1511	BTH_II0855	BMAA0730

^aBMAA0736 is incorrectly annotated in the *B.m* ATCC 23344 genome, the stop codon of *tagA* and the start codon of *tagB* have been ignored.

Table 10.3 List of primers used in this work

Primer	Sequence 5' → 3'	Restriction site
SOE PCR primers		
tssASOEfor2	GCGCGGTACCATCGCATCATGGGCCTCGAATTC	KpnI
tssASOEmidrev	CGCGATCTCGTTAAGCACGTGCGAAATCCTCGGGAAG	
tssASOEmidfor	CTTCCCGAGGATTTTCGACGTGCTTAACGAGATCGCG	
tssASOErev2	GCGCGGATCCCTGGGGTGTCTTCAACACGATCAA	BamHI
tssA-1SOEfor	GCGCGGTACCCTTCAGGTGTTTGACAAGGG	KpnI
tssA-1SOEmidrev	GTCGTCCTTGACGACCGAGATCGCGTCGAATTCGGC	
tssA-1SOEmidfor	GCCGAATTCGACGCGATCTCGGTCTCAAGGACGAC	
tssA-1SOErev	GCGCGGATCCGCACGATCGAGTTCGAGACC	BamHI
tssDSOEfor2	GCGCTCTAGAGCTGCCGTACATCTTCGT	XbaI
tssDSOEmidrev	GTCCGGCACGTAGGTCCAGGAACCCTCGATGCTGCC	
tssDSOEmidfor	GGCAGCATCGAGGGTTCCTGGACCTACGTGCCGGAC	
tssDSOErev2	GCGCCTGCAGCGGACGAGTTCGTCTCGTAAT	PstI
tssKSOEfor2	GCGCGGTACCACTTCATCCAGACGACGCGCTA	KpnI
tssKSOEmidrev	GTCTGCTCGATCCGGAAAAAAGTCTGGTGCAGTTC	
tssKSOEmidfor	GAAGTGCACCAGCAGTTTTTCCGGATCGAGCAGAC	
tssKSOErev2	GCGCGGATCCAGCTGCAGGCACAGCAGATAGA	BamHI
tagASOEfor2	GCGCGGTACCTTCGACCGATCAGAACACGTTC	KpnI
tagASOEmidrev	GAAGAGCGTTCGCTCGACCCGGTCGATTCCTTCGAA	
tagASOEmidfor	TTCGAAGGAATCGACCCGGTTCGAGCGAACGCTCTTC	
tagASOErev2	GCGCGGATCCCCGTTCAAATGCGTCATCGTCA	BamHI
tagABCDSOEmidrev	GTCGTTGTGCTTCGTCGGCCGGTCGATTCCTTCGAA	
tagABCDSOEmidfor	TTCGAAGGAATCGACCCGGCCGACGAAGCACAACGAC	
tagBSOEfor2	GCGCGGTACCGTCGACATCGTTCCGGCAAGC	KpnI
tagBSOEmidrev	GGGATCGGTGCGCAAGCGGCATCCGAAAGATCGAC	
tagBSOEmidfor	GTCGATCTTTCGGATGCCGCTTGCGCGACCGATCCC	
tagBSOErev2	GCGCGGATCCATGCGCGTACGTCGAAGC	BamHI
tagCSOEfor2	GCGCGGTACCTCGTGCAGACGATGTTCTTCGC	PstI
tagCSOEmidrev	GTCGCGCGCGTGAAGGTGCGCAAGAGGATGCGGATG	
tagCSOEmidfor	CATCCGCATCCTCTTGCGCACCTTCACGCGCGCGAC	
tagCSOErev2	GCGCGGATCCGCCGGCATGAAAATCCGTCGAT	BamHI

tagDSOEfor2	GCGCGGTACCCGACCACGTGCTGATCTGGG	KpnI
tagDSOEmidrev	GTCGTTGTGCTTCGTCGGCAGGCCGGTGTTCCGATA	
tagDSOEmidfor	TATCCGAACACCCGGCCTGCCGACGAAGCACAACGAC	
tagDSOErev2	GCGCGGATCCCGTTTTCGCTTCCGTTCCGCGT	BamHI
Complementation primers		
tssAcompfor	GCGCAAGCTTCGTGGAGACGCTATGGGAATGAA	HindIII
tssAcomprev	GCGCGGATCCATTTTCGCGTCACGTCGACAAAC	BamHI
tssKcompfor	GCGCAAGCTTCTAACCGGAACGAACGACATGGAC	HindIII
tssKcomprev	GCGCGGATCCCATCGAATCGGACAGCTTCATCA	BamHI
tagAcompfor	GCGCAAGCTTGTGATAGGCTGACCTGCTCATTCTG	HindIII
tagAcomprev	GCGCGGATCCAACGTGTGTCGGACATGGGTC	BamHI
tagActermFLAGrev	GCGCGGATCCTCACTTATCGTCGTCATCCTTGT AATCGCGGGATGACGCGAGTTCGG	BamHI
tagBcompfor	GCGCAAGCTTCGCGTCATCCCGCTGATTCATT	HindIII
tagBcomprev	GCGCGGATCCCGAGAGTCGTGAGTCATCGTTC	BamHI
tagBctermFLAGrev	GCGCGGATCCTCACTTATCGTCGTCATCCTTGT AATCTCGTTCGGGCGCGGTCCATC	BamHI
tagCcompfor	GCGCAAGCTTGGCGCTGGCCGAACGATGGAC	KpnI
tagCcomprev	GCGCGGATCCGGAAAATCAGCCGAGATCGA	BamHI
tagCctermFLAGrev	GCGCGGATCCTCACTTATCGTCGTCATCCTTGT AATCGCCGAGATCGATGCGCTCGC	BamHI
tagDcompfor	GCGCAAGCTTGCATCTCGGCTGATTTTCCTCT	HindIII
tagDcomprev	GCGCGGATCCCCTTAACTCATCACCATCACTTTC	BamHI
tagDctermFLAGrev	GCGCGGATCCTTACTTATCGTCGTCATCCTTGT AATCACTCATCACCATCACTTTCTGCTG	BamHI
<i>virAG</i> primers		
BthaiVirAGRhaFor	GCGCCATATGCACGGAAATTCATCGATGC	NdeI
BthaiVirAGRhaRev	GCGCGGATCCTCATTCCCATAGCGTCTCCAC	BamHI
Protein expression primers		
tssDpET14bfor	GCGCCATATGCCGATGCCGTGCTATCTCA	NdeI
tssDpET14brev	GCGCGGATCCCGGCCGAAGATGATCGATGATCGA	BamHI
tagAMCS1for	GCGCTCATGAAAATCGTCAAACCCGAGT	BspHI
tagAMCS1rev	GCGCAAGCTTATGAATCAGCGGGATGACGC	HindIII

tagBMCS2for	GCGCCATATGTCCGACACAGTTCACGC	NdeI
tagBMCS2rev	GCGCGGATCCAGGAGTAGAAGGAAGGCATGGT	BamHI
tagCMCS1for	GCGCCCATGGACCGCGCCCGAACGAT	NcoI
tagDMCS2for2	GCGCCATATGTTTCGTAGTCACCACCGCC	NdeI
BACTH primers		
pUT18C-tssAfor	GCGCTCTAGAAGGAATGAACGAACGGCGTCA	XbaI
pKT25tssCfor	GCGCCTGCAGGGGAAGGCGAACACCTGTACTC	PstI
pKT25tssCrev	GCGCTCTAGATCAGCGCTTCTCGAGCTTGC	XbaI
pKNT25tssCfor	GCGCCTGCAGGGGAAGGCGAACACCTGTACTC	PstI
pKNT25tssCrev	GCGCTCTAGAGTGCGCTTCTCGAGCTTGCCGAC	XbaI
pKT25-tsslfor	GCGCTCTAGAATCTTCGTCCCATCGACACTA	XbaI
pKT25-tsslrev	GCGCGGTACCAATGAGCAGGTCAGCCTAGC	KpnI
pKNT25-tsslfor	GCGCTCTAGAATCTTCGTCCCATCGACACTA	XbaI
pKNT25-tsslrev	GCGCGGTACCCCTAGCTGGATCAACTGTCC	KpnI
tagApUT18for	GCGCCTGCAGGAAAATCGTCAAACCCGAGTCGC	PstI
tagApUT18rev	GCGCGGATCCTCGCGGGATGACGCGAGTTCGG	BamHI
tagBpKNT25for	GCGCAAGCTTGTCCGACACAGTTCACGCGG	HindIII
tagBpKNT25rev	GCGCGGATCCCTTCGTTGCGGGCGCGGTCCATC	BamHI
tagCpKT25for2	GCGCCTGCAGACCGCGCCCGAACGATGAC	PstI
pUT18C-tagCfor	GCGCTCTAGAGACTCAGACTCTCGCGCTTC	XbaI
pKT25-tagDfor2	GCGCTCTAGAATTTGTCGTCACCACCGCCTC	XbaI
Screening primers		
TssAscrnfor	AGCGTTTTCCGCTTATCTGC	
TssAscrnrev	GATACGATGAAACTTCCGATCCT	
tssA-1Scrnfors	CGAACGCAAGATGATCACGATC	
tssA-1Scrnrrev	ACCCGACCTACATGATCAAGAAC	
tssDscrnfor	GAGATCCAGAACAAGATCCCGA	
tssDscrnrev	AGGCATCGATTGATCTCGGT	
tssKscrnrev	TCAGATAAAGCGACAGCAGGATCG	
tagAscrnfor	AGTTCGACCTCAAGGAGCTGAT	
tagCscrnfor	AGCGATTTTCAGCGGCACATC	
tagCscrnrev	G TTCAGGTATTGTTGAGCCGTG	
M13forward	TGTAACGACGCGCCAGT	

M13reverse	CAGGAAACAGCTATGACC	
pSCrhaB2for	TCAGTAACGAGAAGGTCGCG	
pSCrhaB2rev	TACTGCCGCCAGGCAAATTC	
virGfor	GCGCCATATGAATGCGACAAGATCGCC	NdeI
T7for	ACGACTCACTATAGGGAGAC	
T7rev	GCTAGTTATTGCTCAGCGGT	
pETDuet-T7-1for	ATGCGTCCGGCGTAGA	
pACYCDuetT7-1rev	GATTATGCGGCCGTGTACAA	
pACYC-T7-1for	GGATCTCGACGCTCTCCCT	
pACYC-T7-2for	TTGTACACGGCCGCATAATC	
pKNT+pUT.seq.for.RJ	GGCTCGTATGTTGTGTGGAAT	
pKNT.rev.seq.RJ	TTGATGCCATCGAGTACGGCT	
pUT.seq.rev.RJ	TTCCACAACAAGTCGATGCGT	
pKT.for.seq.RJ	AAGTTGGACAGATGCGGCATA	
pKT.rev.seq.RJ	ATTAAGTTGGGTAACGCCAGG	
pUTC.for.seq.RJ	TCTCGCCGGATGTACTGGAAA	
pUTC.rev.seq.RJ	TGTCGGGGCTGGCTTAACTAT	

Table 10.4 Proteins detected in all three WT *B.t* supernatant samples

UniProtKB Accession	Description
Q2STF7	Amino acid ABC transporter, periplasmic amino acid-binding protein, putative OS= <i>Burkholderia thailandensis</i> (strain E264 / ATCC 700388 / DSM 13276 / CIP 106301) GN=BTH_I3300 PE=4 SV=1
Q2STQ9	Flagellin OS= <i>Burkholderia thailandensis</i> (strain E264 / ATCC 700388 / DSM 13276 / CIP 106301) GN=BTH_I3196 PE=4 SV=1
Q2STT2	Lipoprotein, putative OS= <i>Burkholderia thailandensis</i> (strain E264 / ATCC 700388 / DSM 13276 / CIP 106301) GN=BTH_I3173 PE=4 SV=1
Q2SU25	Elongation factor Tu OS= <i>Burkholderia thailandensis</i> (strain E264 / ATCC 700388 / DSM 13276 / CIP 106301) GN= <i>tuf1</i> PE=3 SV=1
Q2SU95	Toluene tolerance, Ttg2 superfamily OS= <i>Burkholderia thailandensis</i> (strain E264 / ATCC 700388 / DSM 13276 / CIP 106301) GN=BTH_I3000 PE=4 SV=1
Q2SUC7	Lipoprotein, putative OS= <i>Burkholderia thailandensis</i> (strain E264 / ATCC 700388 / DSM 13276 / CIP 106301) GN=BTH_I2965 PE=4 SV=1
Q2SUE7	Peptidase, M1 family OS= <i>Burkholderia thailandensis</i> (strain E264 / ATCC 700388 / DSM 13276 / CIP 106301) GN=BTH_I2945 PE=4 SV=1
Q2SV12	Filamentous haemagglutinin OS= <i>Burkholderia thailandensis</i> (strain E264 / ATCC 700388 / DSM 13276 / CIP 106301) GN=BTH_I2723 PE=4 SV=1
Q2SV22	Poly(3-hydroxybutyrate) depolymerase OS= <i>Burkholderia thailandensis</i> (strain E264 / ATCC 700388 / DSM 13276 / CIP 106301) GN=BTH_I2713 PE=4 SV=1
Q2SVD6	Endoribonuclease L-PSP superfamily OS= <i>Burkholderia thailandensis</i> (strain E264 / ATCC 700388 / DSM 13276 / CIP 106301) GN=BTH_I2598 PE=4 SV=1
Q2SVX6	Glycosyl hydrolase, family 18 OS= <i>Burkholderia thailandensis</i> (strain E264 / ATCC 700388 / DSM 13276 / CIP 106301) GN=BTH_I2402 PE=3 SV=1
Q2SVY5	FenI protein OS= <i>Burkholderia thailandensis</i> (strain E264 / ATCC 700388 / DSM 13276 / CIP 106301) GN=BTH_I2393 PE=4 SV=1
Q2SWL5	Lipoprotein, putative OS= <i>Burkholderia thailandensis</i> (strain E264 / ATCC 700388 / DSM 13276 / CIP 106301) GN=BTH_I2163 PE=4 SV=1
Q2SWT4	Alkyl hydroperoxide reductase AhpD OS= <i>Burkholderia thailandensis</i> (strain E264 / ATCC 700388 / DSM 13276 / CIP 106301) GN= <i>ahpD</i> PE=3 SV=1

Q2SX80	Peptidyl-prolyl cis-trans isomerase OS= <i>Burkholderia thailandensis</i> (strain E264 / ATCC 700388 / DSM 13276 / CIP 106301) GN=BTH_I1939 PE=3 SV=1
Q2SXN4	Amino acid ABC transporter, periplasmic amino acid-binding protein OS= <i>Burkholderia thailandensis</i> (strain E264 / ATCC 700388 / DSM 13276 / CIP 106301) GN=BTH_I1783 PE=3 SV=1
Q2SXN9	N-succinylglutamate 5-semialdehyde dehydrogenase OS= <i>Burkholderia thailandensis</i> (strain E264 / ATCC 700388 / DSM 13276 / CIP 106301) GN= <i>astD</i> PE=1 SV=1
Q2SXQ5	Phospholipase C OS= <i>Burkholderia thailandensis</i> (strain E264 / ATCC 700388 / DSM 13276 / CIP 106301) GN=BTH_I1762 PE=4 SV=1
Q2SY31	OmpA family protein OS= <i>Burkholderia thailandensis</i> (strain E264 / ATCC 700388 / DSM 13276 / CIP 106301) GN=BTH_I1631 PE=3 SV=1
Q2SY68	Outer membrane porin OpcP OS= <i>Burkholderia thailandensis</i> (strain E264 / ATCC 700388 / DSM 13276 / CIP 106301) GN=BTH_I1592 PE=4 SV=1
Q2SYD9	Putative uncharacterized protein OS= <i>Burkholderia thailandensis</i> (strain E264 / ATCC 700388 / DSM 13276 / CIP 106301) GN=BTH_I1515 PE=4 SV=1
Q2SYJ5	60 kDa chaperonin 1 OS= <i>Burkholderia thailandensis</i> (strain E264 / ATCC 700388 / DSM 13276 / CIP 106301) GN= <i>groL1</i> PE=3 SV=1
Q2SYL9	Activator protein, putative OS= <i>Burkholderia thailandensis</i> (strain E264 / ATCC 700388 / DSM 13276 / CIP 106301) GN=BTH_I1434 PE=4 SV=1
Q2SYM1	Lipoprotein, putative OS= <i>Burkholderia thailandensis</i> (strain E264 / ATCC 700388 / DSM 13276 / CIP 106301) GN=BTH_I1432 PE=4 SV=1
Q2SYM2	Putative uncharacterized protein OS= <i>Burkholderia thailandensis</i> (strain E264 / ATCC 700388 / DSM 13276 / CIP 106301) GN=BTH_I1431 PE=4 SV=1
Q2SYN2	Serine-type carboxypeptidase family protein OS= <i>Burkholderia thailandensis</i> (strain E264 / ATCC 700388 / DSM 13276 / CIP 106301) GN=BTH_I1421 PE=4 SV=1
Q2SYN3	D-(-)-3-hydroxybutyrate oligomer hydrolase OS= <i>Burkholderia thailandensis</i> (strain E264 / ATCC 700388 / DSM 13276 / CIP 106301) GN=BTH_I1420 PE=3 SV=1
Q2SYT1	Outer membrane protein, OmpA family OS= <i>Burkholderia thailandensis</i> (strain E264 / ATCC 700388 / DSM 13276 / CIP 106301) GN=BTH_I1372 PE=3 SV=1
Q2SZ77	Glutamate/aspartate ABC transporter, periplasmic glutamate/aspartate-binding protein OS= <i>Burkholderia thailandensis</i> (strain E264 / ATCC 700388 / DSM 13276 / CIP 106301) GN=BTH_I1225 PE=4 SV=1
Q2SZA6	Glyceraldehyde-3-phosphate dehydrogenase, type I OS= <i>Burkholderia thailandensis</i> (strain E264 / ATCC 700388 / DSM 13276 / CIP 106301) GN= <i>gap</i> PE=3 SV=1

Q2SZE5	Outer membrane lipoprotein OS= <i>Burkholderia thailandensis</i> (strain E264 / ATCC 700388 / DSM 13276 / CIP 106301) GN=BTH_I1157 PE=4 SV=1
Q2T086	OmpA family protein OS= <i>Burkholderia thailandensis</i> (strain E264 / ATCC 700388 / DSM 13276 / CIP 106301) GN=BTH_I0857 PE=3 SV=1
Q2T0J9	Superoxide dismutase OS= <i>Burkholderia thailandensis</i> (strain E264 / ATCC 700388 / DSM 13276 / CIP 106301) GN=BTH_I0744 PE=3 SV=1
Q2T0T0	Phosphoglycerate kinase OS= <i>Burkholderia thailandensis</i> (strain E264 / ATCC 700388 / DSM 13276 / CIP 106301) GN= <i>pgk</i> PE=3 SV=1
Q2T0X3	Cholesterol oxidase OS= <i>Burkholderia thailandensis</i> (strain E264 / ATCC 700388 / DSM 13276 / CIP 106301) GN=BTH_I0619 PE=4 SV=1
Q2T1F2	Lipoprotein OS= <i>Burkholderia thailandensis</i> (strain E264 / ATCC 700388 / DSM 13276 / CIP 106301) GN=BTH_I0439 PE=3 SV=1
Q2T1H6	Carboxy-terminal protease OS= <i>Burkholderia thailandensis</i> (strain E264 / ATCC 700388 / DSM 13276 / CIP 106301) GN=BTH_I0415 PE=3 SV=1
Q2T1N8	Thiol:disulfide interchange protein OS= <i>Burkholderia thailandensis</i> (strain E264 / ATCC 700388 / DSM 13276 / CIP 106301) GN=BTH_I0353 PE=3 SV=1
Q2T1Y0	Putative uncharacterized protein OS= <i>Burkholderia thailandensis</i> (strain E264 / ATCC 700388 / DSM 13276 / CIP 106301) GN=BTH_I0261 PE=4 SV=1
Q2T201	Flagellar basal body rod protein FlgB OS= <i>Burkholderia thailandensis</i> (strain E264 / ATCC 700388 / DSM 13276 / CIP 106301) GN= <i>flgB-1</i> PE=3 SV=1
Q2T2S6	Toluene tolerance, Ttg2 superfamily OS= <i>Burkholderia thailandensis</i> (strain E264 / ATCC 700388 / DSM 13276 / CIP 106301) GN=BTH_II2336 PE=4 SV=1
Q2T3C2	TonB-dependent heme/hemoglobin receptor family protein OS= <i>Burkholderia thailandensis</i> (strain E264 / ATCC 700388 / DSM 13276 / CIP 106301) GN=BTH_II2139 PE=3 SV=1
Q2T3C7	Lipoprotein OS= <i>Burkholderia thailandensis</i> (strain E264 / ATCC 700388 / DSM 13276 / CIP 106301) GN=BTH_II2134 PE=3 SV=1
Q2T3E9	Lipoprotein, putative OS= <i>Burkholderia thailandensis</i> (strain E264 / ATCC 700388 / DSM 13276 / CIP 106301) GN=BTH_II2112 PE=4 SV=1
Q2T3W7	60 kDa chaperonin 2 OS= <i>Burkholderia thailandensis</i> (strain E264 / ATCC 700388 / DSM 13276 / CIP 106301) GN= <i>groL2</i> PE=3 SV=1
Q2T3Y0	Chitin binding domain protein OS= <i>Burkholderia thailandensis</i> (strain E264 / ATCC 700388 / DSM 13276 / CIP 106301) GN=BTH_II1925 PE=4 SV=1

Q2T454	Metallopeptidase domain protein OS= <i>Burkholderia thailandensis</i> (strain E264 / ATCC 700388 / DSM 13276 / CIP 106301) GN=BTH_II1851 PE=4 SV=1
Q2T466	Leucine-, isoleucine-, valine-, threonine-, and alanine-binding protein OS= <i>Burkholderia thailandensis</i> (strain E264 / ATCC 700388 / DSM 13276 / CIP 106301) GN= <i>braC</i> PE=4 SV=1
Q2T471	LasA protease OS= <i>Burkholderia thailandensis</i> (strain E264 / ATCC 700388 / DSM 13276 / CIP 106301) GN=BTH_II1834 PE=4 SV=1
Q2T4B6	Ribonuclease T2 family OS= <i>Burkholderia thailandensis</i> (strain E264 / ATCC 700388 / DSM 13276 / CIP 106301) GN=BTH_II1789 PE=3 SV=1
Q2T4F3	Periplasmic trehalase OS= <i>Burkholderia thailandensis</i> (strain E264 / ATCC 700388 / DSM 13276 / CIP 106301) GN= <i>treA</i> PE=3 SV=1
Q2T4R7	Putative uncharacterized protein OS= <i>Burkholderia thailandensis</i> (strain E264 / ATCC 700388 / DSM 13276 / CIP 106301) GN=BTH_II1638 PE=4 SV=1
Q2T4V6	Amino acid ABC transporter, periplasmic amino acid-binding protein, putative OS= <i>Burkholderia thailandensis</i> (strain E264 / ATCC 700388 / DSM 13276 / CIP 106301) GN=BTH_II1598 PE=4 SV=1
Q2T4W5	Putative uncharacterized protein OS= <i>Burkholderia thailandensis</i> (strain E264 / ATCC 700388 / DSM 13276 / CIP 106301) GN=BTH_II1589 PE=4 SV=1
Q2T4X6	Microbial collagenase, putative OS= <i>Burkholderia thailandensis</i> (strain E264 / ATCC 700388 / DSM 13276 / CIP 106301) GN=BTH_II1578 PE=4 SV=1
Q2T533	Outer membrane porin OpcP OS= <i>Burkholderia thailandensis</i> (strain E264 / ATCC 700388 / DSM 13276 / CIP 106301) GN=BTH_II1520 PE=4 SV=1
Q2T5L4	Putative uncharacterized protein OS= <i>Burkholderia thailandensis</i> (strain E264 / ATCC 700388 / DSM 13276 / CIP 106301) GN=BTH_II1339 PE=4 SV=1
Q2T5W0	Putative ABC transporter ATP-binding protein OS= <i>Burkholderia thailandensis</i> (strain E264 / ATCC 700388 / DSM 13276 / CIP 106301) GN=BTH_II1243 PE=4 SV=1
Q2T637	Lipoprotein, putative OS= <i>Burkholderia thailandensis</i> (strain E264 / ATCC 700388 / DSM 13276 / CIP 106301) GN=BTH_II1165 PE=4 SV=1
Q2T6D3	Gp28 OS= <i>Burkholderia thailandensis</i> (strain E264 / ATCC 700388 / DSM 13276 / CIP 106301) GN=BTH_II1069 PE=4 SV=1
Q2T6Y4	Hcp protein OS= <i>Burkholderia thailandensis</i> (strain E264 / ATCC 700388 / DSM 13276 / CIP 106301) GN=BTH_II0868 PE=4 SV=1
Q2T6Y9	Rhs element Vgr protein OS= <i>Burkholderia thailandensis</i> (strain E264 / ATCC 700388 / DSM 13276 / CIP 106301) GN=BTH_II0863 PE=4 SV=1

Q2T6Z8	Ubiquitin-specific proteinase 31, putative OS= <i>Burkholderia thailandensis</i> (strain E264 / ATCC 700388 / DSM 13276 / CIP 106301) GN=BTH_II0854 PE=4 SV=1
Q2T736	Thermolysin metallopeptidase OS= <i>Burkholderia thailandensis</i> (strain E264 / ATCC 700388 / DSM 13276 / CIP 106301) GN=BTH_II0816 PE=4 SV=1
Q2T769	Putative uncharacterized protein OS= <i>Burkholderia thailandensis</i> (strain E264 / ATCC 700388 / DSM 13276 / CIP 106301) GN=BTH_II0783 PE=4 SV=1
Q2T7C9	Beta-glucosidase OS= <i>Burkholderia thailandensis</i> (strain E264 / ATCC 700388 / DSM 13276 / CIP 106301) GN= <i>bgIB</i> PE=4 SV=1
Q2T7D3	Streptavidin, putative OS= <i>Burkholderia thailandensis</i> (strain E264 / ATCC 700388 / DSM 13276 / CIP 106301) GN=BTH_II0719 PE=4 SV=1
Q2T7P3	NADH dehydrogenase OS= <i>Burkholderia thailandensis</i> (strain E264 / ATCC 700388 / DSM 13276 / CIP 106301) GN=BTH_II0606 PE=4 SV=1
Q2T7W2	N-acetylmuramoyl-L-alanine amidase domain protein OS= <i>Burkholderia thailandensis</i> (strain E264 / ATCC 700388 / DSM 13276 / CIP 106301) GN=BTH_II0537 PE=4 SV=1
Q2T7W7	Extracellular nuclease, putative OS= <i>Burkholderia thailandensis</i> (strain E264 / ATCC 700388 / DSM 13276 / CIP 106301) GN=BTH_II0532 PE=4 SV=1
Q2T7W9	Lipoprotein, putative OS= <i>Burkholderia thailandensis</i> (strain E264 / ATCC 700388 / DSM 13276 / CIP 106301) GN=BTH_II0530 PE=4 SV=1
Q2T8B9	X-pro dipeptidyl-peptidase, putative OS= <i>Burkholderia thailandensis</i> (strain E264 / ATCC 700388 / DSM 13276 / CIP 106301) GN=BTH_II0380 PE=4 SV=1
Q2T8C0	Serine metalloprotease OS= <i>Burkholderia thailandensis</i> (strain E264 / ATCC 700388 / DSM 13276 / CIP 106301) GN=BTH_II0379 PE=4 SV=1
Q2T8I8	Antifungal protein, putative OS= <i>Burkholderia thailandensis</i> (strain E264 / ATCC 700388 / DSM 13276 / CIP 106301) GN=BTH_II0310 PE=4 SV=1
Q2T8R9	Alpha-1,2-mannosidase family protein OS= <i>Burkholderia thailandensis</i> (strain E264 / ATCC 700388 / DSM 13276 / CIP 106301) GN=BTH_II0228 PE=4 SV=1
Q2T8S0	Putative uncharacterized protein OS= <i>Burkholderia thailandensis</i> (strain E264 / ATCC 700388 / DSM 13276 / CIP 106301) GN=BTH_II0227 PE=4 SV=1
Q2T8T4	Probable glucan 1,4-a-glucosidase OS= <i>Burkholderia thailandensis</i> (strain E264 / ATCC 700388 / DSM 13276 / CIP 106301) GN=BTH_II0213 PE=4 SV=1
Q2T8Z6	Flagellin D OS= <i>Burkholderia thailandensis</i> (strain E264 / ATCC 700388 / DSM 13276 / CIP 106301) GN=BTH_II0151 PE=4 SV=1
Q2T934	PqaA OS= <i>Burkholderia thailandensis</i> (strain E264 / ATCC 700388 / DSM 13276 / CIP 106301) GN=BTH_II0113 PE=4 SV=1

Table 10.5 Proteins detected in all three *B.t* Δ tssK supernatant samples

UniProtKB Accession	Description
Q2STE7	ATP synthase subunit alpha 1 OS= <i>Burkholderia thailandensis</i> (strain E264 / ATCC 700388 / DSM 13276 / CIP 106301) GN= <i>atpA1</i> PE=3 SV=1
Q2STE9	ATP synthase subunit beta 1 OS= <i>Burkholderia thailandensis</i> (strain E264 / ATCC 700388 / DSM 13276 / CIP 106301) GN= <i>atpD1</i> PE=3 SV=1
Q2STF7	Amino acid ABC transporter, periplasmic amino acid-binding protein, putative OS= <i>Burkholderia thailandensis</i> (strain E264 / ATCC 700388 / DSM 13276 / CIP 106301) GN=BTH_I3300 PE=4 SV=1
Q2STJ7	GDSL-like Lipase/Acylhydrolase domain protein OS= <i>Burkholderia thailandensis</i> (strain E264 / ATCC 700388 / DSM 13276 / CIP 106301) GN=BTH_I3258 PE=4 SV=1
Q2STK2	Glycine dehydrogenase (decarboxylating) OS= <i>Burkholderia thailandensis</i> (strain E264 / ATCC 700388 / DSM 13276 / CIP 106301) GN= <i>gcvP</i> PE=3 SV=1
Q2STQ9	Flagellin OS= <i>Burkholderia thailandensis</i> (strain E264 / ATCC 700388 / DSM 13276 / CIP 106301) GN=BTH_I3196 PE=4 SV=1
Q2STT2	Lipoprotein, putative OS= <i>Burkholderia thailandensis</i> (strain E264 / ATCC 700388 / DSM 13276 / CIP 106301) GN=BTH_I3173 PE=4 SV=1
Q2STU0	Adenosylhomocysteinase OS= <i>Burkholderia thailandensis</i> (strain E264 / ATCC 700388 / DSM 13276 / CIP 106301) GN= <i>ahcY</i> PE=3 SV=1
Q2STV9	Transporter, putative OS= <i>Burkholderia thailandensis</i> (strain E264 / ATCC 700388 / DSM 13276 / CIP 106301) GN=BTH_I3146 PE=4 SV=1
Q2STX7	Putative uncharacterized protein OS= <i>Burkholderia thailandensis</i> (strain E264 / ATCC 700388 / DSM 13276 / CIP 106301) GN=BTH_I3127 PE=4 SV=1
Q2STZ3	Orotate phosphoribosyltransferase OS= <i>Burkholderia thailandensis</i> (strain E264 / ATCC 700388 / DSM 13276 / CIP 106301) GN= <i>pyrE</i> PE=3 SV=1
Q2SU25	Elongation factor Tu OS= <i>Burkholderia thailandensis</i> (strain E264 / ATCC 700388 / DSM 13276 / CIP 106301) GN= <i>tuf1</i> PE=3 SV=1
Q2SU95	Toluene tolerance, Ttg2 superfamily OS= <i>Burkholderia thailandensis</i> (strain E264 / ATCC 700388 / DSM 13276 / CIP 106301) GN=BTH_I3000 PE=4 SV=1
Q2SUE7	Peptidase, M1 family OS= <i>Burkholderia thailandensis</i> (strain E264 / ATCC 700388 / DSM 13276 / CIP 106301) GN=BTH_I2945 PE=4 SV=1

Q2SUI0	Indole-3-glycerol phosphate synthase OS= <i>Burkholderia thailandensis</i> (strain E264 / ATCC 700388 / DSM 13276 / CIP 106301) GN= <i>trpC</i> PE=3 SV=1
Q2SUV4	Carbamoyl-phosphate synthase small chain OS= <i>Burkholderia thailandensis</i> (strain E264 / ATCC 700388 / DSM 13276 / CIP 106301) GN= <i>carA</i> PE=3 SV=1
Q2SV22	Poly(3-hydroxybutyrate) depolymerase OS= <i>Burkholderia thailandensis</i> (strain E264 / ATCC 700388 / DSM 13276 / CIP 106301) GN=BTH_I2713 PE=4 SV=1
Q2SV97	LysM domain protein OS= <i>Burkholderia thailandensis</i> (strain E264 / ATCC 700388 / DSM 13276 / CIP 106301) GN=BTH_I2637 PE=4 SV=1
Q2SVC6	3-oxoadipate CoA-succinyl transferase alpha subunit OS= <i>Burkholderia thailandensis</i> (strain E264 / ATCC 700388 / DSM 13276 / CIP 106301) GN=BTH_I2608 PE=4 SV=1
Q2SVD6	Endoribonuclease L-PSP superfamily OS= <i>Burkholderia thailandensis</i> (strain E264 / ATCC 700388 / DSM 13276 / CIP 106301) GN=BTH_I2598 PE=4 SV=1
Q2SVH8	Dihydrolipoyl dehydrogenase OS= <i>Burkholderia thailandensis</i> (strain E264 / ATCC 700388 / DSM 13276 / CIP 106301) GN= <i>lpdA-1</i> PE=3 SV=1
Q2SVX6	Glycosyl hydrolase, family 18 OS= <i>Burkholderia thailandensis</i> (strain E264 / ATCC 700388 / DSM 13276 / CIP 106301) GN=BTH_I2402 PE=3 SV=1
Q2SVY5	FenI protein OS= <i>Burkholderia thailandensis</i> (strain E264 / ATCC 700388 / DSM 13276 / CIP 106301) GN=BTH_I2393 PE=4 SV=1
Q2SW43	Alcohol dehydrogenase, iron-containing OS= <i>Burkholderia thailandensis</i> (strain E264 / ATCC 700388 / DSM 13276 / CIP 106301) GN=BTH_I2335 PE=4 SV=1
Q2SWD3	Adenylosuccinate synthetase OS= <i>Burkholderia thailandensis</i> (strain E264 / ATCC 700388 / DSM 13276 / CIP 106301) GN= <i>purA</i> PE=1 SV=1
Q2SWD4	ATP phosphoribosyltransferase regulatory subunit OS= <i>Burkholderia thailandensis</i> (strain E264 / ATCC 700388 / DSM 13276 / CIP 106301) GN= <i>hisZ</i> PE=3 SV=1
Q2SWE7	Nucleoside diphosphate kinase OS= <i>Burkholderia thailandensis</i> (strain E264 / ATCC 700388 / DSM 13276 / CIP 106301) GN= <i>ndk</i> PE=1 SV=1
Q2SWG0	Thioredoxin OS= <i>Burkholderia thailandensis</i> (strain E264 / ATCC 700388 / DSM 13276 / CIP 106301) GN=BTH_I2218 PE=4 SV=1
Q2SWL5	Lipoprotein, putative OS= <i>Burkholderia thailandensis</i> (strain E264 / ATCC 700388 / DSM 13276 / CIP 106301) GN=BTH_I2163 PE=4 SV=1
Q2SWQ6	ATP-dependent Clp protease proteolytic subunit OS= <i>Burkholderia thailandensis</i> (strain E264 / ATCC 700388 / DSM 13276 / CIP 106301) GN= <i>clpP</i> PE=3 SV=1
Q2SWT3	Antioxidant, AhpC/Tsa family OS= <i>Burkholderia thailandensis</i> (strain E264 / ATCC 700388 / DSM 13276 / CIP 106301) GN=BTH_I2092 PE=4 SV=1

Q2SWT4	Alkyl hydroperoxide reductase AhpD OS= <i>Burkholderia thailandensis</i> (strain E264 / ATCC 700388 / DSM 13276 / CIP 106301) GN= <i>ahpD</i> PE=3 SV=1
Q2SWW7	GMP synthase [glutamine-hydrolyzing] OS= <i>Burkholderia thailandensis</i> (strain E264 / ATCC 700388 / DSM 13276 / CIP 106301) GN= <i>guaA</i> PE=3 SV=1
Q2SWY1	Serine protease, subtilase family OS= <i>Burkholderia thailandensis</i> (strain E264 / ATCC 700388 / DSM 13276 / CIP 106301) GN=BTH_I2044 PE=4 SV=1
Q2SWY7	3-hydroxyacyl-[acyl-carrier-protein] dehydratase FabZ OS= <i>Burkholderia thailandensis</i> (strain E264 / ATCC 700388 / DSM 13276 / CIP 106301) GN= <i>fabZ</i> PE=1 SV=1
Q2SWZ5	Ribosome-recycling factor OS= <i>Burkholderia thailandensis</i> (strain E264 / ATCC 700388 / DSM 13276 / CIP 106301) GN= <i>frr</i> PE=3 SV=1
Q2SX33	Putative regulator of ribonuclease activity OS= <i>Burkholderia thailandensis</i> (strain E264 / ATCC 700388 / DSM 13276 / CIP 106301) GN=BTH_I1992 PE=3 SV=1
Q2SX80	Peptidyl-prolyl cis-trans isomerase OS= <i>Burkholderia thailandensis</i> (strain E264 / ATCC 700388 / DSM 13276 / CIP 106301) GN=BTH_I1939 PE=3 SV=1
Q2SXC5	Enolase OS= <i>Burkholderia thailandensis</i> (strain E264 / ATCC 700388 / DSM 13276 / CIP 106301) GN= <i>eno</i> PE=3 SV=1
Q2SXF3	Pyruvate dehydrogenase, E3 component, dihydrolipoamide dehydrogenase OS= <i>Burkholderia thailandensis</i> (strain E264 / ATCC 700388 / DSM 13276 / CIP 106301) GN=BTH_I1866 PE=3 SV=1
Q2SXF5	Pyruvate dehydrogenase E1 component OS= <i>Burkholderia thailandensis</i> (strain E264 / ATCC 700388 / DSM 13276 / CIP 106301) GN=BTH_I1864 PE=3 SV=1
Q2SXN4	Amino acid ABC transporter, periplasmic amino acid-binding protein OS= <i>Burkholderia thailandensis</i> (strain E264 / ATCC 700388 / DSM 13276 / CIP 106301) GN=BTH_I1783 PE=3 SV=1
Q2SXN9	N-succinylglutamate 5-semialdehyde dehydrogenase OS= <i>Burkholderia thailandensis</i> (strain E264 / ATCC 700388 / DSM 13276 / CIP 106301) GN= <i>astD</i> PE=1 SV=1
Q2SXQ5	Phospholipase C OS= <i>Burkholderia thailandensis</i> (strain E264 / ATCC 700388 / DSM 13276 / CIP 106301) GN=BTH_I1762 PE=4 SV=1
Q2SY24	30S ribosomal protein S1 OS= <i>Burkholderia thailandensis</i> (strain E264 / ATCC 700388 / DSM 13276 / CIP 106301) GN= <i>rpsA</i> PE=3 SV=1
Q2SY31	OmpA family protein OS= <i>Burkholderia thailandensis</i> (strain E264 / ATCC 700388 / DSM 13276 / CIP 106301) GN=BTH_I1631 PE=3 SV=1

Q2SY68	Outer membrane porin OpcP OS= <i>Burkholderia thailandensis</i> (strain E264 / ATCC 700388 / DSM 13276 / CIP 106301) GN=BTH_I1592 PE=4 SV=1
Q2SYC4	6,7-dimethyl-8-ribityllumazine synthase OS= <i>Burkholderia thailandensis</i> (strain E264 / ATCC 700388 / DSM 13276 / CIP 106301) GN=ribH PE=3 SV=1
Q2SYD9	Putative uncharacterized protein OS= <i>Burkholderia thailandensis</i> (strain E264 / ATCC 700388 / DSM 13276 / CIP 106301) GN=BTH_I1515 PE=4 SV=1
Q2SYG4	Phosphoglucomutase/phosphomannomutase family protein OS= <i>Burkholderia thailandensis</i> (strain E264 / ATCC 700388 / DSM 13276 / CIP 106301) GN=BTH_I1489 PE=1 SV=1
Q2SYI2	dTDP-4-dehydrorhamnose 3,5-epimerase OS= <i>Burkholderia thailandensis</i> (strain E264 / ATCC 700388 / DSM 13276 / CIP 106301) GN=BTH_I1471 PE=4 SV=1
Q2SYJ5	60 kDa chaperonin 1 OS= <i>Burkholderia thailandensis</i> (strain E264 / ATCC 700388 / DSM 13276 / CIP 106301) GN=groL1 PE=3 SV=1
Q2SYL9	Activator protein, putative OS= <i>Burkholderia thailandensis</i> (strain E264 / ATCC 700388 / DSM 13276 / CIP 106301) GN=BTH_I1434 PE=4 SV=1
Q2SYM1	Lipoprotein, putative OS= <i>Burkholderia thailandensis</i> (strain E264 / ATCC 700388 / DSM 13276 / CIP 106301) GN=BTH_I1432 PE=4 SV=1
Q2SYN2	Serine-type carboxypeptidase family protein OS= <i>Burkholderia thailandensis</i> (strain E264 / ATCC 700388 / DSM 13276 / CIP 106301) GN=BTH_I1421 PE=4 SV=1
Q2SYS4	Serine hydroxymethyltransferase 1 OS= <i>Burkholderia thailandensis</i> (strain E264 / ATCC 700388 / DSM 13276 / CIP 106301) GN=glyA1 PE=3 SV=2
Q2SYS5	Oxidoreductase, short-chain dehydrogenase/reductase family OS= <i>Burkholderia thailandensis</i> (strain E264 / ATCC 700388 / DSM 13276 / CIP 106301) GN=BTH_I1378 PE=3 SV=1
Q2SYT1	Outer membrane protein, OmpA family OS= <i>Burkholderia thailandensis</i> (strain E264 / ATCC 700388 / DSM 13276 / CIP 106301) GN=BTH_I1372 PE=3 SV=1
Q2SYZ4	Chaperone protein DnaK OS= <i>Burkholderia thailandensis</i> (strain E264 / ATCC 700388 / DSM 13276 / CIP 106301) GN=dnaK PE=3 SV=1
Q2SZ39	Putative uncharacterized protein OS= <i>Burkholderia thailandensis</i> (strain E264 / ATCC 700388 / DSM 13276 / CIP 106301) GN=BTH_I1263 PE=4 SV=1
Q2SZ52	Bifunctional purine biosynthesis protein PurH OS= <i>Burkholderia thailandensis</i> (strain E264 / ATCC 700388 / DSM 13276 / CIP 106301) GN=purH PE=3 SV=1

Q2SZ77	Glutamate/aspartate ABC transporter, periplasmic glutamate/aspartate-binding protein OS= <i>Burkholderia thailandensis</i> (strain E264 / ATCC 700388 / DSM 13276 / CIP 106301) GN=BTH_I1225 PE=4 SV=1
Q2SZ78	Glutamate dehydrogenase OS= <i>Burkholderia thailandensis</i> (strain E264 / ATCC 700388 / DSM 13276 / CIP 106301) GN=BTH_I1224 PE=3 SV=1
Q2SZ81	Adenylosuccinate lyase OS= <i>Burkholderia thailandensis</i> (strain E264 / ATCC 700388 / DSM 13276 / CIP 106301) GN= <i>purB</i> PE=4 SV=1
Q2SZ94	4-hydroxy-tetrahydrodipicolinate reductase OS= <i>Burkholderia thailandensis</i> (strain E264 / ATCC 700388 / DSM 13276 / CIP 106301) GN= <i>dapB</i> PE=1 SV=1
Q2SZA6	Glyceraldehyde-3-phosphate dehydrogenase, type I OS= <i>Burkholderia thailandensis</i> (strain E264 / ATCC 700388 / DSM 13276 / CIP 106301) GN= <i>gap</i> PE=3 SV=1
Q2SZA7	Transketolase OS= <i>Burkholderia thailandensis</i> (strain E264 / ATCC 700388 / DSM 13276 / CIP 106301) GN= <i>tkt</i> PE=1 SV=1
Q2SZE5	Outer membrane lipoprotein OS= <i>Burkholderia thailandensis</i> (strain E264 / ATCC 700388 / DSM 13276 / CIP 106301) GN=BTH_I1157 PE=4 SV=1
Q2SZN7	Triosephosphate isomerase OS= <i>Burkholderia thailandensis</i> (strain E264 / ATCC 700388 / DSM 13276 / CIP 106301) GN= <i>tpiA</i> PE=1 SV=1
Q2SZN9	Polyribonucleotide nucleotidyltransferase OS= <i>Burkholderia thailandensis</i> (strain E264 / ATCC 700388 / DSM 13276 / CIP 106301) GN= <i>pnp</i> PE=3 SV=1
Q2T086	OmpA family protein OS= <i>Burkholderia thailandensis</i> (strain E264 / ATCC 700388 / DSM 13276 / CIP 106301) GN=BTH_I0857 PE=3 SV=1
Q2T0B3	Putative uncharacterized protein OS= <i>Burkholderia thailandensis</i> (strain E264 / ATCC 700388 / DSM 13276 / CIP 106301) GN=BTH_I0830 PE=4 SV=1
Q2T0I4	Isocitrate dehydrogenase [NADP] OS= <i>Burkholderia thailandensis</i> (strain E264 / ATCC 700388 / DSM 13276 / CIP 106301) GN= <i>icd</i> PE=3 SV=1
Q2T0J9	Superoxide dismutase OS= <i>Burkholderia thailandensis</i> (strain E264 / ATCC 700388 / DSM 13276 / CIP 106301) GN=BTH_I0744 PE=3 SV=1
Q2T0L1	Ornithine carbamoyltransferase OS= <i>Burkholderia thailandensis</i> (strain E264 / ATCC 700388 / DSM 13276 / CIP 106301) GN= <i>argF-1</i> PE=1 SV=1
Q2T0L3	UPF0234 protein BTH_I0730 OS= <i>Burkholderia thailandensis</i> (strain E264 / ATCC 700388 / DSM 13276 / CIP 106301) GN=BTH_I0730 PE=3 SV=1
Q2T0R8	Serine protease OS= <i>Burkholderia thailandensis</i> (strain E264 / ATCC 700388 / DSM 13276 / CIP 106301) GN=BTH_I0675 PE=4 SV=1

Q2T0T0	Phosphoglycerate kinase OS= <i>Burkholderia thailandensis</i> (strain E264 / ATCC 700388 / DSM 13276 / CIP 106301) GN= <i>pgk</i> PE=3 SV=1
Q2T0X3	Cholesterol oxidase OS= <i>Burkholderia thailandensis</i> (strain E264 / ATCC 700388 / DSM 13276 / CIP 106301) GN=BTH_I0619 PE=4 SV=1
Q2T0Z3	Glycerol kinase OS= <i>Burkholderia thailandensis</i> (strain E264 / ATCC 700388 / DSM 13276 / CIP 106301) GN= <i>glpK</i> PE=3 SV=1
Q2T126	Thiolase family protein OS= <i>Burkholderia thailandensis</i> (strain E264 / ATCC 700388 / DSM 13276 / CIP 106301) GN=BTH_I0566 PE=3 SV=1
Q2T127	3-hydroxyacyl-CoA dehydrogenase/enoyl-CoA hydratase/isomerase family protein OS= <i>Burkholderia thailandensis</i> (strain E264 / ATCC 700388 / DSM 13276 / CIP 106301) GN=BTH_I0565 PE=4 SV=1
Q2T138	Tim44-like domain family OS= <i>Burkholderia thailandensis</i> (strain E264 / ATCC 700388 / DSM 13276 / CIP 106301) GN=BTH_I0554 PE=4 SV=1
Q2T1A8	PTS IIA-like nitrogen-regulatory protein PtsN OS= <i>Burkholderia thailandensis</i> (strain E264 / ATCC 700388 / DSM 13276 / CIP 106301) GN= <i>ptsN</i> PE=1 SV=1
Q2T1F2	Lipoprotein OS= <i>Burkholderia thailandensis</i> (strain E264 / ATCC 700388 / DSM 13276 / CIP 106301) GN=BTH_I0439 PE=3 SV=1
Q2T1J3	Sodium:solute symporter family protein OS= <i>Burkholderia thailandensis</i> (strain E264 / ATCC 700388 / DSM 13276 / CIP 106301) GN=BTH_I0398 PE=3 SV=1
Q2T1Y0	Putative uncharacterized protein OS= <i>Burkholderia thailandensis</i> (strain E264 / ATCC 700388 / DSM 13276 / CIP 106301) GN=BTH_I0261 PE=4 SV=1
Q2T220	Dipeptide ABC transporter, permease protein OS= <i>Burkholderia thailandensis</i> (strain E264 / ATCC 700388 / DSM 13276 / CIP 106301) GN=BTH_I0221 PE=3 SV=1
Q2T267	S-adenosylmethionine synthase OS= <i>Burkholderia thailandensis</i> (strain E264 / ATCC 700388 / DSM 13276 / CIP 106301) GN= <i>metK</i> PE=3 SV=1
Q2T276	ATP-dependent protease subunit HslV OS= <i>Burkholderia thailandensis</i> (strain E264 / ATCC 700388 / DSM 13276 / CIP 106301) GN= <i>hslV</i> PE=3 SV=1
Q2T2S6	Toluene tolerance, Ttg2 superfamily OS= <i>Burkholderia thailandensis</i> (strain E264 / ATCC 700388 / DSM 13276 / CIP 106301) GN=BTH_II2336 PE=4 SV=1
Q2T3D5	Beta-ketoadipyl CoA thiolase OS= <i>Burkholderia thailandensis</i> (strain E264 / ATCC 700388 / DSM 13276 / CIP 106301) GN=BTH_II2126 PE=3 SV=1
Q2T3E9	Lipoprotein, putative OS= <i>Burkholderia thailandensis</i> (strain E264 / ATCC 700388 / DSM 13276 / CIP 106301) GN=BTH_II2112 PE=4 SV=1

Q2T3L9	Aromatic-amino-acid aminotransferase OS= <i>Burkholderia thailandensis</i> (strain E264 / ATCC 700388 / DSM 13276 / CIP 106301) GN=BTH_II2037 PE=3 SV=1
Q2T3W7	60 kDa chaperonin 2 OS= <i>Burkholderia thailandensis</i> (strain E264 / ATCC 700388 / DSM 13276 / CIP 106301) GN= <i>groL2</i> PE=3 SV=1
Q2T3Y0	Chitin binding domain protein OS= <i>Burkholderia thailandensis</i> (strain E264 / ATCC 700388 / DSM 13276 / CIP 106301) GN=BTH_II1925 PE=4 SV=1
Q2T454	Metallopeptidase domain protein OS= <i>Burkholderia thailandensis</i> (strain E264 / ATCC 700388 / DSM 13276 / CIP 106301) GN=BTH_II1851 PE=4 SV=1
Q2T471	LasA protease OS= <i>Burkholderia thailandensis</i> (strain E264 / ATCC 700388 / DSM 13276 / CIP 106301) GN=BTH_II1834 PE=4 SV=1
Q2T4F3	Periplasmic trehalase OS= <i>Burkholderia thailandensis</i> (strain E264 / ATCC 700388 / DSM 13276 / CIP 106301) GN= <i>treA</i> PE=3 SV=1
Q2T4R7	Putative uncharacterized protein OS= <i>Burkholderia thailandensis</i> (strain E264 / ATCC 700388 / DSM 13276 / CIP 106301) GN=BTH_II1638 PE=4 SV=1
Q2T4T8	Malate dehydrogenase 2 OS= <i>Burkholderia thailandensis</i> (strain E264 / ATCC 700388 / DSM 13276 / CIP 106301) GN= <i>mdh2</i> PE=3 SV=1
Q2T4V6	Amino acid ABC transporter, periplasmic amino acid-binding protein, putative OS= <i>Burkholderia thailandensis</i> (strain E264 / ATCC 700388 / DSM 13276 / CIP 106301) GN=BTH_II1598 PE=4 SV=1
Q2T4W1	Aromatic-amino-acid aminotransferase OS= <i>Burkholderia thailandensis</i> (strain E264 / ATCC 700388 / DSM 13276 / CIP 106301) GN=BTH_II1593 PE=3 SV=1
Q2T4W5	Putative uncharacterized protein OS= <i>Burkholderia thailandensis</i> (strain E264 / ATCC 700388 / DSM 13276 / CIP 106301) GN=BTH_II1589 PE=4 SV=1
Q2T4X6	Microbial collagenase, putative OS= <i>Burkholderia thailandensis</i> (strain E264 / ATCC 700388 / DSM 13276 / CIP 106301) GN=BTH_II1578 PE=4 SV=1
Q2T599	Outer membrane porin OpcP OS= <i>Burkholderia thailandensis</i> (strain E264 / ATCC 700388 / DSM 13276 / CIP 106301) GN=BTH_II1454 PE=4 SV=1
Q2T5L4	Putative uncharacterized protein OS= <i>Burkholderia thailandensis</i> (strain E264 / ATCC 700388 / DSM 13276 / CIP 106301) GN=BTH_II1339 PE=4 SV=1
Q2T6D1	Putative uncharacterized protein OS= <i>Burkholderia thailandensis</i> (strain E264 / ATCC 700388 / DSM 13276 / CIP 106301) GN=BTH_II1071 PE=4 SV=1
Q2T6Z8	Ubiquitin-specific proteinase 31, putative OS= <i>Burkholderia thailandensis</i> (strain E264 / ATCC 700388 / DSM 13276 / CIP 106301) GN=BTH_II0854 PE=4 SV=1

Q2T736	Thermolysin metallopeptidase OS= <i>Burkholderia thailandensis</i> (strain E264 / ATCC 700388 / DSM 13276 / CIP 106301) GN=BTH_II0816 PE=4 SV=1
Q2T740	Serine-type carboxypeptidase family protein OS= <i>Burkholderia thailandensis</i> (strain E264 / ATCC 700388 / DSM 13276 / CIP 106301) GN=BTH_II0812 PE=4 SV=1
Q2T769	Putative uncharacterized protein OS= <i>Burkholderia thailandensis</i> (strain E264 / ATCC 700388 / DSM 13276 / CIP 106301) GN=BTH_II0783 PE=4 SV=1
Q2T7C9	Beta-glucosidase OS= <i>Burkholderia thailandensis</i> (strain E264 / ATCC 700388 / DSM 13276 / CIP 106301) GN= <i>bgIB</i> PE=4 SV=1
Q2T7I5	Citrate synthase OS= <i>Burkholderia thailandensis</i> (strain E264 / ATCC 700388 / DSM 13276 / CIP 106301) GN= <i>gltA</i> PE=3 SV=1
Q2T7J2	Malate dehydrogenase 1 OS= <i>Burkholderia thailandensis</i> (strain E264 / ATCC 700388 / DSM 13276 / CIP 106301) GN= <i>mdh1</i> PE=3 SV=1
Q2T7J6	Aconitate hydratase 1 OS= <i>Burkholderia thailandensis</i> (strain E264 / ATCC 700388 / DSM 13276 / CIP 106301) GN= <i>acnA</i> PE=4 SV=1
Q2T7L9	6-phosphogluconate dehydrogenase, decarboxylating OS= <i>Burkholderia thailandensis</i> (strain E264 / ATCC 700388 / DSM 13276 / CIP 106301) GN= <i>gnd</i> PE=3 SV=1
Q2T7W2	N-acetylmuramoyl-L-alanine amidase domain protein OS= <i>Burkholderia thailandensis</i> (strain E264 / ATCC 700388 / DSM 13276 / CIP 106301) GN=BTH_II0537 PE=4 SV=1
Q2T7W7	Extracellular nuclease, putative OS= <i>Burkholderia thailandensis</i> (strain E264 / ATCC 700388 / DSM 13276 / CIP 106301) GN=BTH_II0532 PE=4 SV=1
Q2T7W9	Lipoprotein, putative OS= <i>Burkholderia thailandensis</i> (strain E264 / ATCC 700388 / DSM 13276 / CIP 106301) GN=BTH_II0530 PE=4 SV=1
Q2T7Y2	Putative uncharacterized protein OS= <i>Burkholderia thailandensis</i> (strain E264 / ATCC 700388 / DSM 13276 / CIP 106301) GN=BTH_II0517 PE=4 SV=1
Q2T8B9	X-pro dipeptidyl-peptidase, putative OS= <i>Burkholderia thailandensis</i> (strain E264 / ATCC 700388 / DSM 13276 / CIP 106301) GN=BTH_II0380 PE=4 SV=1
Q2T8C0	Serine metalloprotease OS= <i>Burkholderia thailandensis</i> (strain E264 / ATCC 700388 / DSM 13276 / CIP 106301) GN=BTH_II0379 PE=4 SV=1
Q2T8I8	Antifungal protein, putative OS= <i>Burkholderia thailandensis</i> (strain E264 / ATCC 700388 / DSM 13276 / CIP 106301) GN=BTH_II0310 PE=4 SV=1
Q2T8S0	Putative uncharacterized protein OS= <i>Burkholderia thailandensis</i> (strain E264 / ATCC 700388 / DSM 13276 / CIP 106301) GN=BTH_II0227 PE=4 SV=1
Q2T934	PqaA OS= <i>Burkholderia thailandensis</i> (strain E264 / ATCC 700388 / DSM 13276 / CIP 106301) GN=BTH_II0113 PE=4 SV=1